THE GLUTATHIONE S-TRANSFERASES: KINETICS, BINDING AND INHIBITION

by

Richard David Goold B.Pharm., M.Sc. (Pharm.)

A thesis submitted to the
University of Cape Town Faculty of Medicine,
in partial fulfillment of the
requirements for the degree of

DOCTOR OF PHILOSOPHY

in Medical Biochemistry.

March 1989

ACKNOWLEDGEMENTS

I would like to express my sincere thanks to the following people:

My supervisors, Kathy and Paul, for their invaluable guidance, constructive criticism, and encouragement throughout this study.

The other members of our research group for their help and interest, especially Alfred Thumser, Cynthia Sikakana, Sue Phillips, Mel Ziman and Jo-Ann Harper.

Those many members of the department of Medical Biochemistry who loaned equipment or reagents, or gave advice and technical support.

Professor GMB Berger of the Red Cross War Memorial Childrens' Hospital for access to the Multistat centrifugal analyser, and the staff of the Pathology Laboratory, especially Brian Peak and Bruce Fuller, for their assistance.

Drs EH Merrifield and LL Radulovic for advice with purifications; Professor TJ Stewart for help with model discrimination and statistics; Dr Z van der Spey for permission to use human placental tissue from the maternity centre at Groote Schuur Hospital, Cape Town; Dr A Corrigall for donations of human lung GST samples.

Finally, I am grateful for the financial support afforded by the following:

UCT Postgraduate Research Scholarships (1986, 1987, 1988)
Frank Forman Grant (1986)
JW Duncan Baxter Scholarship (1988)

ABBREVIATIONS, SYMBOLS AND DEFINITIONS

A - absorbance
ANS - 8-anilino-1-naphthalene sulphonate
BSP - bromosulphophthalein
CDNB - 1-chloro-2,4-dinitrobenzene
CM-cellulose - carboxymethylcellulose
Cys - cysteine
DCNB - 1,2-dichloro-4-nitrobenzene
DEAE-cellulose - diethylaminoethylcellulose
DME - 1,2-dimethoxyethane
DMSO - dimethylsulphoxide
DNA - deoxyribonucleic acid
DTNB - 5,5′-dithiobis(2-nitrobenzoic acid)
DTT - dithiothreitol
E - enzyme
ϵ - molar extinction coefficient ($M^{-1}cm^{-1}$)
EDB - ethylene dibromide
EDTA - ethylenediaminetetraacetate
FPLC - fast protein liquid chromatofocusing
GST - glutathione S-transferase
GSH - glutathione, reduced
GSSG - glutathione, oxidised
His - histidine
HPLC - high pressure liquid chromatography
I - inhibitor
I_{50} - [I] causing 50% inhibition of enzyme activity under specified conditions.
$K_{A\ app}$ - (apparent K_m) [A] required for ½ V_{max} at specified finite [B] (similarly for $K_{B\ app}$)
K_i - (inhibitor constant) dissociation constant of EI complex
K_m - (Michaelis constant) [S] required for ½ V_{max} - for reactions involving two substrates (A & B), K_A is used to represent [A] required for ½ V_{max} when [B] is extrapolated to infinity (similarly for K_B)
k_{+n}, k_{-n} - velocity constants for the forward and backward reactions in the *n*th step of an enzymic reaction.
k_p - rate constant for the breakdown of ES to E + P
K_S - the equilibrium constant for the dissociation of the ES complex
λ - wavelength
MP-X - microperoxidase-X; X = number of amino acid residues of cytochrome-*c* retained in haempeptide
π - human placental GST isoenzyme
P - product
pI - isoelectric point
rpm - revolutions per minute
S - substrate
SD - standard deviation
SDS - sodium dodecyl sulphate
SDS-PAGE - sodium dodecyl sulphate polyacrylamide-gel electrophoresis
specific activity - activity units (U) per mg of protein as measured by a specified method and using a specified standard (units: μmol/min/mg)
$t_{½}$ - half-life
TCA - trichloroacetic acid
THF - tetrahydrofuran
Tris - tris(hydroxymethyl)aminomethane
U - (enzyme activity units) one unit is the amount of E catalysing the formation of 1 μmol of P per min under the conditions of the specific assay (μmol/min/ml).
UV - ultraviolet
v - initial velocity of appearance of P or disappearance of S at a given [S]
V_{max} - maximum initial velocity when E is saturated with S, in the absence of I

PUBLICATIONS AND PRESENTATIONS

Some of the work reported in this thesis has been prepared for publication with the approval of my supervisors:

Haem-peptide/Protein Interactions (i): The Binding of Haem Octa- and Undecapeptides; Microperoxidase-8 and 11 to Human Serum Albumin. P.A. Adams, R.D. Goold & A. Thumser. (1989) *J.Inorg.Biochem.*, in press. **(Appendix 1)**

The Kinetics of Haem Octapeptide (Microperoxidase-8; MP-8) Formation Studied by HPLC Monitoring of the Peptic and Tryptic Hydrolysis of Horse Heart Cytochrome-*c*. P.A. Adams, M.P. Byfield, R.D. Goold & A. Thumser (1989) *J.Inorg.Biochem.*, in press. **(Appendix 2)**

The Simplest Steady-State Random Sequential Bi Bi Mechanism is Sufficient to Explain the Non-Hyperbolic Kinetics of the Glutathione S-Transferases. K.M. Ivanetich, R.D. Goold & C.N.T. Sikakana. (1989), manuscript in preparation.

A Rapid Equilibrium Random Sequential Bi Bi Mechanism for Human Placental Glutathione S-Transferase. K.M. Ivanetich & R.D. Goold (1989), manuscript in preparation.

Active Site Solvation Contributes Significantly to Inactivation of the Glutathione S-Transferases (GST). P.A. Adams, R.D. Goold & C.N.T. Sikakana (1989), *Biochem. Pharmacol.*, in press.

Heme-Peptide-Protein Interactions (ii) : The Kinetics and Mechanism of the Interaction of Microperoxidase-8 with Apo-Myoglobin. P.A. Adams, R.D. Goold & A. Thumser. (1989), *J.Chem.Soc. (London) Faraday Transactions 1*, in press.

Heme-Peptide-Protein Interactions (iii) : The Kinetics and Mechanism of the Interaction between Human Placental Glutathione S-Transferase π and the Non-Substrate Ligand Microperoxidase-8 (MP-8). P.A. Adams & R.D. Goold (1989), manuscript in preparation.

Heme-Peptide-Protein Interactions (iv) : Microperoxidase-8-Mediated Inhibition of the Human Placental Glutathione S-Transferase π-Catalysed Conjugation of Glutathione and 1-Chloro-2,4-dinitrobenzene. P.A. Adams & R.D. Goold (1989), manuscript in preparation.

Some of this work has also been presented at scientific meetings:

Glutathione S-Transferase Activity: Effect of Irreversible Inhibition by the Substrate 1-Chloro-2,4-Dinitrobenzene. C.N.T. Sikakana, S. Phillips, R.D. Goold & K.M. Ivanetich. First Joint Conference of the S.A. Biochemical Society, S.A. Genetics Society & S.A. Society for Microbiology, University of the Witwatersrand, Johannesburg, S.A., July 1986.

Glutathione S-Transferase Activity: Effect of Irreversible Inhibition by the Substrate 1-Chloro-2,4-Dinitrobenzene. C.N.T. Sikakana, S. Phillips, R.D. Goold & K.M. Ivanetich. 10th European Drug Metabolism Workshop, Guildford, Surrey, U.K., July 1986.

A Steady-State Random Sequential Mechanism can Explain the Non-Hyperbolic Kinetics of the Glutathione S-Transferases. K.M. Ivanetich, R.D. Goold & C.N.T. Sikakana. 10th Enzyme Mechanisms Conference, Asilomar Conference Centre, Asilomar, California, U.S.A., Jan 2-6 1987.

A Steady-State Random Sequential Mechanism can Explain the Non-Hyperbolic Kinetics of Xenobiotic Metabolism by the Glutathione S-Transferases. K.M. Ivanetich, R.D. Goold & C.N.T. Sikakana. ISSX 2nd European Meeting on Foreign Compound Metabolism, J.W. Goethe-Universität Frankfurt A.M., F.R.G., March 29-April 3 1987.

The Mechanism of Drug Metabolism by the Glutathione S-Transferases. R.D. Goold, C.N.T. Sikakana & K.M. Ivanetich. 22nd S.A. Pharmacological Society Congress, Cape Town, S.A., October 12-14 1987.

The Kinetic Mechanism of Human Placental Glutathione S-Transferase. K.M. Ivanetich & R.D. Goold. 9th S.A. Biochemical Society Conference, Wilderness, S.A., March 27-31 1988.

Glutathione S-transferase Mechanism: Computer Simulation of the Conjugation Reaction and of Inhibition by 1-Chloro-2,4-dinitrobenzene. C.N.T. Sikakana, R.D. Goold & K.M. Ivanetich. 9th S.A. Biochemical Society Conference, Wilderness, S.A., March 27-31 1988.

The Physical and Inorganic Biochemistry of Microperoxidase-8 (MP-8) (4) Interaction of MP-8 with Human Serum Albumin. P.A. Adams & R.D. Goold. 9th S.A. Biochemical Society Conference, Wilderness, S.A., March 27-31 1988.

The Physical and Inorganic Biochemistry of Microperoxidase-8 (MP-8) (5) The Interaction of MP-8 with Human Placental Glutathione S-Transferase. P.A. Adams & R.D. Goold. 9th S.A. Biochemical Society Conference, Wilderness, S.A., March 27-31 1988.

The Physical and Inorganic Biochemistry of Microperoxidase-8 (MP-8) (6) The Kinetics and Mechanism of the Inhibition of Human Placental Glutathione S-Transferase by MP-8. P.A. Adams & R.D. Goold. 9th S.A. Biochemical Society Conference, Wilderness, S.A., March 27-31 1988.

The Physical and Inorganic Biochemistry of Microperoxidase-8 (MP-8) (7) The Interaction of MP-8 with Apo Myoglobin (apo-Mb). P.A. Adams, R.D. Goold & A.E.A. Thumser. 9th S.A. Biochemical Society Conference, Wilderness, S.A., March 27-31 1988.

The Interaction of the Haem Octapeptide Microperoxidase-8 (MP-8) with Haem Binding Proteins. P.A. Adams, R.D. Goold & A.E.A. Thumser. Inorganic 88, Gordon's Bay, S.A., April 7-9, 1988.

Haem Peptide-Protein Interactions: The Mechanism of the Reaction Between Haem Octa- and Undecapeptides (MP-8 and MP-11) with Drug Transporting and Metabolising Proteins. P.A. Adams, R.D. Goold & A. Thumser. 23rd S.A. Pharmacological Society Congress, Port Elizabeth, S.A., October 12-14 1988.

CONTENTS

	Page
Acknowledgements	ii
Abbreviations Symbols and Definitions	iii
List of Publications	iv
Contents	vii
List of Figures	x
List of Tables	xii
Summary	xiii
1. **INTRODUCTION**	1
1.1 THE ISOENZYMES OF GLUTATHIONE S-TRANSFERASE	1
1.1.1 Rat Glutathione S-Transferases	3
1.1.1.1 Characteristics and Tissue Distribution of the Cytosolic Isoenzymes	5
1.1.1.2 Microsomal Glutathione S-Transferases	10
1.1.2 Human Glutathione S-Transferases	11
1.1.3 Glutathione S-Transferases of Other Species	15
1.1.4 Species-Independent Classification of Isoenzymes	16
1.1.5 Primary Protein Structure and Evolution	18
1.2 PURIFICATION AND PHYSICAL CHARACTERISATION	20
1.2.1 Assay Systems	21
1.3 SUBSTRATES AND BIOLOGICAL FUNCTION	23
1.4 KINETICS AND CATALYTIC MECHANISM	29
1.4.1 Catalytic Site	29
1.4.2 Kinetic Mechanism	33
1.5 NON-SUBSTRATE LIGAND BINDING	38
1.5.1 Physiological Significance of Binding	39
1.5.2 Stoichiometry of Binding and Relationship Between Binding and Catalysis	40
1.5.3 Covalent Binding	42
1.6 BIOLOGICAL REGULATION	42
1.7 MICROPEROXIDASE-8: A MODEL COMPOUND FOR STUDIES OF HAEM/PROTEIN INTERACTIONS	43
1.8 OBJECTIVES OF THIS STUDY	45

Page

2. **EXPERIMENTAL METHODS** 47

2.1 MATERIALS AND GENERAL METHODS 47
2.2 ASSAYS FOR GSH S-TRANSFERASE ACTIVITY 47
2.3 PRELIMINARY EXPERIMENTS 51
2.4 GSH S-TRANSFERASE ISOENZYME PURIFICATIONS 54
2.4.1 Purification of Human Placental GSH S-Transferase π 54
2.4.2 Purification of Rat Hepatic GSH S-Transferase 2-2 56
2.5 STEADY-STATE KINETIC STUDIES 58
2.5.1 Initial Velocities in the Absence of Products 58
2.5.2 Initial Velocities in the Presence of Product 59
2.5.3 Synthesis of S-(2,4-Dinitrophenyl)glutathione 60
2.5.4 Model Fitting and Discrimination Between Rival Models 61
2.6 EQUILIBRIUM BINDING OF GSH TO HUMAN PLACENTAL GST π 62
2.7 OPTIMISATION OF THE PREPARATION OF MP-8 63
2.7.1 Preparation of MP-8 63
2.7.2 Kinetics of MP-11 Formation from Cytochrome-*c* 64
2.8 INTERACTION OF HUMAN PLACENTAL GST π AND MP-8 65
2.9 THE INHIBITION OF HUMAN PLACENTAL GST π BY MP-8 66

3. **RESULTS** 67

3.1 PRELIMINARY EXPERIMENTS 67
3.2 GSH S-TRANSFERASE ISOENZYME PURIFICATIONS 72
3.2.1 Purification of Human Placental GSH S-Transferase π 72
3.2.2 Purification of Rat Hepatic GSH S-Transferase 2-2 74
3.3 STEADY-STATE KINETIC STUDIES 76
3.3.1 Rat Liver GST Isoenzymes 3-3 and 3-4 76
3.3.2 Human Placental GST π - Initial Velocities in the Absence of Products 79
3.3.3 Human Placental GST π - Initial Velocities in the Presence of Product 83
3.3.4 Rat Liver GST 2-2 - Initial Velocities in the Absence of Products 88
3.3.5 Rat Liver GST 2-2 - Initial Velocities in the Presence of Product 92
3.4 EQUILIBRIUM BINDING OF GSH TO HUMAN PLACENTAL GST π 94
3.5 OPTIMISATION OF THE PREPARATION OF MP-8 95
3.6 INTERACTION OF HUMAN PLACENTAL GST π AND MP-8 96
3.7 THE INHIBITION OF HUMAN PLACENTAL GST π BY MP-8 103

Page

4. **DISCUSSION** 108

4.1 OPTIMISATION OF GST ASSAY FOR KINETIC STUDIES 108
4.2 THE REVERSIBLE AND IRREVERSIBLE INHIBITION OF GSTs BY ETHYLENE DIBROMIDE 111
4.3 THE SIMPLEST STEADY-STATE RANDOM SEQUENTIAL BI BI MECHANISM ADEQUATELY EXPLAINS THE NON-HYPERBOLIC KINETICS OF THE GSTs. 113
4.4 A RAPID EQUILIBRIUM RANDOM SEQUENTIAL BI BI MECHANISM FOR HUMAN PLACENTAL GLUTATHIONE S-TRANSFERASE 119
4.5 ACTIVE-SITE SOLVATION CONTRIBUTES SIGNIFICANTLY TO INACTIVATION OF THE GSTs. 126
4.6 OPTIMISATION OF THE PREPARATION OF MP-8 130
4.7 THE KINETICS AND MECHANISM OF THE INTERACTION BETWEEN HUMAN PLACENTAL GST π AND MP-8 132
4.8 THE INHIBITION OF HUMAN PLACENTAL GST BY MP-8 140

5. **CONCLUSIONS** 142

Appendix 1 145
Appendix 2 162
References 168

LIST OF FIGURES

		Page
Figure 1.1	The Tissue Distribution of GSH S-Transferases in the Rat	6
Figure 1.2	Inter-Species Classification of GSH S-Transferases	16
Figure 1.3	The Mercapturic Acid Pathway	24
Figure 1.4	Alternative Models of the Topology for the Two Active-Sites of a Dimeric GSH S-Transferase Molecule	32
Figure 1.5	The Haem-Peptides from Cytochrome-*c*	44
Figure 2.1	Multistat Centrifugal Analyser Rotor	49
Figure 3.1	Linearity of CDNB Assay with Time	68
Figure 3.2	The Effect of Solvent on the DCNB Assay	68
Figure 3.3	Inhibition and Activation of GST 3-3 by EDB	70
Figure 3.4	The Variation in GST Activity During Incubations of EDB with DNA	70
Figure 3.5	GSH-Affinity Chromatography of Human Placental GST	73
Figure 3.6	HPLC Separation of Human Placental GST	73
Figure 3.7	SDS-Polyacrylamide Gel Electrophoresis of GSTs	75
Figure 3.8	CM-Cellulose Chromatography of Rat Liver GST	75
Figure 3.9	Reciprocal Plot of Initial Rate Data for Rat Liver GST 3-3 and CDNB.	77
Figure 3.10	Reciprocal Plot of Initial Rate Data for Rat Liver GST 3-4 and DCNB.	77
Figure 3.11	Hill Plot of Rat Liver GST Activity	78
Figure 3.12	Reciprocal Plots of Initial Rate Data in the Absence of Products for Human Placental GST.	80
Figure 3.13	Secondary plots of Initial Rate Data of Figure 3.12	81
Figure 3.14	Reciprocal Plots of Initial Rate Data in the Presence of the Conjugate - Human Placental GST.	84
Figure 3.15	Secondary plots of Initial Rate Data of Figure 3.14	85
Figure 3.16	Reciprocal Plots of Initial Rate Data in the Absence of Products for Rat Liver GST 2-2.	89
Figure 3.17	Secondary plots of Initial Rate Data of Figure 3.16	90
Figure 3.18	Reciprocal Plots of Initial Rate Data in the Presence of the Conjugate - Rat Liver GST 2-2.	93
Figure 3.19	Equilibrium Binding of [^{35}S]GSH to Human Placental GST	94
Figure 3.20	Optimisation of Peptic Digestion of Cytochrome-*c* to MP-11	95

Page

Figure 3.21	Spectral Changes for MP-8/GST Interaction	96
Figure 3.22	Kinetics of the Interaction of Human Placental GST and MP-8	97
Figure 3.23	Interaction of Human Placental GST with Varying Concentrations of MP-8	98
Figure 3.24	Variation of k_1^* and k_2^* with MP-8 Concentration	100
Figure 3.25	Variation of A_r with MP-8 Concentration	100
Figure 3.26	Effect of Bilirubin on the Interaction of MP-8 and GST	101
Figure 3.27	Effect of CDNB on the Interaction of MP-8 and GST	101
Figure 3.28	Effect of GSH on the Interaction of MP-8 and GST	102
Figure 3.29	Time-Dependent Inhibition of Human Placental GST by MP-8	103
Figure 3.30	Inhibition of Human Placental GST by MP-8	105
Figure 3.31	Secondary Plots for Figure 3.30b	106
Figure 3.32	Slope and Intercept Replots of Dixon Plots for Data of Figure 3.30b	107

LIST OF TABLES

		Page
Table 1.1	Sources of Glutathione S-Transferase	2
Table 1.2	Nomenclature for the Cytosolic Rat GSH S-Transferases	4
Table 1.3	Substrate Specificities of Major Rat GSH S-Transferases	8
Table 1.4	Inhibition Characteristics of Major Rat GSH S-Transferases	8
Table 1.5	Nomenclature and Physical Characteristics of Major Human GSH S-Transferases	11
Table 1.6	Substrate Specificities of Major Human GSH S-Transferases	12
Table 1.7	Inhibition Characteristics of Major Human GSH S-Transferases	12
Table 1.8	Class-Discriminating Substrate Specificities and Inhibitor Sensitivities of GSH S-Transferases	17
Table 1.9	Conditions for Spectrophotometric Assays for GSH S-Transferases	22
Table 1.10	Dissociation Constants for the GSH S-Transferases	38
Table 2.1	Sources of Reagents and Solvents Used	48
Table 3.1	GSH-Mediated DNA-Binding of EDB Catalysed by Different GST Isoenzymes	71
Table 3.2	Summary of Human Placental GST Purification	72
Table 3.3	Summary of Rat Liver GST 2-2 Purification	74
Table 3.4	Comparison of the Fitting of Bireactant Reaction Mechanisms to Initial Rate Data for Human Placental GST π.	82
Table 3.5	Comparison of the Fitting of Bireactant Reaction Mechanisms to Initial Rate Data in the Presence of the conjugate, S-(2,4-dinitrophenyl)-glutathione.	87
Table 3.6	Comparison of the Fitting of Bireactant Reaction Mechanisms to Initial Rate Data for Rat Liver GST 2-2.	91
Table 3.7	Kinetic Parameters for the Interaction of MP-8 and Human Placental GST	98
Table 3.8	Parameters for Linear Mixed Type Inhibition of Human Placental GST by MP-8	104
Table 4.1	The Pseudo-First-Order Rate Constant for Irreversible Inactivation of a Range of GSTs	128

SUMMARY

The glutathione S-transferases are a group of enzymes which catalyse the conjugation of reduced glutathione with a variety of electrophilic molecules, and they are therefore thought to play a major role in drug biotransformation and the detoxification of xenobiotics [39,179]. The cytosolic GSH S-transferase isoenzymes of rat, man and mouse have been assigned to three groups, Alpha, Mu and Pi, based on N-terminal amino acid sequences, substrate specificities, immunological cross-reactivity and sensitivities to inhibitors [182].

The kinetic mechanism of the GSH S-transferases is controversial, due to the observation of non-Michaelian (non-hyperbolic) substrate-rate saturation curves. The most detailed investigations of the steady-state kinetics of glutathione S-transferase have been performed with isoenzyme 3-3 (class Mu) and the substrate 1,2-dichloro-4-nitrobenzene (DCNB) [12,215]. Explanations for the apparently anomalous non-hyperbolic kinetics have included subunit co-operativity, steady-state mechanisms of differing degrees of complexity and the superimposition of either product inhibition or enzyme memory on these mechanisms [39,179].

This study has confirmed the biphasic kinetics for isoenzyme 3-3 with DCNB and shown non-hyperbolic kinetics for this isoenzyme with 1-chloro-2,4-dinitro-benzene (CDNB) and for isoenzyme 3-4 with DCNB and CDNB. It is proposed that the basic steady-state random sequential Bi Bi mechanism is the simplest mechanism sufficient to explain the non-hyperbolic kinetics of GSH S-transferases 3-3 and 3-4 under initial rate conditions. Neither more complex steady-state mechanisms nor the superimposition of product inhibition or enzyme memory on the simplest steady-state mechanism are necessary.

The steady-state kinetic analysis involved initial velocity studies performed both in the presence and absence of the product of the enzymic reaction, as well as computer modelling of the experimental data. An initial optimisation of the GSH S-transferase (GST) assay system was performed to ensure a high degree of accuracy and reproducibility in the kinetic studies. Factors considered included the selection of spectrophotometric instrument, choice of solvent for the hydrophobic substrate, order of addition of reactants and linearity of product formation with time.

Since detailed steady-state kinetic studies have only been done for isoenzymes of class Mu, representative isoenzymes from the other two classes of GST (Alpha and Pi) were isolated and their kinetic mechanisms were characterised. Isoenzyme 2-2 (class Alpha) was isolated from rat liver and found to show non-hyperbolic kinetics, although the biphasic nature of the plots was less pronounced than for class Mu. In contrast to isoenzymes 3-3, 3-4 and 2-2, the kinetics of human placental GST π (class Pi) were hyperbolic over wide ranges of both CDNB and GSH concentration. Computer modelling of the initial velocity data showed that this isoenzyme was more adequately described by a rapid equilibrium random kinetic mechanism than by the analogous steady-state system. This was confirmed by the observed pattern of product inhibition with the GSH•CDNB conjugate, which also indicated the presence of a dead-end enzyme•CDNB•conjugate complex. These findings demonstrate that the kinetic mechanism of the GSH S-transferases is isoenzyme-dependent.

The time-dependent inactivation of several GSTs, by a variety of different inactivating agents in unrelated experiments, appears to follow a pseudo-first-order rate law with a pseudo-first-order rate constant of approximately $2.5 \times 10^{-3}\ s^{-1}$. The similarity between this value and that of the pseudo-first-order rate constant for the inhibition observed on dilution of concentrated solutions of GST suggests that these compounds may inactivate GST by facilitating an increase in the extent of solvation of the hydrophobic active-site. It is possible that this phenomenon could account for the various stable activity states which are observed when GSTs are incubated with foreign proteins prior to the addition of inactivating agents [304].

In addition to their enzymic function, the GSH S-transferases bind a variety of non-substrate ligands, such as bilirubin, haemin, bile acids and certain carcinogens, which suggests that they also play a role in the intracellular transport and storage of xenobiotics and endogenous substances [39]. One of the most biologically significant non-substrate ligands is haemin, and although a number of equilibrium binding studies of the interaction of haemin and the GSTs have been performed, no investigations of the kinetics of binding have yet been reported. A major reason for the paucity of kinetic studies is the tendency of haemin to aggregate in aqueous solution, forming oligimers which prevent the acquisition of 'clean' kinetic data. We have used microperoxidase-8 (MP-8), a sterically hindered analogue of protoporphyrin IX which remains monomeric in solution at experimentally useful concentrations, to model the kinetics of binding of haemin to human placental GST π.

In order to obtain MP-8 of highest purity for kinetic studies, the kinetics of the formation of MP-8 were studied by HPLC monitoring of the peptic and tryptic hydrolysis of horse heart cytochrome-*c*, and conditions for the preparation of MP-8 were thus optimised.

The kinetics of the reaction between MP-8 and human placental GST π, and the effects of other substrate/non-substrate ligands on these kinetics, were followed using the quenching of the MP-8 Soret absorbance (396 nm) which is observed on mixing the two species. The binding constants obtained in these 'extra-thermodynamic' studies were assessed directly from microscopic rate constants and therefore are more directly interpretable than those obtained in the thermo-dynamic procedures employed in previous investigations of GST/non-substrate ligand interactions.

Under pseudo-first-order conditions ([MP-8] >> [GST]) and over a concentration range in which the MP-8 is monomeric in aqueous solution, the kinetics of binding are biphasic. The slower binding phase reflects the hydrophobic interaction of MP-8 with or spatially close to the bilirubin binding site on the enzyme, while the more rapid binding phase is associated with MP-8 binding at a hydrophobic site at or close to the binding site for the co-substrate CDNB. From the fact that GSH had only a minimal effect on the interaction of MP-8 with GST π, it can be inferred that the kinetically fast binding site is not identical to the

CDNB binding site but is adjacent to it, with possibly one or more residues of the octapeptide chain able to overlap the CDNB site. These studies have also provided direct confirmation of the independence of the catalytic and bilirubin-binding sites of GST π [308].

In order to further clarify the nature of the MP-8 binding site(s) of human placental GST, the inhibition by MP-8 of the GST-catalysed conjugation of GSH with CDNB was also investigated. Steady-state kinetic studies of the MP-8-mediated inhibition of the GST π-catalysed conjugation of GSH with CDNB were performed after incubation of the enzyme with varying concentrations of MP-8 for 15 minutes prior to initiation of the reaction. At a fixed GSH concentration with varying CDNB concentration, the data conformed closely to inhibition kinetics of the mixed-type (K_i = 3.2 x 10^{-7} M; pH 6.5; 30°C). For varying GSH concentration at a fixed CDNB concentration, the extent of inhibition was insufficient for analysis. These results are in excellent agreement with the results of the MP-8/GST binding kinetics, indicating that MP-8 and GSH affect each others interaction with the enzyme only minimally, and that the effect of MP-8 on catalysis occurs in the region of the CDNB locus at the active-site.

The fact that the K_i value above is consistent with the independently calculated value of the binding constant for MP-8 binding proximal to the CDNB site demonstrates further agreement between the MP-8/GST binding kinetics and the studies of the MP-8-mediated inhibition of the conjugation reaction. This agreement provides strong evidence that the MP-8/GST fast binding site and the MP-8 catalytic inhibition site are one and the same.

Analysis of the time-course of the MP-8-mediated inhibition of GST π indicated a pseudo-first-order partial inactivation of the enzyme (k_{obs} = 2.3 ± 0.4 x 10^{-3} s^{-1}; pH 6.5; 22.5°C). This value is identical to that found for dilutional inactivation of the enzyme in buffer alone, with MP-8 only increasing the extent of inactivation above that observed for dilutional inactivation. In view of the agreement between these values, as well as all the other observations of this study, the mechanism for the interaction of MP-8 and GST π is shown to be of the random sequential form with perturbation due to solvational elimination of the fast site.

These studies recommend the non-substrate ligand MP-8 as a potentially valuable model for monomeric haemin, with which to investigate the nature and location of metalloporphyrin binding sites on the haem-binding GSTs.

1. INTRODUCTION

The greater part of this chapter comprises a review of the glutathione S-transferases; their distribution, properties, purification and biological function. Also described is the current understanding of their kinetic mechanism and of the binding of non-substrate ligands to this family of enzymes, since both topics are of particular relevance to this investigation.

One of the most physiologically important of the non-substrate ligands of the glutathione S-transferases is haemin, yet experimental difficulties complicate studies of haemin binding in aqueous solution. In this study, novel use was made of microperoxidase-8 as a model compound for the binding of haemin to the glutathione S-transferases. A description of microperoxidase-8, and the rationale behind its use in this investigation, is therefore also presented here. Finally, the objectives of this study are briefly outlined.

1.1 THE ISOENZYMES OF GLUTATHIONE S-TRANSFERASE

The glutathione S-transferases (EC 2.5.1.18) are a group of enzymes which catalyse the conjugation of reduced glutathione (GSH) with a variety of electrophilic molecules; these enzymes are therefore thought to play a major role in drug and xenobiotic biotransformation and detoxification. Their importance can be appraised by their abundance in nature. GSH S-transferases have been identified in fungi and bacteria, plants, insects, molluscs, nematodes, fish and birds (see Table 1.1) as well as in mammals. Man and the rat are the most intensively studied species. The physiological significance of the GSH S-transferases is further reinforced by the fact that they account for 10% of the cytosolic protein in rat liver [39].

In addition to their enzymic function, the GSH S-transferases bind a variety of non-substrate ligands, such as bilirubin, haem, bile acids and certain carcinogens, and there is evidence that they play a role in intracellular transport and storage of xenobiotics and endogenous substances [39].

Table 1.1 : **Sources of Glutathione S-transferases**

Source	Organ	Reference
Rat	Liver	142
	Kidney	295
	Testis	38,95,96
	Lung	239,262
	Heart	129
	Skin	162
	Brain	1,270,296
	Microsomes	198,200
	Intestine	226
	Serum	207
Human	Liver	103,318
	Kidney	268
	Lung	160,260
	Placenta	94,186,231,232,308
	Uterus	72
	Muscle	33
	Heart	260
	Retina	265
	Prostate	290
	Erythrocytes	190,260,261
	Platelets	84
Mouse	Liver	169,319
	Lung	263
Sheep	Liver	234
	Lung	170
Ox	Eye	14
Rabbit	Liver	194
Pig	Liver	92
Dog	Liver	320
Rhesus Monkey	Liver	119
Camel	Liver	123
Chicken	Liver	327
Shark	Liver	278
Atlantic Salmon	-	26
Bluegill & Channel Catfish	-	10
Blue Crab	-	149
Flour Beetle	-	60
American Cockroach	-	168
Housefly	-	205
Yellowfever Mosquito	-	117
Australian Sheep Blowfly	-	161
Greater Wax Moth	-	168
Earth worm	-	168
Corn	-	206
Daphnia magna	-	168
Schistosoma mansoni	-	210,287

Purification methods are detailed in most references cited in table. This table is not intended to be complete, but rather to demonstrate the diversity of species in which GSTs are found.

The GSH S-transferases are primarily cytosolic proteins and occur as several homo- and heterodimeric isoenzymes in virtually all species studied. Although the tissue distribution and physical properties have only been determined in detail for a few species, the expression of GSH S-transferase (GST) isoenzymes is clearly species- and tissue-specific [19,115,301].

1.1.1 Rat Glutathione S-Transferases

The earliest and most intensive studies of the GSTs have been performed on the transferases of adult rat liver. The nomenclature describing the rat GST isoenzymes has undergone modification several times over the years; the major notations that have been used are shown in Table 1.2.

Originally the GST isoenzymes of rat liver cytosol were classified on the basis of their assumed substrate specificities with various aryl, alkyl, alkene and epoxide substrates [44], but the inadequacy of this nomenclature became apparent once the broad and overlapping substrate specificity of the GSTs was demonstrated [107]. It was, for example, discovered that 1-chloro-2,4-dinitrobenzene (CDNB) appears to be a substrate for all GST isoenzymes [55], making the classification 'GSH S-aryl transferase' redundant. CDNB, which is a 'universal substrate' for the transferases, has become the basis of the general assay for transferase activity [107] (see Section 1.2.1). Other names that have been used in the past for the GSTs are ligandin [106], azo-dye carcinogen-binding protein, and Y-protein [171]. These terms are based on the binding properties of various GST isoenzymes.

In view of the overlapping substrate specificities of the GSTs, Jakoby [107,138] proposed a nomenclature based on the alphabetical naming of the enzymes in reverse order of their gradient elution from a CM-cellulose column. Subsequently, the GST nomenclature was further modified to reflect the subunit composition of the dimeric proteins. The three major cytosolic subunits were named Y_a, Y_b and Y_c, in order of their increasing apparent molecular weight on SDS-PAGE [23,111].

This more informative system became somewhat complicated when the Y_b band was shown to contain two components, which were named Y_b^1 and Y_b^2 [25]. The possibility that GST variants might become too numerous for an alphabetical system, particularly after recombinant DNA technology demonstrated micro-heterogeniety in the primary structure of subunits [151,223,247,300,314],

Table 1.2 : Nomenclature for the Cytosolic Rat GSH S-Transferases

New[140] Nomenclature	Other/Previous Nomenclature Systems (Reference)						Subunit M_r* ($\times 10^3$)	pI
	(23,25)		(138)	(116)	(25)	(188)		
1-1	Y_aY_a	Ligandin[171]	B	Ligandin	B_1	L_2	25	10
1-2	Y_aY_c			B	B_2	BL	25,28	9.9
2-2	Y_cY_c		AA		AA	B_2	28	9.8
3-3	$Y_{b1}Y_{b1}$		A		A	A_2	26.5	8.4
3-4	$Y_{b1}Y_{b2}$		C		C	AC	26.5	8.1
4-4	$Y_{b2}Y_{b2}$		D‡		"D"	C_2	26.5	6.9
5-5	—		E		E		26.5	7.3
6-6	Y_nY_n[112]	Y_tY_t[38]					26	5.8
7-7[143]	Y_fY_f[125]	Y_pY_p[248]	P[156]				24	8.7
8-8[144]	Y_kY_k[113]		K[113]				24.5	6.0

‡Although not fully characterised by Jakoby *et al.* (138), D is thought to be the same as 4-4
*M_r based on SDS-PAGE
Table adapted from 179 and references cited in table.

References cited in table:

23. Bass, N.M. *et al.* (1977) *Biochim.Biophys.Acta* **492**, 163-175
25. Beale, D. *et al.* (1983) *Eur.J.Biochem.* **137**, 125-129
38. Boyer, T.D. & Kenney, W.C. (1985) *Biochem.J.* **230**, 125-132
112. Hayes, J.D. (1984) *Biochem.J.* **224**, 839-852
113. Hayes, J.D. (1986) *Biochem.J.* **233**, 789-798
116. Hayes, J.D. *et al.* (1981) *Biochem.J.* **197**, 491-502
125. Hussey, A.J. *et al.* (1986) *Biochem.Biophys.Acta* **874(1)**, 1-12
138. Jakoby, W.B. *et al.* (1976) in *Glutathione: Metabolism and Function*, Raven Press, 189-211
140. Jakoby, W.B. *et al.* (1984) *Biochem.Pharmacol.* **33**, 2539-2540
143. Jensson, H. *et al.* (1985) *FEBS Lett.* **187(1)**, 115-120
144. Jensson, H. *et al.* (1986) *FEBS Lett.* **203(2)**, 207-209
156. Kitahara, A. *et al.* (1984) *Cancer Res.* **44(6)**, 2698-2703
171. Litwack, G. *et al.* (1971) *Nature (London)* **234**, 466-467
188. Mannervik, B. & Jensson, H. (1982) *J.Biol.Chem.* **257(17)**, 9909-9912
248. Satoh, K. *et al.* (1985) *Proc.Natl.Acad.Sci. USA* **82**, 3964-3968

prompted the development of a numeric system of nomenclature, capable of expansion as required. In this system, subunits are numbered consecutively, based on the order in which they are characterised as separate entities.

Although some workers in the field retain the Y_a/Y_b nomenclature [115,282,311], the simpler numeric system, which has been endorsed by several other investigators at a workshop on nomenclature [140], has been adopted throughout this thesis.

1.1.1.1 Characteristics and Tissue Distribution of the Cytosolic Isoenzymes

The GST subunits in the cytosol of rat tissues are coded for by three multigenic families and all rat cytosolic GSTs arise from binary combinations of these subunits [19]. For example, subunits 1 and 2 form a family of related isoenzymes consisting of two homodimers (1-1 and 2-2) and one heterodimer (1-2). Likewise another family comprises transferases 3-3, 4-4 and 3-4. Only subunits within the same gene family have been found to hybridise [113,125].

The distribution of GST isoenzymes varies considerably in different tissues (see Figure 1.1). At least ten GST isoenzymes occur in rat hepatic cytosol, which has the highest capacity for conjugation of CDNB with GSH (followed by the testes and then the kidney). Extrahepatic tissues, with the exception of the kidney, express predominantly acidic isoenzymes [115]. A membrane-bound microsomal form which is completely different to the cytosolic forms also occurs in rat liver (see Section 1.1.1.2). There are indications that the cell nucleus also contains GSH S-transferase [27,48]. When GST subunits were isolated from rat hepatocyte nuclei and then reinjected into the cytoplasm of cultured cells, 44% of the reintroduced subunits rapidly migrated to the nuclear fraction [28] (see Section 1.3).

Rat liver cytosol contains the basic subunits 1, 2, 3 and 4 in high concentration. Subunit 1 is also abundant in the kidney but is either absent or present in low concentrations in other tissues [239]. While subunit 2 occurs in most tissues, it is especially predominant in the adrenal [286]. Subunit 3 is apparently absent from the cytosolic fraction of kidney [151] although subunits 1, 2, 4 and transferase 7-7, an isoenzyme not found in liver, have been identified in this tissue [98]. The cytosol of rat testis contains negligible amounts of transferases 1-1 and 1-2 and the major isoenzyme of this tissue (about 50% of the transferase activity) is the acidic

transferase 6-6 [38,95-97], which is not found in rat liver. Another acidic isoenzyme with distinct enzymatic properties (transferase 5-5) is present in proportionally large amounts in the seminiferous tubules [192]. A novel rat transferase isoenzyme (M_r 25 000, pI 6.1) that is present in high concentrations in the colon has been reported [113]. Rat heart lacks the majority of basic isoenzymes, and most of the GST activity in this tissue is associated with near-neutral and acidic proteins [128,129].

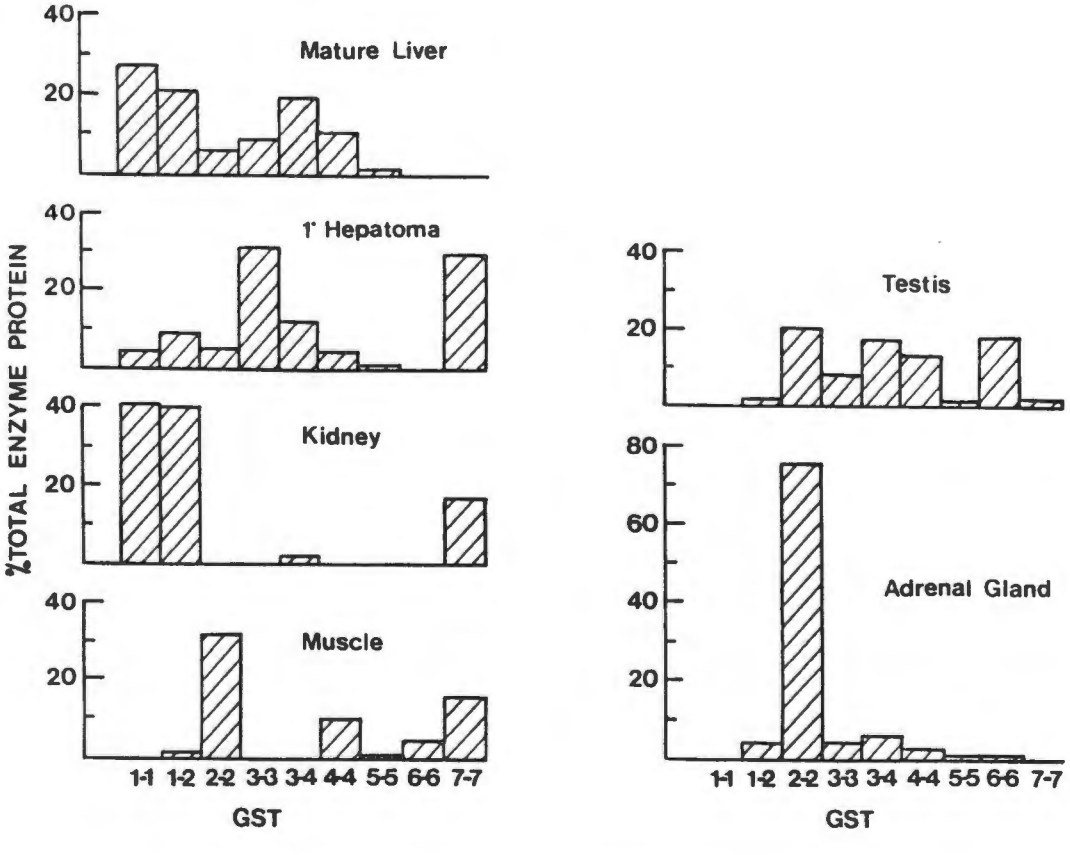

Figure 1.1 : **The Tissue Distribution of GSH S-Transferases in the Rat**
Adapted from reference 151.

It is interesting to note that primary hepatoma, arising from hepatic parenchymal tissue, expresses a quite different profile of isoenzymes to its parent tissue. Subunit 1 decreases in quantity, subunit 2 remains at a high level, and subunit 3 becomes a major component [286]. Particularly significant in hyperplastic nodules and

hepatocellular carcinomas is the predominance of isoenzyme 7-7, which is almost absent in the mature rat liver (see Figure 1.1). This isoenzyme is therefore regarded as a hepatoma marker [195,209,219,243,245,286]. Although the mechanism by which this marked increase in transferase 7-7 content occurs is unknown, proportional increases in tissue mRNA content have indicated at least partial control at the transcriptional level [209].

The rat GST subunits can be differentiated by their apparent molecular weight and isoelectric point, shown in Table 1.2, as well as by their characteristic specific activities with a range of substrates (see Table 1.3) and sensitivities to selective inhibitors (Table 1.4).

Rat GST 1-1 is one of the major hepatic isoenzymes and, together with 1-2, was ascribed the functions of 'ligandin' with respect to binding of haem derivatives [153], and other compounds [171]. The isomerase activity of 1-1 with Δ^5-androstene-3,17-dione is higher than other rat GST isoenzymes [188], and this isoenzyme is strongly inhibited by haematin [325]. When rat liver is treated with inducing agents, such as phenobarbital, 3-methylcholanthrene and *trans*-stilbene oxide, isoenzyme 1-1 is the most effectively induced isoenzyme, with the greatest induction observed for *trans*-stilbene oxide [179].

Isoenzyme 2-2 is characterised by a high specific GSH peroxidase activity [188]. Tributyltin acetate is the strongest inhibitor of those studied, but weak inhibition by bromosulphophthalein (BSP) differentiates isoenzyme 2-2 from other cytosolic GSTs, as these are also strongly inhibited by tributyltin acetate [325]. Inducing agents, such as phenobarbital, 3-methylcholanthrene and *trans*-stilbene oxide, decrease the cytosolic concentration of isoenzyme 2-2 [78].

The heterodimeric isoenzyme 1-2 has a pattern of specific activity toward different substrates [188] and sensitivity to inhibitors [325] intermediate between the homodimeric transferases 1-1 and 2-2. The two non-identical subunits are readily separated using SDS-polyacrylamide gels [23]. Inducing agents increase the levels of transferase 1-2 in the rat hepatic cytosol [78].

Isoenzyme 3-3 is best identified by a high specific activity with BSP, together with strong inhibition by triphenyltin chloride and triethyltin bromide [188,325]. This isoenzyme is induced almost as much as transferase 1-1 by the inducing agents mentioned above [179].

Table 1.3 **Substrate Specificities of Major Rat GSH S-Transferases**

Substrate	Relative Specific Activity (%)‡ Isoenzyme						
	1-1	1-2	2-2	3-3	3-4	4-4	6-6
1-Chloro-2,4-dinitrobenzene	100 (33)	100 (28)	100 (19)	100 (38)	100 (28)	100 (18)	100 (190)
1,2-Dichloro-4-nitrobenzene	<0.2	<0.2	0.2	10	9	1	1.5
Bromosulphophthalein	ND	ND	ND	2	1	0.2	ND
Ethacrynic acid	0.4	3	7	0.3	1	3	0.03
trans-4-Phenyl-3-buten-2-one	ND	ND	ND	0.2	2	9	0.01
1,2-Epoxy-3-(*p*-nitrophenoxy)propane	0.4	0.3	0.3	1.3	1.6	5	ND
Cumene hydroperoxide	8	14	40	1.4	2	7	0.1
Δ^5-Androstene-3,17-dione	13	8	2	0.05	0.03	0.01	ND
p-Nitrophenyl acetate	2	1.3	0.4	2	1.3	1	0.1

‡Values given as percentages of the specific activities determined with CDNB as substrate (specific activity in parentheses). ND = no detectable activity. From reference 179.

Table 1.4 **Inhibition Characteristics of Major Rat GSH S-Transferases**

Inhibitor	ID_{50} (μM)‡ Isoenzyme						
	1-1	1-2	2-2	3-3	3-4	4-4	6-6
Cibacron blue	0.6	4	20	0.25	0.25	0.1	0.02
Tributyltin acetate	2	1	0.5	1	1	2	10
Triethyltin bromide	350	100	3	1	1	70	100
Triphenyltin chloride	0.5	1	30	0.1	0.1	0.2	30
Bromosulphophthalein	2	10	200	10	6	0.5	1
Haematin	0.05	0.2	>2	1	1	1	0.3
S-(*p*-Bromobenzyl)glutathione	50	10	2	25	35	6	25

‡Values are ID_{50}s (μM), i.e. the concentration of inhibitor giving 50% inhibition of enzyme activity at pH 6.5, 30 °C, with 1 mM CDNB and 1 mM GSH as substrates. From reference 179.

Distinctive properties of isoenzyme 4-4 are its catalytic efficiency and stereoselectivity toward arene oxide substrates [59,71]. The characteristic substrate for GST 4-4 is *trans*-4-phenyl-3-buten-2-one [188], and the isoenzyme is most strongly inhibited by BSP [325]. Transferase 4-4 has been shown [64] to be the only GST isoenzyme strongly inhibited by indomethacin, a finding which is useful for its identification. Treatment with inducing agents decreases the relative concentration of isoenzyme 4-4 in hepatic cytosol [78].

Like isoenzyme 1-2, GST 3-4 has properties intermediate between the homodimeric isoenzymes related to it (3-3 and 4-4). A combination of substrates and inhibitors must therefore be used to characterise the isoenzyme (see Tables 1.3 and 1.4).

Transferase 5-5 can be best identified with 1,2-epoxy-3-(*p*-nitrophenoxy)-propane, although iodomethane is also a good substrate [107]. A low specific activity with CDNB is also characteristic.

The specific activity of GST 6-6, the major isoenzyme in rat testis, is characteristically higher with CDNB than any other rat transferase characterised [95,97]. The strongest inhibitor known for this isoenzyme is Cibacron Blue [179]. The isoelectric point of transferase 6-6 (pH 5.8) is considerably lower than those of the isoenzymes containing subunits 1 to 5 (see Table 1.2). Inducing agents do not elevate the levels of this isoenzyme in rat testis [179].

The most characteristic property of isoenzyme 7-7 (pI 8.7) is its low apparent subunit M_r (24 000) compared with the transferases isolated from rat liver cytosol, as well as its relatively high activity with ethacrynic acid [98].

GST 8-8 (pI 6.0; apparent subunit M_r 24 500) has been shown to be the most active of several GST isoenzymes towards 4-hydroxynon-2-enals, major products of the peroxidative degradation of polyunsaturated fatty acids [144], although GST 4-4 is also highly efficient in the detoxification of these compounds [8].

1.1.1.2 **Microsomal Glutathione S-Transferases**

A membrane-bound GST isoenzyme that differs from the soluble forms of the enzyme is found in several rodent species and has also been identified in human liver [67]. Microsomal GST constitutes 3% and 5% of the total protein in the rat liver endoplasmic reticulum and outer mitochondrial membrane, respectively [199,203]. The subunit molecular weight of microsomal GST is 17 000, compared with 25 000 for the subunits of the cytosolic isoenzymes [42]. The amino acid sequence of rat liver microsomal GST lacks obvious homology with any of the characterised cytosolic enzymes [200], and antibodies directed against GSTs 1-1, 1-2, 3-3 and 3-4 do not react with the purified microsomal GST [202]. Microsomal GST has been found to be activated 15-fold by treatment with *N*-ethylmaleimide, and to a lesser extent by other sulphydryl agents, whereas the cytosolic isoenzymes are not similarly activated [198,199,204]. In its purified form, microsomal GST is dependent on detergent for activity and in a protein/Triton X-100 micelle is thought to exist as a trimeric protein [200]. Radiation inactivation studies have demonstrated that the isoenzyme also exists as a trimeric protein in the microsomal membrane, and is dependent on the integrity of all three subunits for catalytic activity [42].

The specific activity of purified rat liver microsomal GST comprises only 10% of that of the cytosolic GSTs [39], although in some species the microsomal activity is greater and may be important in the metabolism of electrophiles produced within the microsomal membrane by lipid peroxidation [198,199].

1.1.2 Human Glutathione S-Transferases

The human cytosolic GSTs are currently denoted by Greek letters (Table 1.5) and can be differentiated into three distinct classes of dimeric isoenzymes, on the basis of an analysis of their structural and kinetic properties. These are referred to as the basic, near-neutral and acidic classes [187]. There has been no evidence to date of major functional differences between the isoenzymes within each class [179]. Some of the physical properties of the human GST isoenzymes are shown in Table 1.5, and their substrate specificities and inhibition characteristics are shown in Tables 1.6 and 1.7, respectively.

The human GSTs are thought to be the products of at least three distinct autosomal gene loci, designated as GST1, GST2 and GST3 [266]. On the basis of their electrophoretic mobility, these gene loci are thought to correspond to the near-neutral, basic and acidic GST isoenzyme types, respectively [20]. Genetic polymorphism has been suggested for some or all of the three loci [125,267]. A minimum of four genes has been proposed by Singh *et al.* [264], each gene resulting in an immunologically and functionally distinct subunit. The human GST isoenzymes are thought to arise from different homo- and heterodimeric combinations of three of these subunits. These subunits are designated A-type (M_r 26 500), B-type (M_r 24 500) and C-type (M_r 22 500) [20,264].

Table 1.5 : **Nomenclature and Physical Characteristics of Major Human GSH S-Transferases**

Isoenzyme	pI	Subunit M_r* ($\times 10^3$)
α	7.8	25
β	8.25	25
γ	8.55	25
δ	8.75	24.5,26
ϵ	8.8	24.5,26
μ	6.0-6.5	26.3
ψ	5.4	26.5
ω	4.6	22.5,24.5
π	4.8	22.5,23
ρ	4.7	24

*M_r based on SDS-PAGE
Table adapted from 179, 39, 137.

Table 1.6 : **Substrate Specificities of Major Human GSH S-Transferases**

Substrate	Specific Activity (μmol/min/mg) GST isoenzymes		
	Basic (α-ϵ)	Near-Neutral (μ)	Acidic (π)
1-Chloro-2,4-dinitrobenzene	64	187	105
1,2-Dichloro-4-nitrobenzene	0.035-0.065	0.032	0.11
Bromosulphophthalein	0.001-0.01	<0.002	<0.002
Ethacrynic acid	0.017-0.044	0.081	0.86
trans-4-Phenyl-3-buten-2-one	0.001-0.002	0.36	0.01
1,2-Epoxy-3-(*p*-nitrophenoxy)propane	0	0.11	0.37
Styrene-7,8-oxide	0.02	2.6	0.07
Benzo(a)pyrene-4,5-oxide	0.047	0.92	0.13
Cumene hydroperoxide	10.6	0.63	0.03
Δ^5-Androstene-3,17-dione	8	0.12	0.01
p-Nitrophenyl acetate	0.18	0.22	0.19

From reference 179.

Table 1.7 : **Inhibition Characteristics of Major Human GSH S-Transferases**

Inhibitor	ID_{50} (μM) GST isoenzymes		
	Basic (α-ϵ)	Near-Neutral (μ)	Acidic (π)
Cibacron blue	5	0.05	0.5
Gossypol acetic acid	50	2	>100
Tributyltin acetate	0.01	0.5	4
Triethyltin bromide	10	5	6
Triphenyltin chloride	0.25	0.5	>10
Bromosulphophthalein	75	2	100
Haematin	0.5	1	5
S-Hexylglutathione	3	10	20
S-(*p*-Bromobenzyl)glutathione	4	1	4

Values are ID_{50}s (μM), i.e. the concentration of inhibitor giving 50% inhibition of enzyme activity at pH 6.5, 30°C, with 1 mM CDNB and 1 mM GSH as substrates. From reference 179.

In human liver there are five isoenzymes with basic isoelectric points (pI 7.8-8.9), called α, β, γ, δ and ε [145]. These GST isoenzymes are homo- and heterodimers of A- and B-type subunits, with M_r values between 24 500 and 26 500 [65,119,264]. The basic isoenzymes are characterised by high GSH peroxidase activity toward organic peroxides [17], and are strongly inhibited by tributyltin acetate [179].

A near-neutral (pI 6.6) isoenzyme (transferase μ), which has high specific activity towards epoxides and a high affinity for the non-substrate ligand haematin [119], is not found in the liver of all humans but, when present, constitutes 15-20% of the total GST activity [316,317]. The near-neutral GST μ is a homodimer of M_r-26 300 subunits and is immunochemically distinct from the cationic isoenzymes [275,315].

The characteristic substrate for the human acidic transferases is ethacrynic acid, and these isoenzymes are best inhibited by Cibacron Blue [179]. Human liver possesses two such anionic transferases, ω and ψ (with pI values of 4.6 and 5.4, respectively) [17,179,266]. Transferase ω is a heterodimer of B-type and C-type subunits [65], while GST ψ is composed of M_r-26 500 subunits, designated A′-type as they are immunochemically distinct from the A-type subunits [264]. It has recently been shown that the anionic GST ψ of human liver is more closely related in structure to the near-neutral (GST μ) than to the acidic isoenzymes [266].

In human liver the five basic isoenzymes α-ε comprise 90% of hepatic GST activity. The remainder of this activity is distributed between the near-neutral GST, which is only expressed in 60% of individuals, and two acidic transferases, ω and ψ [266]. The extrahepatic human organs contain primarily acidic transferases.

The predominant GST of human placenta, isoenzyme π, is an acidic (pI 4.8) homodimer of C-type subunits (M_r 22 500) [66,100,102,119,275]. With respect to physical, catalytic and immunochemical properties, it is distinct from the major, basic human liver isoenzymes, but closely related or identical to the human erythrocyte GST isoenzyme ρ [100,190,305].

Transferase π is found in high concentration in human placenta [186] and might be expected to play a major role in the protection of the developing foetus from the toxic effects of circulating electrophilic substances [232]. However, only one transferase isoenzyme has been found in the placenta [94,228,231] and this appears

to possess narrow substrate specificity, so it would seem that the placental GST provides less protection to the tissue than the liver isoenzymes [16]. Most drugs administered to pregnant women have been found in measurable quantities in the foetal circulation, so the putative role of the placenta as a 'surrogate liver' of the foetus or a 'barrier' against xenobiotic passage is uncertain [74,216]. Conceivably, for some drugs the low drug metabolising activity of the placenta may be sufficient for decisive effects on foetotoxicity [216]. Placental GST activity was reportedly not altered following exposure of pregnant women to cigarette smoke [174,216] nor was it affected by several inducing agents [163].

An acidic GST isoenzyme with properties similar to those of the placental/ erythrocytic form has also been found in human lung [160], breast [73], thyroid [69], lens and kidney [39] as well as in all foetal organs studied [72,102]. The acidic forms of rat liver have also been reported to be immunochemically similar to the erythrocyte/placental enzymes [66].

Isoenzymes representing all three major classes of transferases have been found in human lung [20] and kidney [267], although the patterns of isoenzyme expression differ. The kidney has also been found to possess at least two isoenzymes which have not previously been characterised [267]. Five GST isoenzymes have been isolated from human uterus, including one which may be specific to that organ [72]. Four GSTs, comprised of subunits representing each of the three major transferase classes, have been reported in human prostatic tissue [290]. A new basic transferase (pI 9.9; apparent subunit M_r 26 500) has been found in human skin [68], which also contains two other isoenzymes that are related to the established acidic and basic transferases of human liver. As well as the anionic transferase ρ, human erythrocytes have a cationic (pI > 10) isoenzyme designated GST σ [261].

The ontogeny of the human GST isoenzymes in lung [89], liver, adrenal, kidney and spleen [83] has been investigated. Studies on the development of GST isoenzymes show that, at least after the first trimester, no foetal-specific isoenzymes are present [83,102,217]. A major component of human foetal liver is isoenzyme π, but a basic transferase of the α-ϵ class found in the adult liver is also present [39].

A GST of the Pi class (see Section 1.1.4) has been found to be overexpressed in certain human cancer cells, and this enzyme may therefore have potential as a marker for preneoplastic cells and neoplastic tissues [24,185,246,248,255,297]. Although the properties of this isoenzyme were indistinguishable from transferase π, variant forms within the Pi class may exist [185]. The increased concentrations of GST Pi may also contribute to the characteristic resistance of malignant tissues to cytostatic drugs [24,185,240].

1.1.3 Glutathione S-Transferases of Other Species

Table 1.1 shows the variety of species and tissues from which GSTs have been isolated. With the exception of the microsomal enzyme which is trimeric *in situ* (see Section 1.1.1.2) and a monomeric isoenzyme isolated from the protozoan, *Tetrahymena thermophila* [213], all GSTs discovered so far have been found to be composed of two subunits [137].

Hoesch and Boyer [119] have demonstrated that the hepatic cytosol of rhesus monkeys contains a number of GST isoenzymes that are very similar to those of human liver.

Four isoenzymes have been isolated from the liver of the DBA/2J strain of mouse, and have been named F1, F2, F3 and F4, on the basis of their increasing isoelectric points [169]. Three homodimeric isoenzymes were isolated from the NMRI strain of mouse [319] and named MI, MII and MIII, on the basis of their respective subunit compositions. Forms F1 and F2 seem similar to MII and F3 is apparently analogous to transferase MIII [319]. A new nomenclature for the GST isoenzymes of mouse tissues which signifies the strain of mouse as well as the subunit composition has been proposed [319].

Although few isoenzymes seem to be expressed in insects [149], fish possess a number of acidic, basic and near-neutral GST isoenzymes. Transferases from fish and molluscs have been extensively studied because levels of enzyme induction, caused by environmental pollutants, provide a useful index of marine and freshwater pollution levels [35,39]. The GST forms of insects and crops are of interest from the perspective of resistance to herbicides and insecticides, and those in microorganisms are studied to gain insight into resistance to antimicrobial drugs [39,117,161].

1.1.4 Species-Independent Classification of Isoenzymes

Mannervik [182] has proposed a species-independent classification of the cytosolic GST isoenzymes into three groups, namely Alpha, Mu and Pi (shown in Figure 1.2). This proposal was based on the pattern recognition analysis of data on the substrate specificities, sensitivities to inhibitors, immunochemical cross-reactivity and amino-terminal amino acid sequences of the cytosolic GST isoenzymes of rat, mouse and man. Rat liver microsomal GST is clearly distinct from the cytosolic isoenzymes [202] and is therefore thought to belong to an additional GST class [182].

Figure 1.2 : **Inter-Species Classification of GSH S-Transferases**

Classified by pattern recognition analysis according to amino-terminal amino acid sequences, substrate specificities, sensitivities to inhibitors and immunological cross-reactivity. From reference 182.

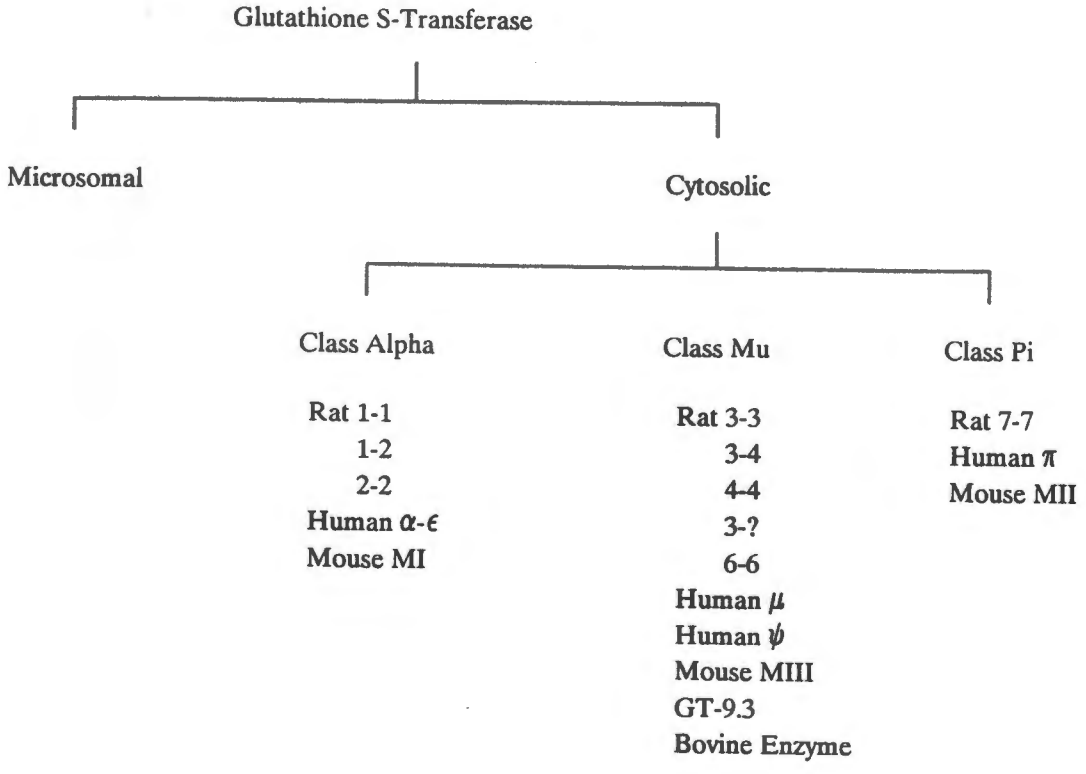

Characteristic substrate specificities and inhibitor sensitivities of the three classes are shown in Table 1.8. Class Alpha isoenzymes exhibit high non-selenium GSH peroxidase activity, class Mu shows high activity with epoxides, and the members of class Pi are characterised by comparatively high activity with ethacrynic acid [182]. Class Pi has the notable characteristic of high stereoselectivity for the proximate carcinogen derived from benzo(a)pyrene, the 'bay-region' diol epoxide (+)-anti-7,8-dihydrodiol-9,10-epoxide [181]. The characteristic inhibitor sensitivities of class Alpha isoenzymes are a low IC_{50} value for haematin and a high value for Cibacron blue, while both groups Mu and Pi show the converse. Class Mu can be distinguished from class Pi by its low IC_{50} values for triphenyltin chloride.

Table 1.8 : **Class-Discriminating Substrate Specificities and Inhibitor Sensitivities of GSH S-Transferases**

	Transferase Class		
	Alpha	**Mu**	**Pi**
Specific Activity with Substrate (μmol/min/mg)			
Ethacrynic acid	0.01-1.2	0.08-0.6	**0.9-4**
Bromosulphophthalein	<0.01	**0.002-0.9**	<0.01
trans-4-Phenyl-3-buten-2-one	<0.01	**0.04-1.2**	0.01-0.02
Cumene hydroperoxide	**3-12**	0.1-0.7	0.03-0.14
Δ^5-Androstene-3,17-dione	**0.04-8**	0.002-0.1	0.01-0.17
ID_{50} values with Inhibitor (μM)			
Cibacron blue	0.6-20	**0.05-0.7**	0.1-0.5
Triphenyltin chloride	0.3-30	**0.04-0.5**	>10
Bromosulphophthalein	**2-200**	0.5-10	20-100
Haematin	**0.05-2**	1-2	4-5
Isoelectric Point (pI)	Alkaline (>8.0)	Neutral (7-8)	Acidic (<7.0)

Characteristically high specific activities and low ID_{50} values are given in bold type. Members of class Alpha or Mu have high activity with at least one of the two substrates indicated. Members of class Pi are distinguished from those of classes Alpha and Mu by low sensitivity to both triphenyltin chloride and haematin. No characteristic inhibitor for class Pi has yet been identified. Adapted from reference 179.

There may however be large differences in the substrate and inhibitor specificities of isoenzymes within the same class [64]. In addition, most isoenzymes have measurable specific activities or inhibitor sensitivities with the substrates/ inhibitors listed in Table 1.8, and considerable overlap in the given ranges is observable between some of the GST classes.

For the three mammalian species studied, immunochemical cross-reactivity was shown among GSTs within each class, but none was observed between isoenzymes in different classes [182,299].

All of the enzymes of class Mu and Pi that have been characterised have an unblocked N-terminus; the isoenzymes within a class have 70-80% amino acid sequence homology, whereas enzymes from different classes have an homology of only 20-30% [68,181,224,236]. A 95% conservation of amino acid sequence has been demonstrated in rat and human microsomal GSTs [67]. Del Boccio *et al.* [68] have also shown a striking relationship between the primary structures of a previously unknown basic transferase isoenzyme from human skin and rat isoenzyme 2-2, both of the Alpha class. Even GST isoenzymes isolated from parasitic schistosomes possessed regions with high homology to isoenzymes of one or other of the vertebrate multigene families [271,287]. This level of conservation of structure between enzymes isolated from different species supports the proposed species-independent classification [182,299].

1.1.5 **Primary Protein Structure and Evolution**

The primary protein structure and evolution of the many isoforms of GST have been described in several recent papers [19,39,83,125,151,179,180,222,286]. It was originally unclear whether or not the GST subunits were the products of a single gene [31]. Scully and Mantle [251] suggested that subunits 1, 2 and 3 arose from the proteolytic cleavage of such a single gene product. Later studies showing differential induction of the subunits and immunochemical dissimilarities among them suggested that these subunits may rather have had separate origins [18,40,269]. The concept that subunits 1, 2 and 3 are the products of separate genes has been further substantiated by numerous reports of heterogeneity within these subunit types [40,88,223,269,298].

The primary structures of several subunits have been determined from a combination of chemical sequencing and analysis of coding sequences from cDNA

clones [76,223,298]. Six of the subunits named to date have been assigned to three multigenic families (the 1/2, 3/4/6, and 7 gene families) and two (5 and 8) have yet to be characterised [25,179,225,286]. A minimum of four GST gene families in the rat has been recently proposed, on the basis of the nucleotide and amino acid sequence analysis of cDNA clones and purified proteins [288].

A high degree of conservation of amino acid sequences is apparent along the full length of subunits of the 3/4/6 family [241], while subunits of the 1/2 family exhibit varying degrees of conservation, but possess two regions of high homology [289]. All the subunits of rat GSTs show three regions of conserved structure, possibly reflecting a common purpose such as the binding of GSH [165,236]. Shared conserved regions of amino acid sequence have also been observed between transferases of different species [179,196] (see Section 1.1.4), further indicating that these regions are important to the structure-function relationship of the transferases [286].

Kinetic and binding data have indirectly inferred certain structural features of the GSTs, and X-ray diffraction investigations with crystallised enzymes are likely to yield more structural information (preliminary studies have been performed with isoenzyme 3-3) [254].

1.2 PURIFICATION AND PHYSICAL CHARACTERISATION

The relative abundance of GST activity in mammalian liver and the fact that some transferases are among the most alkaline of hepatic cytosolic proteins facilitates their purification [39]. The method used depends greatly upon the source from which the enzyme is obtained, and many purification procedures have been reported in the literature (see Table 1.1 for examples). The different techniques utilised for the purification of GST isoenzymes are described in outline only here, while specific details of the purification methods used in this investigation are found in Section 2.4.

In one of the earlier purification methods [107], the rat liver cytosolic fraction was passed through a DEAE-cellulose column, which retained 80% of the cytosolic proteins, but allowed 90% of the GST activity to pass through unbound in the eluent. The GST isoenzymes were subsequently separated by CM-cellulose and hydroxylapatite chromatography [12,107]. The disadvantages of these methods were the many chromatographic steps, irreproducibilities arising from the variability in the properties of hydroxylapatite, and lack of isoenzyme resolution on CM-cellulose [39].

Boyer *et al.* [40] combined some of the features of previous methods with GSH affinity chromatography. The introduction of this step eliminated non-GSH-specific proteins and improved the subsequent purification on CM-cellulose. Several types of affinity columns have been used for GST isolation. Earlier affinity columns employed organic ligands such as BSP [92,322] and cholic acid [218], known to bind to the transferases. However the very tight binding of some transferases to BSP has caused problems in their elution from matrices linked to BSP, and columns utilizing cholic acid as a ligand do not bind subunits 1 and 2 [179]. The most commonly used affinity columns are those with matrices consisting of epoxy-activated agarose derivatives coupled to either GSH or to *S*-alkyl derivatives of GSH, the latter method being based on the high affinity of these compounds for GSTs [39,126].

With the GSH-affinity column [257], GSH is usually covalently linked through the thiol group to epoxy-activated sepharose, although coupling may also occur through the α-amino group of GSH under certain conditions. Transferases are eluted from these columns with high concentrations of GSH. A second method employs *S*-hexylglutathione coupled through the N-terminal α-amino group to

activated sepharose, and elution with low concentrations of *S*-hexylglutathione [100]. Because this compound is a strong inhibitor of the GSTs, it must be removed before use of the enzyme [39]. It has been found that transferase 5-5 does not bind to *S*-hexylglutathione affinity columns, and transferase 1-1 binds more weakly than most other isoenzymes [179].

Isoelectric focusing has also been used to separate GST isoenzymes [12], but this technique is slow and has limited capacity [179]. The introduction of HPLC [231,260] and FPLC (fast protein liquid chromatofocusing) [9] techniques has improved the resolution of GST isoenzymes and shortened separation times considerably. Rapid separation times are considered essential to minimise loss of GST activity and the formation of oxidation or degradation products of the GSTs which can be erroneously interpreted as new isoenzymes [179]. A reverse-phase HPLC method has been proposed for quantifying the GST subunit content of a given tissue [211].

Techniques used to characterise and confirm the homogeneity of the GST isoenzymes include SDS polyacrylamide gels, electrofocusing, chromatofocusing, and immunological procedures (detailed by Boyer [39]). As has been described previously (see Section 1.1.1.1), a variety of substrates and inhibitors may be used to facilitate the identification of different forms of GST [182].

1.2.1 **Assay Systems**

The most convenient and sensitive assay for the GSTs is the spectrophotometric monitoring of the conjugation of GSH with the universal substrate, CDNB (see Section 1.1.1). It has been noted that some isoenzymes exhibit low specific activity toward CDNB, and therefore its exclusive use as a screen for GST activity may impede detection of some isoforms [55]. A number of other useful spectrophotometric methods have been developed [104,107,137]; the most frequently used are summarised in Table 1.9. Details of assays used in this investigation are described in Section 2.2.

Titrimetric methods have been developed for measuring the GST-catalysed metabolism of iodomethane, and radioactive substrates are used for assays of reactions with arene oxides, trisubstituted phosphates and disulphides [137].

Table 1.9 : **Conditions for Spectrophotometric Assays for GSH S-Transferases**

Substrate	[Substrate] mM	[GSH] mM	pH	Wavelength nm	$\Delta\epsilon$ $mM^{-1}cm^{-1}$
1,2-Dichloro-4-nitrobenzene	1.0	5.0	7.5	345	8.5
1-Chloro-2,4-dinitrobenzene	1.0	1.0	6.5	340	9.6
4-Nitropyridine-*N*-oxide	0.2	5.0	7.0	295	7.0
p-Nitrophenethyl bromide	0.1	5.0	6.5	310	1.2
p-Nitrobenzyl chloride	1.0	5.0	6.5	310	1.9
1,2-Epoxy-3-(*p*-nitrophenoxy)propane	5.0	5.0	6.5	360	0.5
1,2-Naphthalene oxide	0.1	5.0	8.5	260	8.1
Bromosulphophthalein	0.03	5.0	7.5	330	4.5
1-Menaphthyl sulphate	0.5	5.0	7.5	298	2.5
trans-4-Phenyl-3-buten-2-one	0.05	0.25	6.5	290	-24.8
Ethacrynic acid	0.2	0.25	6.5	270	5.0
Δ^5-Androstene-3,17-dione	0.068	0.1	8.5	248	16.3

All assays performed in 0.1 M potassium phosphate (25°C). Table adapted from reference 107.

1.3 SUBSTRATES AND BIOLOGICAL FUNCTION

The GSTs are thought to play a central part in the biotransformation and detoxification of a wide range of drugs and xenobiotics. In these reactions, the transferases catalyse the nucleophilic attack by the electrons of the sulphur atom of reduced glutathione on an electrophilic centre of an acceptor substrate such as CDNB:

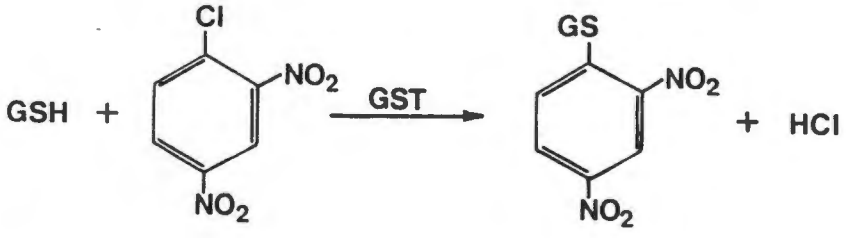

This electrophilic centre may be a carbon, sulphur or nitrogen atom, but the basic chemical mechanism remains as shown below, where the GSH attacks the Cl-bonded carbon atom:

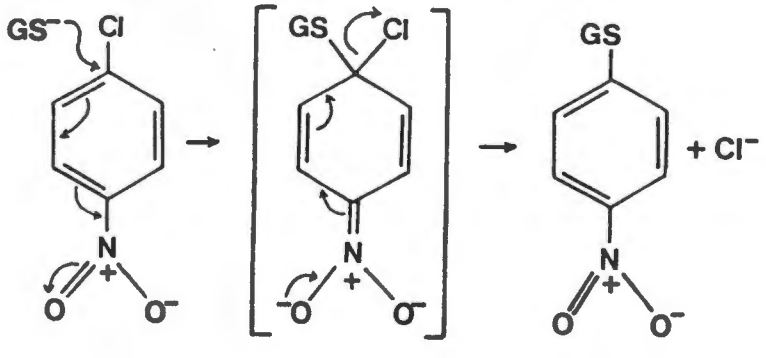

The transferases are thought to catalyse this reaction by bringing the substrates into close juxtaposition, thereby increasing their effective local concentrations, and by enhancing the nucleophilicity of the sulphydryl group of GSH, thereby causing it to react more readily with an electrophile bound at the hydrophobic site [39,249]. The nucleophilic reactivity mentioned above may be enhanced by the ability of the protein to lower the effective pK_a of the sulphydryl group of GSH [54].

The GSH conjugate formed may be excreted from the cell as such or hydrolysed by peptidases to an *S*-(substituted)-cysteine derivative, which may subsequently be N-acetylated in a CoA-linked reaction to yield a mercapturic acid, a classical excretion product of many xenobiotics (see Figure 1.3) [179]. Alternatively, the unacetylated cysteine derivative may be cleaved at the C-S bond with the elimination of pyruvate and NH_3, and the conversion of the *S*-substituent to a mercaptan. The resulting thiol group can be either glucuronidated with uridinediphosphoglucuronate to a thioglucuronide or methylated with *S*-adenosyl-methionine to a methylthio conjugate. The latter product may be sequentially oxidised to a methylsulphinyl and a methylsulphonyl derivative.

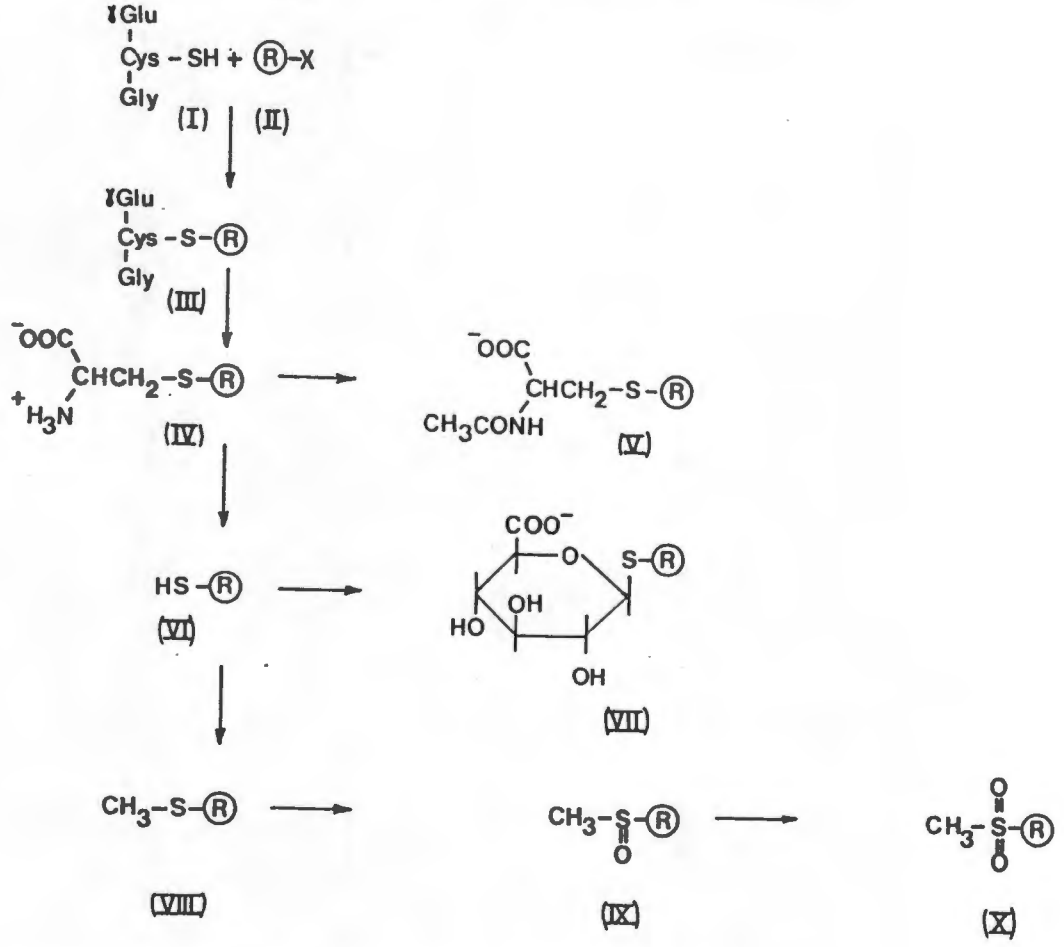

Figure 1.3 : **The Mercapturic Acid Pathway**

Flow scheme of possible biotransformation of an electrophilic species after conjugation with GSH (I). The reactive electrophile (II) forms a stable conjugate (III) with GSH. The conjugate is degraded in two steps to a cysteine conjugate (IV), which on acetylation with acetylcoenzyme-A is converted to a mercapturate (V). Alternatively, the cysteine conjugate may be cleaved to a mercaptan (VI) by elimination of pyruvate and ammonia. The resulting thiol group can either be glucuronidated with uridinediphosphoglucuronate to a thioglucuronide (VII) or methylated with S-adenosylmethionine to a methylthio conjugate (VIII). The latter compound may be oxidised sequentially to a methylsulphinyl (IX) and a methylsulphonyl derivative (X). The reactions do not have to take place in the same cell or organ. Some reactions are probably catalysed by enzymes in the intestinal microbial flora. Compounds V, VIII-X are major excretion products resulting from the initial conjugation with GSH. From reference 179.

As well as their role in the detoxification of xenobiotics, the transferases appear to catalyse the conjugation of GSH with a number of endogenous substrates; these are thought to include steroids, prostaglandins, leukotrienes, and organic hydroperoxides (including lipid hydroperoxides and products of lipid peroxidation) [183].

Both endogenous compounds and xenobiotics may form epoxides, which may undergo conjugation with GSH [52];

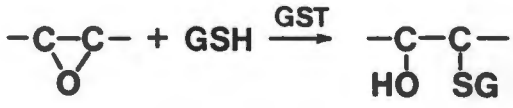

although the GST isoenzymes vary in their specific activities with any particular epoxide. This reaction may have considerable toxicological significance since a proportion of human subjects lack the isoenzyme (transferase μ) which has the highest specific activity with the mutagenic arene oxides such as benzo(a)pyrene-4,5-oxide [315,316].

An important physiological function of transferases which contain subunits 1, 2, 5 or 7 is thought to be their GSH peroxidase activity towards organic peroxides [97]. This peroxidase activity is distinct from that of the selenium-linked GSH peroxidase found in many tissues, and can be distinguished from the latter by the inability of the GSTs to catalyse the reduction of hydrogen peroxide [230]. In the equations below the initial reaction is catalysed by the transferases, and the second proceeds non-enzymatically, resulting in the formation of oxidised glutathione (GSSG) [147];

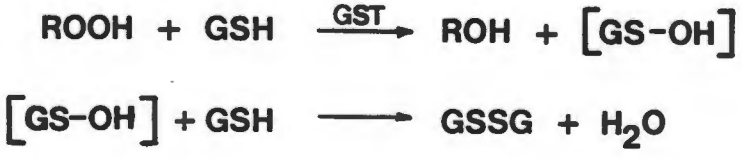

Products of lipid peroxidation, such as cholesterol α-oxide [193] and activated alkenes, for example the hydroxyalkenals [8], are substrates for those GSTs which exhibit peroxidase activity;

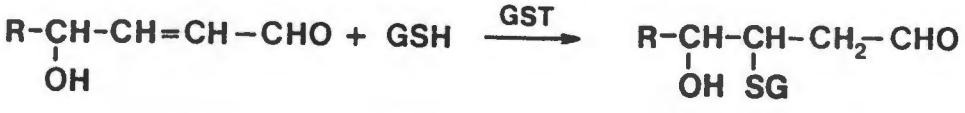

The primary GSH adduct shown above can be subsequently transformed to a cyclic hemimercaptal derivative [180]. An important biological function of the GSTs may therefore be the protection of membranes from damage by the process of lipid peroxidation [152,201,285].

Subunit 1 of the transferases catalyses the GSH-dependent isomerisation about certain double bonds. An example is the conversion of Δ^5-androstene-3,17-dione to Δ^4-androstene-3,17-dione, shown below;

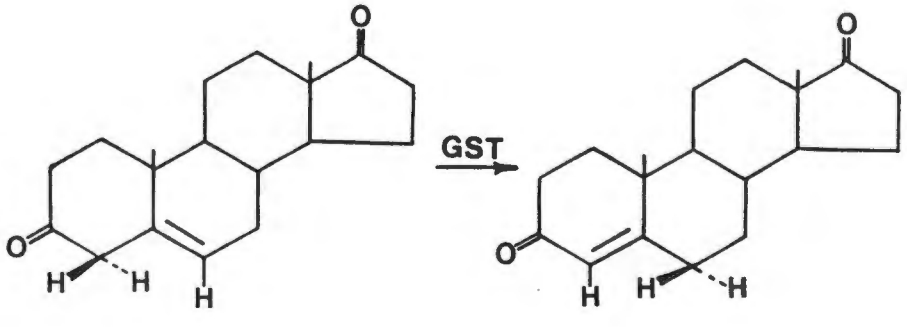

While GSH is not consumed in this reaction, it is thought that an intermediate GSH-adduct exists, which splits to yield GSH and the thermodynamically stable steroid isomer [148].

Some prostaglandins have been shown to be substrates for the GSTs [47,179], and some GST isoenzymes (particularly those belonging to class Mu) are also capable of catalysing the conversion of the epoxide derivative of arachidonic acid, leukotriene A_4 to leukotriene C_4 [189,273,274];

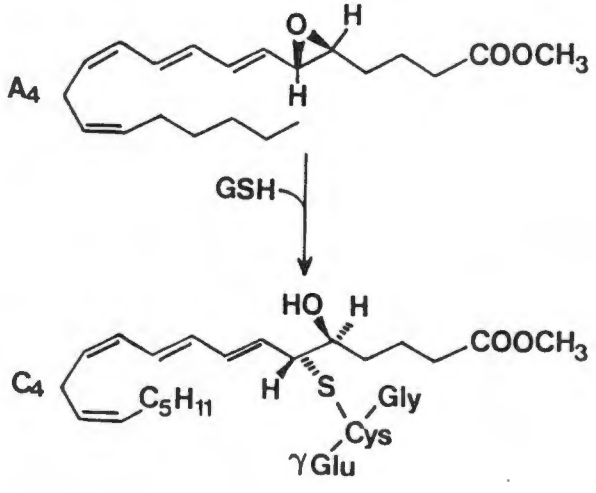

The enzyme was therefore thought to play a role in the biosynthesis of leukotrienes, which are directly responsible for *in vivo* inflammatory effects. However, Söderström *et al.* [273] have shown using mouse mastocytoma cells that the activity of microsomal and cytosolic GSTs towards leukotriene A_4 is too low to account for *in vivo* leukotriene C_4 formation [273]. Instead, a distinct membrane-bound enzyme, leukotriene C synthase, has been found to be primarily responsible for leukotriene C_4 biosynthesis.

Although the GSTs are normally considered to be enzymes of detoxification, they appear to have a role in the bioactivation of certain precarcinogens, principally the vicinal dihaloethanes, such as ethylene dibromide (EDB). Widely used as a grain fumigant, industrial solvent and anti-knock petroleum additive, EDB has been shown to be both mutagenic and carcinogenic [233,324]. Considerable concern has been expressed over EDB residues in foodstuffs as well as over occupational exposure to the chemical.

The compound is converted in a GST-catalysed reaction to a GSH adduct that irreversibly binds to DNA [214,303]. A general scheme for the proposed formation of reactive intermediates from the reaction of EDB (and other dihaloalkanes) with GSH is shown below. GST-catalysed conjugation of EDB with GSH gives rise to half-sulphur mustard compounds with the subsequent production of reactive episulphonium ions [303]. There is evidence that the major DNA adduct formed in rat liver is *S*-[2-(N^7-guanyl)ethyl]glutathione [158].

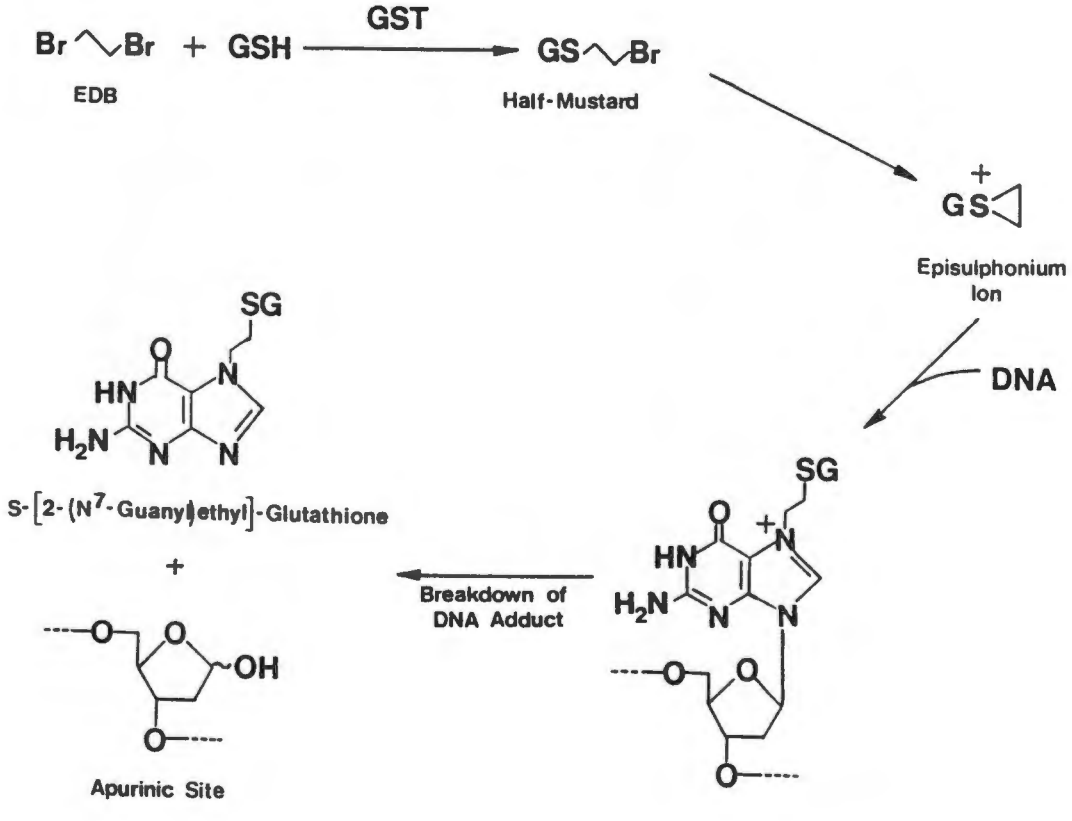

Androgen-repressed DNA-binding proteins which are present at interchromatinic regions of the cell nucleus have been identified as GST subunits 3 and 4 [27,51]. The possibility exists that some GSTs (themselves under negative regulation by androgens) may exert control over organ growth through modulation of nuclear events related to the production, processing, or transport of RNA [51].

1.4 KINETICS AND CATALYTIC MECHANISM

1.4.1 Catalytic Site

The specificity of the GSTs for GSH as the thiol substrate is extremely high. In addition to GSH, the only substrates capable of binding to the GSH site of the transferases are a small number of GSH-analogues such as homoglutathione (in which β-alanine replaces glycine) and γ-glutamylcysteine [53,54,107,145,276]. Several other thiols small enough to fit into the active-site do not have catalytic activity [105,107,145,147,326], although Principato *et al.* [229] have shown that one of these thiols, 2-mercaptoethanol, can serve as a substrate in the presence of a non-substrate GSH analogue, *S*-methylglutathione. In view of this, it has been suggested that the peptide portion of GSH induces a conformational change in the protein to an active state in which catalysis may occur [229]. GSH would therefore have two functions - to induce a catalytically active protein conformation and provide the thiol group for the reaction [229]. Such conformational changes, induced by GSH or by other substances, have been proposed as an explanation for the non-hyperbolic steady-state kinetics of the transferases (see Section 1.4.2) [179,229].

The active-site of the transferases is thought to have reasonably wide space available in the vicinity of the sulphur atom of the bound GSH, due to the similarity in binding properties of the GSH and *S*-alkylglutathione affinity matrices [179]. The three charged groups of the GSH molecule are thought to bind to oppositely charged amino acid side chains at the binding site for GSH (known as the G site) on the enzyme [179]. It has been shown using inhibitors and protective agents that several different functional groups are required for catalytic activity. These may include the thiol, amino and guanidino groups of the protein, although partial modification of the protein thiols is possible without loss of catalytic activity [49,179]. Awasthi *et al.* [15], working with human GST isoenzyme ψ, have shown that a functional histidine residue at or near the GSH binding site is essential for catalytic activity. Hydrogen bonds are probably also formed between the two peptide bonds of GSH and suitable groups in the protein [179].

In contrast to the very strict requirements for binding to the GSH site, the adjacent acceptor substrate binding site of the transferases appears to be much less specific. A large variety of substrates, ranging in size and shape from iodomethane to

steroids and polycyclic hydrocarbons, bind to the active-site. The acceptor substrate binding site may be expected to be hydrophobic in nature [137], since a prerequisite for substrate binding to the site appears to be the possession of a hydrophobic region [148].

While compounds such as maleic acid, L-cystine and *N-N*-diacetyl-L-cystine were not substrates for the transferases, uncharged analogues of these same compounds (maleylacetone, L-cystine dimethyl ester and *N-N*-diacetyl-L-cystine dimethyl ester) were substrates [148]. The hydrophobic nature of the analogues apparently enhanced their ability to act as substrates [39]. A series of *S*-(n-alkyl)-glutathione derivatives with substituents of varying chain length have been used to probe the acceptor binding site on transferases 3-3 and 3-4 [12]. The inhibitory potency of these compounds increased with substituent chain length, providing further evidence of the hydrophobic nature of the acceptor binding site, named the H-site [179]. In addition, the binding of bilirubin to GST 1-2 is associated with the quenching of intrinsic tryptophan fluorescence, and the only tryptophan residue in the polypeptide is situated in the H-site [223].

The H-site of the transferases shows varying degrees of stereoselectivity, depending upon the isoenzyme and substrate. It is thought that although the H-site is capable of accommodating a wide variety of chemical moieties, the scissile bond of the electrophilic substrate may have strict stereochemical requirements with respect to binding to the sulphur atom of GSH and to the catalytic groups of the enzyme [179].

Varying degrees of enantioselectivity have been demonstrated for purified transferase isoenzymes 1-1, 3-3, 3-4 and 1-2 using chiral substrates [175,176]. In the conjugation of GSH and arene oxide substrates, isoenzymes 3-3 and 4-4 from rat liver showed a pronounced preference for the stereocentre of R-absolute configuration on the electrophilic substrate [54,59,71,80]. Cobb *et al.* [59] found that transferase 3-4 showed more stereoselectivity with phenanthrene 9,10-oxide than did transferases 3-3 and 1-2.

Further evidence for the importance of stereospecificity comes from the finding that transferase 3-3 is able to metabolise BSP, while transferases containing subunit 4 are not (and are in fact inhibited by the compound) [179,325]. However, the binding stoichiometry and affinity for BSP are not significantly different for subunits 3 and 4. Therefore the topological orientation of BSP when bound to

subunit 4 seems to be inadequate for catalysis.

Although most studies have been on the rat transferases, investigations with the human GST isoenzymes have also shown qualitative variations in their degree of stereospecificity [179,238]. The near-neutral transferase μ shows high preference for (-)4R,5S benzo(a)pyrene 4,5-oxide, yielding a 4S,5S GSH conjugate. The basic transferases have a similar, but less pronounced, preference, whereas the transferase π primarily yields the two 4R,5R GSH conjugates. Human GST μ is highly stereoselective for reaction of GSH with (*R*)-configured oxirane carbon atom of the polycyclic arene oxides studied [80]. However, high preference for GSH reaction with (*S*)-configured oxirane carbon occurs with human placental GST π [80] (as well as with rat kidney and spleen cytosol [79]).

The functional properties of different GST isoenzymes appear to reflect the structure of their respective active-site regions [62]. It has been suggested that GST isoenzymes from different species may therefore have appreciable differences in the topography of their active-sites, and that stereoselectivity with epoxide substrates might complement existing methods for the functional characterisation of different isoforms of GST [81]. It has been found, for rat [34] and elasmobranch [87] transferases at least, that the stereospecifity of the isoenzymes towards polycyclic arene oxides may be predicted from their subunit compositions and is not dependent on subunit-subunit interactions.

Figure 1.4 shows two alternative models for the localization of the two active-sites of a dimeric GST molecule. Kinetic and equilibrium binding studies indicate that each of the two enzyme subunits contains a complete active-site (composed of both the GSH binding site and the hydrophobic binding site) that is topologically independent of the second subunit (as opposed to the concept of shared catalytic sites formed at the interface of the two subunits) [63,132,179]. It has been suggested that the ability to predict the kinetic behaviour of heterodimeric GST isoenzymes from the kinetic properties of the parent homodimers (see Section 1.1.1.1) seems to exclude the possibility of a shared active-site built by residues from two adjacent subunits [63]. However, the subunits are thought to be mutually dependent for maintaining the correct polypeptide folding for a catalytically active conformation of the enzyme [63,42].

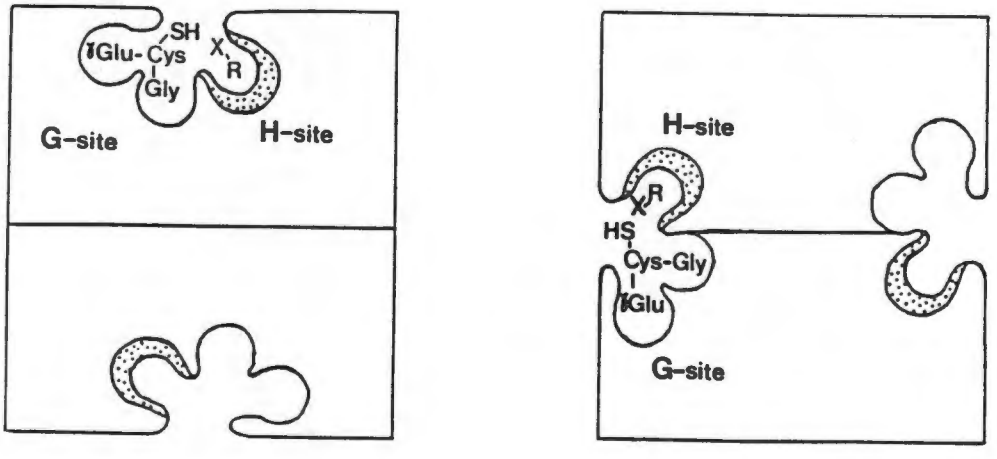

Figure 1.4 : **Alternative Models of the Topology for the Two Active Sites of a Dimeric GSH S-Transferase Molecule**

The topology to the right appears excluded by kinetic and equilibrium binding data (see Section 1.4.1). From reference 179.

1.4.2 **Kinetic Mechanism**

Detailed investigations of the kinetics of GST have only been performed for a few isoenzymes. The most extensive studies have been done with rat liver isoenzyme 3-3, which is fortunate since the contributions of two non-identical subunits need not be considered [179].

Using the substrates GSH and 1,2-dichloro-4-nitrobenzene (DCNB), two different laboratories reported similar kinetic data for isoenzyme 3-3 [12,132,215] although each ascribed different interpretations to their findings. Convex-up 1/v vs 1/[S] plots, analogous to those seen when a mixture of enzymes with different K_m values act on the same substrate, were observed when the concentration of GSH was varied at constant DCNB concentration [12,215,179]. The deviations from Michaelis-Menten kinetics remained even with rigorously purified isoenzyme, which implied that they were not caused by inhomogeneous enzyme preparations. Furthermore, when the concentration of DCNB was varied at constant GSH concentration, the resultant biphasic plots showed the opposite sign of curvature to that expected for a mixture of enzymes individually obeying the Michaelis-Menten equation [132,133,179].

Nonhyperbolic substrate-rate saturation curves are often indicative of co-operativity, where the K_m of the system may alter with changing substrate concentration [138]. However, equilibrium binding studies using GSH and the GSH•CDNB conjugate, *S*-(2,4-dinitrophenyl)glutathione, showed that two binding sites are present on each enzyme molecule, but did not indicate deviations from a simple hyperbolic binding saturation curve [135]. This appeared to exclude co-operative interactions (as described by Huang *et al.* [122]) between two non-identical ligand binding sites of an enzyme molecule as a cause for the non-Michaelian kinetics [179]. For a dimer which has two non-co-operative binding sites, the microscopic rate constants for the binding of a ligand to a subunit are always the same irrespective of the occupancy of the other subunit [135]. The possibility of subunit interaction during catalysis was investigated further by use of the distinct substrate specificities of rat transferase subunits 1, 2, 3 and 4 [63]. These studies demonstrated that the kinetic properties of the heterodimeric isoenzymes could be predicted from their corresponding homodimers and confirmed the kinetic independence of the transferase subunits.

A further possible cause of non-hyperbolic kinetics was thought to be partial

inhibition (entailing alternative reaction pathways) by ethanol, the solvent used to dissolve the electrophilic substrate; this type of inhibition would introduce higher degree terms into the rate equation [134]. However, non-specific inhibition was observed experimentally, and the non-hyperbolic kinetics remained even with extrapolation to zero ethanol concentration [134]. Since measured reaction rates were found to be proportional to the enzyme concentration [13], association-dissociation of the enzyme was also eliminated as a possible explanation. It was therefore concluded that the explanation for the apparently unusual rate behaviour of this homodimeric isoenzyme must be sought in kinetic effects [63].

Based on kinetic and product inhibition data, Pabst *et al.* [215] proposed a hybrid kinetic mechanism in which the concentration of the acceptor substrate governs the flux ratio of two alternative reaction pathways. At concentrations of GSH greater than approximately 0.1 mM, an ordered sequential mechanism prevailed, with GSH binding first and then the electrophilic substrate (with the GSH still bound to the enzyme). The order of addition with high GSH is derived from the finding that the product is competitive with GSH and non-competitive with DCNB [215]. At concentrations of GSH below about 0.1 mM, the reaction followed a ping-pong mechanism, with the electrophilic substrate leaving before the GSH bound to the enzyme [39,215].

In accordance with a prediction of the general rate equation for this mechanism,

$$v = \frac{V_1AB + V_2A^2B + V_3AB^2}{K_2A + K_3B + AB + K_4A^2 + K_5B^2 + K_6A^2B + K_7AB^2} \qquad \text{(Eqn. 1)}$$

where V_i(i = 1-3) and K_j(j = 2-7) are constants and A and B are substrate concentrations [179], the breakpoint in the biphasic double-reciprocal plot for GSH saturation was found to shift to lower GSH concentrations as the concentration of the electrophilic substrate was lowered [138]. Under physiological conditions (1-10 mM GSH) the ordered sequential mechanism would predominate [137,215].

On the basis of kinetic and binding data, Mannervik and his co-workers [12,132] suggested a steady-state random sequential mechanism to explain their non-Michaelian kinetic data. This mechanism, in which either substrate may bind first and both substrates bind before any product is released, is shown below,

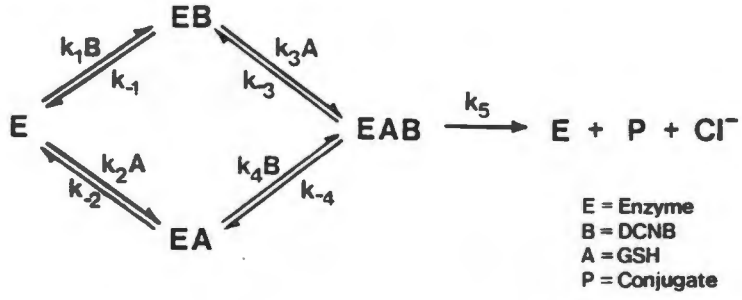

where E = enzyme, B = DCNB, A = GSH and P = the GSH·DCNB conjugate. The observed non-linearity in the kinetic plots was thought to be due to product inhibition, not to a complex kinetic mechanism [132].

In its simplest form, the steady-state random sequential mechanism has the rate equation :

$$v = \frac{V_1AB + V_2A^2B + V_3AB^2}{K_1 + K_2A + K_3B + AB + K_4A^2 + K_5B^2 + K_6A^2B + K_7AB^2} \qquad \text{(Eqn. 2)}$$

where V_i(i = 1-3) and K_j(j = 1-7) are constants, but are not equated, in terms of their elementary rate constant composition, with the coefficients V_i and K_j of Eqn. 1 [179].

Stereochemical investigations of the enzyme-catalysed reaction have helped to clarify the kinetic mechanism of the GSTs. A ping-pong reaction should show a double (or even number of) displacement(s), and retention of the stereochemical configuration on formation of the GSH adduct [39]. On the other hand, a sequential mechanism would result in a single (or odd number of) displacement(s), with inversion of configuration at the reaction site [39,179]. Abdel-Monem and co-workers [176,237], using chiral (1-haloethyl)benzenes and 2-halooctanes as substrates for transferases 3-3 and 1-2, observed inversion of configuration of the S-3 stereoisomer at the benzylic carbon atom. A single (or odd-numbered) displacement was observed at both low and high GSH concentrations, thus favouring a random sequential kinetic mechanism over a ping-pong model [39].

Mannervik and colleagues, in order to discriminate between these rival models, performed an analysis of both their own initial rate data and those of Pabst *et al.* [215] using non-linear regression methods [178,184]. This discrimination was based on the criteria detailed by Mannervik [177], and included an assessment of the 'goodness of fit' of the model rate equations to the experimental data.

Because the constants in multi-parameter models such as Eqn. 1 are highly correlated through the variance-covariance matrix, it was impossible to obtain accurate estimates for individual constants [63]. Use was therefore made of the asymptotic properties of the rate equations [177]. At sufficiently low concentrations of A and B the terms containing second-power concentration factors become negligible. Under these conditions Eqn. 1 degenerates to:

$$v = \frac{VAB}{K''A + K'''B + AB} \qquad \text{(Eqn. 3)}$$

and Eqn. 2 to:

$$v = \frac{VAB}{K' + K''A + K'''B + AB} \qquad \text{(Eqn. 4)}$$

where

$$V = V_1/D,\ K' = K_1/D,\ K'' = \left\{ K_3 - \frac{K_1K_2}{V_1} \right\} / D,$$

$$K''' = \left\{ K_3 - \frac{K_1K_3}{V_1} \right\} / D,$$

and

$$D = \left[1 + \frac{V_2}{V_1} \left\{ \frac{K_1K_3}{V_1} - K_3 \right\} + \frac{V_3}{V_1} \left\{ \frac{K_1K_2}{V_1} - K_2 \right\} \right].$$

The results of the analysis showed that the K_1 term was required for a good fit of the rate equation to the experimental data (in both the complete as well as the degenerate rate equations), and that Eqn. 4 fitted the data better than Eqn. 3 at low substrate concentrations [184]. This was also found to be the case when the original initial rate data of Pabst *et al.* [215] were similarly analysed [184]. Mannervik concluded that this finding ruled out a reaction scheme involving a ping-pong branch, since any such scheme could never yield a constant term in the rate law [179].

Further evidence in support of a steady-state random sequential mechanism has come from double inhibition experiments involving *S*-substituted GSH derivatives with GST 3-3 [133].

A random sequential mechanism has also been proposed for isoenzyme 1-1, based on kinetic and binding studies involving a spin-labelled product analogue [249], and for isoenzyme 4-4, in studies involving product inhibition and alternative substrates [53,54]. An acidic GST isoenzyme isolated from human liver also demonstrated non-hyperbolic kinetics, although the enzyme preparation was apparently not homogeneous [159]. Non-linear kinetics have also been observed for the human erythrocyte GST enzyme with respect to both GSH and CDNB [118].

Still apparently unresolved, however, was the belief that none of the simple classical mechanisms explained the higher-degree dependence of velocity on substrate concentration observed in the absence of inhibitors [133]. Several alternate mechanisms and modifications to the steady-state mechanism were investigated in an attempt to explain the apparently anomalous non-hyperbolic kinetics of GST 3-3 for the conjugation of DCNB and GSH. Explanations have included the superimposition of product inhibition on the steady-state mechanism [132,133], and the suggestion that the basic sequential model may be overlaid with the kinetic complications inherent in an 'enzyme memory' mechanism involving GSH-induced slow transitions [179] (discussed further in Section 4.5). Mannervik [63] has suggested that the only remaining explanation for the non-Michaelian rate behaviour appears to be an enzyme memory mechanism involving slow conformational changes of the protein between kinetically stable states. Conformational changes have also been invoked by Radulovic and Kulkarni [232] to explain the observed non-Michaelian behaviour of human placental GST using ethacrynic acid as the substrate.

1.5 NON-SUBSTRATE LIGAND BINDING

Early investigators identified a protein in rat liver cytosol that bound a number of hydrophobic compounds [154,197], and this protein was termed 'ligandin' in view of its broad affinity for non-substrate ligands [171]. Later, a BSP-binding ligandin in hepatic cytosol was found to possess GST activity [146], and immunochemical studies established that transferase 1-2 and ligandin were one and the same protein [106]. It is now known that the majority of GSTs in both rat and human tissues are able to reversibly bind a variety of non-substrate ligands, including a number of endogenous ligands, such as haem and bilirubin [136,155].

The methods used to measure non-substrate ligand binding to the GSTs have been reviewed by Boyer [39]. These include circular dichroism, equilibrium dialysis and fluorescence spectroscopy. Because the binding characteristics of the transferases for different ligands can vary considerably under different conditions, such variables must be taken into account when comparing the results of different binding studies [41].

The binding of a number of non-substrate ligands has been investigated and some of the reported binding constants for the GSTs are shown in Table 1.10. The inhibitory effect (I_{50} values) of non-substrate ligands on the CDNB-conjugating activity of the transferase subunits has been used to discriminate between the various classes of rat [114,281,325] and human [280,281] isoenzymes (see Section 1.1.1.1).

Table 1.10 : **Dissociation Constants for the GSH S-Transferases**

Non-substrate Ligand	K_D (μM)								
	Rat Isoenzymes				Human Isoenzymes				
	1-2	2-2	3-3	3-4	α	β	γ	δ	ϵ
Bilirubin	2	100	15	2	65	110	34	18	34
Bilirubin diglucuronide	10	40	23	20				33	121
Indocyanine green	3	100	3	1	20			20	
Haematin	0.1	4	2	7	10			10	
ANS*	95	700	330	400					

*8-Anilino-1-naphthalene sulphonate
Adapted from reference 39.

1.5.1 **Physiological Significance of Binding**

The GSTs may function as intracellular transport and storage proteins, perhaps by increasing the solubility of non-polar endogenous compounds and xenobiotics and therefore facilitating their cytosolic transport between intracellular membranes [39]. This suggestion is supported by a mathematical model [291], although some doubt has been cast on the ability of the transferases to remove membrane-associated molecules [43]. This would make facilitation of ligand transport by the transferases dependent on the rates of desorption of ligand into the cytosol, which are thought to vary considerably [39,43].

The correlation between hepatic ligandin levels and the hepatic uptake of organic anions suggested that the transferases may also play a part in the hepatic and renal uptake and excretion of organic anions [43]. However, increasing the intrahepatic ligandin concentration did not influence the rate of influx of bilirubin into the hepatocyte [323]. Scriven *et al.* [250] have suggested that human GSTs may only play a minor role in bile acid transport *in vivo*.

Because of the poor aqueous solubility of haemin (see Section 1.7) it has been suggested that the GSTs may be involved in the intracellular solubilisation of haemin, in much the same manner as serum albumin is thought to function extracellularly [110,136]. The affinity of the GST isoenzyme from human erythrocytes for haemin was found to approximate that of bovine serum albumin for the same compound [110] and in addition, haemin has been found to be the only non-substrate ligand which binds with high affinity to the human GSTs [284]. The binding of haem to the transferases has not been studied extensively, although a specific role for the GSTs in haem transport from mitochondria has been suggested [110,124,306]. Consistent with this suggestion, the protein responsible for haem transfer from the mitochondria to apocytochrome b_5 has been isolated and identified as a cytosolic GST [253].

Rat liver GSTs containing subunits 3 or 4 have been shown to bind dexamethasone and corticosterone with greater affinity than putative glucocorticoid receptors [120,121], suggesting a potential role for these transferases in intracellular steroid hormone transport.

1.5.2 Stoichiometry of Binding and Relationship Between Binding and Catalysis

In many early studies, it was suggested that non-substrate ligand binding occurred at the catalytic site, since ligands were competitive inhibitors of the reactions catalysed by the transferases [37,150,293]. Although competitive inhibition has been observed in subsequent investigations for several substrates and transferases, other combinations displayed complex inhibition patterns [312]. These results have provided evidence for other binding sites distinct from the catalytic site. However, the relationship between the non-substrate ligand binding site(s) and the acceptor substrate site is still unresolved and is therefore of considerable interest.

In addition to the complex non-competitive inhibition patterns described above, there is other experimental evidence in support of non-substrate ligand binding sites which are distinct from the enzyme active-site. For example, blocking the binding of bilirubin to ligandin with dimethylsuberimidate did not decrease enzymic activity, implying that the bilirubin binding site and active-site are discrete entities [30]. Transferase 2-2 and to a lesser extent, transferase 1-2 have also been shown to retain catalytic activity in the presence of bound non-substrate ligand [39,41,307,311].

Furthermore, inhibition by non-substrate ligands has been shown to be dependent on incubation conditions, for example, bilirubin is a much less effective inhibitor of transferase 1-2 at pH 7.4 than at pH 6.5 [307]. Boyer *et al.* [41] also observed less inhibition at higher pH values when transferases 1-2 and 2-2 were incubated with a variety of non-substrate ligands, although the inhibition of transferase 1-1 was the same over the entire pH range. The observed inhibition in both studies could not be explained simply by a pH-induced loss in enzyme affinity for the non-substrate ligands, but was consistent with the formation of different ternary enzyme•substrate•inhibitor conformers at different pH values [39,307]. The conformers formed at pH 6.5 had little enzymic activity, while those formed at pH 7.5 retained significant catalytic activity. Allosteric modifications of the isoenzymes, which may differentially affect substrate binding, are thought to explain these findings [311].

In addition, some non-substrate ligands, notably 2,4,5-trichlorophenoxyacetic acid and several other phenoxyherbicides, have been found to reversibly activate rather than inhibit the activity towards CDNB of GSTs 2-2 and 1-2 [310,311].

Therefore, evidence for distinct binding sites for non-substrate ligands includes the retention of enzymic activity in the presence of some bound non-substrate ligands, the formation of catalytically active enzyme·substrate·inhibitor complexes at high pH values, and the fact that some non-substrate ligands stimulate rather than inhibit enzyme activity.

The stoichiometry of non-substrate ligand binding to the GSTs is still unresolved, but indications are that the number of binding sites may vary for different isoenzyme/non-substrate ligand combinations. Based on patterns of inhibition by non-substrate ligands, Vander Jagt and colleagues [304,306,307] have proposed that GSTs from rat and human liver contain at least two binding sites for non-substrate ligands, one specific for bilirubin and the other(s) capable of binding a number of non-substrate ligands. A bilirubin binding site that was distinct from the catalytic site was also reported for human placental GST, after bilirubin was found not to inhibit the activity of the enzyme even at concentrations sufficiently high to quench most of the protein fluorescence [308]. The GSTs of human liver and placenta bind both bilirubin and haematin at sites distinct from the catalytic site [145,304,306-308]. Interestingly, this property of unique binding sites for bilirubin and haematin is also shared by human serum albumin [305].

The nature of the binding of bilirubin to subunits 1 and 2 is still uncertain. Some investigators found that transferase 1-1 bound, with high affinity, two molecules of bilirubin per enzyme molecule [30-32]. Since transferase 2-2 lacked a high affinity bilirubin site, and transferase 1-2 was found to have only one such site, the high affinity bilirubin binding site was apparently situated on subunit 1 [150,155]. Similar findings were reported for the binding of lithocholic acid to transferases 1-1 and 1-2 [116,282,283]. Other binding studies are at variance with these conclusions, for reasons which are not clear. A single binding site was found for bilirubin [40,49], BSP [40] and oestrone sulphate [49] on transferase 1-1. A single binding site has also been reported for five transferases (1-1, 1-2, 3-3, 3-4 and 4-4) with bilirubin, haematin and BSP [277]. If the transferases have only one binding site for non-substrate ligands, then either the site may not reside on a specific subunit but may be formed by subunit interaction [37,40,49,191] or binding of the first non-substrate ligand molecule may prevent binding of the second [39].

1.5.3 Covalent Binding

In addition to the reversible binding of the non-substrate ligands, a number of compounds (including carcinogenic aminoazo dyes and polycyclic hydrocarbons) covalently bind to the transferases [137]. This 'suicide inhibition' may be an additional protective mechanism for the cell, in which the transferases act as scavengers of potentially harmful electrophiles [139,272].

1.6 BIOLOGICAL REGULATION

A complex regulatory mechanism to control the expression of GSTs is thought to exist, resulting in the observed variations in the distribution of GST isoenzymes and their different substrate specificities (for a review, see reference 222). Differences in GST distribution and activities, both between foetal and adult rats and between male and female rats, have been reported (reviewed in 179). Some studies have described the hypothalamic and pituitary modulation of the gonadal control of GST in rat liver [166,179]. The marked induction of placental GST in preneoplastic tissue (see Section 1.1.2) and the resultant resistance to some cytotoxic drugs has been the subject of considerable research. There is also evidence that interferon is an endogenous inducer of the placental GST, although links between the anti-cancer activity of the interferons and the GSTs remain speculative [2].

Glutathione S-transferase activity can be induced by several classes of compounds, and isoenzyme patterns may also be altered [78,137,179,222,313]. Phenobarbital and 3-methylcholanthrene both induce levels of subunits 1 and 3 in rat liver, as do food additives such as butylated hydroxyanisole [70,75,77,101, 224,263]. Divergent regions of three cDNA clones have been used to demonstrate induction by phenobarbital of levels of the mRNAs corresponding to rat subunits 1, 2 and 3 [224]. Such changes have potential importance in the toxic consequences of xenobiotic metabolism.

1.7 MICROPEROXIDASE-8 : A MODEL COMPOUND FOR STUDIES OF HAEM/PROTEIN INTERACTIONS

Haemin (ferriprotoporphyrin IX) is one of the most physiologically important non-substrate ligands of the GSTs (see Section 1.5.1) and although a number of studies of its interaction with the enzyme have been published [110,277,306], the kinetics of the interaction have not been described. In addition to its physiological significance, haemin is an attractive candidate for a kinetic study of non-substrate ligand/GST interaction, since perturbation of the intense Soret peak of the metalloporphyrin on interaction with proteins facilitates monitoring of the binding reaction at low enzyme and ligand concentrations.

One of the factors which complicates investigations of haem/protein interactions is the poor solubility of haemin in aqueous solutions. Haemin precipitates from aqueous acidic and neutral solutions, and exists as a mixture of monomeric hydroxy and dimeric μ-oxo forms in aqueous alkaline solutions, even at sub-micromolar concentrations [11,110]. Several approaches, such as the use of detergents or aqueous/non-aqueous solvent mixtures, have been used to overcome the problems of haemin aggregation [11]. However, the ligand-binding behaviour of haemin can be altered by the nature and concentration of these detergents and non-aqueous solvents [11].

A possible alternative to the use of haemin *per se* entails the utilisation of water-soluble haempeptide fragments of cytochrome-*c* as model compounds for monomeric haemin. Several of these haempeptides (the microperoxidases) can be obtained by enzymic degradation of cytochrome-*c*, with each haempeptide retaining different numbers of amino acid residues from the parent compound (see Figure 1.5).

Microperoxidase-8 (MP-8) is the ferrihaem-*c* containing octapeptide derived from cytochrome-*c*. Amino acid residues 14 to 21 of cytochrome-*c* are retained and the haem moiety remains covalently linked by thioether bridges to Cys-14 and

Cys-21 [302]. In aqueous solution at pH 5-8, it is thought that the ferric ion of MP-8 is six-coordinate with His-18 and that a water molecule is axially ligating positions 5 and 6 [109]. MP-8 has been found to be monomeric at micromolar/ submicromolar concentrations at pH 7 in aqueous solution [11]. This important property has facilitated the use of MP-8 as a chemical model for both the cytochrome P-450 enzymes [3,4], and the activation of hydrogen peroxide by the peroxidases [22].

Dr Paul Adams, of this university, has proposed that the microperoxidases may also prove valuable as sterically-hindered model compounds for investigating the mechanism of interactions of monomeric haemin with haem-binding proteins in aqueous solution. We have therefore recently investigated the interaction of MP-8 with two such proteins, human serum albumin [6] and apo-myoglobin (Adams, Goold & Thumser, unpublished results). Although details of these investigations are not given in this thesis since they are outside the immediate scope of this study, some of this work has been recently accepted for publication [6], and is included as Appendix 1. These studies have already confirmed that MP-8 may indeed be a valuable mechanistic analogue of monomeric haemin and accordingly, they have now been extended here to the GSTs, another important group of haem-binding proteins.

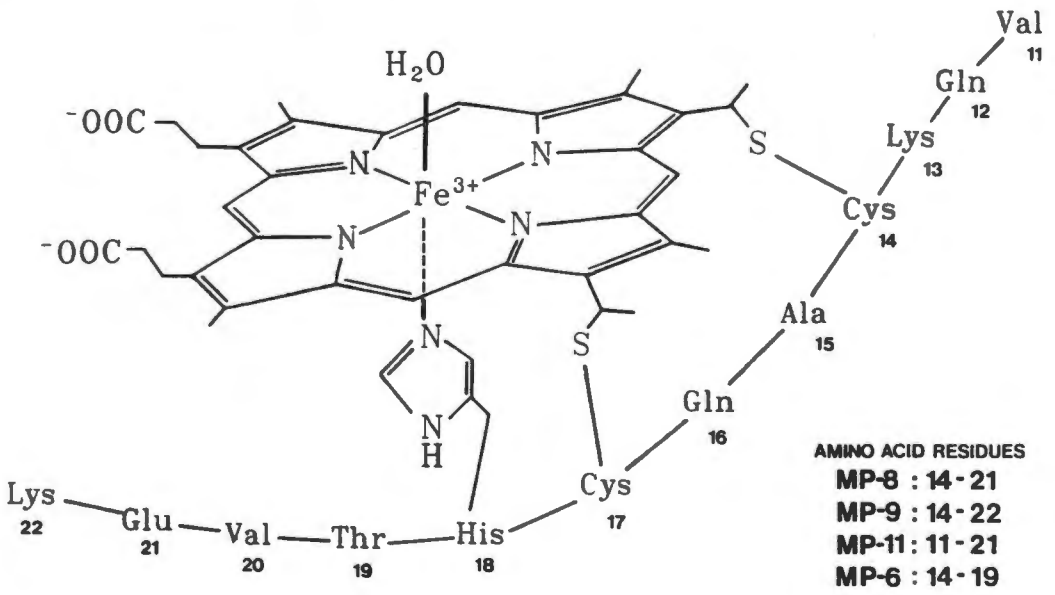

Figure 1.5 : **The Haem-Peptides from Cytochrome-c**
The numbering of the amino acid residues refers to the original protein sequence of horse-heart cytochrome-*c*. Adapted from Reference 21.

1.8 OBJECTIVES OF THIS STUDY

This investigation is broadly concerned with aspects of the kinetics, binding and inhibition of the GSTs, a group of multifunctional enzymes of drug and xenobiotic metabolism (reviewed in this chapter). Both the steady-state kinetics of the GST-catalysed conjugation reaction and the kinetics of binding of substrates and non-substrate ligands to the enzyme have been investigated and are reported here.

One of the primary objectives of this study was to confirm the biphasic kinetics previously reported [12,132,215] for the conjugation of GSH and DCNB by GST isoenzyme 3-3 and to propose an explanation for the apparently unusual steady-state kinetics (see Section 1.4.2). The kinetics of the conjugation of CDNB and GSH by GST 3-3 and of DCNB by GST 3-4 were also investigated. Details of these studies are given in Section 3.3.

In order to carry out steady-state kinetic studies with a high degree of accuracy and reproducibility, a preliminary optimisation of the GST assay system was performed. Factors investigated included the selection and suitability of spectrophotometric instrument, choice of solvent for CDNB and DCNB, the order of addition of reagents, and the linearity of initial rates in the standard GST assay. These preliminary experiments are described in Sections 3.1.

The isoenzymes which have to date been subjected to the most detailed steady-state kinetic analysis, 3-3 and 3-4, both belong to class Mu of the GSTs. Therefore, it was decided to isolate representative homodimeric isoenzymes from the other two classes of GST (Alpha and Pi) and to characterise their kinetic mechanism, in order to determine whether other classes of GST exhibit similar biphasic kinetics. The GST isoenzymes selected for study were human placental GST π (Class Pi) and rat liver GST 2-2 (Class Alpha). The results of these steady-state kinetic studies are reported in Section 3.3.

It was originally thought that the non-Michaelian kinetics observed with rat liver GST 3-3 might be caused by co-operative binding between the enzyme subunits [138]. However, this possibility seems to have been excluded by equilibrium dialysis studies of the binding of the substrate GSH to isoenzyme 3-3 [135] (see Section 1.4.2). In order to investigate the possibility of co-operativity between the subunits of human placental GST, a similar equilibrium dialysis study of GSH binding to GST π was performed (these results are presented in Section 3.4).

Ethylene dibromide reportedly binds to DNA irreversibly in a reaction catalysed by GST when they are incubated together at 37°C for 2 hours [127]. These results were re-evaluated here in view of the observation in this laboratory that EDB irreversibly inhibited selected GST isoenzymes [131]. In these experiments (described in Section 3.1), it was hoped to show that this irreversible inhibition is a factor in determining the extent of DNA binding by EDB *in vivo*.

As described in Section 1.5.1, one of the most biologically significant of the non-substrate ligands of the GSTs is haemin. In this investigation, an attempt has been made to kinetically characterise the interaction of haemin with human placental GST using microperoxidase-8 (MP-8), a sterically hindered analogue of proto-porphyrin IX. Unlike haemin, MP-8 remains monomeric in aqueous solution at experimentally useful concentrations, facilitating its use as a chemical model for monomeric haemin (see Section 1.7).

Conventional methods for the preparation of MP-8 are time-consuming (8-10 days) and result in relatively poor yields of a product that is only approximately 90% pure. Although a recent HPLC-based method [4] has enabled the preparation of MP-8 of higher purity in a shorter time, a requirement for MP-8 of still higher purity in kinetic studies (such as those of this investigation) prompted attempts here to further optimise the preparative schedule for the haempeptide (described in Section 3.5).

Investigations to date into the interaction of non-substrate ligands with the GSTs have been almost exclusively thermodynamic in nature, despite the fact that such studies do not permit unambiguous mechanistic interpretation when taken in isolation (see Section 4.7). In this study, the kinetic mechanism of the interaction of MP-8 and GST was investigated both by examining the inhibition by MP-8 of the steady-state GST-catalysed conjugation between GSH and CDNB (Section 3.7) and by direct observation and analysis of the time-course of the binding process (Section 3.6). The latter technique represents the simplest and most direct 'extra-thermodynamic' method for obtaining information on the ligand/protein interaction. By using MP-8 in this novel manner, it was hoped to obtain unambiguous information on steric aspects of the haemoprotein binding site(s) and their spatial relationship to the catalytic site of the enzyme. The results of these investigations are described in Sections 3.6 and 3.7.

2. EXPERIMENTAL METHODS

2.1 MATERIALS AND GENERAL METHODS

Reagents and solvents were obtained from the sources shown in Table 2.1. Reagents were analytical grade wherever possible. Water was double-distilled in glass.

Buffers were prepared with double-distilled water, degassed and adjusted to the correct pH value at the temperature of use. Measurements of pH and ionic strength were made with a GK 2501C combination glass electrode on a Radiometer model ION83 ion meter (Radiometer, Copenhagen, Denmark), calibrated against commercial pH standard buffers.

2.2 ASSAYS FOR GSH S-TRANSFERASE ACTIVITY

The activity of GST toward various substrates was determined spectrophotometrically by monitoring the rate of formation of product. The wavelength used was the maximum of the difference spectrum between the starting assay mixture and the product [107]. Table 1.9 summarises the more frequently used spectrophotometric methods, details of which are found in several references [39,104, 107,137]. The cumene hydroperoxide assay was performed according to the procedure of Reddy *et al.* [235]. Some detail is given here for the CDNB and DCNB assays since these were the basis of the kinetic studies, and were considerably modified for use with the Multistat centrifugal analyser.

All GSTs conjugate CDNB with GSH, and this 'universal' substrate forms the basis of the standard spectrophotometric assay for GST activity (see Section 1.2.1). The activity of GST toward CDNB was assayed in this study by modification of the method of Habig *et al.* [107]. Assays were either performed in a Beckman UV-5230 spectrophotometer or in a Multistat III Plus centrifugal analyser (Instrumentation Laboratory, Lexington, MA), which facilitated the performance of more assays in a shorter time than possible in conventional spectrophotometers. This was especially important for the kinetic investigations undertaken, where any time-dependent loss of enzyme activity should be minimised. The small cuvette

Table 2.1 : **Sources of Reagents and Solvents Used**

REAGENT	SOURCE	REAGENT	SOURCE
Acetic acid glacial	BDH	GSH (reduced)	Sigma
Acetone	Merck	[^{35}S]GSH (radiochemical purity >99.8%)	New England Nuclear
Acetonitrile	Riedel-de-Haën	GSH Reductase	Sigma
bis-Acrylamide	Merck	GSH S-transferase (Rat Liver Mix)	Sigma
Albumin (bovine serum)	Miles	Haemin (Bovine)	Sigma
Albumin (human serum)	Sigma	Helium	Afrox
Ammonium bicarbonate	Merck	Hoechst 33258	Calbiochem-Behring
Ammonium hydroxide	Merck	Hydrochloric acid	Merck
Ammonium persulphate	BDH	Isoamyl alcohol	Merck
Ammonium sulphate	Merck	2-Mercaptoethanol	Merck
Δ^5-Androstene-3,17-dione	Sigma	Methanol	BDH
Argon	Afrox	Molecular Weight Markers (14 300-71 500)	BDH
Bilirubin	Sigma	NADPH	Sigma
Bio-Rad protein assay dye	Bio-Rad	Nitrogen	Afrox
Bromophenol blue	Merck	Pepsin (porcine)	Sigma
CDNB	Merck	pH standard buffers	Radiometer
CM-Cellulose (CM-52)	Whatman	Phenol	Merck
Chloroform	Merck	*trans*-4-Phenyl-3-buten-2-one	Aldrich
Citric acid	May & Baker	Potassium chloride	Merck
Copper sulphate	Merck	Potassium dichromate	Merck
Cumene hydroperoxide	Fluka	Potassium dihydrogen phosphate	Merck
Cytochrome *c* (horse heart type III)	Sigma	Potassium hydroxide	BDH
DCNB	EGA	Sepharose-6B	Pharmacia
Diethyl ether	BDH	CnBr-activated Sepharose-4B	Pharmacia
1,2-Dimethoxyethane	Merck	Sodium acetate	Merck
Dimethyl sulphoxide	Merck	Sodium azide	BDH
Dipotassium hydrogen phosphate	Merck	Sodium bicarbonate	Merck
5,5'-Dithiobis(2-nitrobenzoic acid)	Merck/Sigma	Sodium borate	Merck
Dithiothreitol	BDH/Sigma	Sodium carbonate	Merck
DNA (calf thymus)	Sigma	Sodium cholride	Merck
EDTA	BDH	Sodium citrate	Merck
1,2-Epoxy-3-(*p*-nitrophenoxy)propane	Sigma	Sodium dihydrogen phosphate	Merck
Ethacrynic acid	Sigma	Sodium dithionite	Riedel-de-Haën
Ethanol (SVR; Absolute)	Merck/BDH	Sodium dodecyl sulphate	Merck
Ethanolamine	BDH	Sodium hydroxide (solid)	Merck
Ethylene dibromide	BDH	Sodium tartrate	Merck
[U-^{14}C]EDB (radiochemical purity >98%)	Amersham	TEMED	Sigma
Folin-Ciocalteau's phenol reagent	Merck	Tetrahydrofuran	Merck
γ-Globulin (bovine)	Bio-Rad	Trifluoroacetic acid	Merck
Glycerol	BDH	Tris	Merck
Trypsin (bovine pancreas type I)	Sigma		

Afrox, Cape Town, RSA
Aldrich Chemicals, Milwaukee, WI, USA
Amersham International plc, Buckinghamshire, UK
BDH Chemicals, Poole, UK
Bio-Rad Laboratories, Munich, FRG
Calbiochem-Behring, La Jolla, CA, USA
EGA Chemie, Steinheim, FRG
Fluka, Buchs, FRG
May & Baker, Dagenham, Essex, UK
Merck Chemicals, Darmsdadt, FR
Miles Laboratories, USA
New England Nuclear, Boston, Mass, USA
Pharmacia, Uppsala, Sweden
Radiometer, Copenhagen, Denmark
Riedel-de-Haën, Seelze-Hannover, FRG
Sigma Chemical Co, St Louis, MO, USA
Whatman, Maidstone, Kent, UK

volume (200 µl) enabled economical usage of the enzyme preparation, and the centrifugal mixing method allowed absorbance measurements from as little as 3 seconds after the initiation of the reaction. The centrifugal analyser also provided controlled temperature conditions (30.0 ± 0.1°C) and enabled more precise and reproducible absorbance/time measurements than possible using conventional manual spectrophotometric methods.

Twenty cuvettes of 0.50 ± 0.010 cm pathlength are contained in each disposable Multistat rotor. Each cuvette consists of two chambers, separated by an internal 'dam' which keeps reactants apart until mixing (see Figure 2.1).

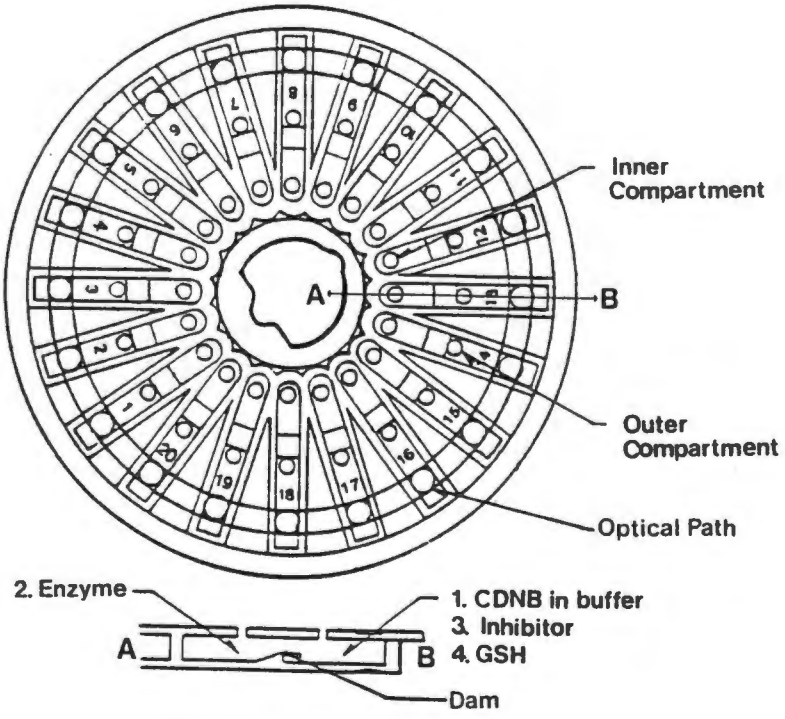

Figure 2.1 : **Multistat Centrifugal Analyser Rotor**
Reagents were added to the inner and outer cuvette compartments as shown in rotor cross-section (A-B), with order of addition as numbered.

The CDNB solution was pipetted into the outer chamber of each cuvette, and the enzyme solution into the inner chamber. Immediately prior to analysis, the GSH solution was added to the same cuvette compartment as the CDNB. After a short incubation period during which the assay temperature was attained, the rotor was accelerated to 4 000 rpm and was then briefly stopped (0.5 sec) causing thorough

mixing of the reactants. The reaction was therefore initiated by the addition of enzyme to the other reactants. Centrifugation then resumed at 1 000 rpm while the analyser measured the absorbances of all cuvettes essentially simultaneously. The centrifugal analyser used a quartz tungsten light source and narrow bandpass 340 nm optical filter.

Absorbances were measured at 5 second intervals for a total period of 60 seconds, commencing 3 seconds after initial mixing. Initial rates were determined by linear least squares regression of these time/absorbance values. Velocities are in nmol/min/ml except where otherwise indicated.

Because GSH reacts at a finite rate with CDNB (and other substrates) in the absence of enzyme, non-enzymatic reaction rates, obtained under identical conditions of ionic strength, pH and temperature as the enzymic rates, served as controls for the spontaneous 'background' rates. Relevant background rates were subtracted from enzymatic rates in all cases.

Stock solutions of GSH were prepared in 0.1 M potassium phosphate (pH 6.5), readjusted to pH 6.5 with 1 mM KOH and kept under nitrogen in an ice-bath to prevent oxidation. Oxidised glutathione (GSSG) is an inhibitor of several of the GST isoenzymes [39]. Because of its limited aqueous solubility, CDNB was first dissolved in dimethyl sulphoxide (DMSO), and then diluted with the buffer used in the assay (0.1 M potassium phosphate (pH 6.5)), to make a premixed stock solution. This technique was employed in order to avoid the precipitation of CDNB on the walls of the cuvette. This has been observed when addition of CDNB solutions in organic solvent is made directly to the assay system [39]. Photosensitive solutions containing CDNB were kept in foil-covered amber vials to minimise light degradation. In the standard assay, the final concentration of GSH and CDNB used was 1 mM, and the final concentration of DMSO in the reaction mixture was 2% (v/v). Although substrate concentrations varied in the steady-state kinetic experiments, the DMSO component of the solvent was always kept constant at 2% (v/v).

The assay using DCNB as substrate was performed in the same manner as the CDNB assay, the only difference being that the assay was performed at pH 7.5 (see Table 1.9).

2.3 PRELIMINARY EXPERIMENTS

After the standard assay volume had been scaled down to 200 μl for the centrifugal analyser, the assay conditions were optimised and the suitability of the instrument confirmed. For CDNB and DCNB, the change in absorbance has been found to be a linear function of enzyme concentration and of time for at least 3 min when the rate of absorbance change was limited to less than 0.05 units per minute (for a pathlength of 1 cm) [104]. Experiments were performed to confirm the linearity of the enzymic reaction in the standard assay (1 mM GSH; 1 mM CDNB) with time and enzyme concentration, and the photometric linearity of the instrument was checked with potassium dichromate standards. Periodically, control enzyme preparations having independently determined ΔA_{340}/min/ml values were used to monitor the performance of the CDNB and DCNB assays.

The time course experiments were performed with both CDNB and DCNB with rat liver GST mix (Sigma), rat liver cytosol, and purified rat liver isoenzyme 3-4, human lung basic, acidic and near-neutral isoenzymes as well as human placental isoenzyme π. Initially, readings were taken at 10 sec intervals for 3 min, since previous reports had indicated that the reaction appeared linear for at least 3 min [104,107]. Also tested were 10 sec intervals for 10 min and 3 sec intervals for 1 min. Absorbance/time data were fitted to straight-lined and quadratic functions and each tested for randomness by a runs test [279]. The effect of bovine serum albumin (120 μM) on the linearity of the standard assay was also investigated. The linearity of the standard CDNB and DCNB assays was studied using enzyme solutions ranging from 0.5-8 times the concentration which resulted in a rate of absorbance change of about 0.025 units (for a pathlength of 0.5 cm).

Background rates were also investigated to determine the best method to correct for non-enzymic conjugation rates. The results of these latter experiments were also checked using a carefully calibrated Varian Techtron 635 UV-vis spectrophotometer with precise temperature control (± 0.02°C), as a standard kinetic instrument.

It is generally considered that solvent concentrations should be kept as low as possible to minimise solvent effects on the enzyme [39,104]. It has been shown that ethanol inhibits the GSTs at concentrations of greater than 1% (v/v) [39], although ethanol is still the most frequently used solvent used for CDNB and DCNB in the GST assay. Ethanol concentrations of less than 4-5% (v/v) are usually

recommended in the standard assay [9,104,107,186,249], although concentrations as high as 10% have been used [12]. Other organic solvents have been found to be less inhibitory to the transferase activity of rat liver cytosolic fraction, at least when used as vehicles for DCNB [7]. The effects of various organic solvents on the activity of the purified transferase isoenzymes used in this study towards both CDNB and DCNB were investigated. CDNB and DCNB assays were performed with different solvents (ethanol, acetone, DMSO, 1,2-dimethoxyethane or tetrahydrofuran) at concentrations of 0.3-4.5% (v/v).

The order of addition of reagents to the assay system was investigated since preincubation with GSH prior to assay has been reported to activate the enzyme [150]. Such effects could be significant in kinetic experiments, and must also be considered when using certain enzyme preparations, such as rat liver cytosolic fraction and the commercially available rat liver GST (Sigma), which both contain varying amounts of GSH. Assays were performed at different CDNB concentrations with 1 mM GSH added either to the same cuvette compartment as the enzyme, or to the compartment containing the CDNB. The purified isoenzyme preparations used (Sigma rat liver GST and rat liver isoenzyme 3-3) were dialysed overnight against buffer containing no GSH, to remove any residual GSH present.

Unpublished observations in this laboratory have indicated that the activity of various GST dilutions was greater when water, rather than 0.1 M potassium phosphate (pH 6.5) buffer, was used as a diluent. Equivalent dilutions (1/10) were therefore prepared in both diluents, using human placental GST, and tested for activity after standing on ice for one hour.

In order to confirm the suitability of the instrument and the reproducibility of previous work done in this laboratory, on the reversible inhibition and activation of rat hepatic GSH S-transferases by ethylene dibromide [130], these experiments were repeated.

Inskeep and Guengerich [127] have reported that EDB bound irreversibly to DNA in a reaction catalysed by GSTs when they were incubated together at 37°C for 2 hours. These results were re-examined and the conditions of the incubation reproduced in view of the observation in this laboratory that EDB irreversibly inhibited selected GST isoenzymes [131]. Incubations were performed at 37°C in polycarbonate centrifuge tubes (Eppendorf, Hamburg, FRG) containing 100 µl 0.1 M Tris.HCl (pH 7.7), 0.2 mg DNA, 2 mM (or 15 mM) GSH, 5 mM EDB and 0.4 mg rat liver GST mix (Sigma). The GST activity of the incubation mixture was determined at intervals, up to two hours.

An attempt was also made to assess the binding of [^{14}C]-EDB to DNA under these incubation conditions, using four different GST sources (Sigma rat liver GST mix, and three GST isoenzymes from human lung - see Section 2.4). Incubations were performed as described above (at 2 mM GSH), although only 15 µg of each GST was used per experiment, due to the limited availability of the purified isoenzymes. The specific radioactivity of the [^{14}C]-EDB used in the incubations was 185 MBq/mmol (5 mCi/mmol). The incubations were terminated by the addition of 50 mM Tris.HCl buffer (pH 7.7) containing 15 mM sodium citrate and 1% (w/v) SDS, and the content of protein, DNA and DNA-bound [^{14}C]-EDB were then determined. EDB-bound DNA was purified by extraction with an equal volume of a saturated aqueous phenol (twice), after which the aqueous supernatant was extracted with an equal volume of chloroform:isoamyl alcohol (24:1). Several extractions using diethyl ether were used to remove excess EDB, and residual ether was removed under vacuum.

DNA was determined by the fluorometric Hoechst 33258 assay described by Cesarone *et al.* [50], using a Perkin-Elmer LS-5 Fluorimeter. Protein determinations were by the Bio-Rad dye-binding method, using bovine γ-globulin as the standard. In order to measure DNA-bound [^{14}C]-EDB, 20 µl aliquots of the incubation mixture were added to 5 ml of Beckman RV liquid scintillation cocktail and radioactivity was determined using a Packard TriCarb 4640 liquid scintillation counter. The results of all the preliminary experiments are presented in Section 3.1.

2.4 GSH S-TRANSFERASE ISOENZYME PURIFICATIONS

The rat liver isoenzymes 3-3 and 3-4 used in this study had been purified and characterised earlier by others in this laboratory, according to a method described previously [131]. Essentially, the method used was similar to that of Guthenberg and Mannervik [99], and employed S-hexylglutathione affinity chromatography and chromatofocusing to isolate the isoenzymes. Human lung acidic, basic and near-neutral isoenzyme samples were the gift of Ms A Corrigall, UCT Department of Medicine. The methods used in this investigation to isolate human placental GST π and rat GST 2-2 are described below.

The protein concentrations of cytosolic tissue fractions were determined by the method of Lowry *et al.* [173], while the Bio-Rad assay (based on the dye-binding method of Bradford [45]) was used for subsequent purification steps. The Bio-Rad microassay (for protein concentrations in the range 1-20 μg) was performed according to the manufacturer's instructions. For both methods of protein determination, bovine γ-globulin was used as the standard. Activity towards CDNB was used to monitor GST throughout the purifications and this activity, together with those towards other substrates, were determined as described in Section 2.2. SDS-PAGE was performed by the method of Laemmli [164], using molecular weight standards (BDH) to determine the homogeneity and apparent M_r of the isoenzyme preparations. The results of the purifications are found in Section 3.2.

2.4.1 Purification of Human Placental GSH S-Transferase π

GSH S-transferase π was isolated from human placental tissue by affinity chromatography and HPLC, essentially according to the method of Radulovic and Kulkarni [231,232] with several modifications, as detailed below.

Placentae were collected from non-smoking women at the time of elective Caesarean deliveries at Groote Schuur Hospital, Cape Town, within 30 min of parturition and were maintained at 4°C thereafter. The placental tissue was cleared of amniotic membranes, and approximately 150 g of tissue was cut into small pieces, washed copiously with cold 50 mM Tris (pH 7.4 at 4°C) to remove residual blood, minced and homogenised in approximately 750 ml of the same

buffer. The cytosol was centrifuged at 12 250 *g* for 20 min in a Beckman J2-21 centrifuge (JA14 rotor), and the supernatant was filtered through cheesecloth to remove floating lipid material. The supernatant was then centrifuged at 100 000 *g* for 60 min in a Beckman L8-70 centrifuge (50.2 Ti rotor).

Epoxy-activated Sepharose 6B (Sigma) was derivatised with GSH by the method of Simons and Vander Jagt [257,259]. Supernatant containing approximately 400 U of enzyme activity was added to a beaker containing the GSH-affinity gel, equilibrated with 50 mM Tris buffer (pH 7.4 at 4°C), and gently stirred for 5-10 min. The coupled gel was then poured into a column (2.2 x 13 cm), which was washed through with the same buffer until protein (A_{280}) was no longer detected in the effluent. The GST activity was eluted from the matrix with 50 mM Tris containing 10 mM GSH (pH 9.6 at 4°C), and collected in 1 ml fractions. The flow rate was maintained at 0.5 ml/min throughout. Fractions with GST activity were pooled, concentrated using an Amicon P10 membrane to a protein concentration of 0.5-10 mg/ml, and then adjusted to pH 7.4 with 1 M KH_2PO_4. The pooled GST was dialysed overnight against 10 mM potassium phosphate buffer (pH 6.0) containing 10 mM GSH before anion exchange HPLC.

A Beckman gradient control HPLC system (comprising two model 110A pumps, a model 420 controller and a model 163 variable wavelength detector set at 280 nm) was used in conjunction with a Spectra Physics SP4290 electronic integrator. In initial purifications, a Beckman DSK SBW anion exchange column was employed, although later the Synchrom AX-300 (Synchrom, Lafayette, IN) became the column of choice. The mobile phase consisted of a 5.5 mM citrate/potassium phosphate buffer† (pH 5.85) containing 1 mM dithiothreitol (DTT) and 10 mM GSH (Buffer A), and Buffer A containing 400 mM KCl (Buffer B). Two different but rapidly inter-convertible charge isomers of GST π may be obtained, depending on the GSH concentration in the mobile phase of the HPLC step [232]. The use of 10 mM GSH, as in this study, results in the purification of human placental GST primarily as conformer A (± 96% of recovered GST activity) [232]. All buffers for HPLC were degassed and filtered (0.22 μm) before use.

---

†19.7 ml of 25 mM citric acid & 30.3 ml of 50 mM dibasic potassium phosphate/100 ml

The enzyme solution was filtered (Millipore Millex GV 0.22 μm) before 500 μl (approximately 0.45 mg protein) aliquots were injected onto the column. Elution gradient was as follows: buffer A (1 ml/min) for 5 min; the percentage of buffer B was increased to 7.5% over 3 min and then to 100% over 1 min. At 16 min, the percentage of buffer B was decreased to zero over 2 min (1.5 ml/min), followed by re-equilibration with buffer A for 25 min. Fractions (1 ml) containing GST activity towards CDNB were pooled and dialysed overnight against 10 mM potassium phosphate buffer (pH 7.4) containing 1 mM DTT, to remove the GSH, before storage at 77 K.

2.4.2 Purification of Rat Hepatic GSH S-Transferase 2-2

This isoenzyme was selected for study because it is a homodimeric representative of the Alpha class of GSTs, for which detailed kinetic investigations have not yet been performed. Initially, attempts were made to isolate 2-2 from rat adrenal tissue, where it is the predominant GST isoenzyme [151]. The purification method used for adrenal tissue was analogous to that described below for isolating 2-2 from rat liver, except where otherwise specified.

Since isoenzyme 2-2 has been reported to be readily isolated using CM-cellulose chromatography [39], this step was central to the chosen purification method. A GSH-affinity column preceded the anion-exchange step, in order to remove non-GSH-specific proteins. The GSH-affinity step was modified from that described by Boyer *et al.* [40].

Male Long-Evans rats (180-200 g) were permitted free access to water and Epol laboratory chow (protein min 20%; fat 2.5%; fibre 6%; calcium 1.4%; phosphorus 0.7%) obtained from Epol Ltd., Goodwood, Cape, RSA.

Two animals were sacrificed by cervical dislocation, and their livers immediately excised and maintained at 4°C thereafter. Approximately 19 g of tissue was cut into small pieces, washed copiously with 25 mM sodium phosphate buffer (pH 9.4) to remove residual blood, minced and homogenised in the same buffer (± 25% homogenate). In the adrenal purification, one hundred rats were sacrificed to obtain 9 g of tissue. The cytosol was centrifuged at 12 250 *g* for 20 min in a Beckman L8-70 centrifuge, and the supernatant carefully removed without disturbing the floating lipid material. The supernatant was then centrifuged at 100 000 *g* for 60 min in the same centrifuge.

The GSH-affinity matrix was prepared as described earlier (Section 2.4.1). The supernatant from the previous step was poured through Whatman No. 1 filter paper into a beaker containing the GSH-affinity gel, equilibrated with 25 mM sodium phosphate buffer (pH 9.4). The slurry was gently stirred for 5-10 min. The coupled gel was then poured into a column (1 x 13 cm), which was then washed through, as soon as the gel had settled, with 25 mM sodium phosphate buffer containing 150 mM NaCl (pH 9.4) until protein (A_{280}) was no longer detected in the effluent (about four column volumes). The GST activity was eluted from the matrix with 25 mM sodium phosphate buffer containing 150 mM NaCl & 100 mM GSH (pH 9.4), and collected in 1 ml fractions. The flow rate was maintained at 0.5 ml/min throughout. Fractions with GST activity were pooled and dialysed overnight against 10 mM potassium phosphate buffer (pH 6.0).

Twenty grams of CM-Cellulose (Whatman CM-52) was prepared according to the manufacturers' instructions (method B), poured into a column (1.5 x 20 cm) and equilibrated with 10 mM potassium phosphate buffer (pH 6.0; μ = 0.1). Care was taken to ensure that the pH of the loaded and effluent buffer was the same to ensure thorough equilibration. The pH and ionic strength of the enzyme sample were corrected (if necessary) before application onto the column, and the gel was then rinsed with one column volume of the same buffer. The transferase isoenzymes were eluted with a 24 hr linear gradient of 0 to 75 mM KCl in 10 mM potassium phosphate buffer (pH 6.0), using LKB Bromma (Ultrograd 11300) gradient mixing apparatus. The flow rate was 0.5 ml/min, and 2.5 ml fractions were collected. Care was taken not to stop the flow through the column for more than 30 sec at any one time during the sample loading or buffer changing operations, to prevent local effects at the interfaces.

The active fractions were separately pooled and dialysed overnight against 10 mM potassium phosphate buffer containing 1 mM DTT (pH 7.4), to remove GSH before storage at 77 K.

2.5 STEADY-STATE KINETIC STUDIES

2.5.1 Initial Velocities in the Absence of Products

The steady-state kinetic experiments of Pabst *et al.* [215] using transferase 3-3 and DCNB were repeated. Similar studies were conducted with isoenzymes 3-3 and CDNB, and 3-4 with DCNB. The activity of the GST isoenzymes toward DCNB and CDNB was determined using the centrifugal analyser as described in Section 2.2. All solutions were prepared freshly each day, and isoenzymes (stored at 77 K) were thawed when required and allowed to stand for a fixed period of time prior to use. Grouped kinetic assays were designed to be performed on one day, using one enzyme sample. The enzyme sample was checked for any loss of activity after the experiment, and all enzymic assays were completed before the control non-enzymic reactions were begun.

Among the substrates commonly used to characterise the GSTs, the compound which has the highest specific activity with human placental GST is CDNB [100,232]. The steady-state kinetics of this isoenzyme were therefore investigated with this substrate. In order to determine the optimum range of substrate concentrations for the estimation of the kinetic parameters (and to ensure that the breakpoint in the expected biphasic kinetics was evident), a number of preliminary experiments were performed using different concentration ranges of GSH and CDNB. The ranges initially used were based on previously reported values of the apparent kinetic constants [16,100,186,216]. Once suitable ranges were determined, initial rate measurements were performed over an eight by eight matrix with respect to the concentrations of GSH (0.04-1 mM) and CDNB (0.1-1 mM) (192 data points). The steady-state kinetics of isoenzyme 2-2 using CDNB as substrate were investigated in a similar manner. The results of the steady-state studies using GST π and GST 2-2 are found in Sections 3.3.2 and 3.3.4, respectively.

The activity toward CDNB was determined using the centrifugal analyser as described in Section 2.2. DMSO was used as the solvent for CDNB, with the final DMSO concentration constant in all assays at 2% (v/v). Assays were performed in triplicate.

For visual assessment, the data were plotted according to the Lineweaver-Burk method, and approximate values of the apparent K_m and V_{max} for each substrate were obtained from the various plots and replots [252]. However, final parameter estimation was always carried out using non-linear least-squares optimisation. Non-linear least squares regression analyses were performed by the iterative method of Duggleby [82] using the software package *Enzfitter* (Elsevier-BIOSOFT) [167]. The initial parameter estimates required for the iterative process were either obtained from replots of the data, or were calculated by the computer program. Throughout this thesis, where a factor is indicated in the label of a figure axis, this is the number by which the values given on the axis must be multiplied to give the actual values observed.

2.5.2 Initial Velocities in the Presence of Product

The products of the reaction of GSH and CDNB are the conjugate, S-(2,4-dinitrophenyl)glutathione, and chloride ion. No inhibition by chloride, at concentrations of up to 0.1 M, has been observed towards rat liver GST 3-3 [132,215] or GST 1-1 [249]. The inhibition of human placental GST and rat liver GST 2-2 by 0.1 M chloride (as KCl) was investigated in the standard CDNB assay.

The inhibition of placental GST π by the CDNB•GSH conjugate (see Section 2.5.3 for method of preparation of the conjugate) was investigated with a five by five matrix of concentrations of GSH (0.15-1 mM) and CDNB (0.3-1 mM). Each point in the matrix was assayed in the absence of conjugate and at 35, 65 and 100 μM conjugate (300 data points). The GST assays were performed in the usual manner (see Section 2.2), and the inhibitor was added to the outer cuvette compartment, immediately prior to the addition of GSH (see Figure 2.1). The experimentally observed pattern of inhibition by the conjugate with respect to each substrate determined the choice of rate equations selected to model the initial velocity data in the presence of the conjugate. Estimates of the parameters of the rate equations were obtained from the various plots and secondary plots as described by Segel [252]. The experimental protocol for product inhibition studies using rat liver GST 2-2 was similar to that described for the human placental isoenzyme. The results of both these investigations are described in the Sections 3.3.3 and 3.3.5.

2.5.3 Synthesis of S-(2,4-Dinitrophenyl)glutathione

The product of the enzymatic conjugation of CDNB and GSH, S-(2,4-dinitrophenyl)glutathione, was synthesised and purified by the method of Schramm *et al.* [249].

Ten mmol of CDNB was suspended in 30 ml 50% (v/v) ethanol in water. Ten mmol of GSH was added in portions over a 40 min period to the solution, while stirring continuously. After each addition of GSH, 2.5 M NaOH was used to return the pH to the range 7-8. The progress of reaction was monitored by following the drop in pH and increase in A_{340} due to the formation of S-(2,4-dinitrophenyl)glutathione.

When the reaction was completed, the volume was reduced by about 50% under vacuum using a Corning rotary evaporator. Unreacted CDNB was removed by three extractions with ethyl ether. Ethanol was added to the aqueous solution to give a faintly turbid solution, and the reaction mixture was stored at 2°C for 48 hours.

The oily precipitate, containing S-(2,4-dinitrophenyl)glutathione and some unreacted GSH, was dissolved in water and loaded onto a 2.5 x 30 cm Sephadex G-50 column, equilibrated with water. Fractions (2 ml) containing the clearly-visible yellow band were collected and assayed for GSH. Glutathione was determined by the 5,5′-dithiobis(2-nitrobenzoic acid) (DTNB) assay [303]: a 0.1 ml sample was added to 1.5 ml 0.5 mM DTNB in 0.1 M phosphate buffer pH 6.5, and mixed thoroughly. After 5-30 min at room temperature, the absorbance at 412 nm was measured. Fractions which were free of GSH were then pooled and lyophilised. A quantitative solution of this material dried to constant weight gave the expected absorbance at 343 nm, consistent with the absence of CDNB and GSSG.

2.5.4 Model Fitting and Discrimination Between Rival Models

Alternative mathematical models were fitted to the experimental data by the BMDPAR (derivative-free) and BMDP3R Gauss-Newton non-linear least squares regression analysis subroutines of the BMDP statistical package (University of California, Los Angeles).

The regression function Y minimised for each model was

$$Y = \sum_{i=1}^{n} w_i(v_i - v'_i)^2$$

where v_i and v'_i are the experimental and predicted velocities, respectively, w_i is a weighting factor, n is the number of measurements and $v_i - v'_i$ is the residual in the *i*th point. An analysis of the error structure of the experimental data showed that variance increased with velocity but not necessarily in proportion to it; the inverse of the predicted variance (from regression analysis) at any observed experimental velocity was therefore used as a weighting factor at that point [91,212].

The adequacy of fit of a model was determined by the examination of parameter values, residuals, and the residual sum of squares, and discrimination between models was based on the criteria of Garfinkel *et al.* [90,91] and Mannervik [177]. In general, a good model should converge to meaningful parameter values with low standard deviations, and have a low residual sum of squares. The resultant residuals should have a normal distribution with a mean of zero, and should lack correlation with any of the dependent or independent variables.

2.6 EQUILIBRIUM BINDING OF GSH TO HUMAN PLACENTAL GST π

Equilibrium dialysis was used to evaluate the binding of GSH to human placental GST. The method was similar to that used for GST 3-3 [135], with modifications as described below.

Equilibrium dialysis cells were formed by sealing 0.5 ml of 10 μM human placental GST in a short length of prepared 10 mm dialysis tubing (Sigma, St.Louis, MO), and then submerging these cells in 1 ml aqueous GSH. The dialysis tubing was prepared according to the manufacturers' instructions. The buffer used for both enzyme and GSH, 50 mM sodium phosphate buffer (pH 7.3), was prepared anaerobically and contained 0.25 mM dithioerythritol (to prevent oxidation of GSH during equilibration [135]).

Seven different GSH concentrations (5-190 μM) were used. The concentration of radiolabelled GSH was kept constant (0.01 μM) in each cell, and the total concentration and specific activity of the ligand was varied by addition of unlabelled GSH. The specific activity of the undiluted [^{35}S]-GSH was 2.42 TBq/mmol (65.4 Ci/mmol) at the time of use.

The [^{35}S]-GSH concentration was determined before equilibration, which took place over 16 hr with shaking (12 rpm) at 25°C under anaerobic conditions. On equilibration, triplicate determinations of [^{35}S]-GSH were performed using 0.1 ml aliquots taken from both compartments of the dialysis cells. Aliquots were added to 5 ml of Beckman RV liquid scintillation cocktail and radioactivity was determined using a Packard TriCarb 4640 liquid scintillation counter. To obtain stable counts of radioactivity, the sulphydryl groups of GSH were blocked by the addition 10 mM *N*-ethylmaleimide to the scintillation vials before counting [135].

The data were fit to the Scatchard equation,

$$r = \frac{n\,[GSH]}{K_d + [GSH]}$$

where r = number of moles of GSH bound per mole of enzyme,
n = number of binding sites,
[GSH] = concentration of free GSH,
and K_d = average dissociation constant,

using non-linear least squares regression [167]. The results of this equilibrium binding study are presented in Section 3.4.

2.7 OPTIMISATION OF THE PREPARATION OF MP-8

Spectrophotometric studies were performed using a Varian Techtron 635 dual beam UV/visible spectrophotometer, calibrated for absorbance linearity and accuracy at 402 nm using the p-nitrophenoxide anion [4]. HPLC studies were performed at room temperature using a Spectra Physics SP-8700 system with both analytical and semi-preparative Microbondpak C18 columns. Eluates were monitored at 395 nm (for haem) or 225 nm (for peptide). HPLC buffers were as follows: buffer A, 0.1% trifluoroacetic acid in deionised water; buffer B, 0.1% trifluoroacetic acid in acetonitrile/deionised water (60/40 v/v). Elution was performed at a flow rate of 2 ml/min and gradients were either isocratic (50% A/50% B) or as specified below. Columns were washed with 100% acetonitrile.

2.7.1 Preparation of MP-8

Preparation of high purity MP-8 was essentially according to the method of Adams *et al.* [4]. The modifications to the published method, which are detailed below, arose from the optimisation of the MP-8 preparative schedule which was performed as part of this study (Section 2.7.2).

Two hundred milligrams of horse heart cytochrome-*c* was dissolved in 4 ml deionised water, and 5.5 mg pepsin (in 100 µl deionised water) was added. The pH of the stirred solution was lowered to 2.0-2.1 with 2 M HCl and the mixture was incubated for 15 min at 40 ± 0.05°C. A further 5.5 mg pepsin (in 100 µl deionised water) was then added and incubation carried out for 2 hours at 40°C. The pH of the reaction mixture was adjusted to 5 with concentrated ammonium hydroxide solution, and solid ammonium sulphate was added to the stirred solution on ice. When the first traces of cloudiness were noted, saturated ammonium sulphate solution was added dropwise to completely precipitate haem-containing material (leaving a colourless supernatant). The dark red precipitate was pelleted by centrifugation, drained thoroughly and redissolved in 0.5 ml deionised water. The pH was adjusted to 8.5 with concentrated ammonium hydroxide and the sample incubated at 40°C for 5 minutes. Trypsin (7.5 mg in 400 µl deionised water) was added with stirring, and the reaction was incubated for a further 20 minutes at 40°C.

The concentrated MP-8 solution, approximately 95% pure in terms of haem-peptide at this stage, was further purified by affinity chromatography to remove trypsin and MP-11-derived tripeptide [321]. The sample was poured onto a bovine serum albumin/CNBr-activated Sepharose 4B affinity column (1 x 10 cm), prepared according to the manufacturer's directions. The column was washed with five column volumes of 0.05 M ammonium bicarbonate (pH 7.5), before elution with 0.8 M ammonium hydroxide. Fractions containing the clearly-visible red band were collected and lyophylised.

Further purification of the MP-8 was performed by HPLC using buffers A and B above (43-55% buffer B over 12 minutes) on a semi-preparative reversed-phase C18 column. Prior to use in kinetic and binding studies, 1 mg samples of the lyophylised MP-8 preparation were routinely repurified (to remove trace amounts of MP-11) by analytical HPLC on an C18 column. This resulted in a product in which no impurities could be detected at either 395 nm (haem) or 225 nm (peptide).

2.7.2 **Kinetics of MP-11 Formation from Cytochrome-c**

In a recently published optimised preparative schedule for MP-8 [4], the peptic digestion of cytochrome-*c* is performed at 26°C and requires 8-10 hours for completion. In order to further refine the preparation of MP-8, the peptic digest (described above) was performed at 40°C and the conversion of cytochrome-*c* to MP-11 was monitored by analytical HPLC. Immediately prior to the second addition of pepsin, and at 30 minute time intervals thereafter, 1 μl samples were withdrawn from the incubation and diluted into 50 μl buffer A at 0°C.

These samples were injected onto an analytical HPLC column, and eluted isocratically (50% A/50% B) for 10 minutes, followed by a gradient increase to 100% B over 10 minutes. The results of this kinetic study are described in Section 3.5.

2.8 INTERACTION OF HUMAN PLACENTAL GST π AND MP-8

The methods of preparation of both human placental GST π and MP-8 have been described earlier in this chapter (Sections 2.4.1 and 2.7.1).

The interaction of monomeric MP-8 and GST were first examined by measuring the spectral and difference spectral changes observed on mixing, using an Hewlett Packard 8450A Diode Array Spectrophotometer. The kinetics of the reaction were then followed, utilising the decrease in A_{396nm}, under pseudo-first-order conditions ([MP-8] >> [GST]) at 22.5 ± 0.02°C. Kinetic studies were performed using a Varian Techtron 635 dual beam UV/visible spectrophotometer. This instrument was selected because of its exceptional photometric stability (drift after 2 hours stabilisation was less than 1×10^{-4} AU/h at 396 nm) and low noise level ($< 2 \times 10^{-4}$ AU peak to peak), factors which are of the utmost importance when carrying out multiphasic kinetic studies over small total absorbance changes (< 0.1 AU 396 nm). The reaction temperature in the cuvette was controlled to ± 0.02°C using a Colora circulating heater/cooler bath.

Each reaction was initiated by the addition of a fixed amount of enzyme (2×10^{-8} M) to solutions of varying concentration of MP-8 (10^{-7} to 10^{-6} M), equilibrated for 5 min in 10 mM potassium phosphate buffer (pH 7.0). For some reactions, the GST was preincubated with bilirubin (15 μM) or GSH (1 mM) for 15 minutes prior to the addition of the enzyme to the MP-8. Other kinetic runs were performed in the presence of 1 mM CDNB, which was added immediately prior to the initiation of the reaction.

The absorbance/time data were digitised prior to numerical analysis using *Enzfitter* [167]. Data were fitted to either single exponential ($Abs = A + Be^{-k^*t}$) or biexponential ($Abs = A + Be^{-k_1^*t} + Ce^{-k_2^*t}$) functions, and the statistical adequacy of the least-squares fits was assessed as described in Section 2.5.4. The results of these investigations are found in Section 3.6.

2.9 THE INHIBITION OF HUMAN PLACENTAL GST π BY MP-8

In order to further elucidate the spatial relationship between the binding site(s) and the catalytic site of the enzyme, the inhibition by MP-8 of the steady-state GST-catalysed conjugation between GSH and CDNB was investigated. Preparation of human placental GST and MP-8 was as detailed above, and the GST assay (activity towards CDNB) was performed as described in Section 2.2.

The time-dependent inhibition of the enzyme-catalysed conjugation of CDNB and GSH was monitored during the incubation of 0.4 μM MP-8 with 0.1 μM GST at 25 ± 0.02°C in 0.1 M potassium phosphate buffer (pH 6.5). Following initiation of the incubation, aliquots of the reaction mixture were assayed for enzyme activity with CDNB at various time intervals. Control incubations (no MP-8 present) were performed and the results of these were subtracted from those in the presence of inhibitor.

In addition, the effect of MP-8 on the steady-state kinetics of the enzyme-catalysed conjugation of GSH and CDNB was investigated. At each of several MP-8 concentrations (0, 0.5, 2 and 5 μM), assays were performed with either a fixed CDNB concentration (1 mM) and varying GSH (0.15 - 1 mM), or a fixed GSH concentration (1 mM) and varying CDNB (0.4 - 3 mM). Assays were performed as described in Section 2.5, except that 5% v/v DMSO (final) was used in the experiments at fixed GSH concentration, to accommodate relatively high CDNB concentrations. MP-8 was preincubated with the enzyme (20 nM) for 15 minutes prior to assay, allowing time for the reaction to proceed essentially to completion. The results of these studies are presented in Section 3.7.

3. RESULTS

3.1 PRELIMINARY EXPERIMENTS

The use of a centrifugal analyser in this investigation permitted the assessment of the linearity of initial rates for the GST-catalysed conjugation of GSH and CDNB from effectively zero reaction time (see Figure 3.1). The residuals that resulted from a fit of the initial rate data over 0-60 seconds to a straight-line function were randomly scattered about the mean (m = 2; n = 3; runs = 6), while systematic non-randomness was observed for the data over a 0-180 seconds period (m = 8; n = 11; runs = 3). Fitting the 0-180 seconds data of Figure 3.1 to a quadratic function resulted in a random distribution of residuals. Curvature was always evident 50-70 seconds after the initiation of reaction with all the rat and human GST isoenzymes used. Rates at 2 and 3 minutes were 90% and 83% of the initial rate (see Figure 3.1). Consequently, initial rates were measured over the first 60 seconds of the reaction, during which time the reaction was apparently linear ($r \geq 0.999$). Albumin (120 μM) diminished but did not eliminate the curvature of the absorbance *versus* time plots over 180 seconds (see Figure 3.1 and Discussion).

Using the centrifugal analyser, the enzymatic reaction rate of the GST isoenzymes investigated was found to be a linear function of enzyme concentration for 60 seconds after initiation, when the rate of absorbance change was limited to a less than 0.15 per minute (for a pathlength of 0.5 cm). The centrifugal analyser was found to give a photometrically linear response over the range of absorbance values of the dichromate concentrations investigated.

Because the 0-60 second time period was found to be insufficient for the determination of non-enzymic reaction rates, these were measured at 30 second intervals over 5 minutes. Background rates were found to be uniformly linear over this period with both the centrifugal analyser and the Techtron 635 spectrophotometer.

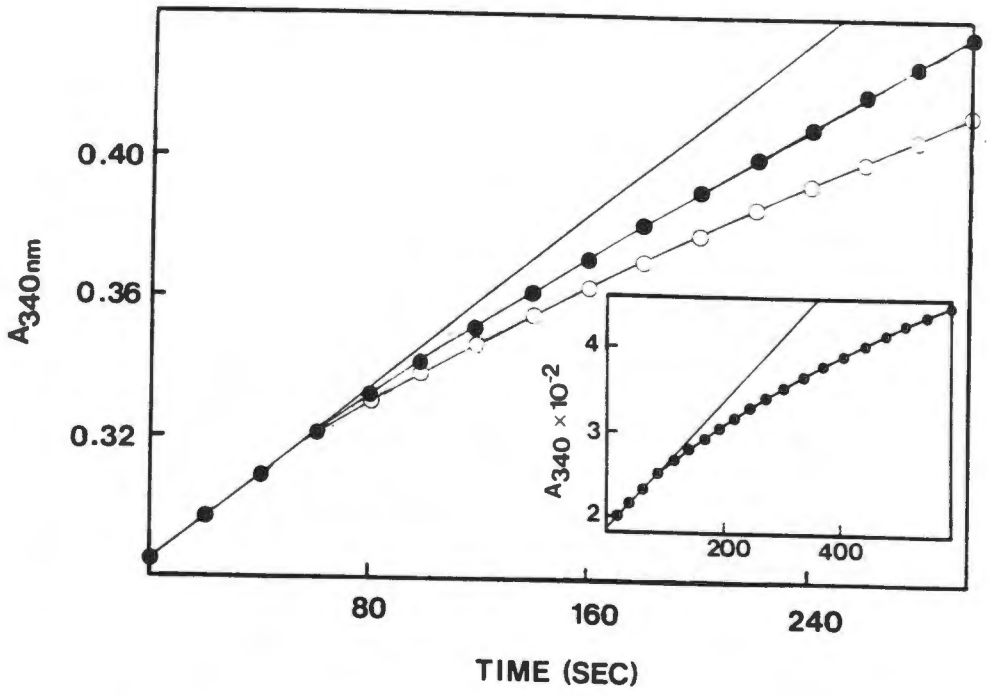

Figure 3.1 : **Linearity of CDNB Assay with Time**

Data shown are for rat liver GST 3-3, although similar results were observed with the other rat and human GST isoenzymes studied. In both the standard assay (○) and when 120 μM bovine serum albumin was added (●), GSH and CDNB were both 1 mM. The straight line represents the tangent to the initial rate. Inset shows another data set, generated under similar conditions, over 10 min (time axis in seconds).

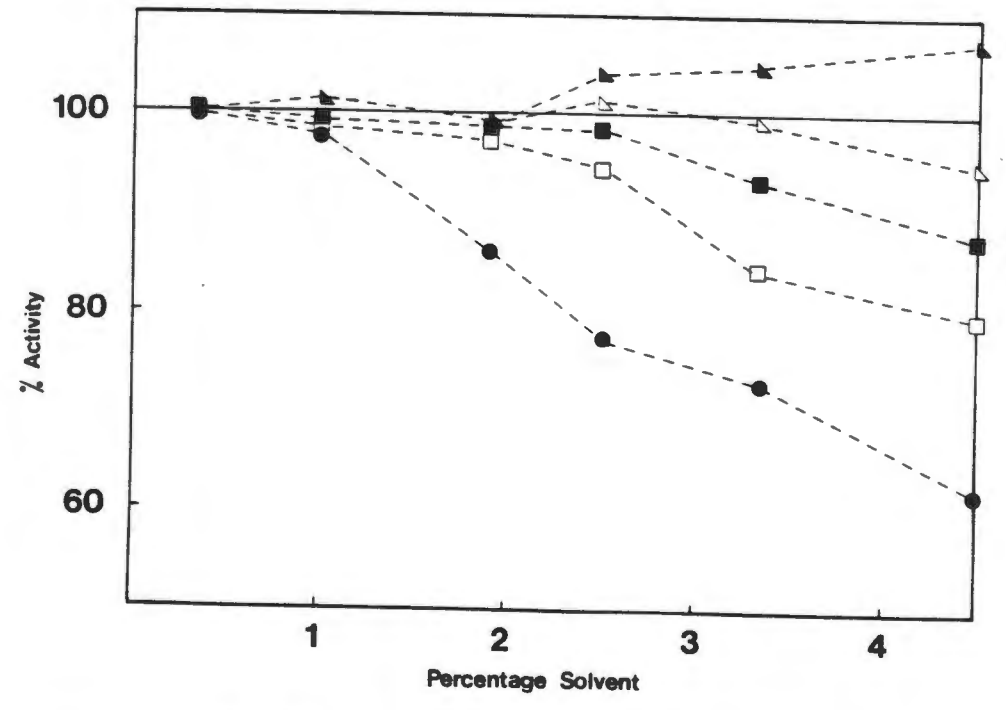

Figure 3.2 : **The Effect of Solvent on the DCNB Assay**

The different solvents used as the vehicle for DCNB were ethanol (●), THF (□), acetone (■), DMSO (◺) and DME (◣). The data shown are for human placental GST π, with 1 mM GSH and 0.1 mM DCNB. Solvent concentrations are expressed as final percentages (v/v). The percentage activity is that remaining of the enzymic activity at the lowest concentration of each solvent (taken to be 100%).

The effects of various organic solvents, used as vehicles for substrates in the CDNB and DCNB assays, on the activity of purified human placental GST are shown in Figure 3.2. The previously reported inhibition of rat liver cytosolic GST activity by ethanol [7,134] was confirmed for the purified isoenzymes studied, and was found to be concentration dependent. All the other solvents tested were less inhibitory than ethanol, and activity towards CDNB seemed to be affected by solvent choice to a lesser extent than DCNB. Both Acetone and DMSO were approximately equivalent, in that no inhibition of CDNB activity, and only slight inhibition of DCNB activity (94% at 4.5% v/v for rat liver isoenzyme 3-3) was observed. DMSO was used as the vehicle for CDNB and DCNB in all further studies, at a concentration of 2% (v/v).

The GST activity of both the purified isoenzyme 3-3 and the commercial rat liver GST mixture was enhanced (by between 8 and 22%) when GSH was added to the cuvette compartment containing the enzyme sample, even though the two were added only 1-2 minutes before assay. When the GST was prepared in buffer containing 0.1 mM or 0.5 mM GSH, and allowed to stand for 5 minutes before assay, the activities were 108% and 114%, respectively, of that of controls prepared in buffer without GSH. Consequently, all assays were initiated by the addition of enzyme, as described in Section 2.2, in order to minimise the effects of the variable enzyme activation by GSH.

Despite the observation in this laboratory that the activity of several rat and human GST preparations seemed greater when water, rather than 0.1 M potassium phosphate buffer (pH 6.5), was used as a diluent, no significant difference was observed in the activity of human placental GST when the enzyme was prepared in either diluent. Dilutions were therefore prepared in phosphate buffer.

The unusual pattern of inhibition and activation of hepatic GSTs by ethylene dibromide (EDB) that has been previously reported from this laboratory [130] was confirmed using the present assay system. As shown in Figure 3.3, EDB inhibited GST activity at lower CDNB concentrations and activated the same at higher CDNB concentrations. A possible mechanistic model for this mixed inhibition has been proposed [130].

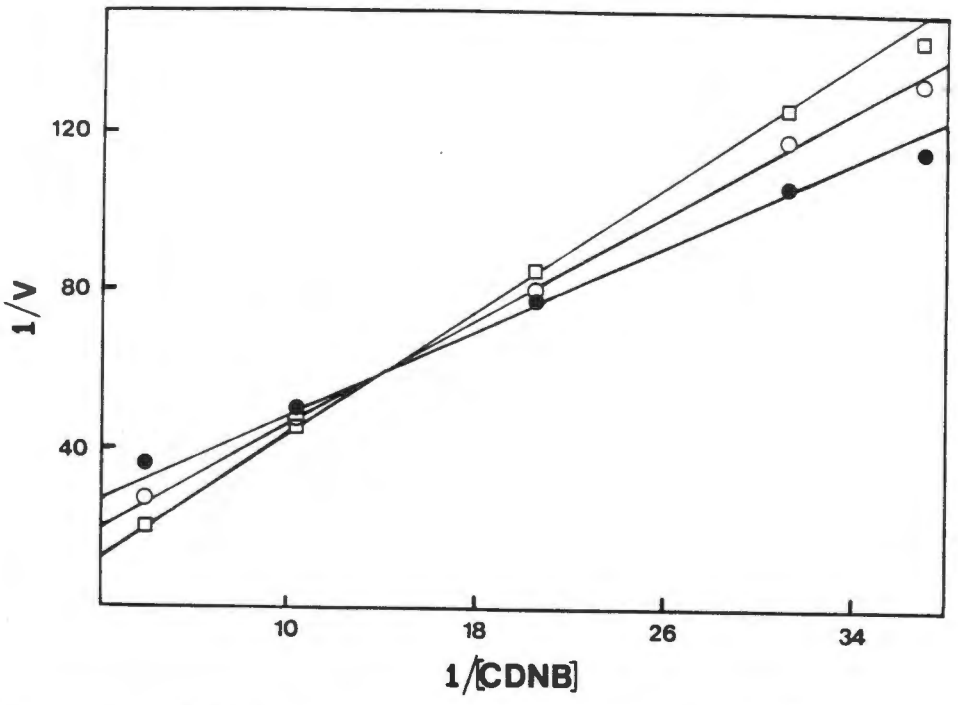

Figure 3.3 : **Inhibition and Activation of GST 3-3 by EDB**

GSH concentration was 1 mM in all assays. Concentrations of CDNB were 0.027, 0.032, 0.049, 0.097 and 0.259 mM. EDB was dissolved in ethanol at either 6 mM (○) or 10 mM (□). Ethanol was 2% (v/v) in these and in control (●) assays. Initial rates (v) are in ΔA_{340nm}/minute.

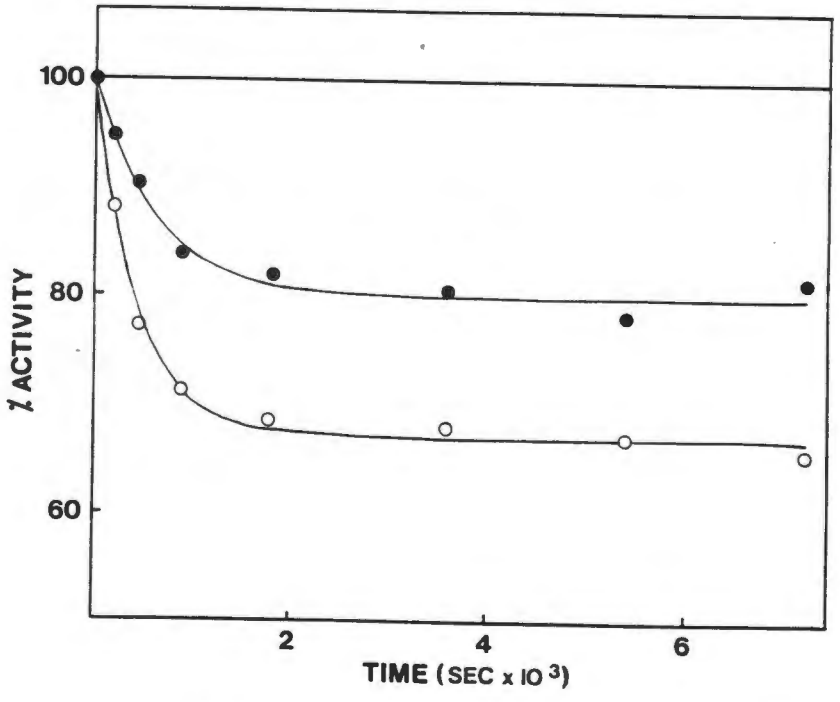

Figure 3.4 : **The Variation in GST Activity During Incubations of EDB with DNA**

GST activity was monitored with CDNB at various times during a 2 hour incubation (37°C) of Sigma rat liver GST mixture (0.2 mg), DNA (0.2 mg), EDB (5 mM) and either 2 mM (○) or 15 mM (●) GSH. The percentage activity is that remaining of the enzymic activity at time zero (taken to be 100%). Data represent the means of triplicate determinations with controls subtracted. The lines drawn are those predicted by fitting the data to the equation $A = A_i + A_d e^{-kt}$, using non-linear least squares regression analysis.

In the presence of EDB, a gradual loss of activity over 2 hours was observed for the commercial rat liver GST mixture at both 2 mM and 15 mM GSH (see Figure 3.4). The loss of activity followed pseudo-first-order kinetics, with rate constants at both 2 mM and 15 mM GSH in close agreement ($2.25 \times 10^{-3} \pm 2.54 \times 10^{-4}$ s^{-1} and $1.64 \times 10^{-3} \pm 3.42 \times 10^{-4}$ s^{-1}, respectively). The extent of the activity loss was greater in the presence of EDB plus 2 mM GSH than EDB plus 15 mM GSH. This may be related to the finding that GSH concentrations above 10 mM resulted in less EDB binding to DNA than GSH concentrations of 2 mM [127]. The implications of this inhibition for GST-mediated toxicity of EDB is discussed in Section 4.2.

The results of the experiments to determine the GSH-mediated binding of [^{14}C]-EDB to DNA, using four different GST sources, are shown in Table 3.1. The neutral human lung GST exhibited the highest activity of those isoenzymes studied. The activities of the human GSTs are considerably greater than the values previously reported for rat isoenzymes [127].

Table 3.1 : **GSH-Mediated DNA-Binding of EDB Catalysed by Different GST Isoenzymes**

GST Isoenzyme per mg DNA	pmol EDB bound
Sigma Rat Liver Mix	4713 ± 133
Human Lung Acidic	3683 ± 184
Human Lung Neutral	5164 ± 535
Human Lung Basic	2206 ± 49

Incubations (100 µl) containing 0.2 mg DNA, 2 mM GSH, 5 mM [^{14}C]-EDB (specific activity 185 MBq/mmol) and 15 µg GST were at 37°C. Each value is the mean ± SD of duplicate determinations.

3.2 GSH S-TRANSFERASE ISOENZYME PURIFICATIONS

3.2.1 Purification of Human Placental GSH S-Transferase π

Table 3.2 summarises the results of a typical purification of human placental GST by the method described in Section 2.4.1. The elution profile of the GSH-affinity column (depicted in Figure 3.5) indicates that a large amount of non-GST protein was efficiently eliminated by this step; no significant GST activity was found in the protein-containing effluent prior to elution. The results achieved by GSH-affinity chromatography (specific activity of 98.4 μmol/min/mg, 94% recovery and 364-fold purification) are comparable with those of previous workers who have used this technique to purify human placental GST [231,232,308].

A typical chromatographic profile for the HPLC separation obtained using the Synchrom AX-300 column is shown in Figure 3.6. Approximately 97% of the recovered activity was present in the major peak (retention time 5.68 min), while other peaks represented 2% (R_T 3.7 min) and 1% (R_T about 12 min) of the activity. This profile is similar to the corresponding profiles of Radulovic and Kulkarni [231,232]. It was found necessary to equilibrate the column extensively between runs for good profile reproducibility.

The presence of a single band on SDS-PAGE with approximate subunit apparent M_r 21 500 (Figure 3.7) suggested that the enzyme had been purified to homogeneity. The specific activities of the placental GST isoenzyme were as follows: CDNB, 133; DCNB, 0.06; cumene hydroperoxide, 0.04; and ethacrynic acid, 1.3. These values are in good agreement with previously published specific activities [100,186,308].

Table 3.2 : **Summary of Human Placental GST Purification**

Step	Volume of Fraction (ml)	Protein Concentration (mg/ml)	Total Activity‡ (μmol/min)	Specific Activity (μmol/min/mg)	Yield (%)	Purification Factor Fold
Supernatant	263	6.99	493.13	0.27	100	1
Affinity Chromatography	47	0.10	462.30	98.36	94	364
Ultrafiltration	3.4	0.91	312.03	100.85	63	374
HPLC	19.5	0.10	259.45	133.05	53	493

‡Activity measured at 30°C and pH 6.5 using 1 mM CDNB and 1 mM GSH.

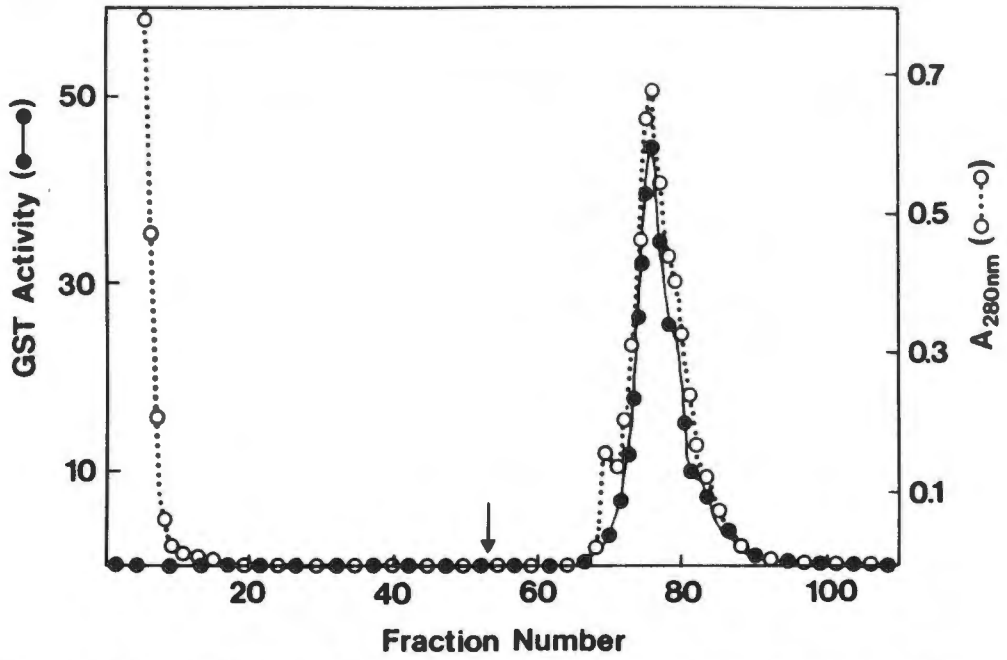

Figure 3.5 : **GSH-Affinity Chromatography of Human Placental GST**
Approximately 400 U of GST activity was applied to the GSH-affinity column (2.2 x 13 cm). The flow rate was maintained at 0.5 ml/min, and 1 ml fractions were collected. Elution (which began where indicated by an arrow) was with 50 mM Tris.HCl containing 10 mM GSH. No GST activity was observed in the effluent prior to elution. GST activity is in μmol/min/ml.

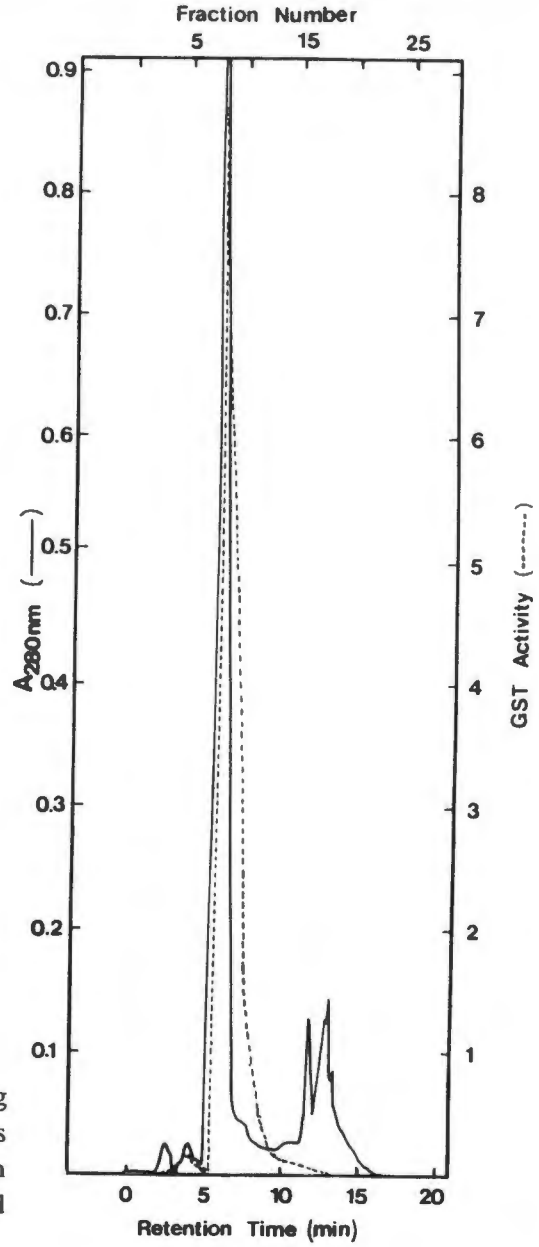

Figure 3.6 : **HPLC Separation of Human Placental GST**
500 μl of concentrated GSH-affinity eluent (approximately 0.45 mg protein) was applied to the Synchrom AX-300 column. The sample was previously dialysed against 10 mM GSH, which was also the concentration in the mobile phase during HPLC. The flow rate was 1 ml/min, and 0.75 ml fractions were collected. GST activity is in μmol/min/ml.

3.2.2 Purification of Rat Hepatic GSH S-Transferase 2-2

Although GST 2-2 is the predominant isoenzyme in rat adrenal gland [151], the total recovery of GST activity from this tissue was found to be too low for practical enzyme isolation (data not shown). It was decided to purify GST 2-2 from rat liver, where the overall GST content is much greater, even though GST 2-2 represents proportionally less of the total tissue GST activity.

Table 3.3 summarises the results of a purification of GST 2-2 from rat liver. The GSH-affinity column resulted in a 17-fold purification, with a recovery of 53.7% total initial activity. The elution profile of the separation on the CM-cellulose column, shown in Figure 3.8, was comparable to previously reported CM-cellulose elution patterns which were run under similar conditions [103,108]. The first peak of GST activity (labelled X), which passed through in the eluant volume, comprised the anionic transferase isoenzymes, which do not bind to CM-cellulose. The last peak eluted (peak 5) corresponded to transferase 2-2 in terms of elution position and substrate specificities. The intermediate peaks, which were not characterised fully, were not well separated (see Figure 3.8 and the gel in Figure 3.7), and probably represented overlapping activities of GSTs 4-4, 5-5, 3-4, 1-2 and 3-3. However, since GST 2-2 is clearly separated from the other isoenzymes by CM-cellulose chromatography [39], the other GST activities were not of great concern.

The results of SDS-PAGE (Figure 3.7) suggested that GST 2-2 had been purified to homogeneity (homodimer with approximate subunit apparent M_r 24 500). The specific activities of GST 2-2 were as follows: CDNB, 18.2; DCNB, 0.01; cumene hydroperoxide, 6.7; and ethacrynic acid, 0.6, in good agreement with previously published values [9,40].

Table 3.3 : **Summary of Rat Liver GST 2-2 Purification**

Step	Volume of Fraction (ml)	Protein Concentration (mg/ml)	Total Activity‡ (μmol/min)	Specific Activity (μmol/min/mg)	Yield (%)	Purification Factor Fold
Supernatant	9	22.78	645.31	0.48	100	1
Affinity Chromatography & Dialysis	19	2.26	346.87	8.08	53.7	17
CM-Cellulose (Peak 5)	35	0.08	6.51	18.23	1	38

‡Activity measured at 30°C and pH 6.5 using 1 mM CDNB and 1 mM GSH.

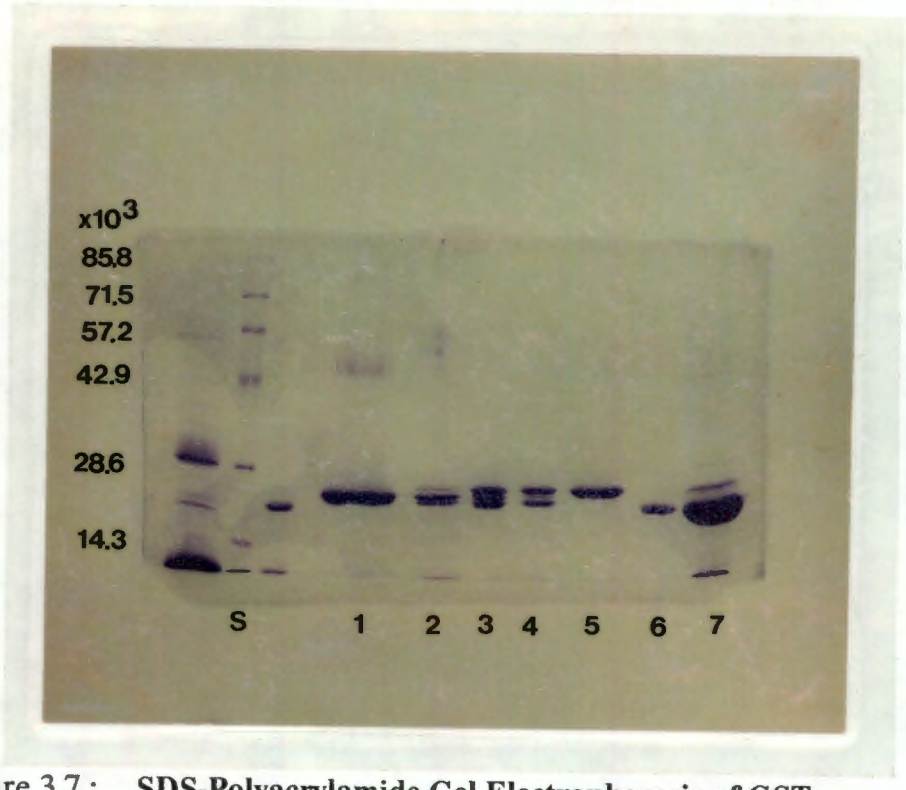

Figure 3.7 : **SDS-Polyacrylamide Gel Electrophoresis of GSTs**

The GSTs were purified and analysed by SDS-PAGE as described in the text. Proteins were applied to the gel as follows: Channel S - protein standards with M_r values of 14 300, 28 600, 42 900, 57 200, 71 500, & 85 800. Channels 1 to 5 contain GST peaks 1 to 5 from CM-cellulose column chromatography of rat liver (see text and Figure 3.8). Channel 6 contained GST π, from HPLC column of the purification of human placental GST, and channel 7 contained the newly available (and recently discontinued) commercial preparation (Sigma) of human placental GST. Approximately 10 μg of each protein was applied to the gel. Approximate M_r values for GST isoenzymes 2-2 and π were 24 500 and 21 500, respectively.

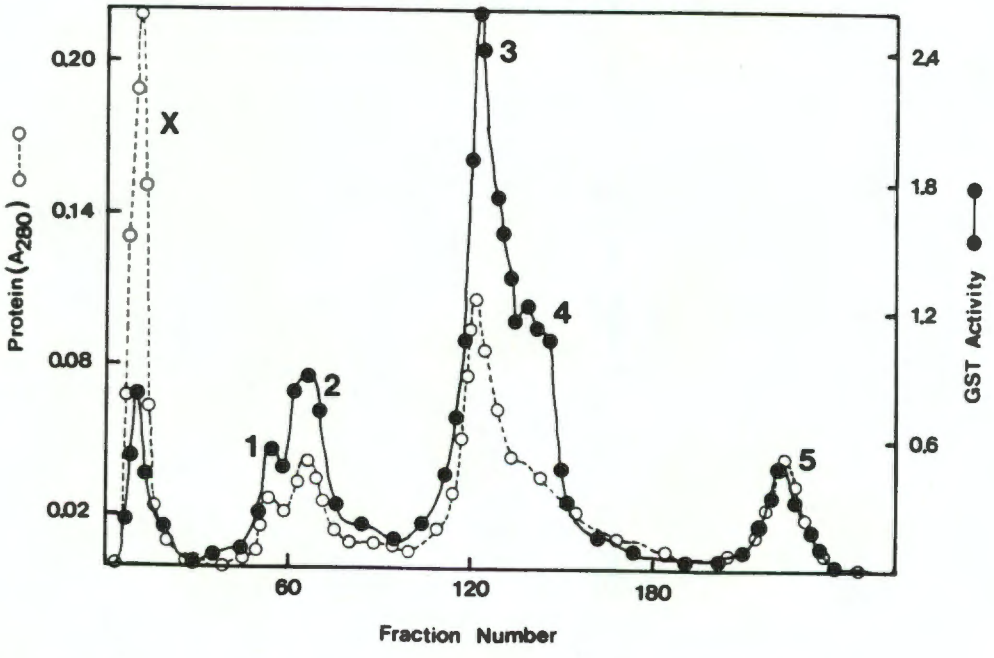

Figure 3.8 : **CM-Cellulose Chromatography of Rat Liver GST**

A 24 hour linear KCl gradient (0-75 mM) was used to elute transferase activity from a CM-cellulose column (1.5 x 20 cm). The flow rate was 0.5 ml/min, and 2.5 ml fractions were collected. GST activity is in μmol/min/ml.

3.3 STEADY-STATE KINETIC STUDIES

3.3.1 Rat Liver GST Isoenzymes 3-3 and 3-4

Families of non-linear concave-down plots were found for the conjugation of CDNB by isoenzyme 3-3 and of DCNB by isoenzyme 3-4 when initial rates were measured over extended substrate ranges (Figures 3.9 and 3.10). Although sufficient data for detailed mechanistic modelling were not collected, the general rate equation for a steady-state random sequential mechanism (Eqn. 5 of Table 3.4) was found to be capable of fitting the data. Although at best two parameters were redundant in the model it provided a better fit, by the criteria of Mannervik [177] for goodness of fit and discrimination between rival models, than the branched reaction scheme of Pabst *et al.* [215] or the rapid equilibrium random Bi Bi mechanism.

The non-linear concave-down double-reciprocal plots of kinetic data for the GSTs are consistent with negative co-operativity. In phenomenological terms [cf. 249], the kinetics of the metabolism of DCNB and CDNB by rat liver GST 3-3 and of DCNB by GST 3-4 exhibit negative co-operativity: Hill plots generated from the data of Pabst *et al.* [215] and the data from Figures 3.9 and 3.10 exhibit Hill coefficients (average $n_{apparent}$ values) of 0.65-0.80 (Figure 3.11). Since linear equilibrium binding Scatchard plots for GSH have been reported for GST iso-enzymes 1-2 and 3-3 [135,292], and for human placental GST (see Section 3.4), it appears that the negative co-operativity of the GSH S-transferases is kinetically generated (see also Section 4.3).

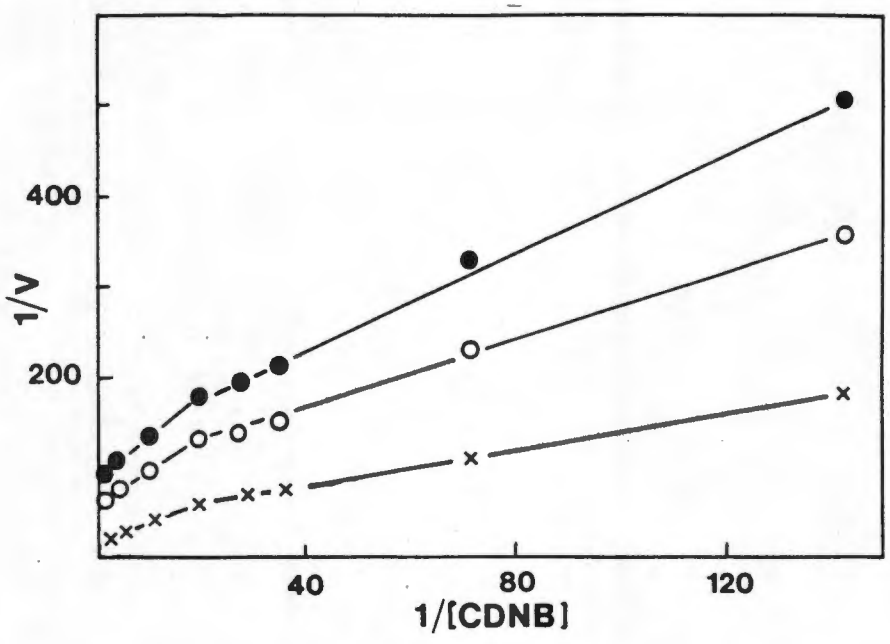

Figure 3.9 : **Reciprocal Plot of Initial Rate Data for Rat Liver GST 3-3 and CDNB.**

With CDNB as the varied substrate, GSH concentrations were (●) 0.05, (○) 0.15 and (×) 1 mM. Velocities are expressed in nmol/min/ml. Enzyme concentration was 0.1 μM. Data points represent the means of triplicate determinations. Lines drawn are those predicted by fitting the data to a steady-state random sequential Bi Bi mechanism using the BMDP program.

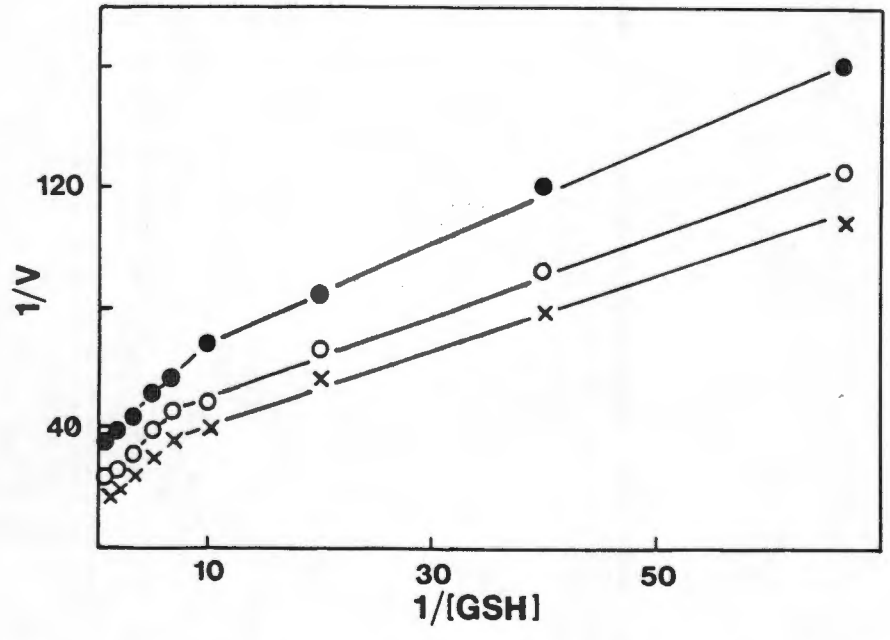

Figure 3.10 : **Reciprocal Plot of Initial Rate Data for Rat Liver GST 3-4 and DCNB.**

With GSH as the varied substrate, DCNB concentrations were (●) 0.2, (○) 0.4 and (×) 0.6 mM. Velocities are expressed in nmol/min/ml. Enzyme concentration was 0.2 μM. Data points represent the means of triplicate determinations. Lines drawn are those predicted by fitting the data to a steady-state random sequential Bi Bi mechanism using the BMDP program.

The apparently anomalous biphasic kinetics observed previously for GST 3-3 with DCNB [132,215], and in this investigation for GST 3-3 with CDNB and GST 3-4 with DCNB, are discussed in Section 4.3. This discussion includes a demonstration that the basic steady-state random sequential Bi Bi mechanism under initial rate conditions is the simplest mechanism consistent with and sufficient to explain the non-hyperbolic kinetics of these GST isoenzymes.

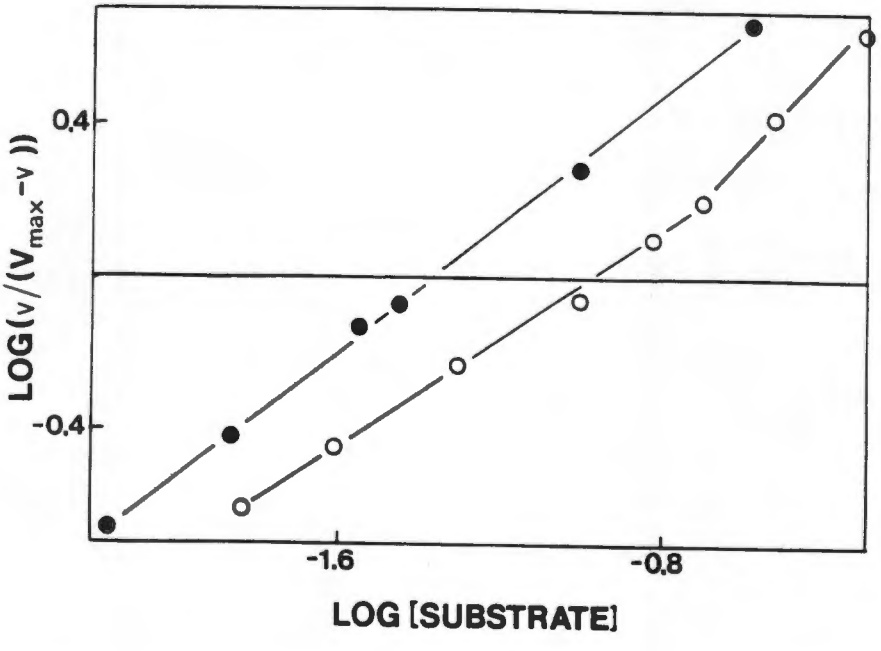

Figure 3.11 : **Hill Plot of Rat Liver GST Activity**
Isoenzyme 3-3 for variable CDNB concentration, at 0.05 mM GSH (●); isoenzyme 3-4 for variable GSH concentration at 0.2 mM DCNB (○).

3.3.2 Human Placental GST π - Initial Velocities in the Absence of Products

In preliminary experiments, double-reciprocal plots of initial velocity data were linear over a 10^3-fold range of GSH (1 μM - 1 mM) at concentrations of CDNB ranging from 0.1-1 mM. Subsequently, initial rate measurements performed over an eight by eight matrix with regard to the concentrations of GSH (0.04-1 mM) and CDNB (0.1-1 mM) (192 data points) gave rise to linear double-reciprocal plots *versus* both substrates (Figure 3.12).

Initial estimates of $K_{m\ app}$ and $V_{max\ app}$ were obtained from the double-reciprocal plots and refined by non-linear regression analysis. Replots of the slope and intercept *versus* the reciprocal of the concentration of the alternate substrate (Figure 3.13) provided estimates of other parameters. These initial parameter estimates were used in further data analysis by non-linear regression (BMDPAR).

The results of fitting five rate equations to the initial rate data are shown in Table 3.4. Included therein are the rate equations, the calculated parameter values and assessments of goodness of fit. In general, a good model should exhibit proper convergence to meaningful parameter values with low standard deviations, a random distribution of residuals which lack correlation with the variables, and a small residual sum of squares [177]. The velocities predicted by fitting the rate data to Eqn. 4 with the BMDPAR program were used to generate the lines in Figures 3.12 and 3.13.

When the initial rate data were fitted to the two rate equations for a rapid equilibrium ordered bireactant system (Eqns. 1 and 2), only the function describing a kinetic system with GSH binding first gave a reasonable fit to the data (Table 3.4). The alternative model exhibited standard deviations for two parameters in excess of 100% and a large residual sum of squares and mean square error.

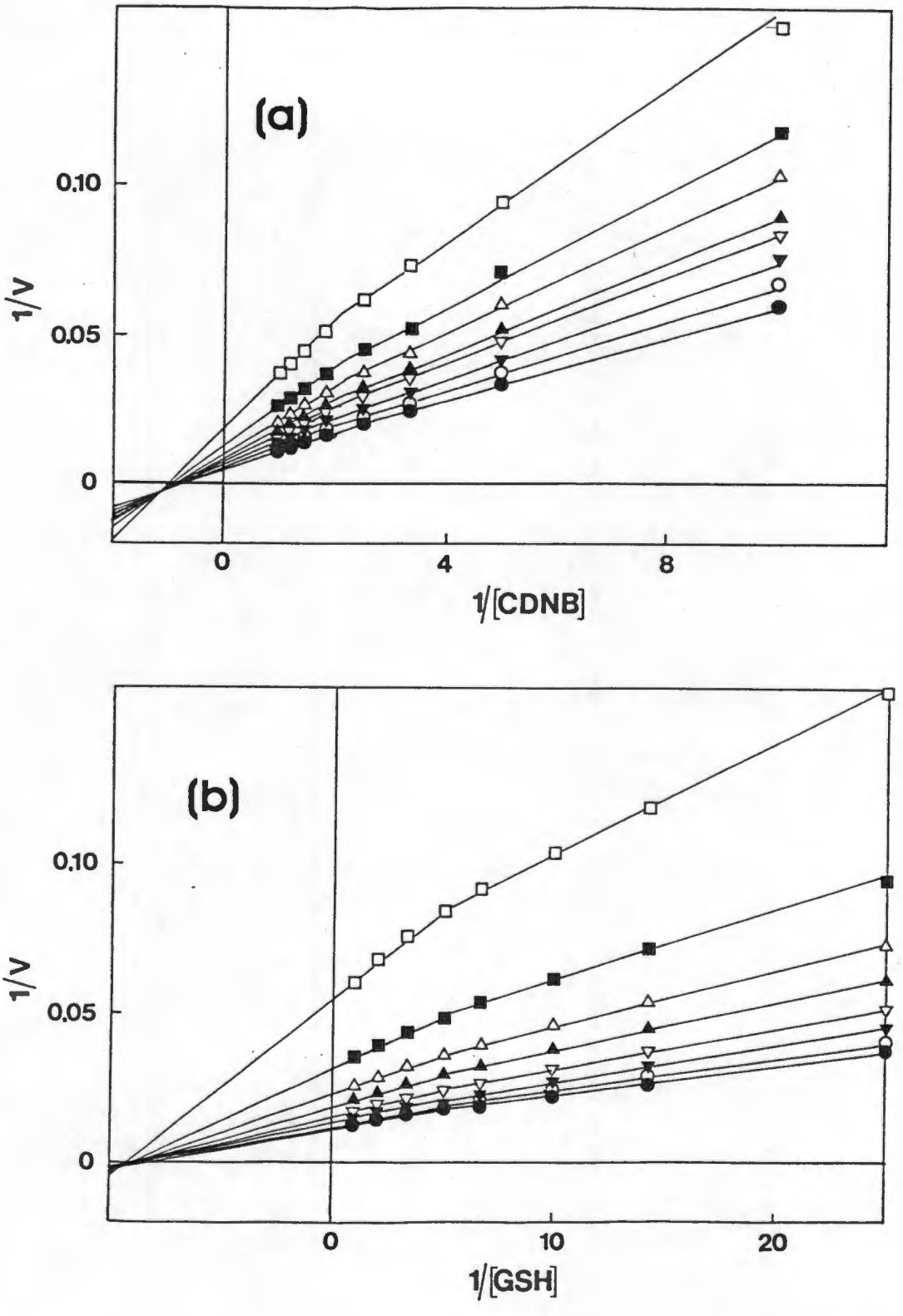

Figure 3.12 : **Reciprocal Plots of Initial Rate Data in the Absence of Product for Human Placental GST.**

(a) With CDNB as the varied substrate, GSH concentrations were (□) 0.04, (■) 0.07, (○) 0.1, (●) 0.15, (◿) 0.2, (◢) 0.3, (△) 0.5, (▲) 1 mM. (b) With GSH as the varied substrate, CDNB concentrations were (□) 0.1, (■) 0.2, (○) 0.3, (●) 0.4, (◿) 0.55, (◢) 0.7, (△) 0.85, (▲) 1 mM. Velocities are expressed in nmol/min/ml. Enzyme concentration was 2 nM. Data points represent the means of triplicate determinations. Lines drawn are those predicted by fitting the data to a rapid equilibrium random Bi Bi mechanism using the BMDP program.

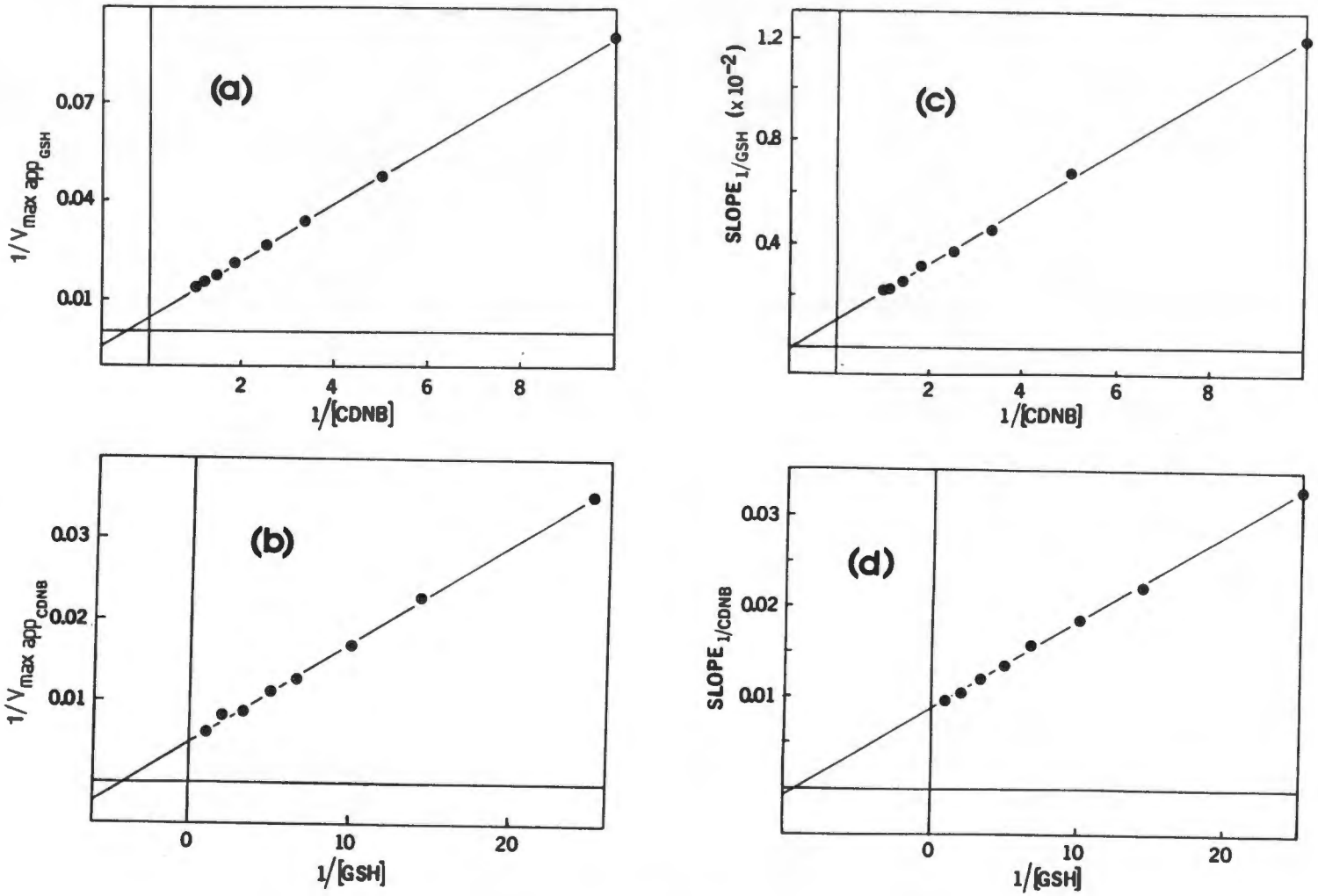

Figure 3.13 : **Secondary Plots of Initial Rate Data of Figure 3.12**
(a) $1/V_{max\ app\ GSH}$ *vs* 1/CDNB (b) $1/V_{max\ app\ CDNB}$ *vs* 1/GSH
(c) $Slopes_{1/GSH}$ *vs* 1/CDNB (d) $Slopes_{1/CDNB}$ *vs* 1/GSH.
Lines are generated as in Figure 3.12. The initial parameter estimates needed for non-linear regression analysis were obtained from these replots as follows: from the $1/V_{max\ app\ GSH}$ *vs* 1/CDNB plot, y-intercept = $1/V_{max}$, x-intercept = $-1/\alpha K_{CDNB}$; from the $Slopes_{1/GSH}$ *vs* 1/CDNB plot, x-intercept = $-1/K_{CDNB}$; from the $1/V_{max\ app\ CDNB}$ *vs* 1/GSH plot, x-intercept = $-1/\alpha K_{GSH}$.

Table 3.4 : **Comparison of the Fitting of Bireactant Reaction Mechanisms to Initial Rate Data for Human Placental GST π**

MECHANISM	RATE EQUATION	EQN	PARAMETER VALUES (± STD.DEV.)	RESIDUAL SUM OF SQUARES	MEAN SQUARE ERROR
RAPID EQUILIBRIUM ORDERED BI BI - GSH BINDS FIRST	$v = \frac{V_{max}AB}{K_AK_B + K_BA + AB}$	1	$V_{max} = 125.5 \pm 4.4$ $K_A = 0.29 \pm 0.01$ $K_B = 0.79 \pm 0.05$	4988.9	26.4
RAPID EQUILIBRIUM ORDERED BI BI - CDNB BINDS FIRST	$v = \frac{V_{max}AB}{K_AK_B + K_AB + AB}$	2	$V_{max} = 86.7 \pm 7.1$ $K_A = 0.006 \pm 0.039$ $K_B = 46.8 \pm 199.4$	83375.1	441.1
STEADY-STATE ORDERED BI BI‡	$v = \frac{V_{max}AB}{K_{ia}K_{mB} + K_{mA}B + K_{mB}A + AB}$	3	$V_{max} = 216.7 \pm 10.2$ $K_{ia} = 0.125 \pm 0.006$ $K_{mA} = 0.26 \pm 0.02$ $K_{mB} = 1.82 \pm 0.11$	1403.5	7.5
RAPID EQUILIBRIUM RANDOM SEQUENTIAL BI BI‡	$v = \frac{V_{max}AB}{\alpha K_AK_B + \alpha K_AB + \alpha K_BA + AB}$	4	$V_{max} = 216.7 \pm 10.2$ $K_A = 0.125 \pm 0.006$ $K_B = 0.87 \pm 0.07$ $\alpha = 2.09 \pm 0.27$	1403.5	7.5
STEADY-STATE RANDOM SEQUENTIAL BI BI	$v = \frac{V_1AB + V_2A^2B + V_3AB^2}{K_1 + K_2A + K_3B + AB + K_4A^2 + K_5B^2 + K_6A^2B + K_7AB^2}$	5	$V_1 = 77.7 \pm 34.0$ $V_2 = 73.5 \pm 36.5$ $V_3 = 0 \pm 0$ $K_1 = 0.13 \pm 0.06$ $K_2 = 0.5 \pm 0.4$ $K_3 = 0 \pm 0$ $K_4 = 0.7 \pm 0.3$ $K_5 = 0 \pm 0$ $K_6 = 0 \pm 0$ $K_7 = 0 \pm 0$	3118.27	17.04

‡These two mechanisms cannot be distinguished by computer modelling (see text).
GSH and CDNB correspond to A and B, respectively, in the equations given in the table. Units of concentration and velocity are mM and nmol/min/ml respectively.
Equations from references 179 and 252.

The steady-state ordered Bi Bi mechanism (Eqn. 3) cannot be distinguished from a rapid equilibrium random mechanism by computer modelling since the rate equations are identical where $K_{ia} = K_A$, $K_{mA} = \alpha K_A$ and $K_{mB} = \alpha K_B$ (see Table 3.4). Therefore, these models give equivalent fits to the data [252]. Both models rapidly converged to the lowest residual sum of squares and mean square error values and gave meaningful parameter values with low standard deviations. These values were close to the estimates obtained from the plotted data (Table 3.4, and Figures 3.12 and 3.13). Very similar parameter values and error estimates were obtained when no weighting procedure was used in fitting the data to the rapid equilibrium random mechanism (data not shown).

Modelling the steady-state random Bi Bi mechanism (Eqn. 5) resulted either in convergence with a larger residual sum of squares than the rapid equilibrium random model (Eqn. 4, Table 3.4), or in a smaller residual sum of squares but no convergence and a non-random distribution of residuals. All attempts to fit the steady-state model resulted in several redundant parameters (parameters with values of zero or not significantly different from zero).

The kinetic data were best fitted by the rapid equilibrium random equation or the equivalent steady-state ordered mechanism. This model exhibited the lowest residual sum of squares, meaningful parameter values with low standard deviations and a random distribution of residuals.

3.3.3 Human Placental GST π - Initial Velocities in the Presence of Product

The products of the reaction of GSH and CDNB are the conjugate, S-(2,4-dinitrophenyl)glutathione, and chloride ion. As previously reported for GST isoenzymes 3-3 [132,215] and 1-1 [249], no significant inhibition of human placental GSH S-transferase by chloride ion was apparent at concentrations of up to 0.1 M (data not shown). The finding that chloride ion was too weak an inhibitor for product inhibition studies [132,215,249] was therefore confirmed.

The initial rate data for the inhibition of GST π by the conjugate were plotted as double-reciprocal plots with varying substrate concentration at fixed co-substrate concentration. The families of lines on each plot represent different inhibitor concentrations; two examples are shown in Figure 3.14. Replots of the slope *versus* inhibitor concentration are shown in Figures 3.15a and b. Secondary replots of the

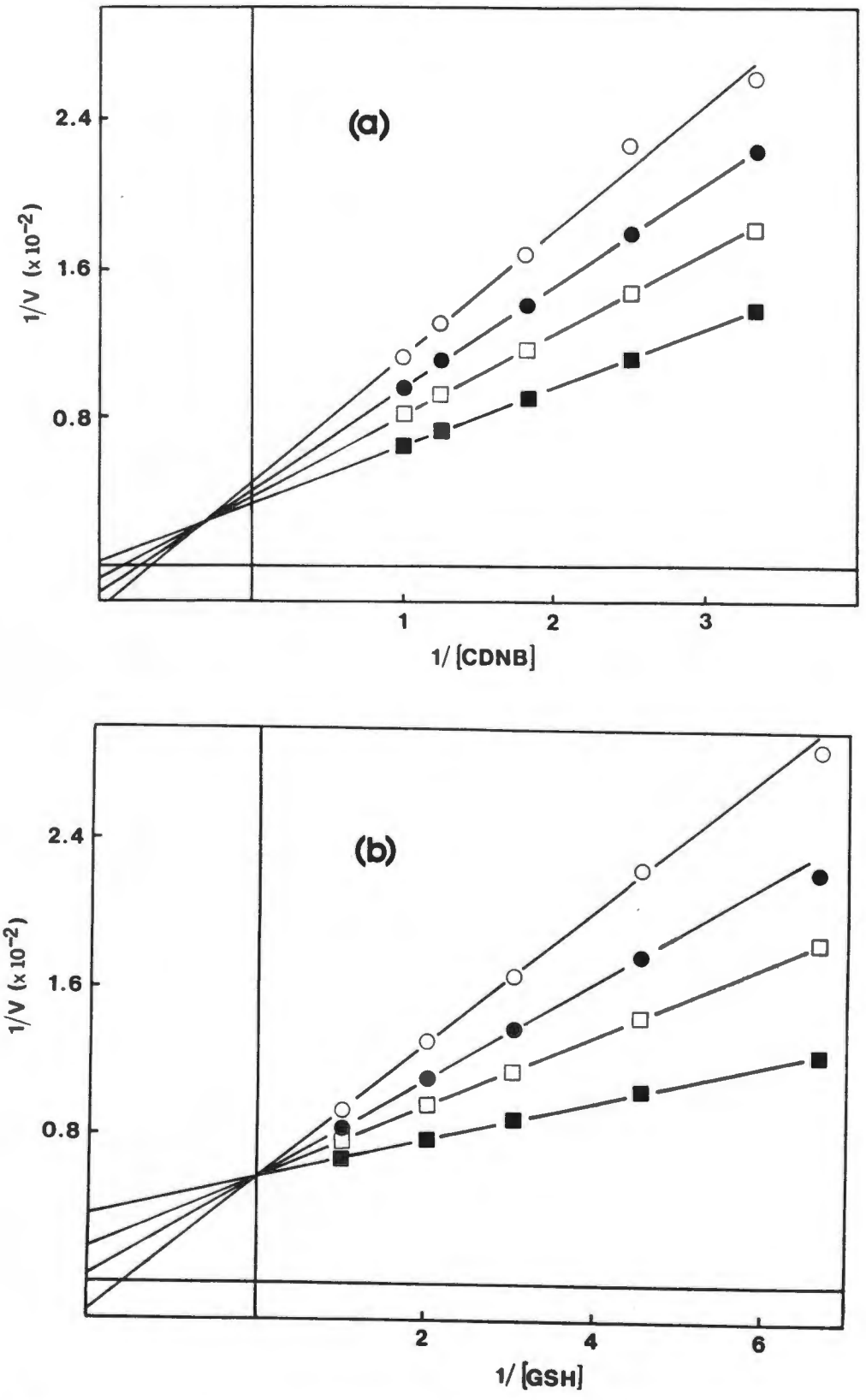

Figure 3.14 : **Reciprocal Plots of Initial Rate Data in the Presence of the Conjugate - Human Placental GST.**

(a) With CDNB as the varied substrate at a fixed GSH concentration of 0.33 mM. **(b)** With GSH as the varied substrate at a fixed CDNB concentration of 0.55 mM. In both plots, concentrations of the conjugate were (■) 0, (□) 35, (●) 65, and (○) 100 μM. Velocities are expressed in nmol/min/ml. Enzyme concentration was 10 nM. Data points represent the means of triplicate determinations. Lines drawn are those predicted by fitting the data to a rapid equilibrium random Bi Bi mechanism with a dead-end enzyme·CDNB·conjugate, using the BMDP program.

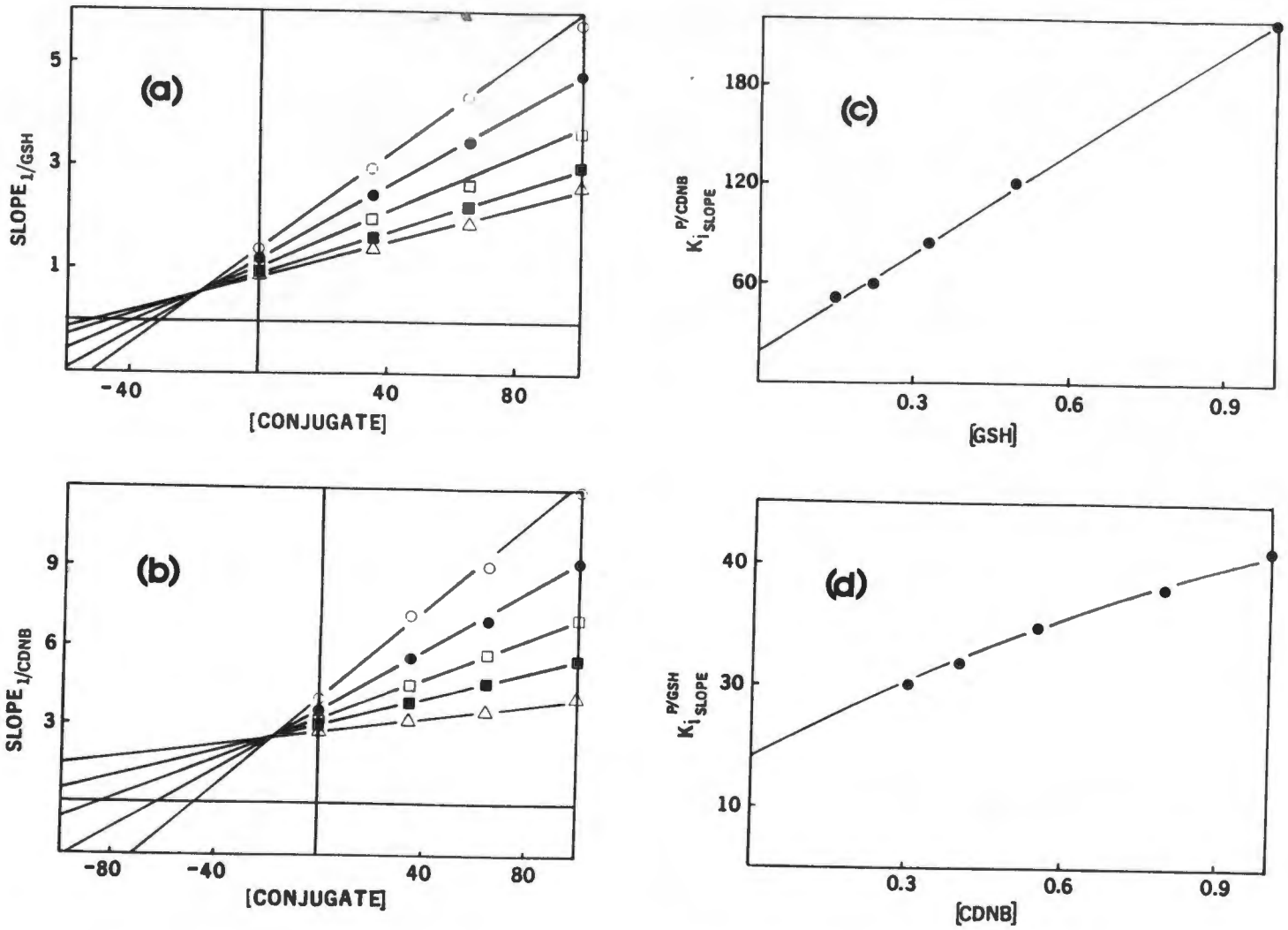

Figure 3.15 : Secondary Plots of Initial Rate Data of Figure 3.14

(a) $Slopes_{1/GSH}$ *vs* [Conjugate]. At a CDNB concentration of 0.55 mM, GSH concentrations were (○) 0.15, (●) 0.22, (□) 0.33, (■) 0.5, (△) 1 mM. (b) $Slopes_{1/CDNB}$ *vs* [Conjugate]. At a GSH concentration of 0.33 mM, CDNB concentrations were (○) 0.3, (●) 0.4, (□) 0.55, (■) 0.8, (△) 1 mM. (c) $K^{P/CDNB}_{islope}$ *vs* [GSH] (d) $K^{P/GSH}_{islope}$ *vs* [CDNB]. Concentrations are μM for conjugate and mM for substrates. Lines are generated as in Figure 3.14.

horizontal-axis intercepts (the $K_{islope}^{P/A}$ values†) of the slope replots (i.e. Figures 3.15a and b) *versus* the concentration of co-substrate were also constructed (Figures 3.15c and d). The conjugate showed mixed-type inhibition towards CDNB (Figure 3.15a). The $K_{islope}^{P/CDNB}$ increased linearly with increasing GSH concentration (Figure 3.15c), indicating that saturation with GSH overcomes the inhibition by the conjugate. The conjugate was a competitive inhibitor toward GSH (Figure 3.15b). The hyperbolic increase in the $K_{islope}^{P/GSH}$ with increasing CDNB concentration (Figure 3.15d) indicates that the conjugate remains a competitive inhibitor at all concentrations of CDNB.

An analysis (described in Section 4.4) of the observed pattern of product inhibition allowed the elimination of several bireactant mechanisms from further consideration, and determined the selection of two rate equations for modelling the initial velocity data in the presence of the conjugate. Both of these rate equations describe rapid equilibrium random systems, one without dead-end complexes, and the other with a catalytically inactive enzyme·CDNB·conjugate complex. Table 3.5. shows the results of fitting the product inhibition data to these equations (Eqns. 6 and 7, respectively). Estimates of the parameters of the rate equations were obtained from the various plots and secondary plots as described by Segel [252].

The equation which includes the dead-end complex, and consequently the additional parameter γ, provided a superior fit to the data by all statistical criteria. The velocities predicted by fitting the rate data to Eqn. 7 with the BMDPAR program were used to generate the lines in Figures 3.14 and 3.15.

---

†$K_{islope}^{P/A}$ is the apparent inhibitor constant expressing the effect of P on the slope of the 1/v *versus* 1/[A] plots. The latter is indicated as $slope_{1/A}$. The apparent constant is obtained by replotting $slope_{1/A}$ *versus* [P].

Table 3.5 : **Comparison of the Fitting of Bireactant Reaction Mechanisms to Initial Rate Data in the Presence of the conjugate, S-(2,4-dinitrophenyl)-glutathione**

MECHANISM	RATE EQUATION	EQN	PARAMETER VALUES (± STD.DEV.)	RESIDUAL SUM OF SQUARES	MEAN SQUARE ERROR	CHARACTERISTIC PRODUCT INHIBITION PATTERN[‡]				
							Varying A		Varying B	
						Inhibitor	Unsaturating B	Saturating B	Unsaturating A	Saturating A
RAPID EQUILIBRIUM RANDOM BI BI WITH NO DEAD-END COMPLEXES	$v = \frac{V_{max}(AB/\alpha K_A K_B)}{1 + A/K_A + B/K_B + P/K_P + AB/\alpha K_A K_B}$	6	V_{max} = 664.6 ± 52.4 K_A = 0.085 ± 0.018 K_B = 0.30 ± 0.08 K_P = 0.013 ± 0.002 α = 5.1 ± 1.9	860.8	9.1	P	C	-	C	-
						Q	C	-	C	-
RAPID EQUILIBRIUM RANDOM BI BI WITH DEAD-END ENZYME·CDNB·CONJUGATE COMPLEX	$v = \frac{V_{max}(AB/\alpha K_A K_B)}{1 + A/K_A + B/K_B + P/K_P + AB/\alpha K_A K_B + BP/\gamma K_B K_P}$	7	V_{max} = 718.3 ± 57.8 K_A = 0.092 ± 0.016 K_B = 0.36 ± 0.08 K_P = 0.018 ± 0.003 α = 4.9 ± 1.6 γ = 8.1 ± 3.3	718.7	7.6	P	C	C	MT	-
						Q	C	-	C	-

[‡]C = Competitive; MT = Mixed-type; - = No inhibition occurs.
In the equations given in the table, A = GSH, B = CDNB, P = Conjugate and Q = Chloride.
Units of concentration and velocity are mM and nmol/min/ml respectively. Equations are from reference 252.

3.3.4 Rat Liver GST 2-2 - Initial Velocities in the Absence of Products

The results of the initial rate measurements performed using GSH and CDNB as substrates for GST 2-2 are shown as double-reciprocal plots *versus* both substrates in Figure 3.16. The 1/V *versus* 1/[GSH] plot (Figure 3.16b) was clearly biphasic (concave-down), as observed for GST isoenzymes 3-3 and 3-4, although the degree of curvature was not as great as for those isoenzymes. Even more slight was the curvature of the 1/V *versus* 1/[CDNB] plot (Figure 3.16a). Replots, corresponding to those for human placental GST π in Section 3.3.3, are shown in Figure 3.17.

Table 3.6 shows the results of fitting five rate equations to the initial rate data. Using the statistical criteria described already (Section 2.5.4), the general rate equation for a steady-state random sequential mechanism (Eqn. 5 of Table 3.6) was found to be superior to the rapid equilibrium random Bi Bi mechanism (Eqn. 4 of Table 3.6) and the other bireactant models. The alternative models were excluded on the basis of lack of convergence, large residual sum of squares values, non-random residual distribution and/or parameter values with high standard deviations. The velocities predicted by fitting the rate data to Equation 5 with the BMDPAR program were used to generate the lines in Figures 3.16 and 3.17.

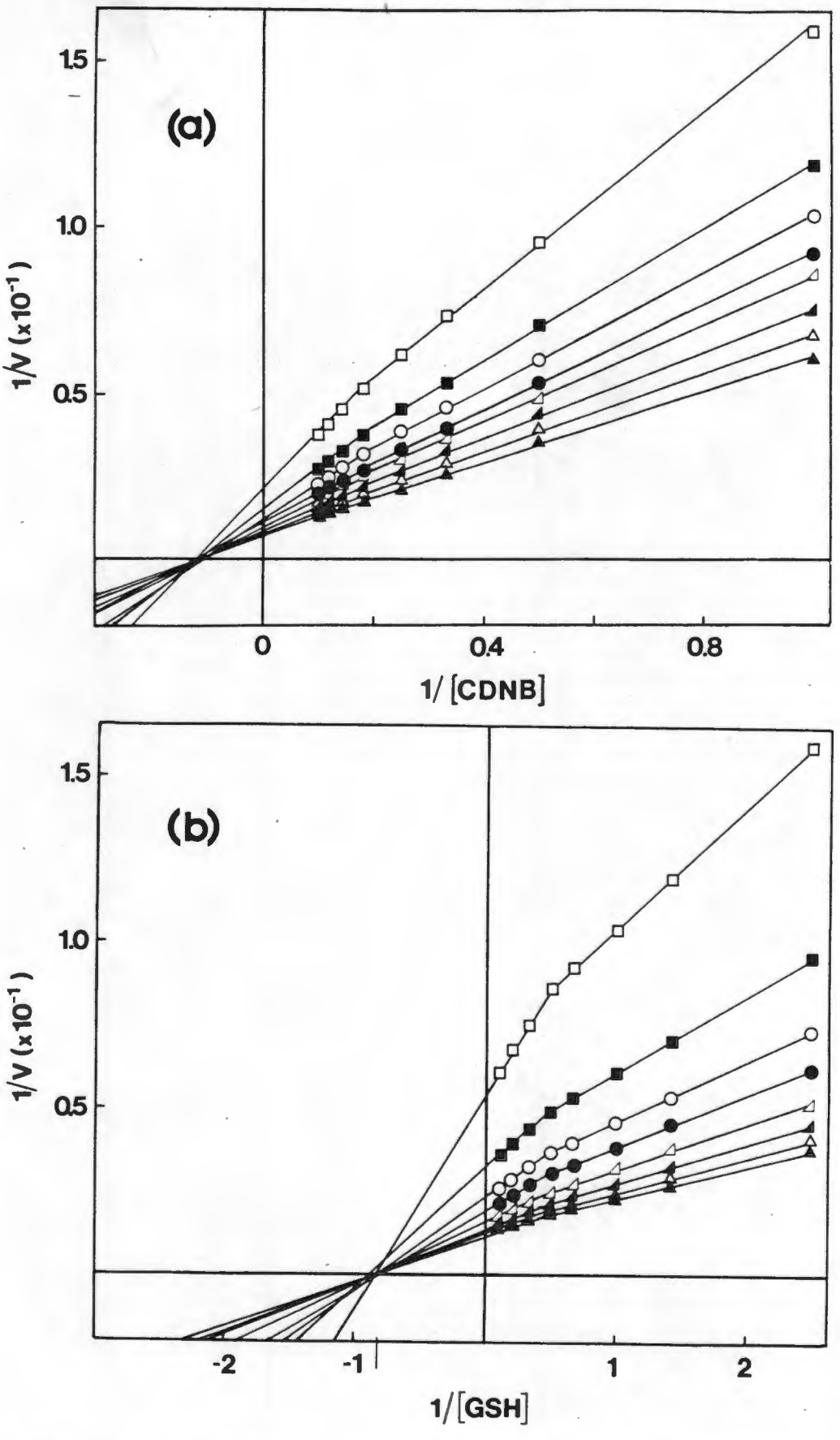

Figure 3.16 : **Reciprocal Plots of Initial Rate Data in the Absence of Product for Rat Liver GST 2-2.**

(a) With CDNB as the varied substrate, GSH concentrations were (□) 0.04, (■) 0.07, (○) 0.1, (●) 0.15, (◿) 0.2, (◢) 0.3, (△) 0.5, (▲) 1 mM. (b) With GSH as the varied substrate, CDNB concentrations were (□) 0.1, (■) 0.2, (○) 0.3, (●) 0.4, (◿) 0.55, (◢) 0.7, (△) 0.85, (▲) 1 mM. Velocities are expressed in nmol/min/ml. Enzyme concentration was 0.14 μM. Data points represent the means of triplicate determinations. The lines drawn are those predicted by fitting the data to Equation 5 of Table 3.6, by non-linear least squares regression analysis, using the BMDP program.

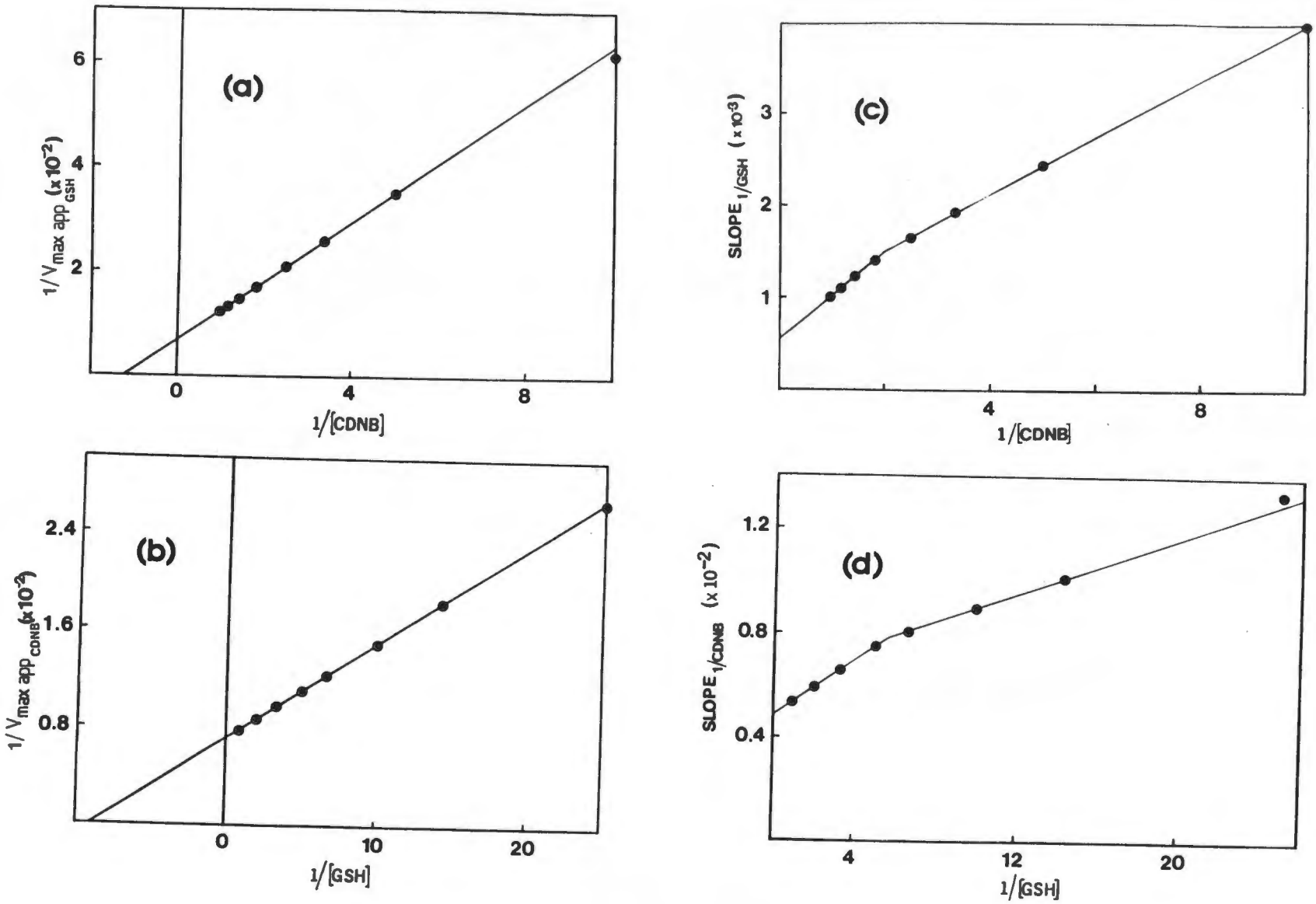

Figure 3.17 : **Secondary Plots of Initial Rate Data of Figure 3.16**
(a) $1/V_{max\ app\ GSH}$ *vs* 1/CDNB (b) $1/V_{max\ app\ CDNB}$ *vs* 1/GSH
(c) $Slopes_{1/GSH}$ *vs* 1/CDNB (d) $Slopes_{1/CDNB}$ *vs* 1/GSH.
Lines are generated as in Figure 3.16.

Table 3.6 : **Comparison of the Fitting of Bireactant Reaction Mechanisms to Initial Rate Data for Rat Liver GST 2-2**

MECHANISM	RATE EQUATION	EQN	PARAMETER VALUES (± STD.DEV.)	RESIDUAL SUM OF SQUARES	MEAN SQUARE ERROR
RAPID EQUILIBRIUM ORDERED BI BI - GSH BINDS FIRST	$v = \frac{V_{max}AB}{K_AK_B + K_BA + AB}$	1	V_{max} = 116.8 ± 3.8 K_A = 0.22 ± 0.01 K_B = 0.47 ± 0.04	210.6	3.45
RAPID EQUILIBRIUM ORDERED BI BI - CDNB BINDS FIRST	$v = \frac{V_{max}AB}{K_AK_B + K_AB + AB}$	2	V_{max} = 80.1 ± 3.4 K_A = 0.001 ± 0.003 K_B = 91.8 ± 215.2	3285.7	354.1
STEADY-STATE ORDERED BI BI‡	$v = \frac{V_{max}AB}{K_{ia}K_{mB} + K_{mA}B + K_{mB}A + AB}$	3	V_{max} = 152.4 ± 4.74 K_{ia} = 0.085 ± 0.008 K_{mA} = 0.102 ± 0.01 K_{mB} = 0.81 ± 0.04	54.2	0.9
RAPID EQUILIBRIUM RANDOM SEQUENTIAL BI BI‡	$v = \frac{V_{max}AB}{\alpha K_AK_B + \alpha K_AB + \alpha K_BA + AB}$	4	V_{max} = 152.4 ± 4.81 K_A = 0.085 ± 0.008 K_B = 0.67 ± 0.09 α = 1.21 ± 0.22	54.2	0.9
STEADY-STATE RANDOM SEQUENTIAL BI BI	$v = \frac{V_1AB + V_2A^2B + V_3AB^2}{K_1 + K_2A + K_3B + AB + K_4A^2 + K_5B^2 + K_6A^2B + K_7AB^2}$	5	V_1 = 18.8 ± 6.3 V_2 = 205.8 ± 54.9 V_3 = 95.5 ± 27.3 K_1 = 0.001 ± 0.0006 K_2 = 0.2 ± 0.1 K_3 = 0.06 ± 0.01 K_4 = 1.02 ± 0.27 K_5 = 0.04 ± 0.02 K_6 = 1.17 ± 0.37 K_7 = 0.55 ± 0.20	7.13	0.1

‡These two mechanisms cannot be distinguished by computer modelling (see text).
GSH and CDNB correspond to A and B, respectively, in the equations given in the table. Units of concentration and velocity are mM and nmol/min/ml respectively.
Equations from references 179 and 252.

3.3.5 Rat Liver GST 2-2 - Initial Velocities in the Presence of Product

The initial rate data were plotted as for the human placental GST isoenzyme (two examples are shown in Figure 3.18). Although the reciprocal plots were non-linear, the conjugate showed apparent mixed-type inhibition towards both substrates.

No attempt was made to model the product inhibition data, because of the complex nature of rate equations describing steady-state bireactant systems in the presence of the products of the enzymic reaction [252]. However, the data for each varied substrate concentration at fixed co-substrate concentration were found to fit the general rate equation for hyperbolic mixed-type inhibition, as predicted for the random Bi Bi mechanism [252]. The non-hyperbolic kinetics observed for GST isoenzymes 3-3, 3-4 and 2-2 are discussed in Section 4.3.

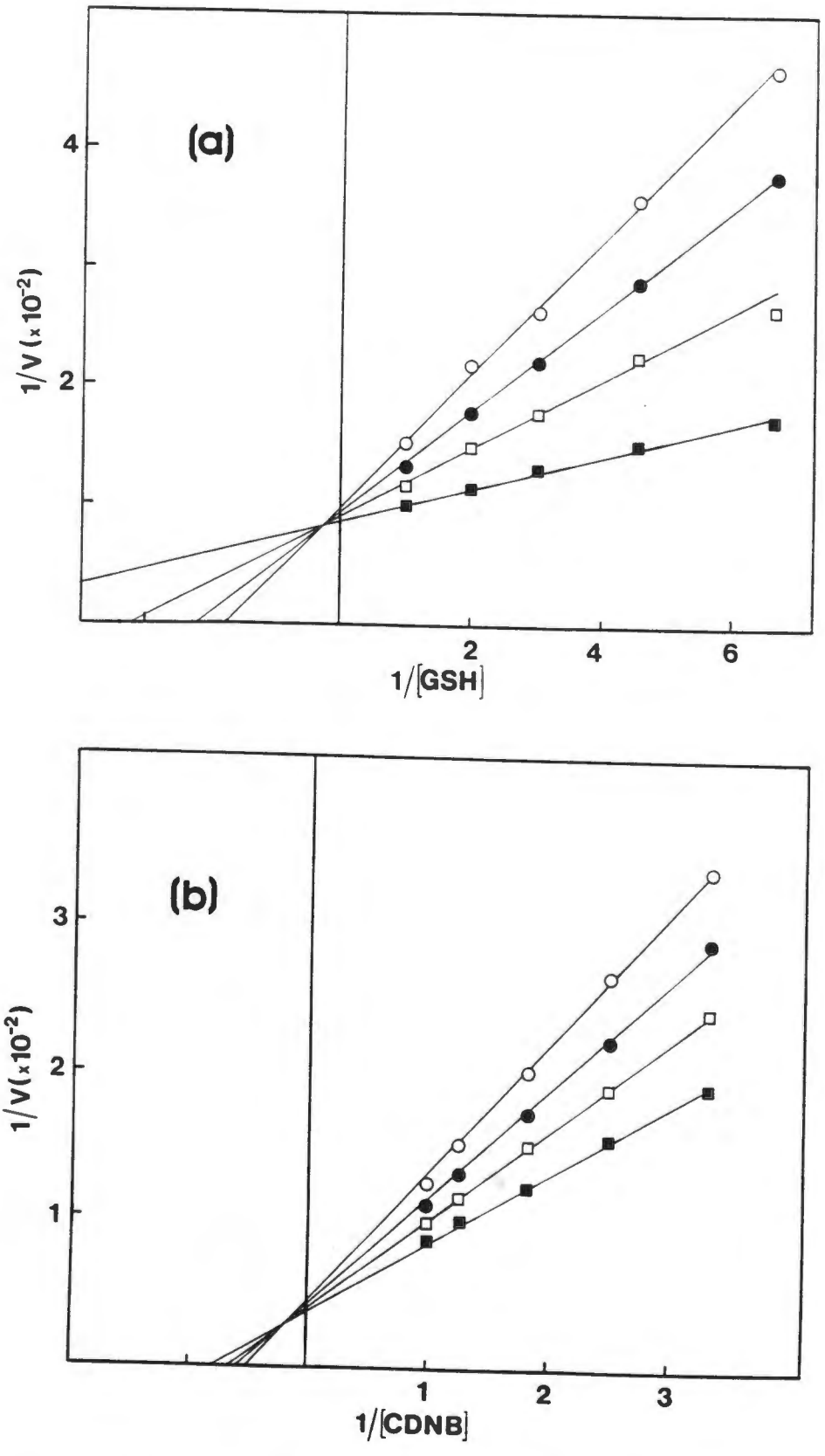

Figure 3.18 : **Reciprocal Plots of Initial Rate Data in the Presence of the Conjugate - Rat Liver GST 2-2.**

(a) With CDNB as the varied substrate at a fixed GSH concentration of 0.5 mM. (b) With GSH as the varied substrate at a fixed CDNB concentration of 0.8 mM. In both plots, concentrations of the conjugate were (■) 0, (□) 35, (●) 65, and (○) 100 μM. Velocities are in nmol/min/ml. Enzyme concentration was 0.2 μM. Data points represent the means of triplicate determinations. Lines drawn are those predicted by fitting the data to an equation describing hyperbolic mixed-type inhibition [252], using the BMDP program.

3.4 EQUILIBRIUM BINDING OF GSH TO HUMAN PLACENTAL GST π

A Scatchard plot of the results of the equilibrium binding studies performed with GSH and human placental GST (Section 2.6) is shown in Figure 3.19. The straight-line graph indicates hyperbolic (i.e. non-co-operative) binding of the substrate to GST, and binding to identical and independent sites. A stoichiometry of two molecules of ligand (n = 1.92 ± 0.07) per molecule of enzyme was apparent, with an average K_d value of 33.84 ± 1.71. These results are consistent with the hyperbolic binding isotherm and stoichiometry of two reported for rat liver GST 3-3 [135], although a single binding site per dimer of rat liver GST 1-1 was found for a spin-labelled GSH analogue [249]. The reported K_d (28 μM) for this latter isoenzyme was close to that observed in this investigation (33 μM), while the dissociation constant for GST 3-3 was 10 μM [135].

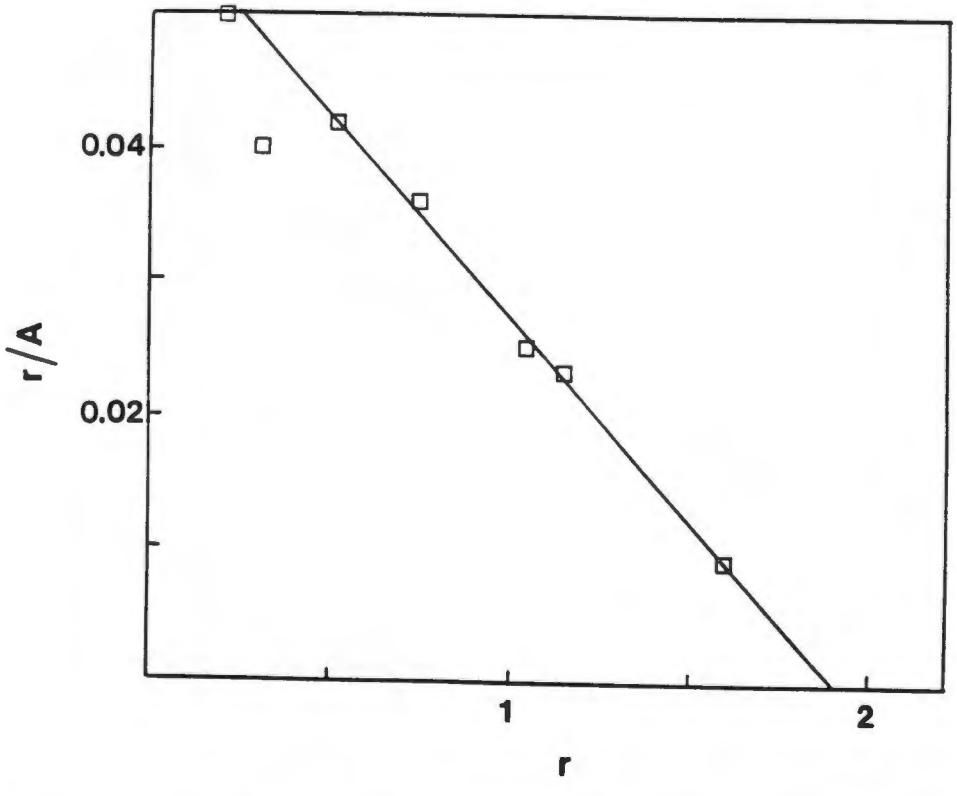

Figure 3.19 : **Equilibrium Binding of [^{35}S]GSH to Human Placental GST π by Equilibrium Dialysis**

The enzyme concentration was 10 μM, and equilibration was at 25°C for 16 hrs in 50 mM sodium phosphate buffer (pH 7.3). Data represent the means of triplicate determinations. The line drawn is that predicted by fitting the data to the Scatchard equation, using non-linear least squares regression analysis (with the outlying point shown excluded). GSH had an average dissociation constant (K_d) of 33.4 ± 1.71 μM, with a binding stoichiometry of 1.91 ± 0.09 (two binding sites per enzyme molecule).

3.5 OPTIMISATION OF THE PREPARATION OF MP-8

The effect of temperature on the kinetics of the peptic digestion of cytochrome-*c* was investigated (Section 2.7). It is clear from analytical HPLC of the incubation mixture (Figure 3.20a) that performing the peptic digestion at 40°C significantly reduced the incubation time, from about 8-10 hours required previously at 26°C [4], to less than 2 hours. Furthermore, contamination by the other haem-containing peptides was reduced. Figure 3.20b shows the reduction in contamination by non-haem peptides that resulted from the inclusion of an ammonium sulphate precipitation step. These results are discussed in Section 4.6.

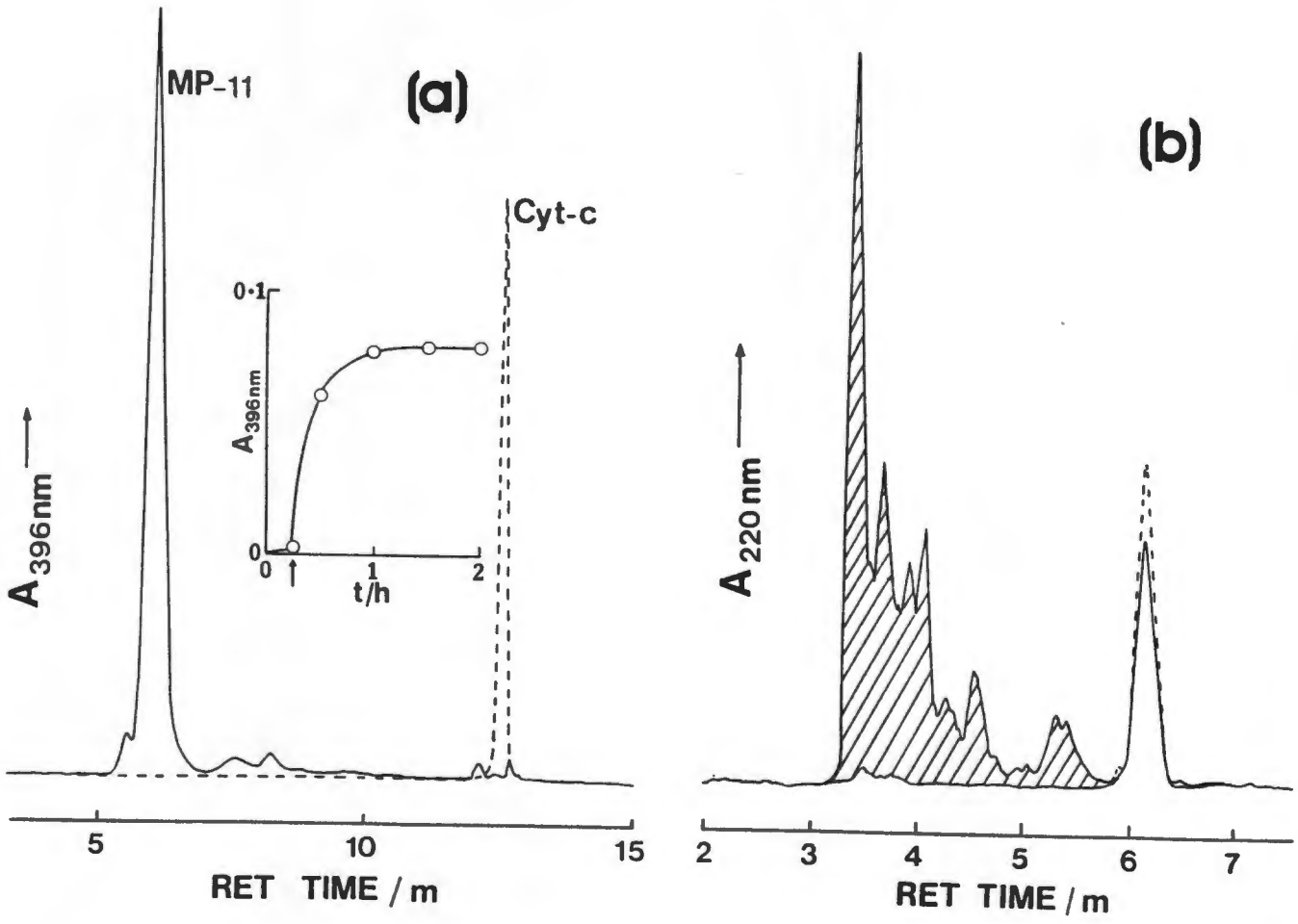

Figure 3.20 : **Optimisation of Peptic Digestion of Cytochrome-c to MP-11**

(a) Conversion of cytochrome-*c* (dashed line, at t = 0) to MP-11 (solid line) by pepsin digestion for 2 hours at 40 ± 0.05°C and pH 2.1. Inset to Figure 3.20a shows the kinetics of formation of MP-11 from cytochrome-*c*. The point at which the second addition of pepsin occurred is arrowed. (b) Removal of non-haem peptides (shaded) by quantitative ammonium sulphate precipitation (at pH 5) of MP-11. The dashed line shows the position at which MP-11 elutes at 396 nm. In both (a) and (b) the HPLC gradient was 50% A/50% B, isocratic for 10 minutes then to 100% B over a further 10 minutes.

3.6 INTERACTION OF HUMAN PLACENTAL GST π AND MP-8

Figure 3.21 shows the spectral and difference spectral changes observed on incubation of 0.5 μM MP-8 and 0.02 μM human placental GST for 10 minutes. Addition of GST to the MP-8 solution typically resulted in a quenching (by about 50% after complete reaction) of the MP-8 Soret peak at 396 nm, although no shift in the peak maximum was observed.

The kinetics of quenching were shown to follow a biexponential time course. A representative trace, generated by the addition of 0.02 μM GST to an MP-8 solution (0.35 μM), is shown in Figure 3.22a. Figure 3.22b depicts the digitised data from Figure 3.22a modelled by a biexponential function. The inset to Figure 3.22b demonstrates the inability of a single exponential function to adequately describe the data. Table 3.7 shows the parameter values obtained when many more points from the experimental trace in Figure 3.22 were included in the biexponential fit. Since the parameter values were closely similar whether 47 or 250 points were included in the data analysis, no advantage was gained by the inclusion of as many as 250 data points in the fit. Figure 3.23 demonstrates the applicability of a biexponential model over a range of MP-8 concentrations. In all cases, only a biexponential function adequately modelled the kinetic data, with respect to the statistical criteria for discrimination between rival models described in Section 2.5.4.

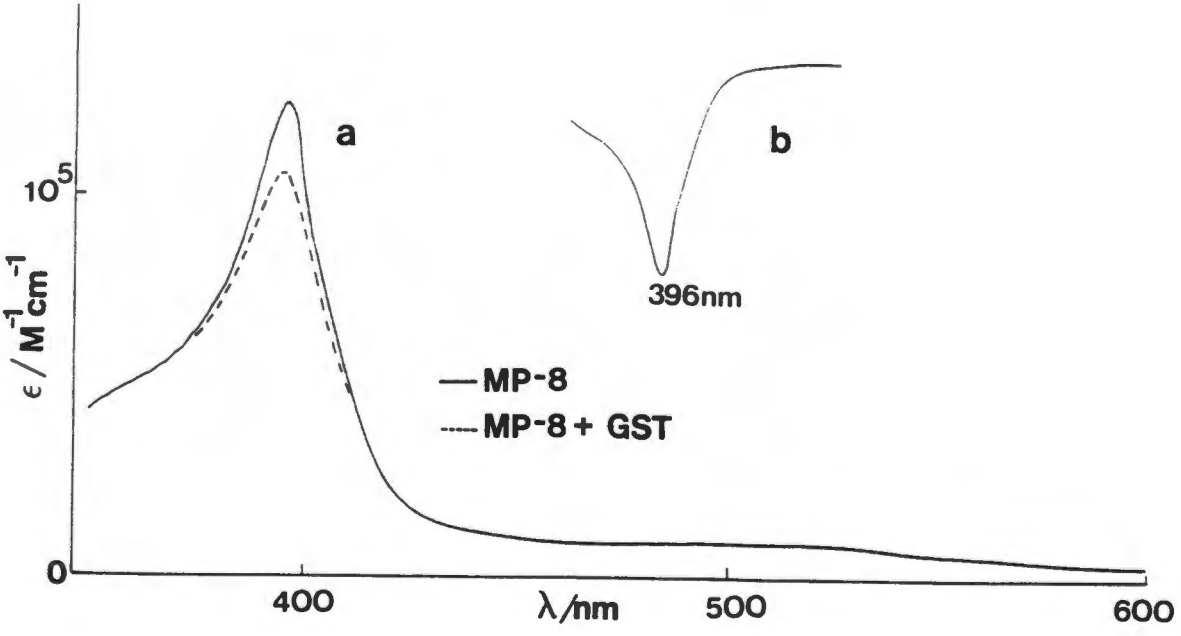

Figure 3.21 : **Spectral Changes for MP-8/GST Interaction**
Spectral (a) and difference spectral (b) changes observed on incubation of 0.5 μM MP-8 with human placental 0.02 μM GST at 22.5 ± 0.02°C and pH 7.00. The quenching shown (approximately 10% after 10 minutes) attains a final value of about 50% when the reaction proceeds to completion.

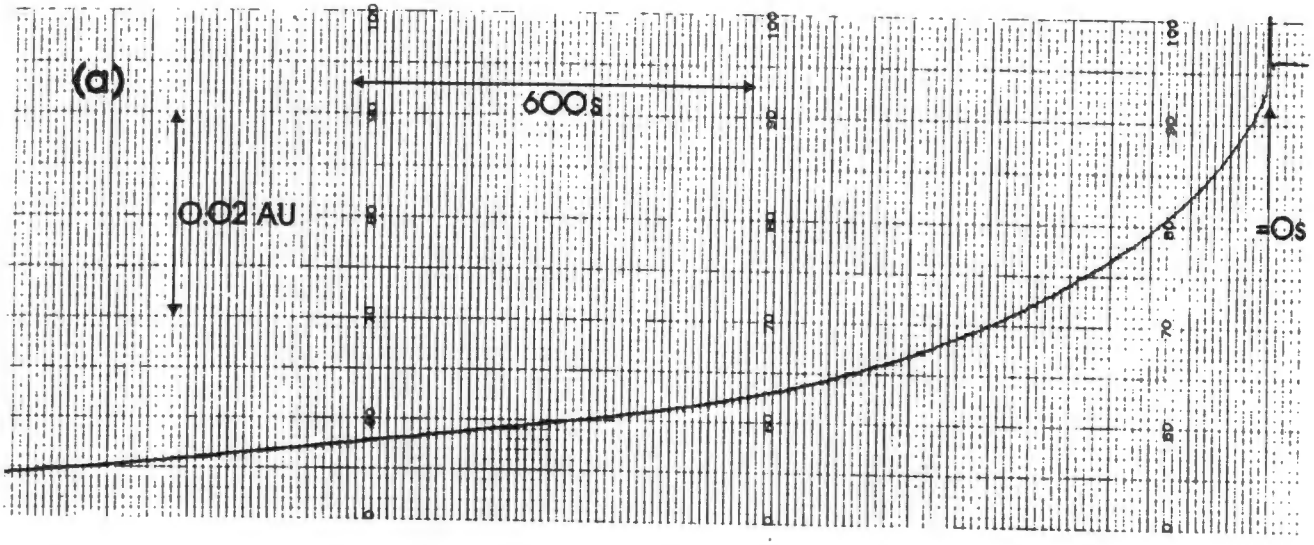

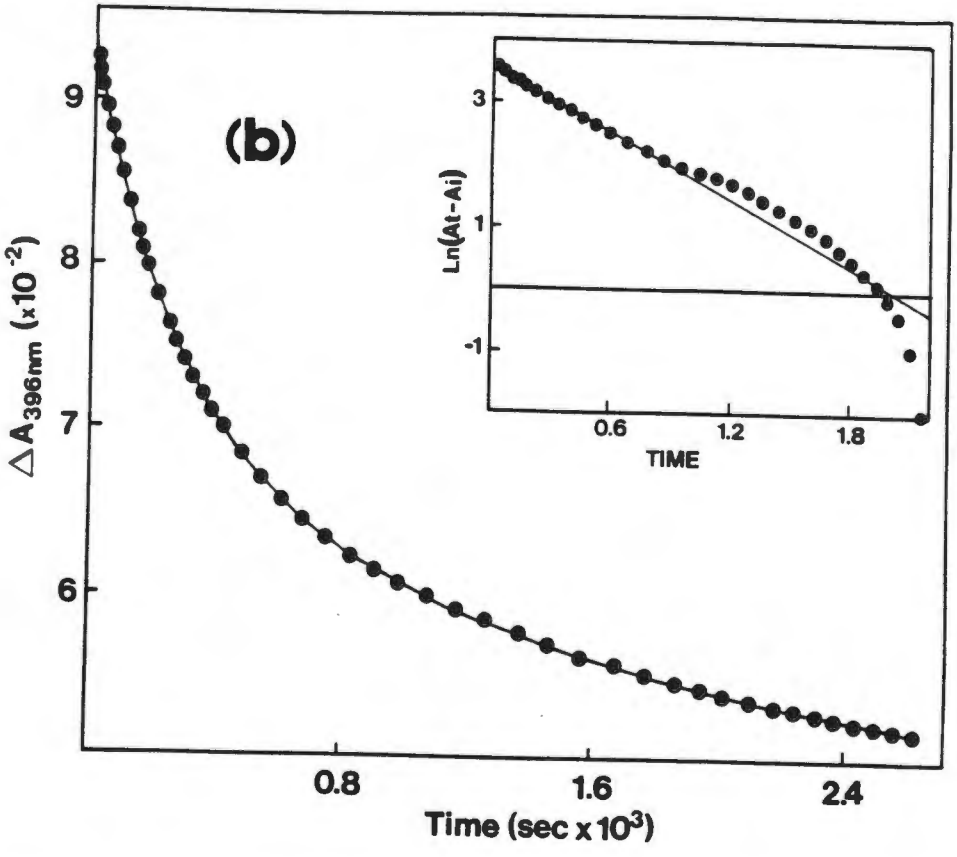

Figure 3.22 : **Kinetics of the Interaction of Human Placental GST and MP-8**

(a) Absorbance/time trace describing the interaction of MP-8 (0.35 μM) and human placental GST (0.02 μM) (decrease in A_{396nm}). Reaction was performed at 22.5 ± 0.02°C in 10 mM potassium phosphate buffer (pH 7.00). (b) Biexponential fit to the data of a). Line drawn in main plot is that predicted by fitting the data to the biexponential function $\Delta A_T + \Delta A_f e^{-k1*t} + \Delta A_s e^{-k2*t}$. The resultant parameter values are shown in Table 3.7 (Fit A). The inset shows the inadequate fit of the same data set when modelled by a single exponential function.

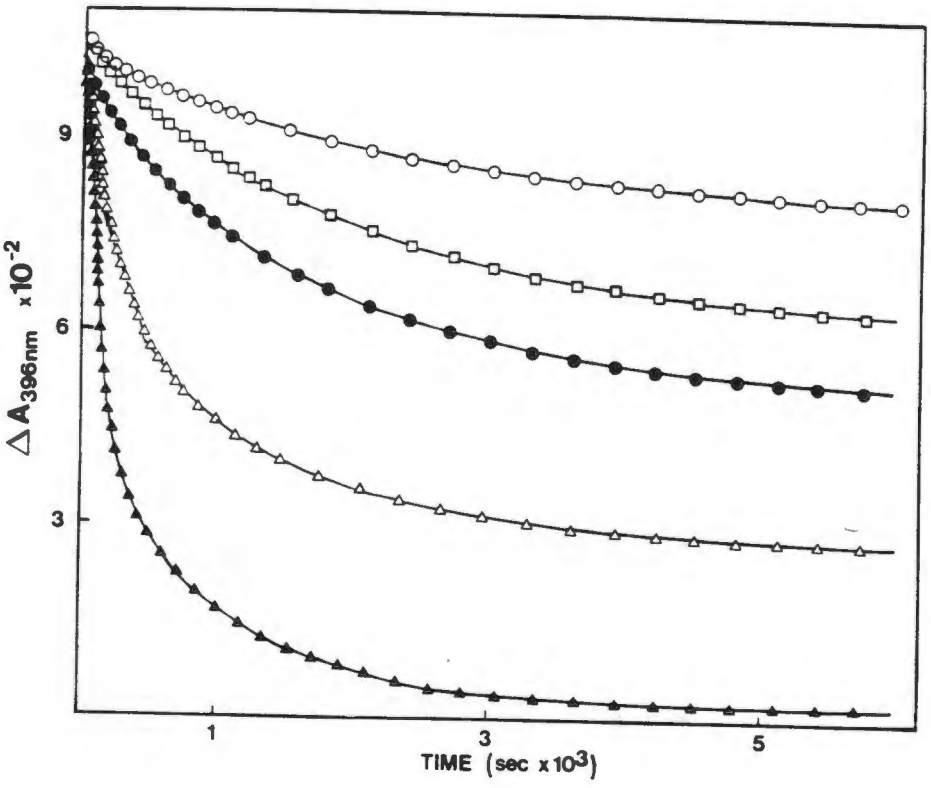

Figure 3.23 : **Interaction of Human Placental GST with Varying Concentrations of MP-8**

Biexponential modelling of the absorbance/time data for the interaction of human placental GST (0.02 μM) and a range of MP-8 concentrations (0.25 (○), 0.35 (□), 0.5 (●), 0.7 (△), and 1 μM (▲), respectively). All reactions were performed at 22.5 ± 0.02°C in 10 mM potassium phosphate buffer (pH 7.00). Lines drawn are those predicted by fitting the data to the biexponential function $\Delta A_T + \Delta A_f e^{-k1^*t} + \Delta A_s e^{-k2^*t}$. The data show clearly that a biexponential model is applicable over the whole MP-8 concentration range employed.

Table 3.7 : **Kinetic Parameters for the Interaction of MP-8 and Human Placental GST**

Parameter	Fit A (± S.D.)	Fit B (± S.D.)
ΔA_T	$4.62 \times 10^{-2} \pm 1.41 \times 10^{-3}$	$4.63 \times 10^{-2} \pm 7.19 \times 10^{-4}$
ΔA_f	$2.34 \times 10^{-2} \pm 4.53 \times 10^{-4}$	$2.19 \times 10^{-2} \pm 2.26 \times 10^{-4}$
k_1^*	$5.42 \times 10^{-4} \pm 8.80 \times 10^{-5}$	$5.25 \times 10^{-4} \pm 4.49 \times 10^{-5}$
ΔA_s	$2.32 \times 10^{-2} \pm 1.26 \times 10^{-3}$	$2.45 \times 10^{-2} \pm 5.78 \times 10^{-4}$
k_2^*	$3.65 \times 10^{-3} \pm 1.88 \times 10^{-4}$	$3.56 \times 10^{-3} \pm 8.22 \times 10^{-5}$

The kinetic parameters above are those predicted by fitting the data shown in Figure 3.22 to the biexponential function: $\Delta A_T + \Delta A_f e^{-k1^*t} + \Delta A_s e^{-k2^*t}$. Only 47 points on the curve were included in fit A, while 250 points were used in fit B.

The biexponential fits to the data yielded pseudo-first-order rate constants (k_1* and k_2*) for the fast and slow phases of the process, respectively, as well as values for the contributions of each phase (f ≡ fast and s ≡ slow) to the total (T) absorbance change ($\Delta A_{f(ast)}$, $\Delta A_{s(low)}$, and $\Delta A_{T(otal)}$, respectively). When the values of $k_{1/2}$* are plotted against MP-8 concentration (Figure 3.24), a straight-line dependence of the individual rate constants on MP-8 concentration is observed. Figure 3.25 shows the change, with increasing MP-8 concentration, in the relative proportion of the total displacement occupied by the fast phase. A mechanistic interpretation of these results is proposed in Section 4.7.

Preincubation of the GST with bilirubin (15 μM) for 15 minutes prior to addition to MP-8 completely eliminated the slow phase of the kinetic binding curve, which became monophasic. Figure 3.26 shows a typical trace obtained after preincubation with bilirubin (data plotted as a first-order kinetic process) with a logarithmic plot of the data inset. The addition of 1 mM CDNB to the enzyme immediately prior to initiation of the kinetic run completely eliminated the fast binding phase (Figure 3.27 and inset), while in the presence of 1 mM GSH, the kinetics of the MP-8/GST interaction remained biphasic in nature (Figure 3.28). These results are discussed in Section 4.7.

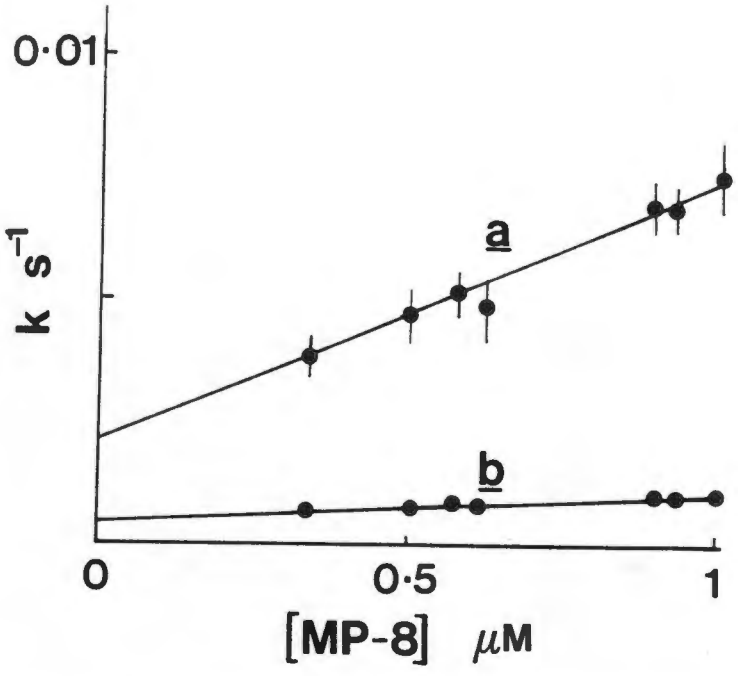

Figure 3.24 : **Variation of k_1* and k_2* with MP-8 Concentration**
The pseudo-first-order rate constants for the fast and slow phases of the interaction between GST (0.02 M) and MP-8 were evaluated by non-linear regression at a number of MP-8 concentrations (0.3-1 μM). The straight lines were fitted to the data by the method of least-squares. Evaluation of the apparent rate constants was possible from the slopes and intercepts of these plots (see text).

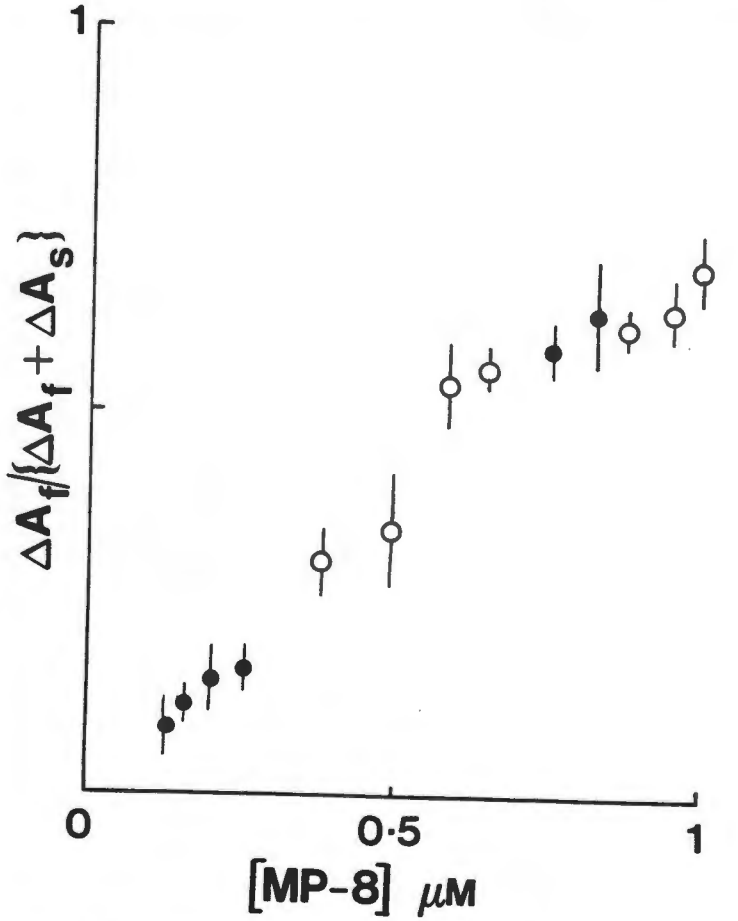

Figure 3.25 : **Variation of A_r with MP-8 Concentration**
The relative absorbance change due to the fast phase ($A_r = \Delta A_f/(\Delta A_f + \Delta A_s)$) is shown for a range of MP-8 concentrations up to 1 μM. The open circles (○) refer to data obtained at 22.5°C (± 0.02°C), while the filled circles (●) represent data from preliminary experiments conducted at room temperature (20-25°C), which were therefore not included in the kinetic analysis.

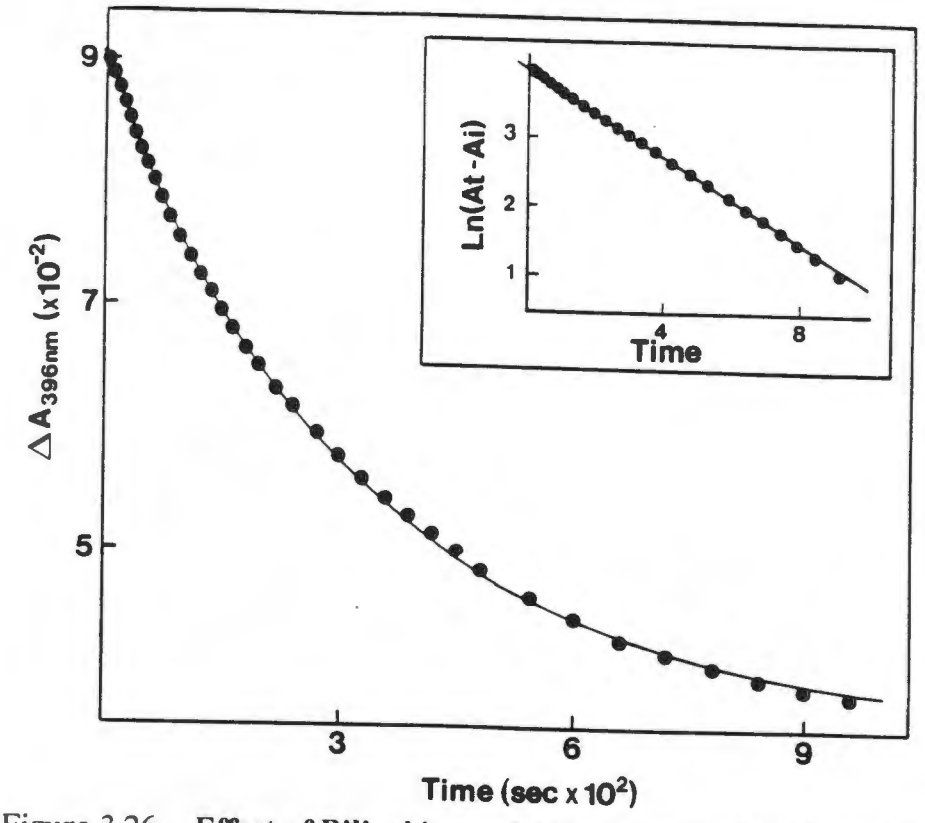

Figure 3.26 : **Effect of Bilirubin on the Interaction of MP-8 and GST**
Kinetic trace describing the interaction of MP-8 and human placental GST after preincubation of the enzyme with 15 μM bilirubin for 15 minutes prior to addition of MP-8. The data now show adherence to a single first-order kinetic process over > 95% of the reaction extent. Inset shows a logarithmic plot of the data. Concentrations of MP-8 and GST were 0.35 μM and 0.02 μM, respectively, and reaction (decrease in A_{396nm}) was performed at 22.5 ± 0.02° C in 10 mM potassium phosphate buffer (pH 7.00).

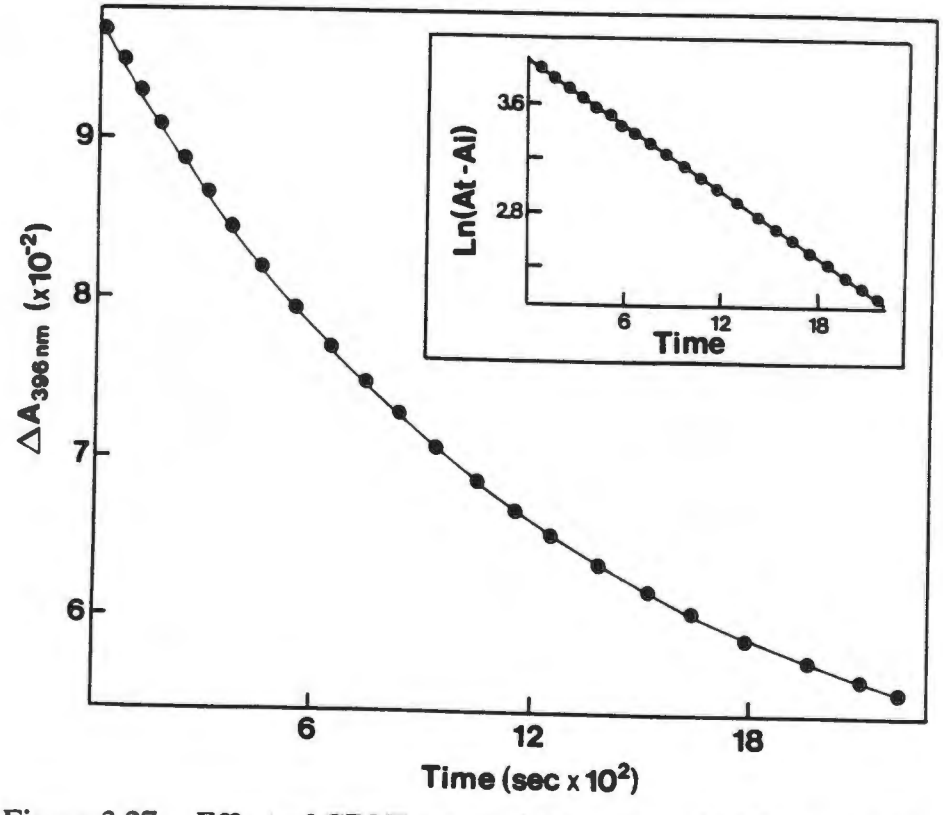

Figure 3.27 : **Effect of CDNB on the Interaction of MP-8 and GST**
Kinetic trace describing the interaction of MP-8 and human placental GST in the presence of 1 mM CDNB, added immediately prior to initiation of the kinetic run. Accurate adherence to a first-order rate law is again observed over > 95% reaction. Reaction conditions and concentrations of reactants were as described in Figure 3.26.

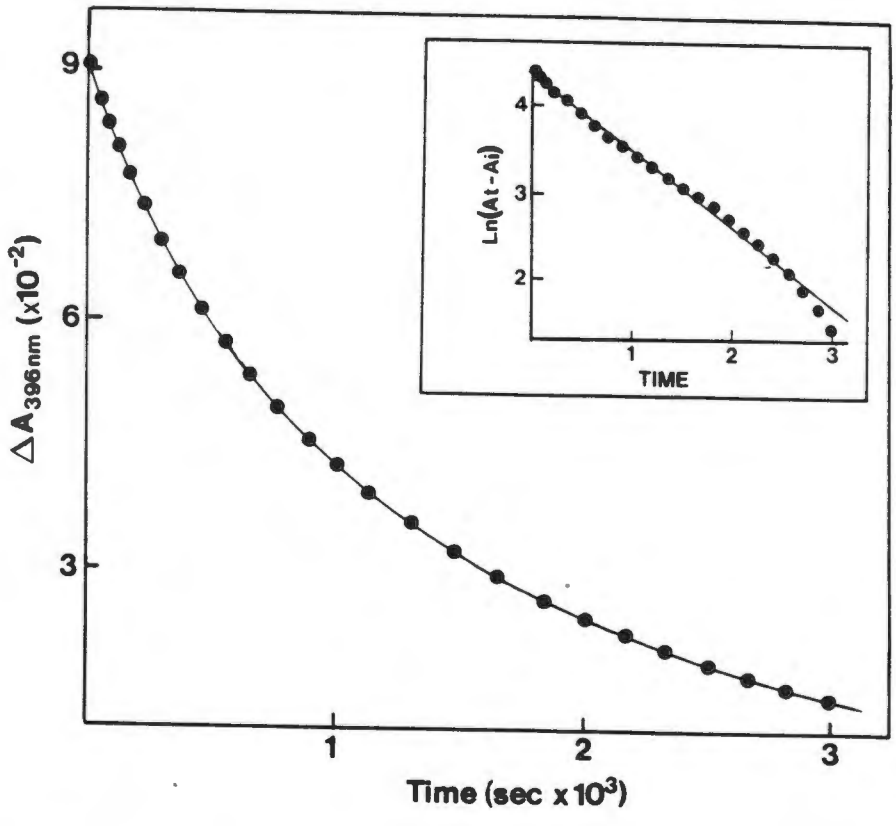

Figure 3.28 : **Effect of GSH on the Interaction of MP-8 and GST**
Kinetic trace describing the interaction of MP-8 and human placental GST after preincubation of the enzyme with 1 mM glutathione for 15 minutes prior to addition of MP-8. The inset demonstrates the inadequacy of a single exponential for modelling the reaction process. Reaction conditions and concentrations of reactants were as described in Figure 3.26.

3.7 THE INHIBITION OF HUMAN PLACENTAL GST π BY MP-8

The time-dependent inhibition of human placental GST by MP-8 is depicted in Figure 3.29. The decrease in enzyme activity towards CDNB followed a pseudo-first-order rate law, with a rate constant (k_{obs}) of 2.3 (± 0.4) x 10^{-3} s^{-1}, determined by a non-linear least squares procedure.

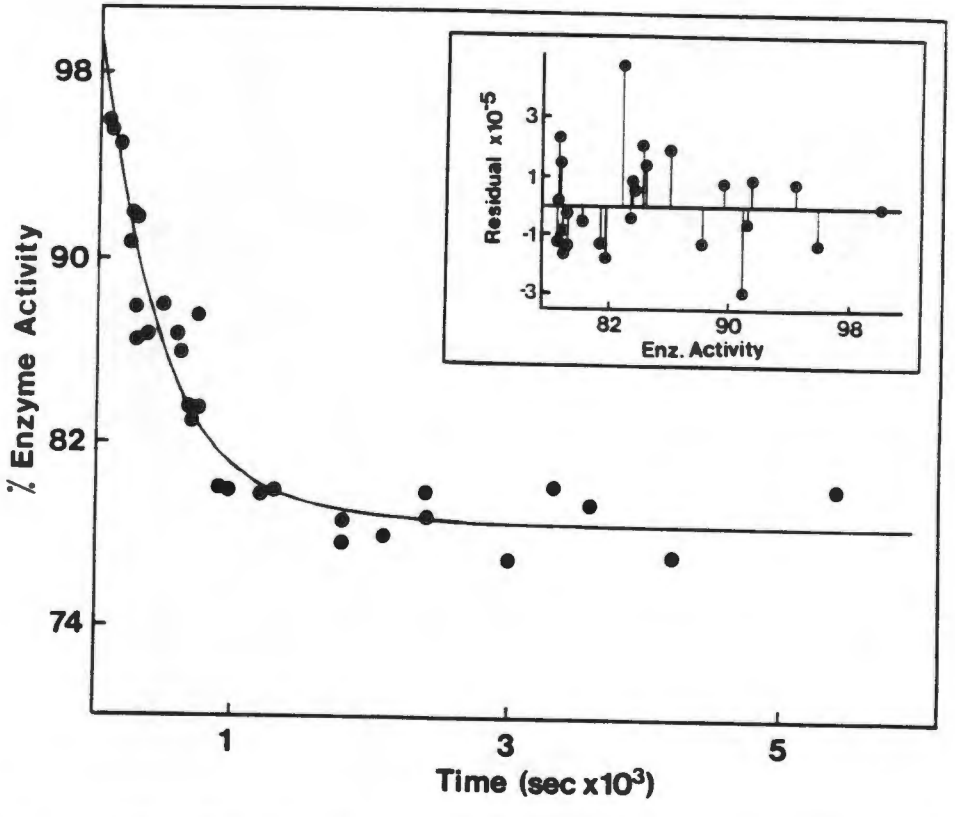

Figure 3.29 : **Time-Dependent Inhibition of Human Placental GST by MP-8**

The time-dependent inhibition of the enzyme-catalysed conjugation of CDNB and GSH was followed by incubation of 0.4 μM MP-8 with 0.1 μM GST at 25 ± 0.02°C in 0.1 M potassium phosphate buffer (pH 6.5). The results of control incubations (no MP-8 present) were subtracted. The line shown is that predicted by the fit of a first-order rate equation to the pooled data from three separate experiments. The first-order rate constant, determined by non-linear least squares regression, was 2.3 (± 0.4) x 10^{-3} sec^{-1}.

Figure 3.30 depicts the effect of MP-8 on the steady-state kinetics of the GST-catalysed conjugation of GSH and CDNB. The inhibition of GST by MP-8 at constant CDNB and varying GSH was apparently of the mixed type (Figure 3.30a), although the inhibition was too slight for further analysis. Preincubation of GST with MP-8 resulted in mixed-type inhibition of the enzyme with respect to CDNB also (Figure 3.30b). The straight-line replots of the 1/v-axis intercepts and slopes (of Figure 3.30b) *versus* MP-8 concentration shown in Figure 3.31 confirm that the inhibition is of the linear mixed-type (scheme shown in Section 4.8) [252].

The value of K_i (0.34 μM), determined from the slope *versus* MP-8 concentration replot, allowed a value for α to be determined using the intercept *versus* MP-8 concentration replot. The value thus calculated for α (3.54) was in good agreement with the value (3.03) determined from the intersection point of the primary reciprocal plot (Figure 3.30b). All the parameter values evaluated from these plots for the linear mixed inhibition mechanism are shown in Table 3.8. The data of Figure 3.30b were also subjected to a Dixon-type analysis, which gave results in full agreement with the alternative (Lineweaver-Burk) analysis. Figure 3.32 shows replots of the Dixon plot slopes and intercepts according to a linear mixed-type inhibition mechanism, and the parameter values derived from the Dixon analysis are included in Table 3.8 for comparison. Also shown in Table 3.8 are the values of K_S and K_i for the data of Harvey and Beutler [110], for human erythrocyte GST (see discussion in Section 4.8).

Table 3.8 : **Parameters for Linear Mixed Type Inhibition of Human Placental GST by MP-8**

	K_S ($M \times 10^{-3}$)	K_i ($M \times 10^{-6}$)	α
Direct Replot	0.73 (± 0.2)	0.33 (± 0.05)	3.5 (± 0.4)
Dixon Analysis	1.3 (± 0.3)	0.51 (± 0.04)	2.2 (± 0.5)
Dixon Analysis of Data of Ref. 110‡	0.77	0.1	—

‡For human erythrocyte GST ρ.

Thermodynamic parameters obtained from direct repolts of $K_{m(app)}$ and $V_{max(app)}$ (Figure 3.31) and from replots of the slope and intercept of Dixon plots (Figure 3.32).

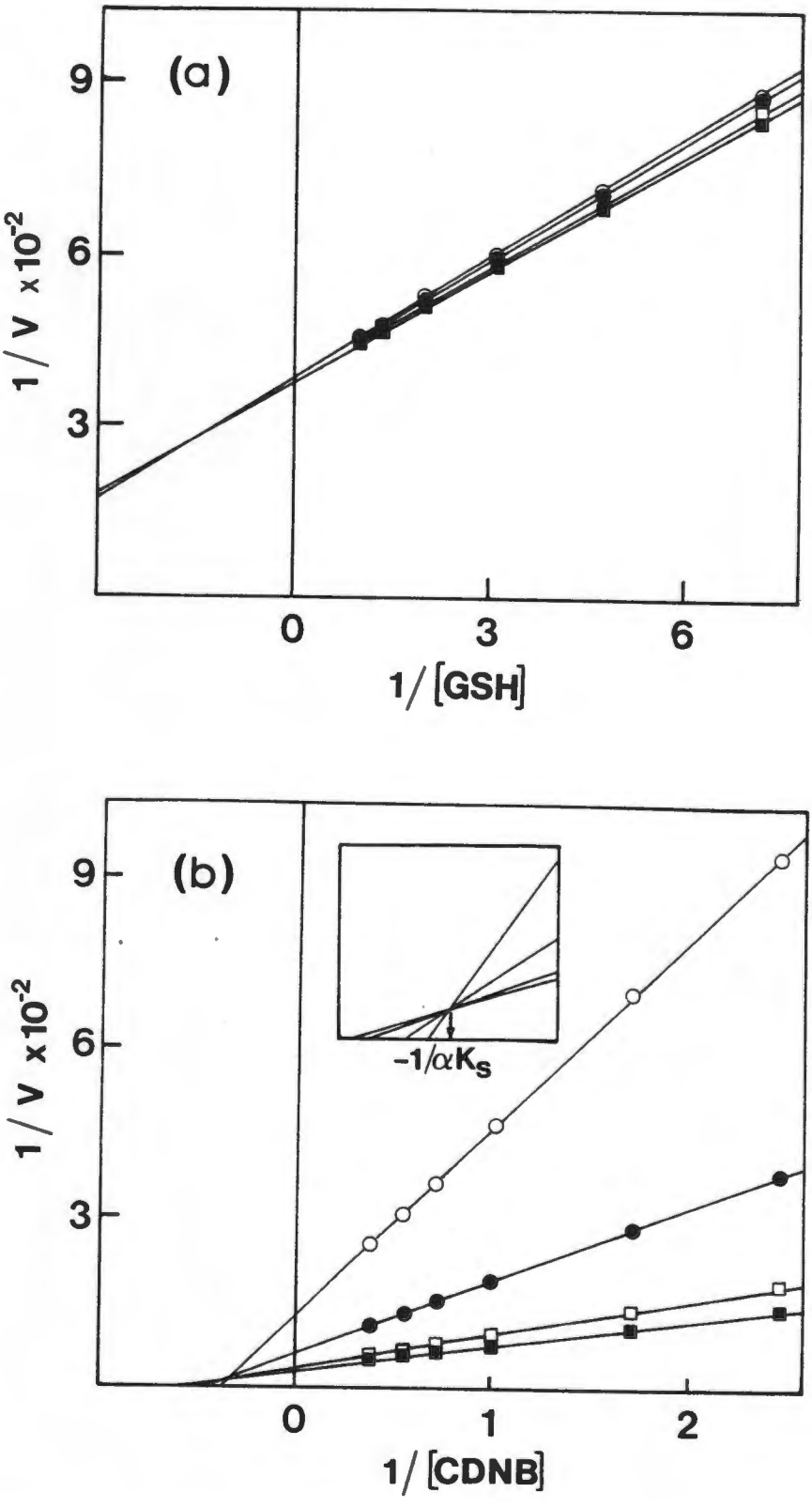

Figure 3.30 : **Inhibition of Human Placental GST by MP-8**
(a) With GSH as the varied substrate at a fixed CDNB concentration of 1 mM. **(b)** With CDNB as the varied substrate at a fixed GSH concentration of 1 mM. In both plots, enzyme concentration was 20 nM and MP-8 concentrations were (■) 0, (□) 0.5, (●) 2 and (○) 5 μM. Velocities are expressed in nmol/min/ml. Data points represent the means of triplicate determinations. Lines are those predicted by non-linear regression of the experimental data. Inset to (b) shows the region of intersection of the straight lines enlarged.

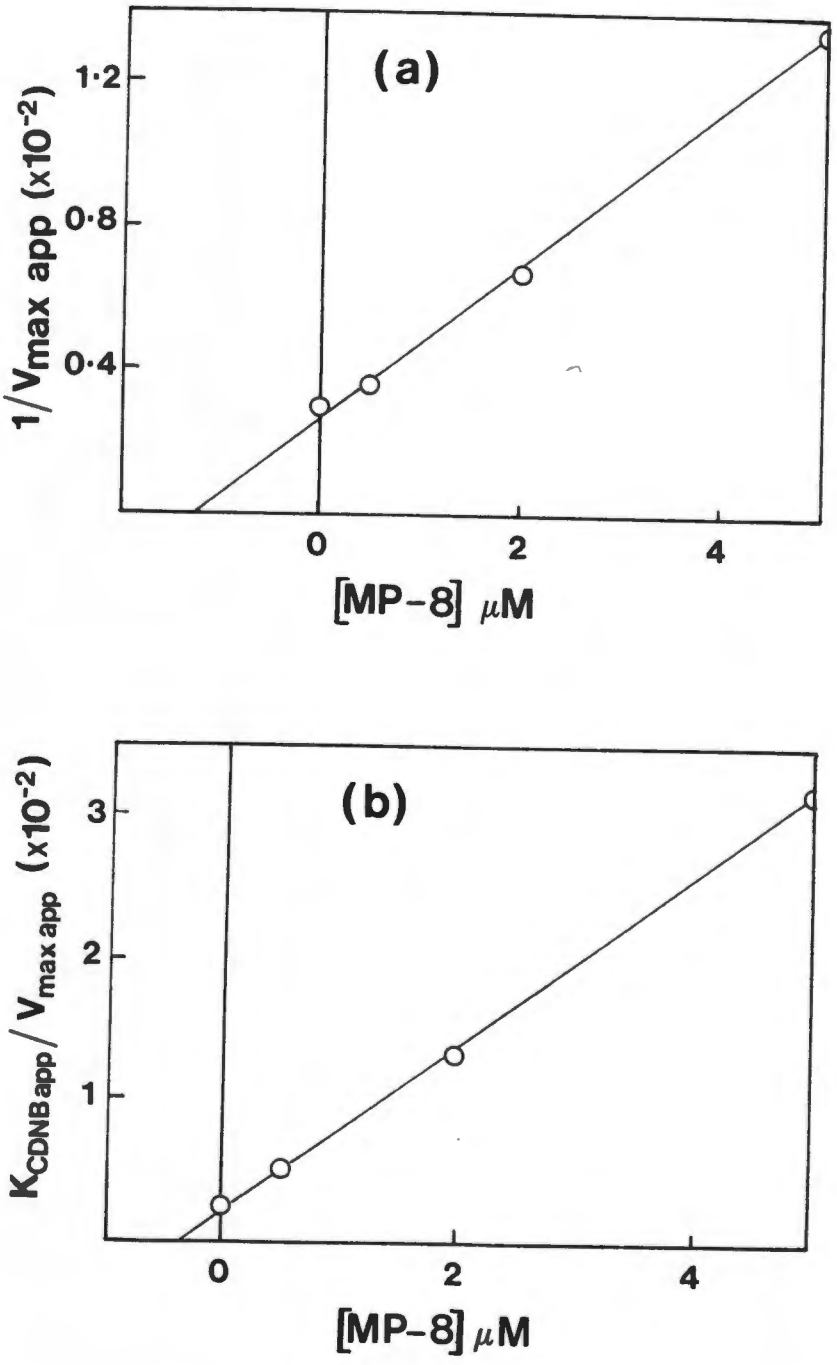

Figure 3.31 : **Secondary Plots for Figure 3.30b**

(a) $1/V_{max\ app}$ *vs* [MP-8]. (b) $K_{CDNB\ app}/V_{max\ app}$. Concentrations are μM for MP-8 and mM for substrate. In Figure 3.31b, the point representing an MP-8 concentration of zero uses the accurate value of K_{CDNB} calculated in the full kinetic analysis reported in Section 3.3.2 (Table 3.3). Derived steady-state parameters for the linear mixed-type inhibition scheme (see text) are shown in Table 3.8. Lines are generated by linear regression of the experimental data.

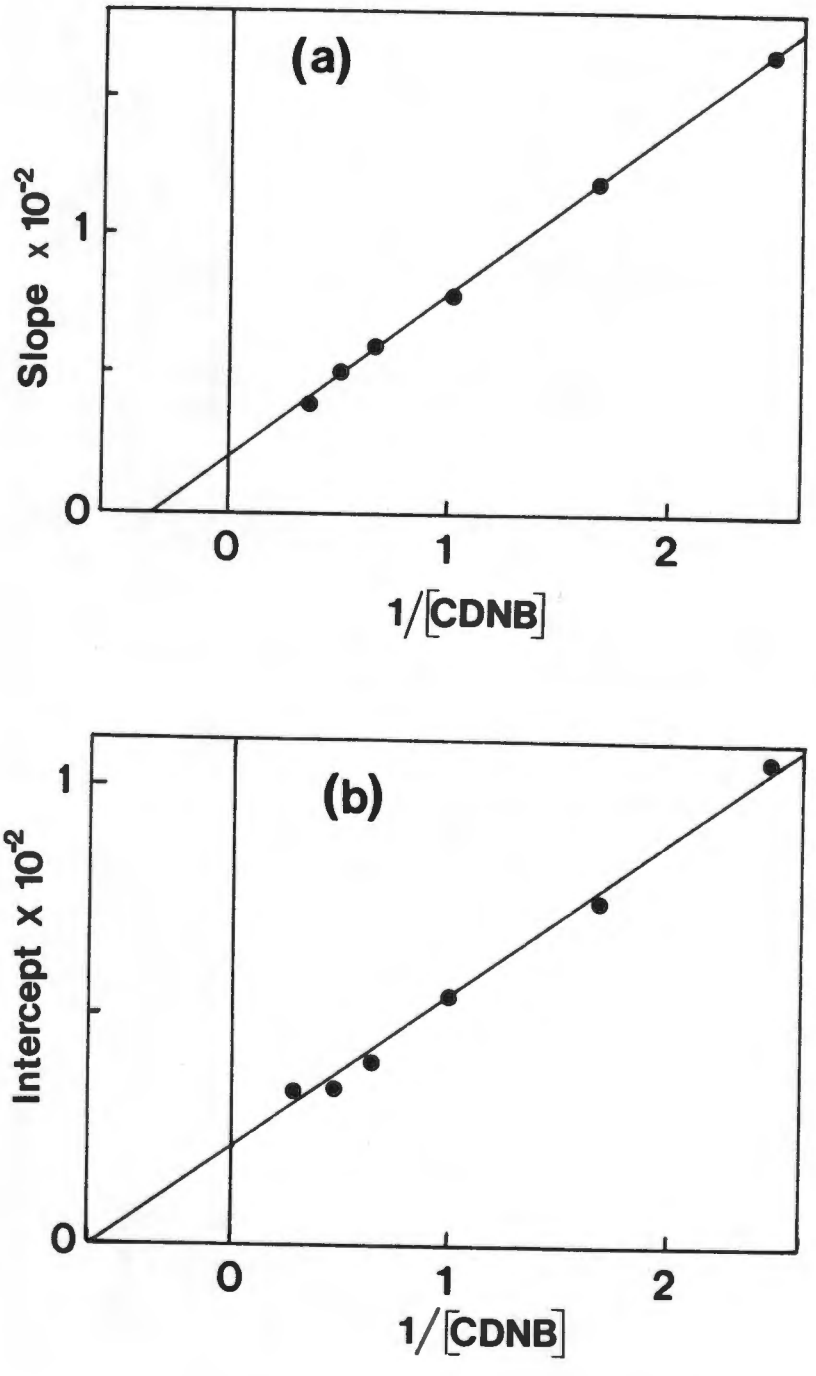

Figure 3.32 : **Slope and Intercept Replots of Dixon Plots for Data of Figure 3.30b**

The straight line is predicted for mixed-type inhibition with the species ESI catalytically inactive. Steady-state parameters for the linear mixed-type inhibition scheme obtained from the Dixon analysis are shown in Table 3.8.

4. DISCUSSION

4.1 OPTIMISATION OF GST ASSAY FOR KINETIC STUDIES

In order to optimise the GST assay system prior to detailed kinetic studies, a number of preliminary experiments were performed. These included investigations of the choice of solvent for CDNB and DCNB, the order of addition of reagents, and the linearity of initial rates in the standard GST assay.

Integral to this optimisation was the selection of the centrifugal analyser as the spectrophotometric instrument of choice. More conventional spectrophotometers are limited by several factors in investigations of this nature, where a large number of assays (up to 600 per experiment) must be performed in as short a time as possible to minimise time-dependent enzyme activity losses. The ability of the centrifugal analyser to process 20 cuvettes simultaneously, as well as the elimination of the need to wash out and dry cuvettes at intervals, reduced the overall experimental time considerably. In addition, economical use of the purified isoenzymes was facilitated by the small cuvette volume (minimum volume of 150 μl). The centrifugal mixing method allowed absorbance measurements from as little as 3 seconds after the initiation of the reaction (in contrast to the variable and sometimes considerably longer times of manual mixing methods). More precise absorbance measurements and temperature control (30.0 ± 0.1°C) than permitted by other available instruments were possible with the Multistat.

Using the centrifugal analyser, it was possible to assess the linearity of initial rates for the reaction from effectively time zero. The results of this investigation (Section 3.1) indicate that initial rates are not linear for as long as previously thought; in fact curvature is evident after only 1 minute (Figure 3.1). For accurate kinetic studies with GST isoenzymes, initial rates should therefore be measured using data obtained over the first 60 seconds of the reaction only. Using manual mixing methods, the time taken between initiation of the reaction and recording of

the reaction rate is operator-dependent and variable, and may encroach substantially on the first 60 seconds of reaction. The centrifugal analyser is therefore well suited to kinetic studies of the transferases, since mixing is automated and measurements are always taken from 3 seconds after initiation of the reaction.

One possible cause of the curvature observed after 60 seconds, which is diminished in the presence of albumin (see Section 3.1), may be irreversible inhibition of GST activity by CDNB [61]. Incubation of CDNB with a mixture of rat liver GST isoenzymes resulted in a time-dependent pseudo-first-order loss of activity (k_{obs} = 2.5×10^{-3} s^{-1}) [61, Sikakana *et al.*, unpublished results]. The extent of this inhibition was dependent on CDNB concentration (I_{50} = 0.3 mM), and was not reversed on removal of CDNB by either dialysis or Sephadex G-75 chromatography. CDNB has also been reported to covalently bind to and irreversibly inhibit rat liver GSTs 1-2 and 3-3 [136,215].

Previous reports [150,179] of an increased enzymic activity in assays performed after preincubation of GST preparations with GSH have been confirmed in this study (see Section 3.1). This activation by GSH may well have introduced uncertainty into the results of some previous kinetic studies [132,184], where GST was preincubated for 5 minutes at 30°C with GSH, at each of the varying GSH concentrations used. In order to minimise the possible variable activation of the enzyme that could result from this phenomenon, the enzyme (in buffer) was always added alone to the inner cuvette chamber of the Multistat rotor (see Figure 2.1) in these kinetic studies. The other reactants were added (in the order shown in Figure 2.1) to the outer chamber, and the reaction was initiated by the addition of enzyme.

Some commonly used solvents have profound substrate-dependent effects on various enzymatic reactions *in vitro* [7]. For example, ethanol, the most commonly used solvent for CDNB and DCNB in the GST assay, has been shown to reversibly inhibit GST activity towards these halo-aromatic substrates at solvent concentrations greater than 1% (v/v) [39,134]. Despite this, some GST assay methods [9,104,257] have recommended ethanol concentrations as high as 5% for substrates with limited aqueous solubility.

Using mathematical modelling of limit-velocity values obtained by extrapolating ethanol concentrations to zero, Jakobson *et al.* [134] have concluded that inhibition by ethanol was not the cause of the non-hyperbolic kinetics observed for GST isoenzyme 3-3. However, it is generally held that solvent concentration in enzyme assays should be kept as low as possible in order to minimise solvent effects on the enzyme and that these effects should be investigated for each enzyme/substrate combination prior to any detailed kinetic studies [7,39]. Although the concentration of ethanol in some early initial velocity studies [132,184] was kept constant at 3% (v/v) because of this fact, considerable inhibition was observed at that concentration in the present investigation (see Figure 3.2).

This study has also demonstrated that DMSO is considerably less inhibitory than ethanol towards GST activity (Figure 3.2) and is thus a more suitable solvent for both CDNB and DCNB for the GST isoenzymes of this investigation. The concentration of DMSO in these kinetic studies was limited to 2% (v/v), at which no significant inhibition was observed (Figure 3.2). Therefore, the contribution of solvent effects could be eliminated from the mechanistic interpretation of the kinetic data.

In view of the findings of these preliminary experiments, the standard assay conditions were reassessed and relatively stringent conditions imposed with respect to solvent choice, order of addition of reactants, linearity of reaction with time, etc., to ensure accurate initial rates, a particularly relevant requirement for mechanistic studies of the GSTs.

4.2 THE REVERSIBLE AND IRREVERSIBLE INHIBITION OF GSTs BY ETHYLENE DIBROMIDE

The experiments to reproduce work previously performed in this laboratory on the reversible inhibition and activation of the GSTs by EDB [130] successfully confirmed the suitability of the centrifugal analyser for kinetic studies on the transferases (Figure 3.3). A mechanistic interpretation of this work has already been proposed [130] and therefore the results of those experiments are not discussed further here.

Inskeep and Guengerich [127] reported that both GSH and GST were necessary for the irreversible binding of [^{14}C]-EDB to DNA to occur *in vitro*. Although no binding of EDB to DNA was observed when GSH was absent, GSH concentrations of greater than 10 mM resulted in less EDB binding to DNA than GSH concentrations of 2 mM [127]. Inskeep and Guengerich [127] concluded that the extent of DNA binding by EDB and other dihaloethanes *in vivo* may be the net result of a complicated balance between the detoxicating and activating processes of GSH conjugation. The results of the present investigation (Section 3.1) suggest that another factor in this balance which has not been previously considered may be irreversible inhibition of GST activity by EDB. This irreversible inhibition of the GSTs by EDB may be a further example of the demonstrated ability of these enzymes to sequester potentially toxic compounds [39,155].

Pseudo-first-order inhibition of GST activity by EDB has been observed previously in this laboratory, for both rat liver GST 3-3 and a mixture of rat cytosolic GSTs [131]. In the present investigation, measurements of GST activity at various time intervals has confirmed this inhibition occurs for human placental GST under the incubation conditions of Inskeep and Guengerich [127]. The observed pseudo-first-order rate constants in the presence of 2 mM or 15 mM GSH (2.25×10^{-3} and 1.64×10^{-3} s^{-1}, respectively) were in good agreement with that previously reported for the inhibition of a mixture of rat liver cytosolic GSTs by EDB ($2\text{-}2.6 \times 10^{-3}$ s^{-1}) [131]. Although the first-order rate constants for the loss of activity of human placental GST π were similar at both GSH concentrations, the extent of inhibition was greater at 2 mM (see Figure 3.4). This phenomenon may be related to the finding that GSH concentrations of greater than 10 mM resulted in less EDB binding to DNA than GSH concentrations of 2 mM [127], and may well be accounted for by the partial protection of GST from inactivation that is observed on preincubation with GSH [61,131,308] (see also Section 4.5).

One passing point of interest concerns the observation of Inskeep and Guengerich [127] that GST 1-2 and Sigma rat liver GST mix were equivalently effective in producing binding of EDB to DNA. This may well be accounted for, at least in part, by a report that the commercial preparation is primarily composed of isoenzyme 1-2 [237]

The ultimate toxicity of EDB *in vivo* may be the net result of several processes, including activation to a DNA-binding GSH adduct by at least some GST isoenzymes, irreversible binding of EDB to these isoenzymes (both inhibiting the metabolic activation of the precarcinogen and sequestering the compound), the physiological concentration of GSH and other GST-independent processes of activation and detoxication.

4.3 THE SIMPLEST STEADY-STATE RANDOM SEQUENTIAL BI BI MECHANISM ADEQUATELY EXPLAINS THE NON-HYPERBOLIC KINETICS OF THE GSTs.

"The kinetic mechanism of the glutathione S-transferases is controversial. The uncertainty reflects, in large part, the non-linear behaviour of the kinetic data obtained with purified glutathione S-transferases." This is how Boyer and Kenney [39] described the kinetics of the GSTs in their recent major review of the subject. In his review of the same year [179], Mannervik concluded "...virtually all GSH transferases studied in detail display distinct deviations from Michaelis-Menten rate-behaviour when the concentration of GSH is varied. Thus, it seems likely that the basic sequential model is overlaid with the kinetic complications arising from an enzyme memory mechanism involving GSH-induced slow transitions. Further investigations are necessary to evaluate this suggestion".

The non-hyperbolic kinetics of the GSTs were first observed in early studies of the conjugation of GSH and DCNB by rat liver GST 3-3 (reviewed in Section 1.4.2). Families of concave-down reciprocal plots were also observed in this investigation for the conjugation of CDNB by isoenzyme 3-3 (Figure 3.9) and of DCNB by isoenzyme 3-4 (Figure 3.10) and for the conjugation of CDNB by rat liver GST 2-2 (Figure 3.16).

The reported data for GST 3-3 and DCNB are generally thought to fit the steady-state random sequential Bi Bi model best [39,179,184]. Although sufficient data for detailed mechanistic modelling were not collected in this study for GSTs 3-3 and 3-4, and although the contributions of the different subunits of the heterodimer cannot be overlooked, it was found that this model was also capable of fitting the data for both these isoenzymes (Section 3.3.1). The initial velocity data collected in this investigation for GST isoenzyme 2-2 were considerably more substantial than those for GSTs 3-3 and 3-4, and these too were found to be best described by the steady-state random model. In fact, where Mannervik and Askelöf [184] reported one redundant parameter when their data were fitted to this model, no redundant parameters were found in this study with the data for GST 2-2 (see Table 3.6). The observed pattern of inhibition by the CDNB•GSH conjugate (see Section 3.3.5) also supported a steady-state random mechanism for GST 2-2.

The kinetic, equilibrium binding and product inhibition data for GSTs 3-3, 3-4 and 2-2 therefore appear to favour a steady-state random sequential mechanism. However, over the years, several models have been proposed to account for the apparent deviations from Michaelis-Menten kinetics of GST 3-3 (these are reviewed in Section 1.4.2) [39,179]. These suggestions have included subunit co-operativity [63], steady-state mechanisms of differing degrees of complexity [132], and the superimposition of product inhibition [132,133] or enzyme memory [179] on the latter. As recently as 1988, GSH-induced conformational transitions have been invoked to account for the non-hyperbolic steady-state kinetics of the GSTs [229].

As described in Section 1.4.2, no evidence has been found for co-operative interactions between the subunits of the dimeric GST isoenzymes studied, apparently eliminating negative co-operativity as a possible cause of the non-linearity (see also Section 4.4) [63,135,179,292].

A steady-state random mechanism involving kinetically significant enzyme•product complexes was proposed by Jakobson *et al.* [132]. They demonstrated that although the classical rate equation for a steady-state random mechanism fitted the data for GST 3-3 satisfactorily, their more complex model (which included > 10 parameters and terms of 4th degree in concentration of each substrate) fitted the data with a lower residual sum of squares. Despite the admission that this model was considerably overdetermined (having several redundant parameters and many other parameters with standard deviations of 100%), they concluded that this model best described the kinetic mechanism of GST 3-3 [132].

It is demonstrated here that the simplest steady-state random sequential Bi Bi mechanism, in the absence of products, is consistent with and sufficient to explain the non-hyperbolic kinetics of GST 3-3. Neither more complex steady-state mechanisms nor the superimposition of product inhibition or enzyme memory on the basic steady-state random sequential mechanism are necessary.

The simplest steady-state random sequential mechanism, as applied by Mannervik and Askelöf [184] to GST 3-3 in the absence of P and Cl^-, is shown below,

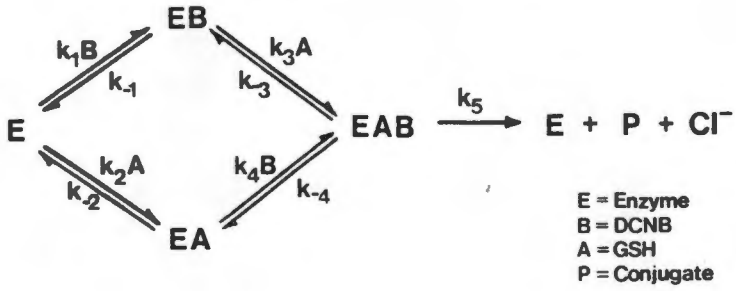

(1)

where E = enzyme, B = DCNB, A = GSH and P = the GSH·DCNB conjugate.

The rate equation corresponding to this mechanism is:

$$v = \frac{V_1AB + V_2A^2B + V_3AB^2}{K_1 + K_2A + K_3B + AB + K_4A^2 + K_5B^2 + K_6A^2B + K_7AB^2} \qquad \text{(Eqn. 1)}$$

where V_i (i = 1-3) are constants containing E_T, and V_i and K_j (j = 1-7) are combinations of the rate constants shown in scheme (1) [184].

For fixed concentrations of DCNB, Eqn. 1 simplifies to:

$$v = \frac{iA^2 + jA}{k + lA^2 + mA} \qquad \text{(Eqn. 2)}$$

where $i = V_2B$, $j = V_1B + V_3B^2$, $k = K_1 + K_3B + K_5B^2$,
$l = K_4 + K_6B$, and $m = K_2 + B + K_7B^2$ [85,221,252].

An analogous expression can be derived for constant concentrations of GSH. These simplified rate equations (like Eqn. 2) are 2/1 functions, i.e., in reciprocal form (after dividing through by A^2) $1/A^2$ appears in the numerator and $1/A$ appears in the denominator [252]. Both the reciprocal equation (Eqn. 3) derived from Eqn. 2 and the first derivative of the reciprocal form (Eqn. 4) are shown below.

$$1/v = \frac{k/A^2 + l + m/A}{i + j/A} \qquad \text{(Eqn. 3)}$$

$$\frac{dy}{dx} = \frac{kjx^2 + 2kix + (im - jl)}{(i + jx)^2} \qquad \text{(Eqn. 4)}$$

where $y = 1/v$ and $x = 1/A$.

The presence of squared terms in the rate equations means that the steady-state random mechanism *predicts* non-linear reciprocal plots with either substrate [58,85,221,252]. In fact, several distinct types of non-hyperbolic kinetics can be obtained in the steady-state random system (where E, EA, EB, A and B are not at equilibrium and k_5 of scheme (1) is greater than any of the other forward rate constants). For example, plots of v *versus* substrate concentration may exhibit zero, one, or even two inflection points if one route to EAB is kinetically more favourable than another [85,86,221,252].

Only under certain conditions, such as with saturating substrate concentrations or where special relationships exist between the kinetic parameters and the constant concentration of one substrate (see Section 4.4), will Eqn. 2 simplify so that linear double-reciprocal plots are obtained for the simplest steady-state random Bi Bi mechanism [58,85,252].

The required conditions for concave-down double-reciprocal plots are met when jl/im, ki/mj, $i^2k/j(mi - jl)$ and K_6A^2/m are all less than unity for fixed DCNB concentrations (or if the equivalent conditions hold for fixed GSH concentrations) [85,252]. Using the reported values of V_i and K_i for the metabolism of DCNB by GST 3-3 [184], which provided a good fit to the experimental data, it can be shown that Eqn. 2 predicts concave-down double-reciprocal plots over the whole range of substrate concentrations used experimentally (data not shown). Conditions for linearity of the double-reciprocal plots would only be met, using these V_i and K_i values, at very much lower concentrations of GSH (≤ 2 μM) or DCNB (< 5 μM) or at saturating concentrations of either substrate.

Using the converged values of V_i and K_i for the metabolism of CDNB by GST 2-2 (Table 3.6) it was also found that concave-down double-reciprocal plots are predicted over the whole range of substrate concentrations used experimentally (data not shown). As was the case for the reported values of V_i and K_i above [184], conditions for linearity of the double-reciprocal plots would only be met at very much lower concentrations or at saturating concentrations of either substrate.

As mentioned above, although concave-down reciprocal plots are consistent with negative co-operativity, hyperbolic binding isotherms have been reported for the equilibrium binding of GSH to GST isoenzymes 1-2 and 3-3 [135,292]. Contributions from co-operative subunit interactions cannot be completely ruled out, though the binding studies do not support this possibility. It therefore appears that the negative co-operativity of the GSTs is kinetically generated via the branched pathway of scheme (1). In theory, kinetically generated negative co-operativity disappears as the concentration of the fixed substrate becomes high enough to essentially force the reaction into an ordered mechanism (see Section 4.4). It was not possible to observe such a trend in this investigation because of the limited solubility of DCNB and CDNB in aqueous solution. The trend might however be observable with GSH concentrations in the range of 100 - 1000 mM.

Generally, in steady-state bisubstrate systems in which there is a preferred (but not exclusive) kinetic pathway to a ternary complex, there is no need to assume subunit-subunit interactions or ligand-induced conformational changes in order to explain sigmoidal responses [252]. This is because the complexities inherent in bisubstrate enzymic reactions can adequately account for 'allosteric' phenomena without necessarily involving protein-protein interactions. The non-hyperbolic kinetics of 3-deoxy-D-*arabino*-heptulosonate-7-phosphate synthetase of

Rhodomicrobium vannielli [141] and phosphofructokinase of *E. coli* [85] have also been interpreted in terms of such a kinetic model. This kinetic explanation for non-hyperbolic kinetics is not valid for rapid equilibrium systems (where the breakdown of EAB is rate-limiting), nor for systems in which either both routes to EAB are equally favourable or in which A and B add in an obligate order [252].

As Segel [252] has emphasised, "the possibility that a sigmoid velocity curve arises as a consequence of a random path to the central complex should be considered seriously by investigators dealing with 'allosteric' bireactant or terreactant enzymes."

In conclusion, the simplest steady-state random sequential Bi Bi mechanism is consistent with and is sufficient to explain the reported non-hyperbolic kinetics of GST 3-3 [184] and those observed here for GSTs 3-3, 3-4 and 2-2. This is the simplest mechanism consistent with all the kinetic, equilibrium binding and product inhibition data. Therefore, invoking Occam's razor†, neither more complex steady-state mechanisms nor the superimposition of product inhibition or enzyme memory on a steady-state random sequential mechanism are required to explain the non-hyperbolic kinetics.

---

†William of Occam's (1280-1349) dictum - *Entia non sunt multiplicanda practer necessitatem.*

4.4 A RAPID EQUILIBRIUM RANDOM SEQUENTIAL BI BI MECHANISM FOR HUMAN PLACENTAL GLUTATHIONE S-TRANSFERASE

For human placental GST π, double-reciprocal plots of initial rate data were linear over wide concentration ranges of both substrates (Section 3.3.2). This is in contrast to the initial rate data for rat liver isoenzymes 3-3 and 3-4 with CDNB and DCNB, which exhibit concave-down double-reciprocal plots (Section 4.3).

The intersecting initial velocity patterns shown in Figure 3.12 indicate that the kinetics of human placental GST π are consistent with a sequential mechanism, with both substrates adding to the enzyme before products are released [252]. This is in agreement with the available kinetic and stereochemical data for the interaction of GST isoenzymes with all substrates studied [175,179,249]. Although this pattern distinguishes the kinetic mechanism from a Ping-Pong system, in which one product leaves before the second substrate binds to the enzyme (and parallel lines are observed), these plots do not yield information on whether an ordered or random addition and release of reactants occurs [252].

The inhibition of GST π by the products of the enzymic conjugation reaction, was also investigated (Section 3.3.3). Initial rate data both in the absence and presence of the CDNB·GSH conjugate were fitted by non-linear least squares regression analysis to several rate equations describing bisubstrate mechanisms. Since the rapid equilibrium random mechanism was the simplest one consistent with all the kinetic experimental data for GST π, the kinetic constants are interpreted in terms of this mechanism. For example, since both the plots in Figure 3.12 intersect below the 1/[Substrate]-axes, the binding of either substrate decreases the affinity (dissociation constant) for the other substrate by a factor α (i.e., $\alpha > 1$), and the apparent K value for the varied substrate increases as the concentration of fixed substrate increases [252].

The linear double-reciprocal plots of substrate saturation are consistent with rapid equilibrium random substrate addition, and this model also provided the best fit to the experimental data (Table 3.4). Since steady-state initial rate equations for a random bisubstrate mechanism contain squared terms with respect to each substrate [252], biphasic plots would be expected at the unsaturating experimental

substrate concentrations (see Section 4.3). It must be noted, however, that both a steady-state random mechanism and a steady-state ordered mechanism may also give rise to straight-lined double-reciprocal plots [252], and therefore such plots may not be good criteria for discriminating between steady-state and rapid equilibrium substrate interactions (see below).

In addition to the linear initial velocity plots, the experimentally observed pattern of inhibition by the CDNB-GSH conjugate also indicated that the placental isoenzyme was not adequately described by the steady-state random mechanism which best fits GST 3-3 (see Section 3.3.3). For a steady-state random sequential Bi Bi mechanism, at fixed unsaturating substrate concentrations, 1/V-axis intercept replots should be hyperbolic, and slope replots would be more complex functions of the product inhibitor concentrations [252].

Although a rapid equilibrium ordered system with GSH binding first gave a reasonable fit to the data (Table 3.4), this mechanism could be eliminated on the basis of the characteristics of the reciprocal plots in the absence of inhibitors and also by the product inhibition pattern. In a rapid equilibrium ordered system with GSH binding first, the family of lines in the 1/v *versus* 1/[CDNB] plots (at fixed GSH concentrations) should intersect on the 1/v axis and above the horizontal axis [252]. This pattern of competitive activation by GSH is a method of distinguishing a rapid equilibrium ordered system from the rapid equilibrium random and steady-state ordered or random reactions [252]. The observed pattern of product inhibition is also inconsistent with that expected for a rapid equilibrium ordered mechanism (see Table 3.5).

Although a steady-state ordered Bi Bi mechanism could not be excluded by the initial velocity data in the absence of product (see above), and could not be distinguished from a rapid equilibrium random Bi Bi mechanism by computer modelling (see Section 3.3.2), the two mechanisms can be differentiated by product inhibition studies [252]. In a steady-state ordered Bi Bi system, the $K_{islope}^{P/GSH}$ is independent of CDNB concentration, and both slope and $K_{islope}^{P/GSH}$ replots would reflect this constant value [252]. However, the experimental value of $K_{islope}^{P/GSH}$ was observed to vary with CDNB concentration (Figure 3.15d), which is characteristic of a rapid equilibrium random mechanism where $\gamma \neq 1$.

The product inhibition data suggest that the mechanism may be a random one in which the interconversion of central complexes is largely the rate-limiting step (rapid equilibrium random), and in which at least one dead-end complex may form, namely that between enzyme, CDNB and the CDNB•GSH conjugate, as shown below [252],

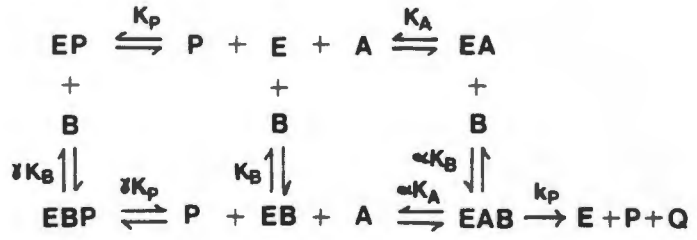

(2)

where E = Enzyme, B = CDNB, A = GSH, P = Conjugate, and Q = Chloride.

In this scheme, the binding of the conjugate to the enzyme does not competitively exclude CDNB, and the formation of a catalytically inactive (dead-end) enzyme•CDNB•conjugate complex is possible. Binding of the conjugate to the enzyme changes the dissociation constant for CDNB by a factor, γ, which results in the mixed-type inhibition observed in the 1/v *versus* 1/[CDNB] plots at varying conjugate concentrations and fixed GSH concentrations (see Figure 3.14). The binding of the conjugate is competitive with respect to GSH, and saturating GSH concentrations overcome inhibition by the conjugate. Saturation with CDNB will not reverse the inhibition by the conjugate, since some conjugate and CDNB can still bind to the enzyme to form the inactive enzyme•CDNB•conjugate complex. Therefore the conjugate remains a competitive inhibitor with respect to GSH at all CDNB concentrations.

Although the product inhibition data and the results of the computer modelling are consistent with this model, they provide only indirect evidence of the existence of a dead-end complex. Confirmation might be obtained experimentally by measurement of the binding of radiolabelled CDNB to GST π in the presence of the conjugate. If radiolabelled CDNB binds to the enzyme in the presence of the conjugate, this would provide direct evidence for the existence of an enzyme•CDNB•conjugate complex.

The evaluation of reports that other GST isoenzymes exhibit hyperbolic kinetics with CDNB and other substrates [107,177,249] is restricted by the use of limited ranges of substrate concentrations. It is known that the non-linearity of reciprocal plots may be difficult to observe over narrow ranges of substrate concentrations, and most kinetic studies have employed too narrow a range of substrate concentrations to establish whether the kinetics are truly hyperbolic or non-hyperbolic.

For example, Schramm *et al.* [249] proposed a rapid equilibrium random mechanism for rat liver isoenzyme 1-1, on the basis of linear double-reciprocal plots over a fivefold range of concentrations for both substrates. Their initial rate measurements were performed over a five by five matrix with regard to the concentrations of GSH (0.1 - 0.5 mM) and CDNB (0.2 - 1 mM). Over a similar GSH concentration range (0.15 - 1 mM), the kinetics of isoenzyme 3-3 with DCNB would also appear to be linear [215]. However, over a 67-fold GSH range (0.015 - 1 mM) the non-linear kinetics of isoenzyme 3-3 become apparent, with the discontinuity at about 0.1 mM GSH [215]. In contrast, the double-reciprocal plots for human placental GST π in this investigation were linear over a 10^3-fold range of GSH concentration and a tenfold CDNB range.

As mentioned above, straight-lined double-reciprocal plots do not necessarily preclude a steady-state random sequential mechanism. If assumptions are made concerning the relative significance of various terms, the rate equation for a steady-state random mechanism (Eqn. 1) will simplify, so that linear double-reciprocal plots are obtained [58,252]. Theoretical analysis of the rate equation has identified several sets of such conditions [58,252]:

1. If one substrate is saturating, the reaction flux is via one pathway to EAB and the randomness disappears, thereby essentially forcing the reaction to a steady-state ordered mechanism.

2. If both routes to EAB are approximately equally favourable, departure from linearity may be impossible to detect. The curvature of the reciprocal plot will occur close to the 1/v axis and the system will appear to be rapid equilibrium random.

3. At very low concentrations of the variable substrate, Eqn. 2 reduces to $1/v = k/(jA) + m/j$ and the curve approaches a linear asymptote.

4. Linear double-reciprocal plots occur over a wide range of DCNB or GSH concentrations if the first derivative (Eqn. 4) is invariant for all concentrations of variable substrate, i.e. if $i^2k = j(im - jl)$. Under these conditions, the second derivative of the reciprocal form, i.e.,

$$\frac{d^2y}{dx^2} = \frac{2\{i^2k - j(im - jl)\}}{(i + jx)^3} \qquad \text{(Eqn. 5)}$$

where $y = 1/v$ and $x = 1/A$, is zero.

For favourable reactions, isotope exchange may provide a means to determine whether or not a random system is rapid equilibrium [252]. If the interconversion of central complexes is the sole rate-limiting step, then all exchanges in a given direction must proceed at the same rate at any given set of reactant concentrations, since they are all limited by the flux through this step [93,252]. The kinetic mechanisms of both yeast hexokinase [242] and *E. coli* galactokinase [93] have been shown to be truly steady-state random, although the initial velocity and product inhibition patterns are fully consistent with the rate equation derived for the rapid equilibrium random model. In both cases, the exchange along one pathway was found to be at least double the exchange along the alternative route [242], indicating the presence of a kinetically preferred pathway (see Section 4.3).

Isotope exchange may in some cases also be able to discriminate between a steady-state ordered Bi Bi and a steady-state random Bi Bi mechanism [252]. For both liver [58,256] and yeast [256] alcohol dehydrogenase, all the kinetic data were consistent with a steady-state ordered mechanism, until isotope exchange revealed that the mechanism was random. Since the reaction catalysed by the GSTs is very exothermic and is considered to be irreversible for practical purposes [132], isotope exchange studies are unsuitable for further elucidation of the kinetic mechanism.

It is evident then that reaction kinetics adequately described by the rapid equilibrium random model may in fact represent a more complex mechanism in unusual cases [57]. Specifically, differences in the relative significance of various terms may account for the apparent difference in kinetic mechanism for the rat liver and human placental GST isoenzymes.

The phenomenon of isoenzymes from different sources exhibiting different kinetic mechanisms is not without precedent [157]. For example, lactate dehydrogenase of rabbit skeletal muscle cytosol has an ordered sequential Bi Bi mechanism, whereas the mitochondrially-bound isoenzyme exhibits non-hyperbolic kinetic behaviour [172]. Differences in kinetic mechanism have been described for the alcohol dehydrogenases from different sources [36,56,208,244]. Pig heart mitochondrial malate dehydrogenase operates via an ordered mechanism at pH 8, yet becomes partly random at pH 9 [56]. In contrast to the kinases mentioned earlier (which were truly steady-state, although fully consistent with the rapid equilibrium random model), isotope exchange revealed that creatine kinase from rabbit skeletal muscle has a truly rapid equilibrium random mechanism, with all exchanges occurring at equal rates under different conditions [56]. Furthermore, arginine kinase from Australian crayfish and nucleoside diphosphokinase from human erythrocytes both exhibit ping-pong mechanisms, as do hexokinases from mammalian brain and muscle [56].

In summary, although a more complex steady-state random mechanism cannot be unequivocally excluded, the rate equation describing the rapid equilibrium random model accurately predicts all the experimental findings. As is usual in such cases, the general principle of interpreting the data by the simplest consistent model is applied, and therefore it is entirely appropriate to interpret the initial velocity data in terms of this model [93,242,249,252].

The straight-lined Scatchard plot (Figure 3.19) indicates hyperbolic (i.e. non-co-operative) binding of the substrate to GST, and binding to identical and independent sites [252]. This binding study is fully consistent with a rapid equilibrium random sequential Bi Bi mechanism, and also with the equivalent steady-state mechanism. These results are also consistent with the hyperbolic binding isotherm and the stoichiometry of two reported for rat liver GST 3-3 [135], also obtained using equilibrium dialysis. A single binding site per dimer of rat liver GST 1-1 was found for a spin-labelled GSH analogue, using electron paramagnetic resonance spectroscopy [249]. The reported K_d (28 μM) for this latter isoenzyme was close to that observed in this investigation (33 μM), while the dissociation constant for GST 3-3 was 10 μM [135].

One interpretation of the non-linearity of the double-reciprocal plots observed with GST 3-3 has been to postulate the existence of negative co-operativity between subunits, although this is not supported by much of the binding data (see Section 1.4.2). While the binding studies with human placental GST π, in which only a single substrate (GSH) was used, might not detect negative co-operativity caused by the binding of the substrate in the presence of the co-substrate, the linear plots of substrate saturation observed for this isoenzyme do not call for explanation in terms of co-operative interactions. The finding of a hyperbolic binding isotherm for GSH with GST π, which has a rapid equilibrium random mechanism, gives indirect evidence for the unlikelihood of negative co-operativity between the subunits of GSTs generally. As demonstrated here, it is conceivable that a steady-state random mechanism could simplify to a rapid equilibrium model by alterations in rate constants, however it seems unlikely that negative co-operativity should be important in the mechanism of some GST isoenzymes, but not of others.

4.5 ACTIVE-SITE SOLVATION CONTRIBUTES SIGNIFICANTLY TO INACTIVATION OF THE GSTs.

An important aspect of GST chemistry is the fact that the isoenzymes are inactivated to varying extents, both reversibly and irreversibly, by several non-substrate ligands and highly reactive substrates/co-substrate conjugates [61,131,308,309]. Examples of the time-dependent inactivation of GST activity have been documented for GST isoenzymes from rat [61,131,307] and human liver [258], human placenta [227,308] and human erythrocytes [110]. The presence of GSH [61,131,308] or a variety of proteins [304] has been found to protect or partially protect the GSTs from time-dependent inactivation.

Vander Jagt and co-workers [304] explained this phenomenon by proposing that, in the presence of any of a variety of inhibitors, GSTs of rat and human liver exhibit conformational changes which are both time- and concentration-dependent, and which may lead to inactivation of the enzyme [258,304]. Foreign proteins (and GSH) are able to interact with the enzyme, preventing or partially preventing it from adopting an inactive conformation, and resulting in the formation of different active conformations of GST, each showing distinct specific activities depending on the nature of the protein [304]. These 'protein-protein interactions' are apparently weak (occurring without the formation of stable complexes) and non-selective, since almost any protein (including the enzyme itself) is able to participate in them. Furthermore, the foreign protein is only able to prevent the inhibitor exerting its conformational effect on the enzyme if the protein is added prior to the enzyme adopting the inactive conformation, or during the time of the conformational changes. Vander Jagt and colleagues [304] described these protein-protein interactions as a form of 'enzyme memory', involving the transmission of information through macromolecular interactions, with each conformation reflecting the prior history of events involving interaction of inhibitor, GST and foreign protein.

The kinetic complications inherent in an 'enzyme memory' mechanism have subsequently been used to explain the apparent deviations of GST 3-3 from Michaelis-Menten rate behaviour [179], although the discussion in Section 4.3 has shown that the imposition of enzyme memory on the basic steady-state random sequential model is not necessary. The finding that incubation with GSH enhanced the activity of purified GSTs [12,132,150] has also been related to the kinetically stable activity states of the 'enzyme memory' mechanism [179].

In this laboratory, a number of studies of the time-dependent inactivation of GSTs from rat liver and human placenta have been performed (see Table 4.1). During the course of these investigations, we have observed that a further type of inactivation, which does not appear to have been previously characterised, occurs on dilution of concentrated stock solutions of GST in buffer. We have proposed (Adams, Goold & Sikakana, unpublished results) that this type of inhibition, which follows pseudo-first-order kinetics, with a rate constant of 0.0025 s^{-1} at 25°C (pH 6.5) and does not proceed to 100% inactivation, is the result of solvation of the hydrophobic active-site of the enzyme.

The studies conducted in this laboratory [131, Table 4.1], as well as results compiled from a survey of the literature [61,110,227,308], have revealed that a first-order inactivation of GST - with a rate constant close to that observed for dilutional inactivation above - was widespread over a range of GST isoenzymes and inactivating agents in unrelated experiments (summarised in Table 4.1).

In this thesis, examples of this first-order inactivation phenomenon may be found in the time-dependent inhibition of human placental GST activity by MP-8 (Section 3.7) and in the inhibition of Sigma rat liver GST by EDB (Section 3.1). The first-order rate constant was 2.2 (± 0.4) x 10^{-3} s^{-1} for the former, and 1.64-2.25 x 10^{-3} s^{-1} for the latter.

The remarkable constancy of the inactivation rate constant in all these cases, together with the fact that the various inactivating agents affect the extent of inactivation but not the rate constant for the process, suggests that these compounds are not inactivating agents *per se*. They merely facilitate an increase in the extent of solvation by increasing the degree to which water can penetrate the hydrophobic active-site. The resultant loss of hydrophobicity (which would differ in extent, depending on the nature and concentration of inhibitor) would determine the activity loss of the enzyme preparation.

Table 4.1 : **The Pseudo-First-Order Rate Constants for Irreversible Inactivation of a Range of GSTs**

Inactivating Agent	GST Isoenzyme	Mean k_{obs} s^{-1} (x 10^{-3})	Ref.
CDNB (1 mM)	Human Placental π	2.5	308
CDNB (1 mM EDTA), 30°C	Human Placental π	1.2	227
CTX (1 mM EDTA), 30°C	Human Placental π	0.5	227
Solvent (1 mM EDTA), 30°C	Human Placental π	0.7	110
Solvent	Human Placental π (Sigma)	2.5	‡
CDNB (1 mM)	Human Placental π (Sigma)	1.7	‡
Solvent	Human Placental π (this prep)	2.7	‡
CDNB (0.8 mM)	Human Placental π (this prep)	1.7	‡
CDNB (1.2 mM)	Human Placental π (this prep)	1.6	‡
MP-8 (0.4 μM)	Human Placental π (this prep)	2.2	Section 3.7
CDNB (0.5 mM), 37°C	Human Erythrocyte ρ	10.5	110
CDNB (1.2 mM)	Human Acidic Lung GST	5.3	61
EDB (37 mM)	3-3 (Rat Liver)	2.0	131
Solvent	3-4 (Rat Liver)	2.8	‡
CDNB (1.2 mM)	3-4 (Rat Liver)	1.7	‡
CDNB (1.2 mM)	3-4 (Rat Liver)	2.5	*
EDB (37 mM)	Rat Liver GST Mix (Sigma)	2.6	131
EDB (5 mM)	Rat Liver GST Mix (Sigma)	2.2	Section 3.1
CDNB (1.2 mM)	Rat Liver GST Mix (Sigma)	2.5	*

‡Adams, Goold & Sikakana, unpublished results

*Sikakana *et al.*, unpublished results

CTX - cefataxine; EDB - Ethylene dibromide; Solvent - phosphate buffer pH 6.5, μ = 0.1. Except where otherwise noted, T = 25°C. Standard deviations on the above rate constants are of the order of ± 15%.

We have also proposed (Adams, Goold & Sikakana, unpublished results) that the observed partial protection of GST from this type of inactivation by preincubation with GSH [61,131,308 (and in this thesis, Sections 3.1 and 3.7)] is caused by the tripeptide physically blocking the approach of water molecules into the catalytic centre. Similarly, the differing degrees of protection of GST activity observed on preincubation with foreign proteins (or with higher concentrations of enzyme) [304] are explicable in terms of the preservation, to varying extents, of the hydrophobic nature of the enzyme active-site by localised interactions in the environment of the site. The concentration-dependence of this protection, the finding that no stable enzyme•inhibitor•protein complexes are observed [304], and the fact that protection is only afforded the enzyme if the protein is added prior to the inactivating agent, are all fully consistent with the proposed solvational inactivation of the GSTs. In addition solvational inactivation adequately accounts for the observed irreversiblity of the inhibition of GST activity by CDNB [61,136,215,304] and EDB [131], previously attributed to stable conformational states [61,304] or covalent binding [61,131].

The pH-dependence of the inhibition of GSTs by non-substrate ligands has been explained in terms of the allosteric formation of different enzyme•substrate•inhibitor conformers at different pH values [39,311]. It may be speculated that changes in pH create perturbations in the hydrophobicity of the enzyme active-site, which result in different degrees of solvation inactivation (this hypothesis is under investigation in this laboratory).

Independent confirmation of the role of dilutional inactivation in the mechanism of human placental GST has been obtained in the studies, reported in this thesis, of the binding kinetics of the interaction between GST π and MP-8 (see Section 4.7).

While solvation of the active-site provides a simple alternative explanation for a number of the observed phenomena concerning the type of inactivation of GST described here, it does not preclude the existence of other types of enzyme inactivation (such as that caused by cross-linking at sulphydryl groups), which may occur in addition to solvation inactivation.

4.6 OPTIMISATION OF THE PREPARATION OF MP-8

The preparation of MP-8 from cytochrome-*c* using proteolytic enzymes has undergone several improvements in recent years. In general terms, however, the procedure involves the cleavage of cytochrome-*c* by peptic digestion to produce the haem undecapeptide (MP-11), which is then further degraded to the haem octapeptide (MP-8) by tryptic digestion. Conventional methods for the preparation of MP-8 require extensive column chromatography, are time consuming and result in relatively poor yields (≈ 50%) of approximately 90% pure MP-8 in 8-10 days [11]. The commercial product is consequently expensive. These factors, together with an increasing interest in MP-8 as a model for monomeric haemin and the recognition of a need for product of higher purity, have led to attempts to develop a more rapid optimised preparative schedule for MP-8.

Analytical HPLC has provided a convenient method for monitoring the kinetics of the conversion of cytochrome-*c* to haempeptides as well as an efficient means of separating closely related haempeptides. As a result, a considerably more rapid (≈ 30 h) and efficient (≈ 90% yield) HPLC-based preparative method for MP-8 has recently been proposed, which results in a product containing no detectable impurities by analytical HPLC (> 99% pure) [4].

The HPLC study of temperature effects on the kinetics of the peptic digestion of cytochrome-*c* which was performed as part of this investigation, together with a similar study of the tryptic digestion of MP-11, have facilitated further optimisation of the conditions for the preparation of MP-8 [5]. By performing both the peptic and tryptic digestions at 40°C, it has become feasible to purify pure MP-8 (to the point of lyophylisation) from cytochrome-*c* within 4 hours [5]. In addition, a reduction in contamination by other haem-containing peptides has been achieved.

While the shorter incubation time must reflect, in part, an Arrhenius-law rate increase, the fact that non-MP-11 haem-containing contaminants are reduced suggests that the higher temperature may be causing the cytochrome-*c* to adopt a less ordered conformation, allowing the pepsin easier access to the MP-11 cleavage sites and resulting in a cleaner conversion of cytochrome-*c* to MP-11.

An important feature of this optimised preparation was the removal of non-haem peptide contaminants by ammonium sulphate precipitation of MP-11 after peptic digestion of cytochrome-*c* (Figure 3.20b). Non-haem-containing amino acids and peptides account for about 85% by weight of the pepsin digestion, and this material could act as tryptic substrates or inhibitors and, by competition with the MP-11, retard the conversion of MP-11 to MP-8. The removal of hydrophilic peptide impurities (Figure 3.20b) by ammonium sulphate precipitation reduces the half-life for MP-8 formation at 40°C from approximately 30 minutes for the non-precipitated sample to approximately 80 seconds. These results are in agreement with those of Petersen *et al.* [220] who, using a similar but slower ammonium sulphate precipitation procedure, concluded that the precipitation step alone represents a considerable purification of MP-11.

The use of a bovine serum albumin affinity column to purify MP-11 from non-haem peptides was first proposed by Wilchek [321]. In this study, the inclusion of such a step enabled the removal of trypsin and MP-11-derived tripeptide from the tryptic digest. In contrast to the observations of Wilchek, it was found that binding of haem-peptide to the affinity column was much less effective when human serum albumin was substituted for bovine serum albumin as an affinity ligand. This may be explicable in terms of the kinetic differences observed, in this laboratory, between bovine and human serum albumin in their reaction with MP-8. MP-8 reacts with bovine serum albumin in a single stage first-order manner, while a more complex, multistage and slower interaction is observed with human serum albumin [6 - see Appendix 1].

4.7 THE KINETICS AND MECHANISM OF THE INTERACTION BETWEEN HUMAN PLACENTAL GST π AND MP-8

A survey of the literature on the interaction of non-substrate ligands with the GSTs revealed that investigations to date have been exclusively thermodynamic (e.g., competitive binding, equilibrium dialysis and direct absorption spectroscopy) or quasi-thermodynamic (e.g., effects of non-substrate ligands on the steady-state kinetics of the enzyme-catalysed conjugation reaction) in nature. While undoubtedly of considerable value, such studies may not be amenable to unambiguous interpretation when taken in isolation. Klotz and co-workers [46] have recently cautioned against using purely thermodynamic grounds to determine the number and nature of ligand/protein binding sites. In addition to highlighting the difficulties associated with thermodynamic studies of GST/ligand interactions, Boyer and Kenney [39] have emphasised that considerable care must be exercised in the mechanistic interpretation of steady-state studies of the inhibition of GSTs by non-substrate ligands.

In this investigation, the interaction of the non-substrate ligand MP-8 and human placental GST was studied by observation and analysis of the time-course of the binding process (Section 3.6). This represents the simplest and most direct 'extra-thermodynamic' procedure by which the mechanism of ligand/protein interaction can be studied, and to the author's knowledge, no such study of the reaction between substrate/non-substrate ligands and any of the GSTs has yet been published.

The observed quenching of the MP-8 Soret peak on addition of GST to solutions of MP-8 (Section 3.6) suggests a hydrophobic interaction between haem peptide and protein, involving the porphyrin macrocycle interacting via π-π bonding with aromatic amino acid residues at the binding site, rather than axial ligation of the iron by donor ligands (imidazole of histidines) on the protein. In support of this statement, it is noted that the interaction of MP-8 with human serum albumin and apo-myoglobin (both of which bind haemin by axial ligation of the iron) leads to a red shift in the λ_{max} (Soret) of approximately 15 nm [6 (Appendix 1)]. In contrast to this, when uroporphyrin I (a largely monomeric porphyrin) interacts hydrophobically with ligandin, changes in the λ_{max} (Soret) have been found to be very small (2 nm) [294]. This result is also consistent with the concept of an enzyme which interacts with a wide range of non-iron-containing hydrophobic substrates and non-substrate ligands.

As described in Section 3.6, the kinetics of quenching followed a biexponential time course over the whole range of MP-8 concentrations used in this study. Attempts to model the kinetics using a single exponential function gave statistically inadequate fits. The observed straight-line dependence of the individual pseudo-first-order rate constants on MP-8 concentration (Figure 3.24) suggests that the biexponential kinetics are due to two separate uncoupled pseudo-first-order processes.

Bilirubin is a non-substrate ligand which has previously been shown to interact with human placental GST at a site which is spatially distinct from the catalytic site on the enzyme [308]. Preincubation of bilirubin with GST prior to addition of MP-8 eliminated the slow binding phase of MP-8 to GST (Section 3.6), so that the resultant kinetic data were best described by a first-order process (Figure 3.26). The pseudo-first-order rate constant obtained from the data of Figure 3.26 ($3.2 \times 10^{-3}\ s^{-1}$) agrees well with the value of $3.4 \times 10^{-3}\ s^{-1}$ interpolated at an MP-8 concentration of 3.5×10^{-7} M from the variation of k_1^* shown in Figure 3.24. It is therefore concluded that the slow kinetic phase reflects interaction at or spatially very close to the hydrophobic bilirubin binding site on the enzyme.

Addition of the co-substrate CDNB completely eliminated the rapid phase of the MP-8/GST interaction (Figure 3.27 and inset). The rate constant calculated for the resultant first-order process ($7.9 \times 10^{-4}\ s^{-1}$) is in good agreement with the value of $5.9 \times 10^{-4}\ s^{-1}$ interpolated from the slow phase data of Figure 3.24. Therefore the rapid phase of the MP-8/GST interaction reflects binding of MP-8 close to or at the CDNB binding site.

The MP-8/GST binding kinetics observed in the presence of GSH were biphasic (Figure 3.28). The values of k_1^* ($3.5 \times 10^{-3}\ s^{-1}$) and k_2^* ($6.5 \times 10^{-4}\ s^{-1}$) obtained from the biexponential fit are again close to the corresponding values interpolated from Figure 3.24 (i.e., $k_1^* = 3.4 \times 10^{-3}\ s^{-1}$ and $k_2^* = 5.9 \times 10^{-4}\ s^{-1}$). Since GST catalyses the conjugation of GSH and CDNB, it is reasonable to assume that the binding sites for these co-substrates are adjacent on the enzyme. Therefore, the fact that CDNB eliminated the fast MP-8 binding site, while GSH had minimal effect on the binding kinetics of MP-8, suggests that the fast MP-8 binding site is adjacent to but not identical to the CDNB site (possibly situated on the opposite side of the CDNB site to that at which GSH binds). If the CDNB and fast MP-8 sites were in fact identical, the greater size of the MP-8 would undoubtedly overlap to a considerable extent with the GSH binding site, resulting in significant

GSH effect on the fast binding stage. Since only a minimal GSH effect is observed to occur, we conclude that the MP-8 haem binds close to the CDNB locus distal to the GSH site, with the possibility that one or more residues from the octapeptide chain overlap the CDNB site.

These observations can thus be summarised by stating that MP-8 binds to GST at two discrete, non-interacting sites on the GST subunit. The kinetically faster site is proximal to the CDNB site and possibly on the side opposed to the GSH binding site. The slower site is at or spatially close to the hydrophobic bilirubin binding site.

Several possible models can be proposed to account for the biexponential kinetics of the binding of MP-8 to GST. One explanation might be that MP-8 binds in a reversible two-step manner to a single site on the enzyme, but this is precluded by the fact that the two sites are dissectable (with bilirubin eliminating the slow phase and CDNB the fast phase). The biexponential kinetics therefore represent not a two-step binding to a single site, but rather a random binding to two separate sites with different rate constants.

The simplest mechanism apparently consistent with the observation of two discrete non-interacting MP-8 binding sites on the enzyme is of the random sequential type shown below,

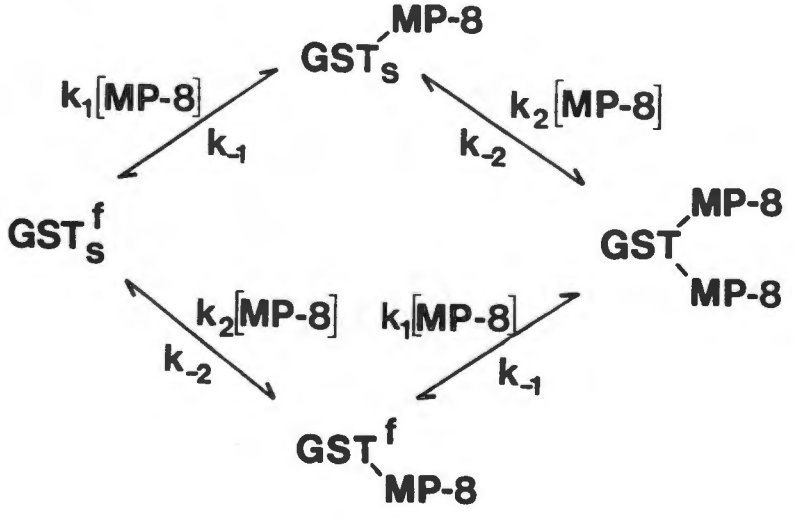

(3)

where 'f' and 's' represent the fast and slow MP-8-binding sites, respectively.

Since site 'f' is observed to be kinetically much faster than site 's', the system can be simplified and closely approximated by

(4)

Under pseudo-first-order conditions, the following expressions can be written for k_1^* and k_2^*:

$$k_1^* = k_1[\text{MP-8}] + k_{-1} \qquad \text{(Eqn. 6)}$$

$$k_2^* = \frac{k_2 k_1[\text{MP-8}]^2}{k_1[\text{MP-8}] + k_{-1}} + k_{-2} \qquad \text{(Eqn. 7)}$$

and when $k_1[\text{MP-8}] >> k_{-1}$, Eqn. 7 reduces to:

$$k_2^* = k_2[\text{MP-8}] + k_{-2} \qquad \text{(Eqn. 8)}$$

Evaluation of the apparent rate constants from the slope and intercepts of the plots in Figure 3.24 yields the following values:

$k_1 = 5500\ (\pm 230)\ M^{-1}\,s^{-1}$; $\quad k_2 = 630\ (\pm 25)\ M^{-1}\,s^{-1}$
$k_{-1} = 2.2\ (\pm 0.4) \times 10^{-3}\ s^{-1}$; $\quad k_{-2} = 3.7\ (\pm 0.6) \times 10^{-4}\ s^{-1}$,

at pH 7.0, $\mu = 0.1$, and 22.5°C.

Immediately, it is apparent that both mechanisms (3) and (4) are over-simplifications, since the condition $k_1[\text{MP-8}] >> k_{-1}$ required for the straight-line dependence of k_2^* on MP-8 concentration (Eqns. 7 and 8 above) clearly does not hold in this case.

It is hoped to demonstrate that a slightly more complex model for the interaction of MP-8 and GST, based on the phenomenon of solvation of the enzyme active-site, is fully consistent with the observed kinetic data. The contribution of active-site solvation towards the inactivation of the GSTs has been discussed in Section 4.5. In the proposed model, shown below

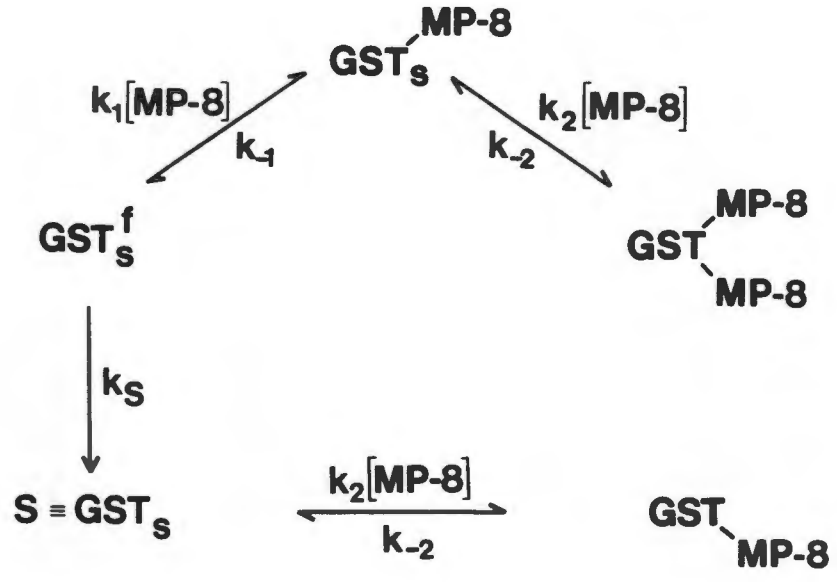

(5)

the species S is a solvated form of the enzyme in which the 'fast' MP-8 binding site is eliminated, but the binding integrity of the 'slow' MP-8 binding site is retained. In terms of the concept outlined above, the loss of hydrophobicity which is resultant upon solvation of the catalytic site of the enzyme (the CDNB interaction locus) profoundly affects further hydrophobic binding at the site. MP-8 is therefore prevented from binding at the CDNB site (represented by the kinetically fast phase), but can still bind at the bilirubin site (slow phase). When CDNB is incubated with GST prior to the addition of MP-8 (as in Figure 3.27), the CDNB facilitates solvation of the active-site and therefore the kinetically fast phase of the MP-8 binding kinetics is eliminated.

This explanation for the biphasic binding kinetics of MP-8 and GST is suggested by the observation that the limiting value of k_1^* at zero MP-8 concentration ($0.0021 \pm 0.0004\ s^{-1}$) is virtually identical to the pseudo-first-order rate constant observed for dilutional inactivation of GST π ($0.0024 \pm 0.0004\ s^{-1}$ at 25 °C).

Moreover, it can be demonstrated kinetically that mechanism (5) is consistent with the experimental observations. If the 'fast' phase of mechanism (5) is isolated, it is equivalent to the simple system describing two parallel and independent first-order reactions [29], *viz.*

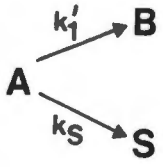

(6)

,

where A and B correspond to GST and the GST•MP-8 complex, respectively, S is the solvated form of the enzyme and k_S corresponds to the solvation rate constant.

For this system, the overall rate of disappearance of free A is the sum of both reactions, i.e.,

$$\frac{-d[A]}{dt} = k_1'[A] + k_S[A] \qquad \text{(Eqn. 9)}$$

$$= (k_1' + k_S)[A]$$

$$= k[A]$$

where $k = (k_1' + k_S)$.

In its integrated form, Eqn. 9 yields

$$[A] = [A]_o e^{-kt} \qquad \text{(Eqn. 10)}$$

where $[A]_o$ is the initial concentration of GST.

The rate of formation of B (the GST•MP-8 complex monitored in the fast kinetic phase) is given by

$$\frac{d[B]}{dt} = k_1'[A]_o e^{-kt} \qquad \text{(Eqn. 11)}$$

which integrates to yield

$$[B] = \frac{k_1'[A]_o}{k} \left[1 - e^{-kt} \right] \qquad \text{(Eqn. 12)}$$

The first-order 'fast' rate constant k_1^*, evaluated experimentally from the biexponential kinetic fits, is now equivalent to k in Eqn. 12, which is itself equivalent to $k_1' + k_S$. Also, since k_1' in mechanism (6) is equal to k_1[MP-8] in mechanism (5), we thus obtain $k_1^* = k_1$[MP-8] + k_S. The dependence of k_1^* on MP-8 concentration is therefore predicted to be straight-line, with slope k_1 and intercept equal to k_S at [MP-8] = 0, in agreement with the experimental observations.

An independent measurement of k_S, determined by following the pseudo-first-order dilutional inactivation of GST (see Table 4.1), was found to be 2.5 (± 0.3) x 10^{-3} s^{-1} (at 25°C, pH 6.5, μ = 0.1), in good agreement with the value of 2.2 (± 0.4) x 10^{-3} s^{-1} obtained from Figure 3.24 at 22.5°C. Furthermore, the error limits on the values of k_S allow us to estimate approximately a maximum value for k_{-1} (the rate constant for dissociation of MP-8 from the fast site) to be of the order of 4 x 10^{-4} s^{-1}.

It is possible to discriminate further between mechanism (5) and mechanism (3). For mechanism (3), the relative proportion of the total absorbance change occupied by each phase should be independent of MP-8 concentration. However, for mechanism (5), the relative absorbance change due to the fast phase of the reaction (A_r), where

$$A_r = \Delta A_f / (\Delta A_f + \Delta A_s) \qquad \text{(Eqn. 13)}$$

should approach zero as the [MP-8] → 0 [29]. Figure 3.25 demonstrates such a dependence of A_r on MP-8 concentration, thereby favouring mechanism (5).

Using the values for k_1, $k_{-1\ max}$, k_2 and k_{-2} calculated from Figure 3.24, we can calculate dissociation constants for the fast and slow kinetic sites. These are found to be $K_f = 7.2 \times 10^{-8}$ M (upper limit) and $K_s = 5.9 \times 10^{-7}$ M, respectively. These values lie well within the range of K_D values observed for other GSTs [39] and are in good agreement with the value of $K_i = 10^{-7}$ reported for the inhibition of human erythrocyte GST ρ by haemin [110].

4.8 THE INHIBITION OF HUMAN PLACENTAL GST BY MP-8

Studies of the steady-state inhibition of the GST-catalysed conjugation reaction are an important technique by which the spatial relationship between non-substrate ligand binding loci and the enzyme catalytic site may be investigated [39] and, when viewed in the context of the kinetics of binding of the non-substrate ligand to the enzyme, such studies can provide a particularly valuable insight into the detailed nature of non-substrate ligand/GST interaction (see Section 4.7). Accordingly, the investigations reported here of the MP-8-mediated inhibition of the GST π-catalysed GSH/CDNB conjugation reaction are interpreted in the light of the direct GST/MP-8 binding kinetic studies discussed in Section 4.7.

Incubation of MP-8 with GST for various times prior to assay (using CDNB and GSH as substrates) resulted in a pseudo-first-order loss of enzyme activity with time (Figure 3.29). Since control values (enzyme incubated in buffer alone) were subtracted from each data point in Figure 3.29, the data are corrected for the first-order inactivation which occurs on dilution of the enzyme in buffer (see Section 4.5). However, the pseudo-first-order rate constant calculated for the MP-8-mediated inactivation (k_{obs} = 2.3 (± 0.4) x 10^{-3} s^{-1}, at 22.5 °C) was identical to the value found for dilutional inactivation alone (2.4 (± 0.2) x 10^{-3} s^{-1}), with only the extent of inactivation differing in the presence of MP-8.

Steady-state kinetic studies at constant GSH and varying CDNB concentrations established the inhibition by MP-8 as being of the linear mixed-type [252], shown below,

$$\begin{array}{ccccccc} E & + & S & \overset{K_S}{\rightleftharpoons} & ES & \xrightarrow{k_p} & E + P \\ + & & & & + & & \\ I & & & & I & & \\ K_i \Big\| & & & & \alpha K_i \Big\| & & \\ EI & + & S & \overset{\alpha K_S}{\rightleftharpoons} & ESI & & \end{array} \qquad (7)$$

From the parameter values shown in Table 3.8 for the linear mixed-type inhibition system, it is noted that K_i at 30°C (3.3×10^{-7} mol) is in reasonable agreement with the $K_{f(max)}$ value of 7.2×10^{-8} mol for MP-8 binding proximal to the CDNB binding site at 22.5°C, inferred independently from microscopic rate constants (Section 4.7). This agreement provides good evidence that the MP-8/GST fast binding site and the MP-8 catalytic inhibition site are one and the same.

For human erythrocyte GST ρ (an enzyme physically, catalytically and immunochemically identical to the placental isoenzyme studied here [100,305]) Harvey and Beutler [110] have concluded that haemin inhibits the enzyme competitively. This conclusions was based on the observation that Dixon plots (at two CDNB concentrations) intersected at a point clearly above the concentration axis. However, the Dixon plots obtained for pure competitive inhibition are known to be identical to those for the mixed-type system (scheme 7) elucidated here [252]. Indeed, assuming mechanism (7) for the data of Harvey and Beutler [110], values for K_S and K_i could be obtained for the erythrocyte isoenzyme at 37°C. These values are shown in Table 3.8, and are in excellent agreement with the results obtained here for human placental GST. Accordingly, a detailed study of haempeptide interaction with human erythrocyte GST is being conducted in this laboratory.

This investigation has shown that the MP-8-mediated inhibition of the steady-state GST-catalysed conjugation reaction between GSH and CDNB is caused by MP-8 binding close to the CDNB interaction locus at the active-site. MP-8 and GSH affect each others interaction with the enzyme only minimally. These results are in excellent accord with the conclusions reached in the direct study of MP-8/GST binding kinetics (Section 4.7). Interestingly, it appears that whereas the binding of CDNB blocks that of MP-8 to the kinetically fast binding site (Section 4.7), incubation of the enzyme with MP-8 gives a complex which can still apparently bind CDNB, resulting in the catalytically inactive ESI complex of scheme (7).

5. CONCLUSIONS

The simplest steady-state random sequential Bi Bi mechanism is sufficient to explain the reported non-hyperbolic kinetics of GST 3-3 [184] and those observed here for GSTs 3-3 and 3-4. This mechanism is consistent with all the kinetic, equilibrium binding and product inhibition data for these isoenzymes. Neither more complex steady-state mechanisms nor the superimposition of product inhibition or enzyme memory on the basic steady-state random sequential mechanism are necessary to account for the non-hyperbolic steady-state kinetics of the GSTs.

Steady-state studies of other GST isoenzymes in this investigation have indicated that rat liver GST 2-2 is similarly best described by a steady-state random mechanism, while the hyperbolic kinetics observed for human placental GST π over wide ranges of substrate concentrations are consistent with a simpler rapid equilibrium random sequential Bi Bi mechanism.

Isoenzymes 2-2, 3-3 and π, are representative of the Alpha, Mu and Pi categories of GST, respectively. The first two isoenzymes originate from rat liver, while GST π originates from human placenta. It remains to be established whether the kinetic mechanisms of the GSTs varies between species or isoenzyme classes. It would therefore be of value to investigate the nature and extent of the kinetic variability of GST isoenzymes, as it may be possible that kinetic mechanism may be a further criterion to distinguish GST isoenzyme categories.

The time-dependent inactivation of various GSTs, by a variety of different inactivating agents in unrelated experiments, follows a first-order rate law with a pseudo-first-order rate constant of approximately 2.5×10^{-3} s^{-1}. The similarity between this value and that of the pseudo-first-order rate constant for the inhibition observed on dilution of concentrated solutions of GST suggests that these compounds are not inactivating agents *per se*. They merely facilitate an increase in the extent of solvation of the hydrophobic active-site. The proposed concept of solvation inactivation provides a simple explanation for the observation of various kinetically stable conformational states for different GST isoenzymes. These conformational states result from the interaction of GST with different inactivating agents and/or agents (such as GSH and foreign proteins) capable of providing partial protection from inactivation (see Section 4.5).

This investigation has resulted in a much more rapid method for preparation of MP-8, with higher yield and greater purity than possible by conventional methods. This was achieved by the optimisation of digest temperature and the introduction of steps designed to reduce contamination by non-MP-8 and non-haem impurities (Section 3.5). Clearly, HPLC procedures will have a major impact on studies of the haempeptides of cytochrome-c, by facilitating the rapid preparation in high yield of ultra-pure samples of these compounds. Further studies are at present in progress in this laboratory designed to exploit HPLC procedures in the optimisation and purification of haem-peptides MP-6, MP-7 and MP-9 in a time period of hours, rather than the days currently required.

The nature of the binding sites for the non-substrate ligand MP-8 on human placental GST has been investigated here by examining the binding kinetics of MP-8 with the enzyme, and the effects of other substrate/non-substrate ligands on these kinetics (Section 4.7). The binding constants obtained in these 'extra-thermodynamic' studies are assessed directly from microscopic rate constants and are therefore more directly interpretable than those obtained in the thermodynamic procedures usually employed to study GST/non-substrate ligand interactions.

Microperoxidase-8 (as an aqueous phase model for monomeric haemin) has been shown to bind to GST π at two sites, the first of which is identified with the hydrophobic bilirubin-binding locus, and the second being adjacent to the hydrophobic CDNB co-substrate binding site. These studies have therefore provided direct confirmation of the independence of the catalytic and bilirubin-binding sites of GST π [306,308]. On the basis of the kinetic studies described, it is plausible that the kinetically more rapid site is at or close to the CDNB binding site, while the slower binding site is the same as or close to the bilirubin binding site. From the fact that GSH has only a minimal effect on the interaction of MP-8 with GST π, we can infer that the kinetically fast binding site is adjacent but not identical to the CDNB binding site.

Furthermore, the direct kinetic binding studies reported here have proved valuable in allowing unambiguous interpretation of the inhibition by MP-8 of the steady-state kinetic of the GSTs. The agreement between the MP-8/GST binding kinetics and the studies of the MP-8-mediated inhibition of the conjugation reaction (Section 4.8) provides strong evidence that the effect of MP-8 on catalysis occurs in the region of the CDNB locus at the active-site.

The rate constant observed for the time course of MP-8-mediated GST inhibition ($2.3 \times 10^{-3}\ s^{-1}$), which was also found independently in the binding studies in Section 4.7, is identical to that found for dilutional inactivation of GST in buffer alone at pH 6.5, 22.5°C. The excellent agreement between these values probably signifies the occurrence of some type of solvational interaction at the catalytic site. It is conceivable that the binding of MP-8 close to the CDNB site may well increase the extent of solvation of the active-site with a concomitant increase in polarity and decrease in catalytic efficiency of the enzyme-catalysed conjugation reaction.

Finally, this study has demonstrated that MP-8 is a potentially valuable analogue of monomeric haemin with which to investigate the nature and location of metalloporphyrin binding sites on the haem-binding GSTs.

APPENDIX 1

Heme-peptide/Protein Interactions : The Binding of the Heme Octa- and Undecapeptides, Microperoxidase-8 and -11, to Human Serum Albumin.

By

Paul A Adams[1]*, Richard D Goold[2] and Alfred A Thumser[2]

[1] MRC Biomembrane Research Unit
Department of Chemical Pathology

and

[2] Department of Medical Biochemistry
University of Cape Town
Medical School
Observatory 7925
Cape Province
Republic of South Africa

*Author to whom all correspondence is addressed

Abstract : The interaction of the heme octa- (MP-8) and undeca- (MP-11) peptides derived from cytochrome-*c* with lipidated human serum albumin (HSA) has been investigated in aqueous solution. It is demonstrated that complex formation occurs in each case with a 1:1 stoichiometry. CN^- binding has been used to investigate the accessibility of the heme in each complex by comparison with CN^- interaction with methemalbumin. A preliminary study of the kinetics of the Fe^{3+}MP-8(11)/HSA interaction demonstrates a clear ligand size related effect on mechanism of interaction - an *ad hoc* explanation of which is given in terms of HSA existing as two non-converting conformers in solution.

Introduction : The kinetics of the interaction between hemin and human serum albumin is more complex than observed for the corresponding reaction with hemopexin (1,2). Further complicating the interpretation of small ligand-binding studies with HSA has been the recent suggestion that HSA exists as two non- (or very slowly inter-) converting conformers, which show different affinities toward hemin (2,3). These conformers (designated I (one) and II (two)) are present in the ratio I/II $\simeq$ 2 and bind deuteroporphyrin IX with $K_a = 1.5 \times 10^7\ M^{-1}$ and $4.9 \times 10^8\ M^{-1}$, respectively.

Equilibrium binding studies of the hemin/HSA reaction (4) and comparative kinetic studies of metalloporphyrin/defatted HSA interaction (5) indicate one primary high-affinity HSA hemin-binding site; in addition, as many as 10 weaker binding sites - which also bind fatty acid residues - were observed per molecule of HSA. The primary binding site for the metalloporphyrin appears to be in a hydrophobic region of the protein, with limited access to the bulk aqueous solvent (6), a conclusion which is in agreement with kinetic studies of the reaction between monomeric hemin and lipidated HSA (7). This study interpreted the binding mechanism as a two stage process (1),

$$\text{Hm} + \text{HSA} \underset{k_{-1}}{\overset{k_1}{\rightleftharpoons}} \text{I} \underset{k_{-2}}{\overset{k_2}{\rightleftharpoons}} \text{Met·Hm·Alb} \qquad (1)$$

the first stage of the process is a reversible bimolecular reaction followed by a reversible unimolecular 'internalization' of the bound hemin to its transport site within the protein.

As part of a general study of the interaction of pure heme-peptides derived from

cytochrome-*c* (the microperoxidases) and their derivatives, with a number of heme-binding proteins and apo-proteins, we have investigated the interaction between the heme octa- and undeca-peptides (MP-8 and MP-11, respectively) with lipidated HSA.

Materials and Methods : Human serum albumin (HSA) crystalline and essentially globulin free obtained from fraction V, was from Sigma Chemical Co. MP-11 and MP-8 were prepared by peptic and tryptic digestion of horse heart cytochrome-*c* (Sigma Chemical Co.) and purified by HPLC as described elsewhere (8). Hemin was recrystallized by the chloroform-pyridine method, and stored under N_2 at 4°C until required. Concentration of stock solutions were determined spectrophotometrically using the following extinction coefficients;

1.57×10^5 M^{-1} cm^{-1}	(pH 7.00, μ = 1);	MP-8 (9)
1.78×10^5 M^{-1} cm^{-1}	(pH 2.25);	MP-11 (10)
1.74×10^5 M^{-1} cm^{-1}	(Neat DMSO, 405 nm);	Hemin (11)
3.74×10^4 M^{-1} cm^{-1}	(pH 7.00, μ = 0.01, 279nm);	HSA (12)

The purity of the KCN used here was determined by $AgNO_3$ titration (13), and found to be 98.1%. CN^- ion concentrations at each pH were calculated according to

$$[CN^-] = [KCN] / (1 + [H^+]/K_{HCN})$$

where pK_{HCN} = 9.21 in aqueous solution at 25°C (14). Kinetic data was fitted to mono-, bi- and tri-exponential functions

$$Abs = a_0 + a_1 e^{k1*t} (+ a_2 e^{k2*t} + (a_3 e^{k3*t}))$$

by a non-linear least-squares procedure (15) utilizing the Marquhardt algorithm, to give pseudo-first-order rate constants k_1^*, k_2^* and k_3^*.

Spectrophotometric studies were carried out using a Varian 635 or Hewlett Packard 8450A UV/Visible spectrophotometer. Absorbance linearity and accuracy were checked using pure *p*-nitrophenoxide anion as described elsewhere (16). The photometric stability of the 635 machine was reflected in an absorbance drift of $< 2 \times 10^{-4}$ $AU_{396/409nm}$ per hour after stabilization for 2 hr. Peak to peak noise level was $< 3 \times 10^{-4}$ AU.

Results : *Interaction of MP-8 and MP-11 with HSA* : Addition of HSA (2×10^{-5} mol dm^{-3}) to MP-8 (2×10^{-6} mol dm^{-3}) at pH 7.0, μ = 0.1, 25°C results in the

spectral and difference spectral changes shown in Fig. 1. Similar changes were observed when MP-8 was replaced by MP-11.
Spectrophotometric titration of these concentrations of MP-8 and MP-11 at 15°C was carried out by incubation of the heme peptides with varying concentrations of HSA. Samples were removed and $A_{409} - A_{396}$ in the difference spectrum (*vs* MP-8/11) was measured, results (corrected for HSA absorbtion) are shown for the MP-11/HSA system in Fig. 2. Values for the Hill parameter 'n' and the association constant were determined for the MP-11/HSA interaction as described previously (16), values of 0.99 and 5 (± 1) x 10^4 mol^{-1} dm^3 respectively being obtained. In the case of MP-8/HSA the stoichiometry was 1:1 but K_a was too high to measure using this technique.

Binding of CN^- by Fe^{3+}MP-8·HSA and Fe^{3+}MP-11·HSA : Addition of CN^- ([KCN] = 1.8 x 10^{-3} mol dm^{-3} ≡ [CN^-] = 1 x 10^{-5} mol dm^{-3}) to the Fe^{3+}MP-8·HSA conjugate gave no detectable change in the visible absorbtion spectrum of the conjugate over a period of 1 hr (Fig. 3b). Difference spectroscopy showed that a very slight broadening of the soret peak was occurring with no shift in λ_{max}, we do not attribute this change to formation of a CN^-/hemeprotein complex.

In contrast to this observed lack of CN^- interaction with MP-8·HSA, addition of CN^- to Fe^{3+}MP-11·HSA resulted in a soret shift from 406 to 408 nm with a decrease in intensity of ≃ 10% (Fig. 3c). Difference spectroscopy showed the final complex to be indistinguishable from CN^-·Fe^{3+}MP-11. The pseudo-first-order rate constant for the spectrophotometric change was 0.05 (± 0.008) s^{-1} at 25°C and this may be compared to a rate-constant for MP-11 dissociation from the HSA complex of 0.0108 s^{-1} measured at 15°C (see later).

A comparative study of CN^- binding was carried out using methemalbumin prepared by incubation of hemin (5 μM) with a 5 x 10^{-5} mol dm^{-1} solution of HSA at pH 7. Binding of CN^- to this species was observed to occur slowly and in an accurately first-order manner. At constant pH the observed first-order rate constant was independent of [CN^-] over a ten-fold concentration range (Fig. 4) implying that CN^- is not reacting with methemalbumin directly in a second-order manner (such interaction would require - under the concentration conditions of the experiment - that $k_{obs} = k_f[CN^-] + k_r$) but with free hemin as it dissociates from the methemalbumin complex. The pH variation of k_{obs} was investigated in the region pH 7 to 7.6 and the results are shown in Fig. 5. Included in Fig. 5 is the limiting rate constant for the dissociation of hemin from methemalbumin (k_{-2} in

scheme (1)) determined in 37.5% DMSO/H_2O by asymptotic kinetic studies of monomeric hemin HSA interaction (7), μ = 0.05. These values may also be compared to values of 0.005 s^{-1}, obtained for the limiting dissociation rate constant of methemalbumin measured by interprotein transfer kinetics in 40% DMSO/ Buffer, μ = 0.3 (1) and 0.002 s^{-1} obtained by dithionite reduction of methemalbumin in 2.5% DMSO/Buffer μ = 0.3 pH 7.0 (2). We conclude therefore that the spectral changes observed when CN^- is added to Fe^{3+}MP-11·HSA and methemalbumin result not from CN^- hemeprotein interaction, but from CN^- trapping of the heme(peptide) as it dissociates from the heme(peptide)·HSA complex. The complete lack of reaction observed on addition of CN^- to Fe^{3+}MP-8·HSA indicates that the dissociation of MP-8 from the final complex is exceedingly slow.

Addition of CN^- to Fe^{3+} myoglobin at similar concentrations to those used for the heme peptide/HSA complexes led to complete formation of the CN^- Mb complex within 5 sec. Addition of CN^- to Fe^{3+} cyt b_5, where the Fe^{3+} is inaccessible due to bis axial ligation by histidine imidazoles, gave no detectable change in either the spectrum or the difference spectrum. We thus conclude that the heme in the HSA complex is not accessible to small anionic ligands (see discussion).

Dithionite reduction of Fe^{3+}MP-8/11·HSA conjugates : Addition of small amounts of solid sodium dithionite to the Fe^{3+}MP-8/11 HSA conjugates produces typical Fe^{2+} hemoprotein spectra (Fig. 6). The α/β band intensity ratio in each case is 1.31, typical of low-spin hemoproteins with one strong axial ligand. Reduction of methemalbumin with solid sodium dithionite in 10% DMSO/aq. gave similar spectral changes, the α/β ratio was again found to be 1.31. Addition of dithionite (at half the concentrations used for reduction of the protein complexes) to solutions of MP-8/11 of the same concentration as above gave immediate bleaching of the Soret peak (Fig. 6).

Kinetics of the Fe^{3+}MP-8/11-HSA interaction : A preliminary investigation of the Fe^{3+}MP-8(11)/HSA reaction kinetics has been carried out. The reaction of the heme-peptides with HSA was followed by UV/visible spectrophotometry with manual mixing, monitoring the absorbance increase at 409 nm or decrease at 396 nm. Kinetic traces were obtained under conditions of [HSA]/[MP-8/11] > 10 over a 7.5 fold range of HSA concentrations. Kinetic traces for the MP-8/HSA reaction were in all cases multiphasic, as can be seen in Fig. 7. Mono- and bi-exponential functions did not adequately model the experimental curves. The

former was rejected on the basis of both non-random distribution of residuals, and gross underfitting of experimental data as assessed by the ratio estimated/observed precision (σ^*/σ) (17). The biexponential fit, although giving $\sigma^*/\sigma \simeq 1$, was rejected on the basis of non-random distribution of residuals (18) at the 95% level. A triexponential function was found in all cases to model the data adequately, i.e. without overfitting and with residuals distributed randomly at the 95% level or greater. In the case of the MP-11/HSA interaction, a single exponential function was found to model the data adequately at all MP-11 concentrations. Pseudo-first-order rate constants (k_1^*, etc.) for the three phases of the MP-8/HSA reaction were obtained (with Std. Deviations) at all HSA concentrations. These are plotted in Figs. 8 a-c *vs* [HSA], included in Fig. 8a are the data for the first-order Fe^{3+}MP-11/HSA interaction.

Discussion : We have provided strong evidence in this study that both Fe^{3+}MP-8 and Fe^{3+}MP-11 interact with lipidated HSA with a 1:1 stoichiometry to form discrete heme-peptide protein complexes. Spectral features shown by the dithionite-reduced heme peptide protein complexes are consistent with a low spin state configuration, in which the iron (II) is coordinated by a strong donor axial ligand.

The inability of CN^- to interact with heme or heme peptide when bound to HSA shows that the iron porphyrin is not accessible to the approach of small ligands in these complexes (see results), in agreement with our previous contention that the heme in methemalbumin is internalized by the protein for transport (7). Clearly such internalization can be rationalized from a physiological point of view as it would be undesirable to have protein-bound, and thus potentially enzymatically-active heme circulating freely *in vivo*.

The lack of CN^- trapping observed with MP-8·HSA is consistent with a very low, or zero rate constant for dissociation from Fe^{3+}MP-8·HSA. This is in agreement with both the very high K_a inferred from the titration data, and a limiting dissociation rate constant of $<0.00002\ s^{-1}$ observed for formation of the final Fe^{3+}MP-8·HSA complex (Fig. 8c and discussed later).

The kinetics of the MP-11/HSA reaction conform to a simple second-order reversible mechanism as shown in (2).

$$Fe^{3+}MP\text{-}11 \quad + \quad HSA \quad \underset{k_{-1}}{\overset{k_1}{\rightleftharpoons}} \quad Fe^{3+}MP\text{-}11{\cdot}HSA \qquad (2)$$

Rate constants for the process were evaluated from Fig. 8a, assuming (2), and give $k_1 = 4.40\ (\pm\ 0.62) \times 10^2\ mol^{-1}\ s^{-1}\ dm^3$, $k_{-1} = 0.0108\ (\pm\ 0.001)\ s^{-1}$. This gives a $K_{a(calc)} = 4.1\ (\pm\ 0.5) \times 10^4\ mol^{-1}\ dm^3$, in good agreement with the value of $K_{a(app)} = 5\ (\pm\ 1) \times 10^4\ mol^{-1}\ dm^3$ calculated from the equilibrium binding studies.

In contrast to the MP-11/HSA system, the MP-8/HSA reaction is by no means simple. The secondary plots of the rate constants k_1^* and k_2^* (Figs. 8a/b) suggest a mechanism of the type (1) found for methemalbumin. Indeed, if we evaluate the forward and reverse rate constants for each stage of the reaction using the data of Figs. 11a/b values of $k_1 = 4.3\ (\pm\ 0.4) \times 10^2\ mol^{-1}\ s^{-1}\ dm^3$, $k_{-1} = 0.030\ (\pm\ 0.003)\ s^{-1}$, $k_2 = 0.023\ (\pm\ 0.004)\ s^{-1}$, and $k_{-2} = 0.002\ (\pm\ 0.004)\ s^{-1}$ are obtained, in addition a value of $K_1\ (= k_1/k_{-1})$ of $1.9 \times 10^4\ mol^{-1}\ dm^3$ is obtained as a parameter from the transient state equation fit to Fig. 8b (7).

Several points should be made at this stage for the MP-8/HSA kinetics :
(i) k_1 and k_{-1} are extremely close to the values obtained for the MP-11/HSA reaction above.
(ii) K_1 calculated from the ratio of the microscopic rate-constants k_1/k_{-1} obtained from the data shown in Fig. 8a, is $1.4\ (\pm\ 0.3) \times 10^4\ mol^{-1}\ dm^3$, again in good agreement with the value of $1.9\ (\pm\ 0.5) \times 10^4\ mol^{-1}\ dm^3$ obtained when K_1 is evaluated as a parameter in the analysis of the k_2^* *vs* concentration data (7) - this part of the model is therefore internally self consistent.

The data of Fig. 8c suggest that a slow parallel reaction of the type (3) is also occurring,

$$Fe^{3+}MP\text{-}8 \quad + \quad HSA \quad \underset{k_r}{\overset{k_f}{\rightleftharpoons}} \quad Fe^{3+}MP\text{-}8{\cdot}HSA \qquad (3)$$

rate constants evaluated for this model give $k_f = 70\ (\pm\ 3)\ mol^{-1}\ s^{-1}\ dm^3$, $k_r < 0.00002\ s^{-1}$, and we note that this implies a $K_a > 3.5 \times 10^6\ mol^{-1}\ dm^3$, in agreement with the fact that the K_a is too high to measure by spectrophotometric titration. In addition lack of reaction of CN^- with MP-8 when mixed with $Fe^{3+}MP\text{-}8{\cdot}HSA$ is in good agreement with $k_r < 0.00002\ s^{-1}$.

Before discussing the possible causes of the complex kinetics exhibited by the MP-8/HSA system, we will state, with reasons, several factors which we consider not to be responsible for the observed effects.

(a) *Aggregation* : In common with most iron porphyrins in aqueous solution, MP-8/11 aggregate to form dimers and possibly higher oligomers (9). In the present system however, MP-8 is > 90% monomeric at 15°C and exhibits complex interaction kinetics while MP-11 (which shows a greater tendency to aggregation due to the α and ϵ-NH_2 groups of Valine and Lysine respectively) shows particularly simple second-order binding kinetics. We do not therefore consider aggregation to be responsible for the observed kinetics.

(b) *HSA preparation* : The HSA preparation used in this study was shown by gel-filtration to be >95% monomeric, we do not consider therefore that the effects observed reflect binding kinetics for a heterogeneous population of HSA molecules (monomer, dimer and trimer) each with different numbers (1, 2 and 3 respectively) of identical primary binding sites. Indeed, this possibility is also rejected by the 1:1 binding stoichiometry observed for each hemepeptide/protein system.

A simple *ad hoc* model, which allows a semiquantitative interpretation of the observed transition in binding kinetics as the ligand size increases from monomeric ferriprotoporphyrin IX to Fe^{3+}MP-11 can be put forward if the HSA is considered to exist as two non-converting conformers, as referred to in the Introduction. The model assumes that the accessibility of ligands greater than a certain size is sterically more hindered in the HSA conformer II than in conformer I. Thus if ferriprotoporphyrin IX has equivalent access to each site, and if the interaction rate constants for the two parallel reactions are of the same order of magnitude, then the kinetics observed for two parallel reactions of type (1) will be a biphasic process (an average of the two reactions) as found previously (7).

In the case of Fe^{3+}MP-11 we assume that access to the primary site of the second conformer-II is totally restricted, however the undecapeptide can react with conformer I to the intermediate stage of mechanism 1. Fe^{3+}MP-8 interaction kinetics would be expected to lie somewhere between these extremes, as is indeed, observed. Interaction with the less restricted primary site of conformer one proceeds at a rate comparable to Fe^{3+}MP-11, followed by partial internalization by conformer one, to a final form in which the heme is closer to the protein surface than for methemalbumin. At the same time a parallel but much slower interaction

occurs with the more restricted site of conformer two, to give the intermediate (I in (1)) which again due to steric constraint by the octapeptide chain cannot internalize the Fe^{3+}MP-8, but in which the heme peptide is more tightly bound ($k_r \simeq 0$).

While we accept that the above model is to a large extent conjectural it should be stressed that the experimental results presented here are reasonably explained e.g., the high K_a for Fe^{3+}MP-8/HSA observed after 48 hr incubation results from the fact that - due to the very low k_r of (3) - eventually most of the Fe^{3+}MP-8 will bind to conformer two. The CN^- binding studies, in which we have shown that reaction only occurs on dissociation of MP-11 from the intermediate (I) complex with conformer one, while no reaction is observed with the complex of MP-8 with conformer two (since $k_{-1} \simeq 0\ s^{-1}$ for this intermediate), suggest that the initial association reaction (characterized by k_1) consists of heme-binding in a pocket or cleft in the protein where the heme is inaccessible to small anionic ligands. We therefore consider that the heme in the intermediate I is not bound at the protein surface in a form freely accessible from the bulk medium, but is a heme-inaccessible complex which rearranges via the k_2 stage to a completely heme-enveloped form.

This concept is also supported by rate constant data for the initial association stage of heme protein binding processes, namely "I" formation characterized by k_1. Literature data for the binding of carboxy hemes (assumed monomeric) to "globin", prepared by the relatively harsh denaturing acid-acetone procedure, shows that k_1 values are of the order of 10^7 - 10^8 $mol^{-1}\ s^{-1}\ dm^3$ and approach the diffusion limiting value expected for sterically unconstrained binding (19).

In the case of apo-myoglobin prepared by the mild acid-butanone procedure of Teale (20), k_1 is found in the range 3-6 x 10^5 $mol^{-1}\ s^{-1}\ dm^3$ for hemin (21,22), and a value of 1.6 x 10^6 $mol^{-1}\ s^{-1}\ dm^3$ is obtained for monomeric MP-8 (Adams, Goold and Thumser, manuscript in preparation), indicating that while subject to more rigorous steric requirements than for denatured "globin", access to the primary binding site is equally facile for the iron porphyrin and heme peptide. In the case of HSA however, the binding rate constant k_1 for monomeric hemin is 1.6 x 10^5 $mol^{-1}\ s^{-1}\ dm^3$ (in 37.5% DMSO/buffer) (7), while that for the heme peptides is a factor of $\simeq 4 \times 10^2$ less, indicating that the peptide moiety is now exercising a constraint on the process, possibly by restricting the depth to which the peptide-bound heme can penetrate unrestricted into a "cleft" in the protein. We therefore

consider that the association rate constant k_1 provides a useful index of the accessibility of the primary heme-binding locus.

Detailed studies are at present being made of the kinetics of interaction of the suite of peptides MP-6, 7, 8, 9 and 11 (and their acetylated derivatives) with both HSA and bovine serum albumin in 20% DMSO/Aqueous buffer, and 20% MeOH /Aqueous buffer, in which the peptides are >95% monomeric at a concentration of 10^{-6} mol dm^{-3}. These studies are hoped to clearly demonstrate the size-mechanism relationship postulated above.

In conclusion we note that cytochrome-*c* ingested in mammalian diet is subject to initially peptic and subsequent tryptic digestion in the gut which will result in MP-11 and MP-8 formation. If these soluble heme peptides cross the intestinal mucosa relatively easily then they will certainly become available for albumin transport *in vivo*, and may thus constitute a significant route by which iron enters the mammalian system.

References

1. Pasternak, R.F., Gibbs, E.J., Hoeflin, E., Kosar, W.P., Kubera, G., Skowronek, C.A., Wong, N.M., and Muller-Eberhard, V., (1983) *Biochemistry*, **22**, 1753-1758

2. Pasternak, R.F., Gibbs, E.J., Mauk, G.A., Reid, L.S., Wong, N.M., Kurokawa, Ko., Hashim, M., and Muller-Eberhard, V., (1985) *Biochemistry*, **24**, 5443-5448

3. Moehring, G.A., Chu, A.H., Kurlansik, L., and Williams, T.J., (1983) *Biochemistry*, **22**, 3381-3386

4. Beaven, G.H., Shi-Haa Chen., D'Albis, A., and Gratzer, W.B., (1974), *Eur. J. Biochem.*, **41**, 539-546

5. Parr, G.R., and Pasternak, R.P., (1977) *Bioinorg. Chem.*, 7, 277-282

6. Cannistraro, S., (1983) *Stud. Biophys.*, **98**, 133-145

7. Adams, P.A., and Berman, M.C., (1980) *Biochem. J.*, **191**, 95-102

8. Adams, P.A., Byfield, M.P., Milton, R.C.deL., and Pratt, J.M., (1988) *J. Inorg. Biochem.*, in press

9. Aron, J., Baldwin, D.A., Marques, H.M., Pratt, J.M., and Adams, P.A., (1986) *J. Inorg. Biochem.*, **27**, 227-243

10. Peterson, J., Saleem, M.M.M., Silver, J., Wilson, M.T., and Morrison, I.E.G., (1983) *J. Inorg. Biochem.*, **19**, 165-178

11. Collier, G.S., Pratt, J.M., De Wet, C.R., and Tschabalala, C.F., (1979) *Biochem. J.*, **179**, 281-289

12. Clark, P., Rachinsky, J.R., and Foster, J.F., (1962) *J. Biol. Chem.*, **237**, 2509-2513

13. Kolthoff, I.M., Sandall, E.B., Meehan, E.J., and Brukenstein, S., (1969) Quantitative Chemical Analysis 4th Ed., Macmillan, London, 811-812

14. Tsonopoulos, C., Coulson, D.M., and Inman, L.B., (1976) *J. Chem. Eng. Data*, **21**, 190-193

15. Leatherbarrow, R.J. (1987) *ENZFITTER*, Elsevier, Netherlands

16. Adams, P.A., Adams, C., and Baldwin, D.A., (1986) *J. Inorg. Biochem.*, **28**, 441-454

17. Kohnstam, G., (1967) *Adv. Phys. Org. Chem.*, (Academic Press, London and New York) **5**

18. Swed, F.S., and Eisenhardt, C., (1943) *Ann. Math. Stat.*, **14**, 66-87

19. Gibson, A., and Antonini, E., (1963) *J. Biol. Chem.*, **238**, 1384-1388

20. Teale, F.W.J., (1959) *Biochim. Biophys. Acta*, **35**, 543 21. Adams, P.A., (1976) *Biochem. J.*, **159**, 371-376

22. Adams, P.A., (1977) *Biochem. J.*, **163**, 153-158

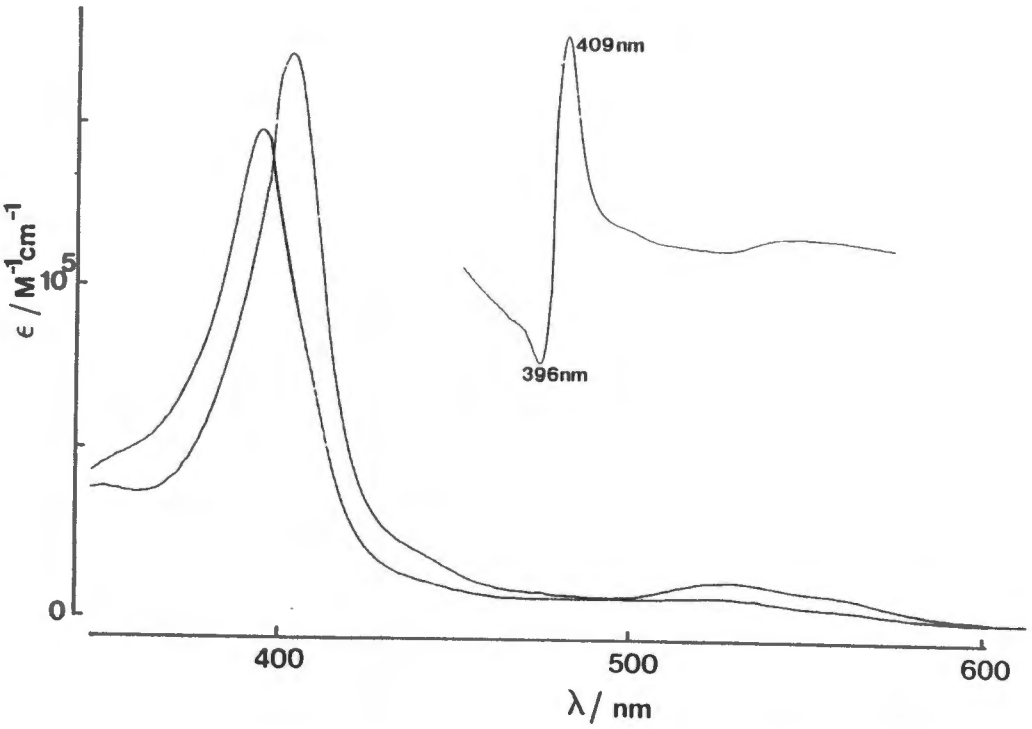

Figure 1. Spectrophotometric changes observed on addition of HSA (2×10^{-5} mol dm^{-3}) to MP-8 (2×10^{-6} mol dm^{-3}). Inset shows the difference spectrum Fe^{3+}MP-8·HSA *vs* Fe^{3+}MP-8. Trace **a** : MP-8; Trace **b** : MP-8·HSA.

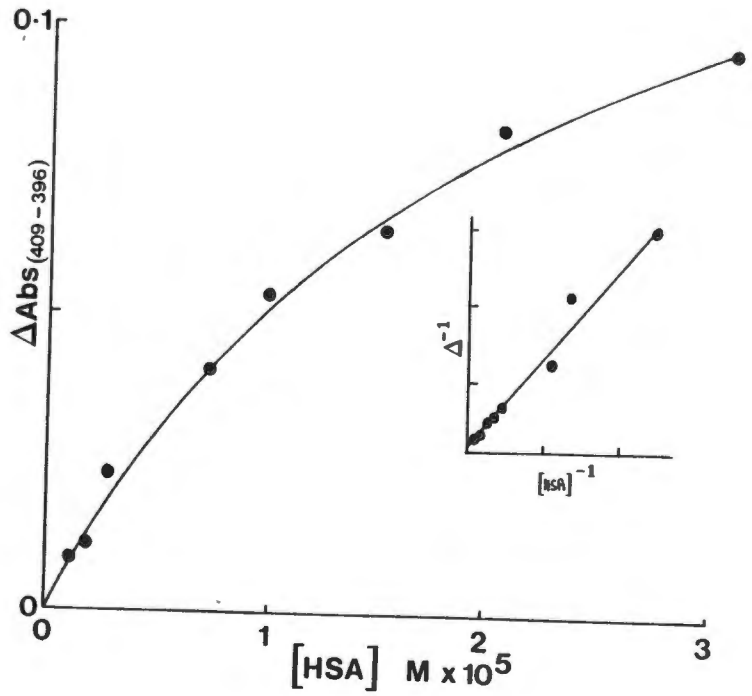

Figure 2. As for Fig. 1 but Fe^{3+}MP-11 in place of Fe^{3+}MP-8. Points shown are at 48 hr and are essentially unchanged from the 30 min values. Inset shows a double reciprocal plot of the data, indicating a hyperbolic relationship between Δ_{Abs} and concentration, implying n = 1 as found.

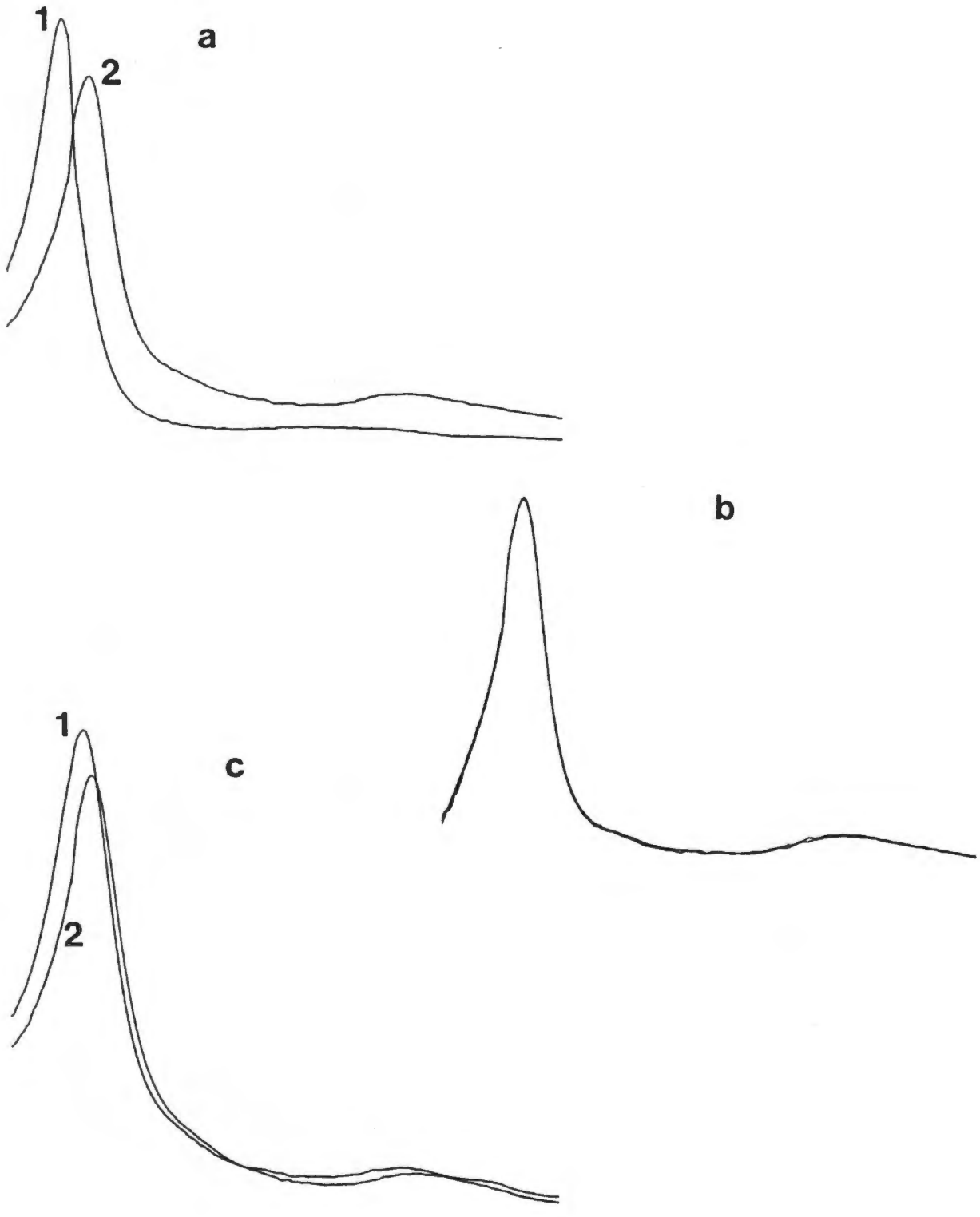

Figure 3. Spectral changes observed in addition of CN^- (1×10^{-5} mol dm^{-3}) to a) Fe^{3+}MP-8, b) Fe^{3+}MP-8·HSA and c) Fe^{3+}MP-11·HSA (all 2×10^{-6} mol dm^{-3}; [HSA] = 1×10^{-4} mol dm^{-3}). In all cases (1) is the species prior to addition of CN^- (2). In a) the spectrum (2) was obtained 10 s after CN^- addition; in b) the spectra (1) and (2) are indistinguishable after 60 min, and in c) the spectrum (2) was obtained 1 min after addition of CN^-. λ_{max} for 1 and 2 in a) are 396 nm and 408 nm respectively; in b) 406 nm, and in c) 406 nm and 408 nm respectively.

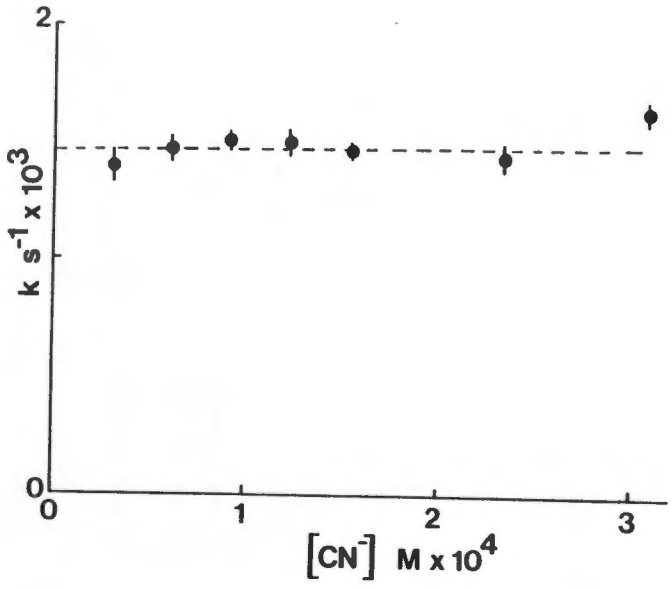

Figure 4. Variation of the rate constant for CN^- interaction with methemalbumin (5×10^{-6} mol dm^{-3}) over a range of CN^- concentrations (pH 7.15, 25°C).

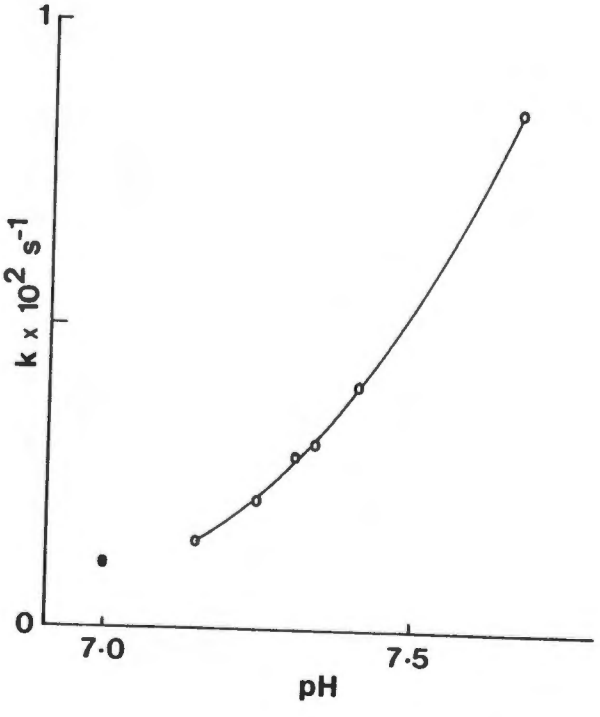

Figure 5. (O) pH variation of the 1st order rate constant for CN^- interaction with methemalbumin at 25°C. The solid point represents the value of k_{-2} (mechanism (1)) obtained previously using asymptotic kinetic procedures (7).

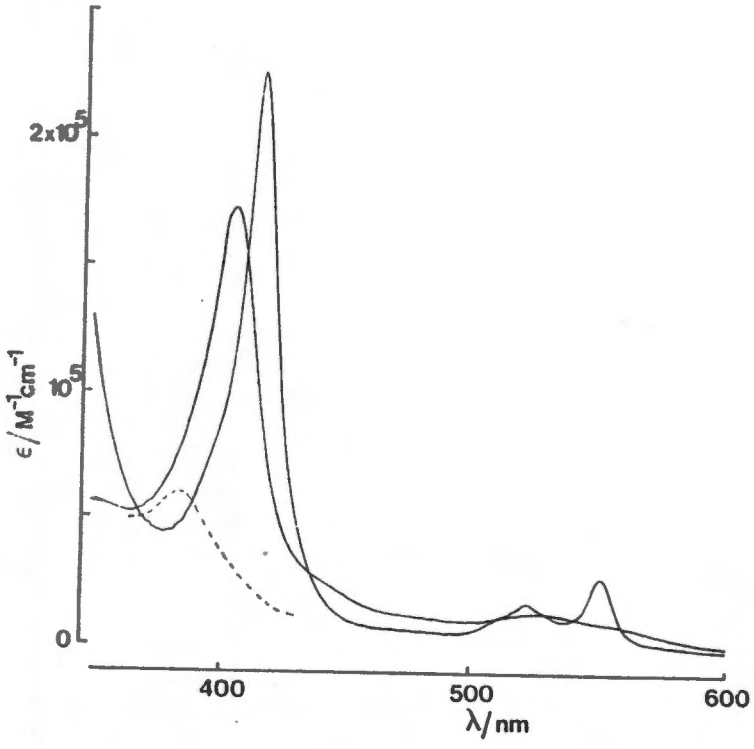

Figure 6. The solid line spectrum a shows the dithionite reduction product of the Fe^{3+}MP-8·HSA complex b (MP-8 :- 2×10^{-6} mol dm^{-3} + HSA :- 1×10^{-4} mol dm^{-3}). The dashed line shows the spectrum obtained 2 sec after addition of half the amount of dithionite to Fe^{3+}MP-8.

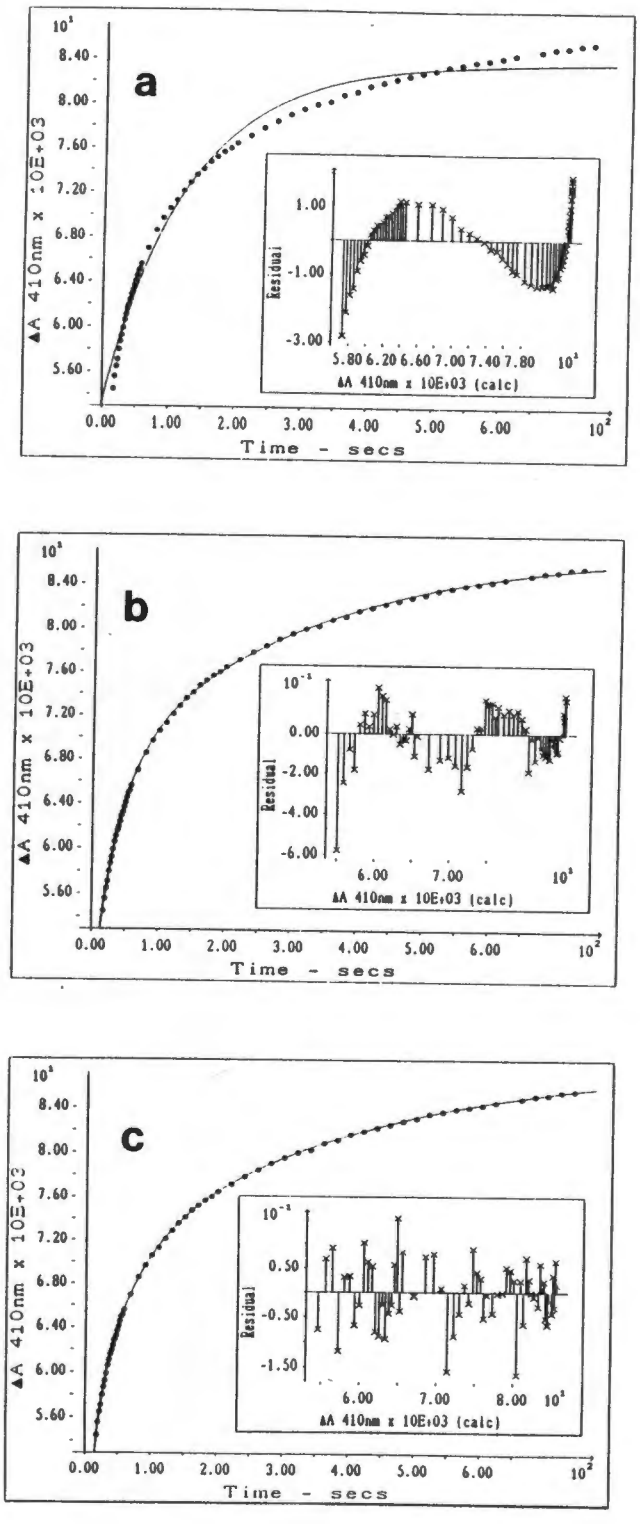

Figure 7. (a) Fitting of a single exponential function to Fe^{3+}MP-8. HSA interaction data, [HSA] = 7.5×10^{5} mol dm^{-3} [MP-8 = 1×10^{-6} mol dm^{-3}, T = 15°C, pH = 7.0, μ = 0.1. The solid line is: Abs = 83.78 - 30.05 $e^{0.007858t}$ (b) As in a) but double exponential fit to data. Solid line is: Abs = 87.15 - 19.80 $e^{0.0265t}$ - 21.02 $e^{0.00338t}$ (c) As in a) but triple exponential function fitted. Solid line is: Abs = 88.511 - 11.32 $e^{0.0641t}$ - 16.44 $e^{0.0140t}$ - 18.71 $e^{0.0025t}$ The Abs axis is in arbitrary units obtained on digitization. The inset show the distribution of residuals.

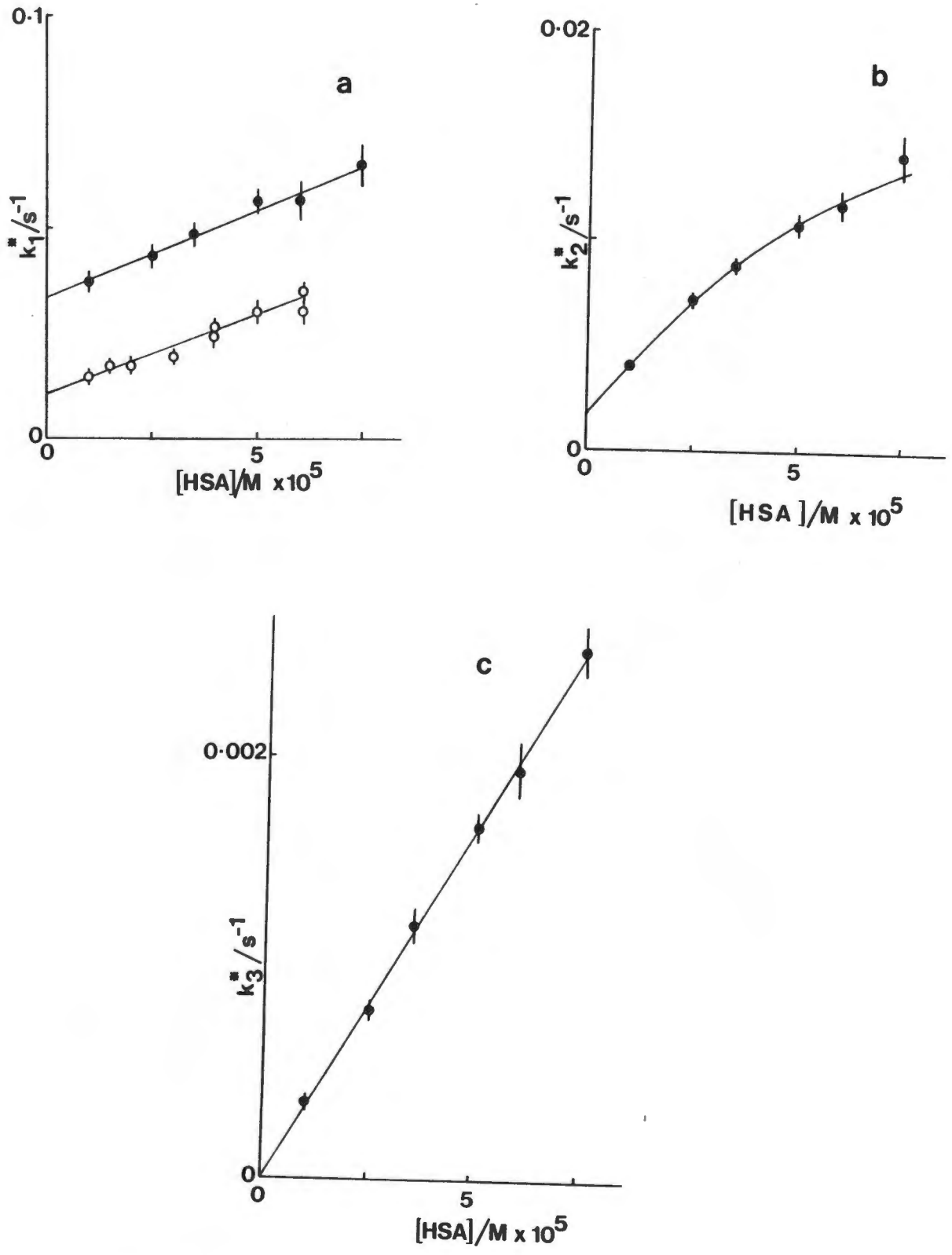

Figure 8. (a) - (c) Secondary plots of the pseudo-first-order rate constants evaluated for the binding of MP-8(11) to HSA. The open circles in Fig. 11a are the results for the MP-11/HSA reaction. The closed circles in all cases reflect the MP-8/HSA data. Concentration of MP-8 = 1×10^{-6} mol dm^{-3}.

APPENDIX 2

The kinetics of heme octapeptide (Microperoxidase-8; MP-8) formation studied by HPLC monitoring of the peptic and tryptic hydrolysis of horse heart cytochrome-c.

By

Paul A Adams[1]*, Mark P Byfield[2], Richard D Goold[3] and Alfred E Thumser[3]

[1] MRC Biomembrane Research Unit
Department of Chemical Pathology

and

[2] Department of Medical Biochemistry
University of Cape Town
Medical School
Observatory 7925
Cape Province
Republic of South Africa

[2] Dept of Chemistry
University of Surrey
Guildford GU2 5XH
Surrey
England

* To whom correspondence should be addressed

Abstract : The kinetics of the sequential peptide and tryptic hydrolysis of cytochrome-c to give the heme-peptides microperoxidase-11 (MP-11) and -8 (MP-8) respectively has been investigated by HPLC and we demonstrate that MP-8 can be prepared from cytochrome-c to the point of lyophilization within 4 hr.

Introduction : The heme octapeptide, Microperoxidase-8 (MP-8), is potentially one of the most useful models for hemeprotein function yet developed, however relatively few studies of the chemistry of this compound have been published (see reference [1] and those contained therein). The barrier to its wider use appears to derive either from the tedious and inefficient column chromatographic methods used for preparation, or from its exceptional cost when obtained commercially. There is thus a real need for the development of optimised preparative schedules for these heme peptides species.

We have recently reported [2] a rapid ($\approx$30 hr) efficient ($\approx$90% yield) HPLC-based preparation of pure (> 99%) MP-8, and have conducted preliminary studies on ligand binding and O_2 activation at high pH using this pure preparation.

In this note we report a systematic HPLC study of the kinetics of peptic and tryptic digestion of cytochrome-c and MP-11 and demonstrate the feasibility of preparing pure MP-8 (to the point of lyophilization) from cytochrome-c within 4 hr.

Materials and Methods : HPLC procedures and buffers A and B were as described previously [2], minor changes in HPLC gradients are indicated where appropriate.

Sixty mg of horse heart cytochrome-c was incubated with pepsin (1.6 mg) in 1 cm^3 buffer pH 2.1 for 15 min at 40°C. At this point 1 μl mixture was removed and diluted into 50 μl buffer A at 0°C. A further 1.6 mg pepsin was added at this point and the mixture was sampled at t = 30 min, 1 hr, 1.5 hr and 2 hr as previously described. Analytical HPLC of the reaction mixture indicated complete reaction after 2 hr (Fig. 1a), no further change in the HPLC trace occurred after 4 hr.

The pH of the reaction mixture was adjusted to 5 with ammonia solution, and solid $(NH_4)_2SO_4$ added slowly to the stirred solution on ice. When the first traces of cloudiness were noted, saturated $(NH_4)_2SO_4$ solution was added dropwise to completely precipitate heme-containing material, leaving a colourless supernatant. The heme peptide(s) were centrifuged down, drained thoroughly, and redissolved

in 1 cm^3 deionised water. The pH was adjusted to 8.5, and the sample incubated at the required temperature for 5 min. Trypsin (1.7 mg) was added, the solution mixed, and sampled at intervals of 15 or 30 sec into buffer A at 0°C. These samples were run isocratically on the HPLC (50% buffer A : 50% buffer B) monitoring the eluant at 396 nm. At the pH ($\approx$3) and peptide concentrations ($\approx 10^{-7}$ mol dm^{-3}) used, both MP-8 and MP-11 have similar extinction coefficients ($\approx$175 000), thus (peak height MP-8)/Σ(peak heights) is a convenient dimensionless measure of MP-8 formation.

Results and Discussion : In agreement with the views of Petersen *et al.* [3] we attempt to minimise the number of concentration/purification steps in the preparation. It is clear from Fig. 1a that carrying out the pepsin digestion at 40°C dramatically reduces the incubation time from the total of $\approx$8-10 hr at 26°C used previously [2], to < 2 hr. Furthermore contamination by the other non-MP-11 "stable" heme-containing peptides was reduced. While the incubation time reduction in part must reflect an Arrhenius-law rate increase, the fact that non-MP-11 heme-containing contaminants are reduced suggests that the higher temperature may be causing the cytochrome-c to adopt a less ordered conformation, allowing the pepsin easier access to the MP-11 cleavage sites and resulting in a cleaner cyt-c → MP-11 conversion.

Removal of non-heme-containing material prior to trypsin digestion (Fig. 1b) is important. Non heme-containing amino acids and peptides account for $\approx$85% by weight of the pepsin digestion, and this material could certainly act as trypsin substrate or inhibitor. When the $(NH_4)_2SO_4$ precipitation step is carried out to remove hydrophilic peptide impurities (Fig. 1b) the trypsin incubation at 40°C (Fig. 2) has a half life of $\approx$80 sec, as opposed to $\approx$30 min for the non-precipitated sample. Our results are therefore in agreement with Peterson *et al.* [4] who, using a similar but slower $(NH_4)_2SO_4$ precipitation procedure, conclude that the precipitation step is in itself a considerable purification of MP-11.

Conversion of MP-11 to MP-8 is quantitative (> 98%) with no byproduct other than non-heme peptide. The kinetics adhere closely to a pseudo-first-order rate law (Fig. 3) indicating that (assuming Michaelis-Menten kinetics) [MP-11] << K_m for the process, Arrhenius behaviour is adhered to with E_a = 16.2 Kcal $mole^{-1}$.

The MP-8 solution, which at this stage is > 95% pure in terms of heme-peptide, can be rapidly purified free from trypsin and MP-11 derived tripeptide by affinity chromatography (5) on a BSA-Sepharose 4B column (HSA-Sepharose 4B is not efficient due to the slow reaction of MP-8 with HSA). We have found it convenient to lyophilise the affinity column purified MP-8 at this stage and ultrapurify 1 mg samples by analytical HPLC to > 99% purity as required.

Further studies are at present in progress designed to exploit HPLC procedures in the optimization and purification of heme-peptides MP-6, MP-7 and MP-9 in a time period of hours, rather than days as previously taken.

Since the HPLC procedure for studying the kinetics of the MP-11 → MP-8 digestion is independent of the amount of reaction mixture injected into the machine it represents a simple highly accurate technique for studying the kinetics of the reaction of trypsin with its natural substrate - peptides. The fact that reaction can be monitored at 396 nm means that interference from non-heme peptides is absent. Thus the HPLC study suggests that both pepsin and trypsin digestion be performed at 40°C, and recommends the MP-11 → MP-8 conversion as a convenient reaction to study the peptidase activity of trypsin.

References

1. Marques, H.M., Baldwin, D.A., and Pratt, J.M., (1988) *S. Afr. J. Chem.* **41(2)**, 68-70

2. Adams, P.A., Byfield, M.P., Milton, R.C.deL., and Pratt, J.M., (1988) *J. Inorg. Biochem.* **34**, 167-176

3. Peterson, J., Saleem, M.M.M., Silver, J., Wilson, M.T., and Morrison, I.E.G., (1983) *J. Inorg. Biochem.* **19**, 165-178

4. Peterson, J., Silver, J., Wilson, M.T., and Morrison, I.E.G., (1980) *J. Inorg. Biochem.* **13**, 75

5. Wilchek, M., (1972) *Anal. Biochem.* **49**, 572-575

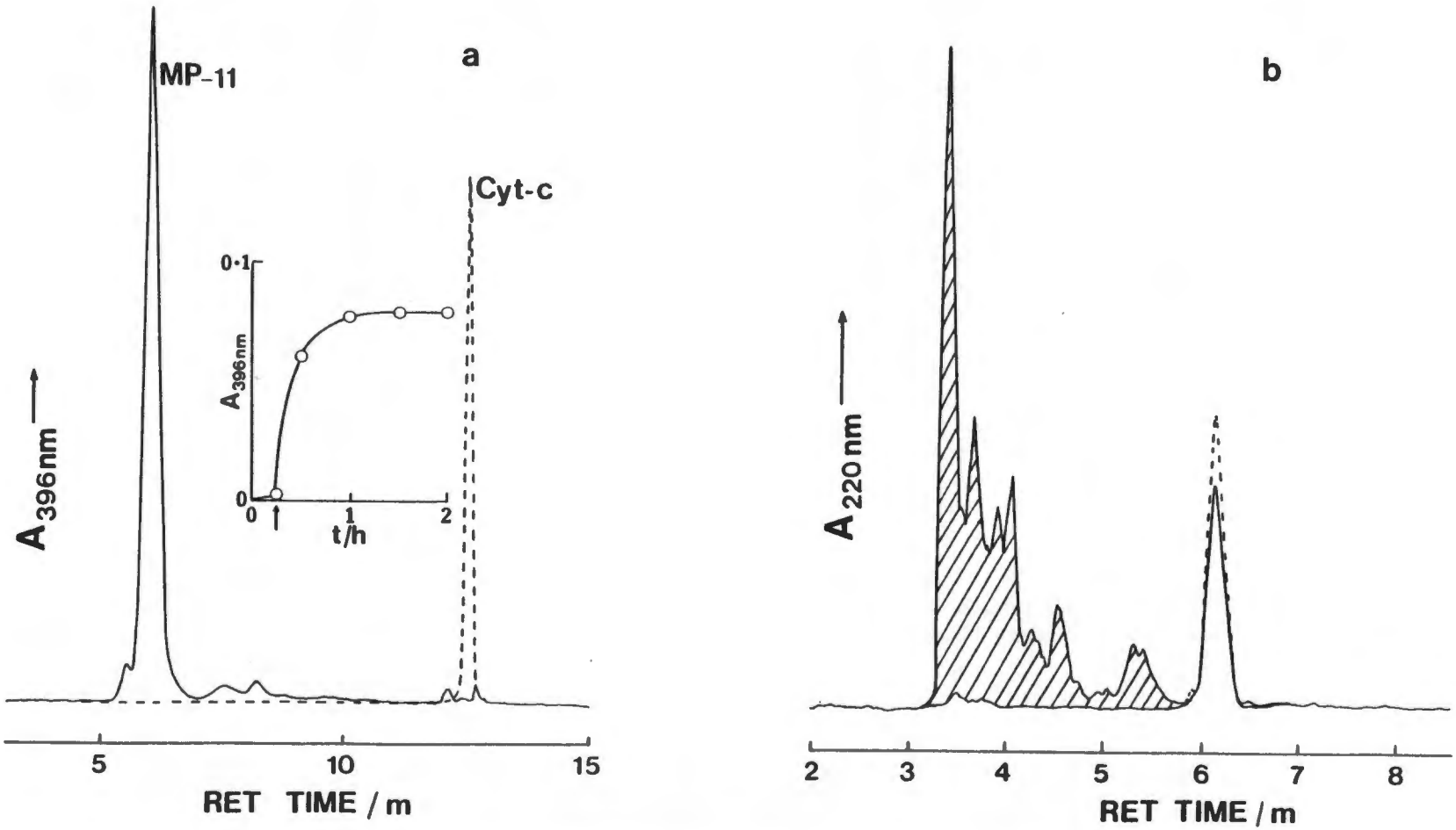

Figure 1. (a) Conversion of cytochrome-*c* (—— at t = 0) to MP-11 (solid line) by pepsin digestion for 2 hr at 40°C, pH 2.1. Inset to Fig. 1a shows kinetics of formation of MP-11 from cyt-c. Arrowed is the point at which the second pepsin addition is made. (b) Removal of non-heme peptides (shaded) by quantitative $(NH_4)_2SO_4$ precipitation (at pH 5) of MP-11. The dashed line shows the position at which MP-11 elutes at 396 nm. In both cases the HPLC gradient was 50% A/50% B, isocratic for 10 min then to 100% B over a further 10 min.

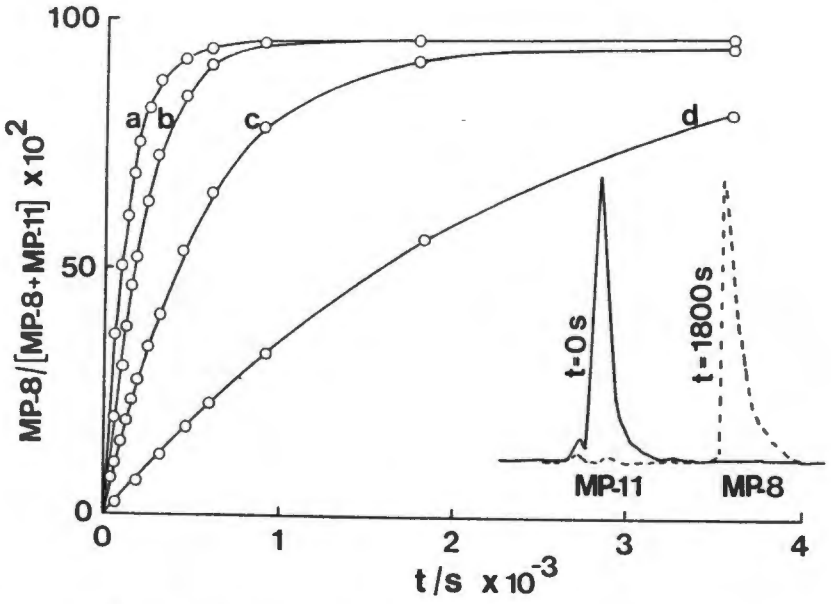

Figure 2. Kinetics of the trypsin catalysed MP-11 → MP-8 conversion monitored at 396 nm, pH 8.5, Ratio of MP-11:trypsin was 5:1 by weight (assuming quantitative conversion of cyt-c to MP-11). Digestion temperatures a) 40°C, b) 30°C, c) 20°C, d) 10°C. The inset shows the MP-11 → MP-8 conversion at t = 0 and t = 1800 s after addition of trypsin. MP-8/[MP-8 + MP-11] calculated from peak heights.

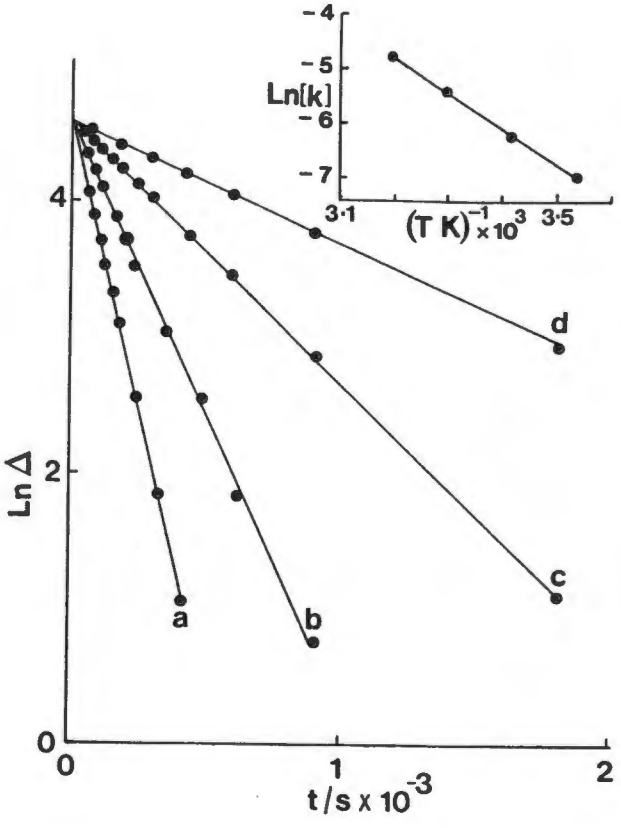

Figure 3. Demonstration of accurate adherence of the MP-11 → MP-8 reaction to a first order rate law to extents of reaction in excess of 90%. Δ = {100 - (MP-8/[MP-8 + MP-11] x 10^2)}. Inset - Arrhenius plot of ln(k) vs $1/_T$. E_a = 15.7.

REFERENCES

1. Abramovitz, M., Homma, H., Ishigaki, S., Tansey, F., Cammer, W. & Listowsky, I. (1988) Characterization and Localization of Glutathione S-Transferases in Rat Brain and Binding of Hormones, Neurotransmitters and Drugs. *J.Neurochem.* **50(1)**, 50-57

2. Adams, D.J., Balkwill, F.R., Griffin, D.B., Hayes, J.D., Lewis, A.D. & Wolf, C.R. (1987) Induction and Suppression of Glutathione Transferases by Interferon in the Mouse. *J.Biol.Chem.* **262(10)**, 4888-4892

3. Adams, P.A. & Adams, C. (1988) Ferriprotoporphyrin IX Mediated Oxygen Activation/Insertion Reactions: The Anerobic Reduction of the Aniline Fe^{3+}-Microperoxidase-8 Complex by NADH. *J.Inorg.Biochem.* **34(3)**, 176-186

4. Adams, P.A., Byfield, M.P., de L. Milton, R.C. & Pratt, J.M. (1988) Oxygen Activation and Ligand Binding by Pure Heme-octapeptide Microperoxidase-8 (MP-8). *J.Inorg.Biochem.* **34(3)**, 170-175

5. Adams, P.A., Byfield, M.P., Goold, R.D. & Thumser, A.E. (1989) The Kinetics of Heme-octapeptide (Microperoxidase-8; MP-8) Formation Studied by HPLC Monitoring of the Peptic and Tryptic Hydrolysis of Horse Heart Cytochrome-c. *J.Inorg.Biochem.*, in press.

6. Adams, P.A., Goold, R.D. & Thumser, A.E. (1989) Heme-peptide/Protein Interactions: The Binding of the Heme Octa- and Undecapeptides, Microperoxidase-8 and -11, to Human Serum Albumin. *J.Inorg.Biochem.*, in press.

7. Aitio, A. & Bend, J.R. (1979) Inhibition of Rat Liver Glutathione S-Transferase Activity by Aprotic Solvents. *FEBS Lett.* **101(1)**, 187-190

8. Ålin, P., Danielson, U.H. & Mannervik, B. (1985) 4-Hydroxyalk-2-enals are Substrates for Glutathione Transferase. *FEBS Lett.* **179(2)**, 267-270

9. Ålin, P., Jensson, H., Guthenberg, C., Danielson, U.H., Tahir, M.K. & Mannervik, B. (1985) Purification of Major Basic Glutathione Transferase Isoenzymes from Rat Liver by Use of Affinity Chromatography and Fast Protein Liquid Chromatofocusing. *Anal.Biochem.* **146**, 313-320

10. Ankley, G.T. & Agosin, M. (1987) Comparative Aspects of Hepatic UDP-Glucuronosyltransferases and Glutathione S-Transferases in Bluegill and Channel Catfish. *Comp.Biochem.Physiol.* **B87(4)**, 671-674

11. Aron, J., Baldwin, D.A., Marques, H.M., Pratt, J.M. & Adams, P.A. (1986) Hemes and Hemoproteins. 1: Preparation and Analysis of the Heme-Containing Octapeptide (Microperoxidase-8) and Identification of the Monomeric Form in Aqueous Solution. *J.Inorg.Biochem.* **27**, 227-243

12. Askelöf, P., Guthenberg, C., Jakobson, I. & Mannervik, B. (1975) Purification and Characterization of Two Glutathione S-Aryltransferase Activities from Rat Liver. *Biochem.J.* **147**, 513-522

13. Askelöf, P., Korsfeldt, M. & Mannervik, B. (1976) Error Structure of Enzyme Kinetic Experiments. Implications for Weighting in Regression Analysis of Experimental Data. *Eur.J.Biochem.* **69**, 61-67

14. Awasthi, Y.C., Ahmad, H., Medh, R.D., Kurosky, A. & Singh, S.V. (1988) Subunits of Glutathione S-Transferases are Differentially Expressed in Bovine Lens, Cornea and Retina. *Invest.Opthalmol.Visual Sci.* **29**, 99

15. Awasthi, Y.C., Bhatnagar, A. & Singh, S.V. (1987) Evidence for the Involvement of Histidine at the Active Site of Glutathione S-Transferase ψ from Human Liver. *Biochem.Biophys.Res.Commun.* **143(3)**, 965-970

16. Awasthi, Y.C. & Dao, D.D. (1981) Glutathione-Mediated Detoxification Mechanisms of Human Placenta. *Placenta (Supplement)* **3**, 289-301

17. Awasthi, Y.C., Dao, D.D. & Saneto, R.P. (1980) Interrelationship Between Anionic and Cationic Forms of Glutathione S-Transferases of Human Liver. *Biochem.J.* **191**, 1-10

18. Awasthi, Y.C., Partridge, C.A., Theodore, C. & Dao, D.D. (1984) Comparative Effect on the Induction of the Subunits of Rat Liver Glutathione S-Transferases by Butylated Hydroxytoluene. *Comp.Biochem.Physiol.* **78C**, 39-41

19. Awasthi, Y.C. & Singh, S.V. (1985) Subunit Structure of Human and Rat Glutathione S-Transferases. *Comp.Biochem.Physiol.* **82B**, 17-23

20. Awasthi, Y.C., Singh, S.V., Ahmad, H., Moller, P.C. (1987) Immunocytochemical Evidence for the Expression of GST1, GST2, and GST3 Gene Loci for Glutathione S-Transferase in Human Lung. *Lung* **165(6)**, 323-332

21. Baldwin, D.A., Mabuya, M.B. & Marques, H.M. (1987) Haems and Haemoproteins. Part 4. Preparation, Analysis, and Solution Chemistry of Microperoxidase-9 - Comparison with Microperoxidase-8. *S.Afr.J.Chem.* **40(2)**, 103-110

22. Baldwin, D.A., Marques, H.M. & Pratt, J.M. (1985) Mechanism of Activation of H_2O_2 by Peroxidases: Kinetic Studies on a Model System. *FEBS Lett.* **183**, 309-312

23. Bass, N.M., Kirsch, R.E., Tuff, S.A., Marks, I. & Saunders, S.J. (1977) Ligandin Heterogeneity: Evidence that the Two Non-Identical Subunits are the Monomers of Two Distinct Proteins. *Biochim.Biophys.Acta* **492**, 163-175

24. Batist, G., Tulpule, A., Sinha, B.K., Katki, A., Myers, C.E. & Cowan, K.H. (1986) Overexpression of a Novel Anionic Glutathione Transferase in Multidrug-Resistant Human Breast Cancer Cells. *J.Biol.Chem.* **261(33)**, 15544-15549

25. Beale, D., Meyer, D.J., Taylor, J.B. & Ketterer, B. (1983) Evidence that the Y_b Subunits of Hepatic Glutathione Transferases Represent Two Different but Related Families of Polypeptides. *Eur.J.Biochem.* **137**, 125-129

26. Bell, J.G., Cowey, C.B., Adron, J.W. & Pirie, B.J.S. (1987) Some Effects of Selenium Deficiency on Enzyme Activities and Indices of Tissue Peroxidation in Atlantic Salmon Parr (*Salmo salar*). *Aquaculture* **65(1)**, 43-54

27. Bennett, C.F., Spector, D.L. & Yeoman, L.C. (1986) Nonhistone Protein BA is a Glutathione S-Transferase Localized to Interchromatinic Regions of the Cell Nucleus. *J. Cell Biol.* **102**, 600-609

28. Bennett, C.F. & Yeoman, L.C. (1987) Microinjected Glutathione S-Transferase Y_b Subunits Translocate to the Cell Nucleus. *Biochem.J.* **247(1)**, 109-112

29. Bernasconi, C.F. (1976) Relaxation Kinetics, p.288, Academic Press, New York

30. Bhargava, M.M., Listowsky, I. & Arias, I.M. (1978) Ligandin: Bilirubin Binding and Glutathione S-Transferase Activity are Independent Processes. *J.Biol.Chem.* **253(12)**, 4112-4115

31. Bhargava, M.M., Ohmi, N., Listowsky, I. & Arias, I.M. (1980) Structural, Catalytic, Binding, and Immunological Properties Associated with each of the Two Subunits of Rat Liver Ligandin. *J.Biol.Chem.* **255(2)**, 718-723

32. Bhargava, M.M., Ohmi, N., Listowsky, I. & Arias, I.M. (1980) Subunit Composition, Organic Anion Binding, Catalytic and Immunological Properties of Ligandin from Rat Testis. *J.Biol.Chem.* **255(2)**, 724-727

33. Board, P.G., Suzuki, T. & Shaw, D.C. (1988) Human Muscle Glutathione S-Transferase GST-4 Shows Close Homology to Human Liver GST-1. *Biochim.Biophys. Acta* **953(3)**, 214-217

34. Boehlert, C.C. & Armstrong, R.N. (1984) Investigation of the Kinetic and Stereochemical Recognition of Arene and Azaarene Oxides by Isozymes A_2 and C_2 of Glutathione S-Transferase. *Biochem.Biophys.Res.Commun.* **121(3)**, 980-986

35. Boryslawskyj, M., Garrood, A.C., Pearson, J.T. & Woodhead, D. (1988) Elevation of Glutathione S-Transferase Activity as a Stress Response to Organochlorine Compounds, in the Freshwater Mussel, *Sphaerium corneum*. *Marine Environ.Res.* **24**, 101-104

36. Bosron, W.F., Magnes, L.J. & Li, T.-K. (1983) Kinetic and Electrophilic Properties of Native and Recombined Isoenzymes of Human Liver Dehydrogenase. *Biochemistry* **22**, 1852-1857

37. Boyer, T.D. (1986) Covalent Labeling of the Nonsubstrate Ligand-Binding Site of Glutathione S-Transferases with Bilirubin-Woodward's Reagent K. *J.Biol.Chem.* **261(12)**, 5363-5367

38. Boyer, T.D. & Kenney, W.C. (1985) Acidic Glutathione S-Transferases of Rat Testis. *Biochem.J.* **230**, 125-132

39. Boyer, T.D. & Kenney, W.C. (1985) Preparation, Characterization, and Properties of Glutathione S-Transferases. in *Biochemical Pharmacology and Toxicology* (Zakim, D. & Vessey, D.A., eds.), vol 1, 297-364, John Wiley and Sons, New York

40. Boyer, T.D., Kenney, W.C. & Zakim, D. (1983) Structural, Functional and Hybridization Studies of the Glutathione S-Transferases of Rat Liver. *Biochem.Pharmacol.* **32(12)**, 1843-1850

41. Boyer, T.D., Vessey, D.A., Holcomb, C. & Saley, N. (1984) Studies of the Relationship Between the Catalytic Activity and Binding of Non-Substrate Ligands by the Glutathione S-Transferases. *Biochem.J.* **217**, 179-185

42. Boyer, T.D., Vessey D.A. & Kempner, E. (1986) Radiation Inactivation of Microsomal Glutathione S-Transferase. *J.Biol.Chem.* **261(36)**, 16963-16968

43. Boyer, T.D., Zakim, D. & Vessey, D.A. (1983) Do the Soluble Glutathione S-Transferases Have Direct Access to Membrane-Bound Substrates? *Biochem.Pharmacol.* **32(1)**, 29-35

44. Boyland, E. & Chasseaud, L.F. (1969) Glutathione and Glutathione S-Transferases in Mercapturic Acid Biosynthesis. *Adv.Enzymol.* **32**, 173-219

45. Bradford, M.M. (1976) A Rapid and Sensitive Method for the Quantification of Microgram Quantities of Protein Utilizing the Principle of Protein-Dye Binding. *Anal.Biochem.* **72**, 248-254

46. Brodersen, R., Honoré, B., Pedersen, A.O. & Klotz, I.M. (1988) Binding Constants for Ligand-Carrier Complexes. *Trends Pharmacol.Sci.* **9**, 252-257

47. Burgess, J.R., Yang, H., Chang, M., Rao, M.K., Tu, C.-P.D. & Reddy, C.C. (1987) Enzymatic Transformation of PGH2 to PGF2α Catalyzed by Glutathione S-Transferases. *Biochem.Biophys.Res.Commun.* **142(2)**, 441-447

48. Campbell, J.A.H., Bass, N.M. & Kirsch, R.E. (1980) Immunohistological Localization of Ligandin in Human Tissues. *Cancer* **45(3)**, 503-509

49. Carne, T., Tipping, E. & Ketterer, B. (1979) The Binding and Catalytic Activities of Forms of Ligandin after Modification of its Thiol Groups. *Biochem.J.* **177**, 433-439

50. Cesarone, C.F., Bolognesi, C. & Santi, L. (1979) Improved Microfluorometric DNA Determination in Biological Material Using 33258 Hoechst. *Anal.Biochem.* **100**, 188-197

51. Chang, C., Saltzman, A.G., Sorensen, N.S., Hiipakka, R.A. & Liao, S. (1987) Identification of Glutathione S-Transferase Y_{b1} Messenger RNA as the Androgen-Repressed Messenger RNA by Complementary DNA Cloning and Sequence Analysis. *J.Biol.Chem.* **262(25)**, 11901-11903

52. Chasseaud, L.F. (1979) The Role of Glutathione and Glutathione S-Transferases in the Metabolism of Chemical Carcinogens and Other Electrophilic Agents. *Adv.Cancer Res.* **29**, 175-274

53. Chen, W.-J., Boehlert, C.C., Rider, K. & Armstrong, R.N. (1985) Synthesis and Characterization of the Oxygen and Desthio Analogues of Glutathione as Dead-End Inhibitors of Glutathione S-Transferase. *Biochem.Biophys.Res.Commun.* **128(1)**, 233-240

54. Chen, W.-J., Graminski, G.F. & Armstrong, R.N. (1988) Dissection of the Catalytic Mechanism of Isozyme 4-4 of Glutathione S-Transferase with Alternative Substrates. *Biochemistry* **27(2)**, 647-654

55. Clark, A.G., Smith, J.N. & Speir, T.W. (1973) Cross Specificity in Some Vertebrate and Insect Glutathione-Transferases with Methyl Parathion (Dimethyl *p*-nitrophenyl phosphorothionate), 1-Chloro-2,4-dinitrobenzene and *S*-Crotonyl-*N*-acetylcysteamine as Substrates. *Biochem.J.* **135**, 385-392

56. Cleland, W.W. (1967) Enzyme Kinetics. *Ann.Rev.Biochem.* **36**, 77-112

57. Cleland, W.W. (1977) Determining the Chemical Mechanisms of Enzyme-Catalyzed Reactions by Kinetic Studies. *Adv.Enzymol.Relat.Areas Mol.Biol.* **45**, 273-387

58. Cleland, W.W. & Wratten, C.C. (1969) Studies on the Kinetic Mechanism of Liver Alcohol Dehydrogenase. in *The Mechanism of Action of Dehydrogenases* (Schwert, G.W. & Winer, A.D., eds.), 103-129, University Press of Kentucky, Lexington

59. Cobb, D., Boehlert, C., Lewis, D. & Armstrong, R.N. (1983) Stereoselectivity of Isozyme C of Glutathione S-Transferase Toward Arene and Azaarene Oxides. *Biochemistry* **22**, 805-812

60. Cohen, E. (1987) Purification of Glutathione S-Transferase from the Flour Beetle *Tribolium castaneum*. *Comp.Biochem.Physiol.* **B88(2)**, 675-680

61. Corrigall, A.V., Ivanetich, K.M. & Kirsch, R.E. (1986) Inhibition of Human Glutathione S-Transferases by 1-Chloro-2,4-Dinitrobenzene. *Hepatology* **6(5)**, 1136

62. Danielson, U.H., Esterbauer, H. & Mannervik, B. (1987) Structure-Activity Relationships of 4-Hydroxyalkenals in the Conjugation Catalyzed by Mammalian Glutathione Transferases. *Biochem.J.* **247(3)**, 707-714

63. Danielson, U.H. & Mannervik, B. (1985) Kinetic Independence of the Subunits of Cytosolic Glutathione Transferase from the Rat. *Biochem.J.* **231**, 263-267

64. Danielson, U.H. & Mannnervik, B. (1988) Paradoxical Inhibition of Rat Glutathione Transferase 4-4 by Indomethacin Explained by Substrate-Inhibitor-Enzyme Complexes in a Random-Order Sequential Mechanism. *Biochem.J.* **250(3)**, 705-712

65. Dao, D.D., Partridge, C.A. & Awasthi, Y.C. (1982) Subunit Structure of Glutathione S-Transferases of Human Liver and Placenta. *IRCS Med.Sci.* **10**, 175

66. Dao, D.D., Partridge, C.A., Kurosky, A. & Awasthi, Y.C. (1984) Human Glutathione S-Transferases: Characterization of the Anionic Forms from Lung and Placenta. *Biochem.J.* **221(1)**, 33-41

67. DeJong, J.L., Morgenstern, R., Jornvall, H., DePierre, J.W. & Tu, C.-P.D. (1988) Gene Expression of Rat and Human Microsomal Glutathione S-Transferases. *J.Biol.Chem.* **263(17)**, 8430-8436

68. Del Boccio, G., Di Ilio, C., Ålin, P., Jörnvall, H. & Mannervik, B. (1987) Identification of a Novel Glutathione Transferase in Human Skin Homologous with Class Alpha Glutathione Transferase 2-2 in the Rat. *Biochem.J.* **244(1)**, 21-26

69. Del Boccio, G., Di Ilio, C., Casalone, E., Pennelli, A., Aceto, A., Sacchetta, P. & Federici, G. (1987) Purification and Characterization of Glutathione Transferase of Human Thyroid. *ItalJ.Biochem.* **36(1)**, 8-17

70. DePierre, J.W., Seidegård, J., Morgenstern, R., Balk, L., Meijer, J., Åström, A., Norélius, I. & Ernster, L. (1984) Induction of Cytosolic Glutathione Transferase and Microsomal Epoxide Hydrolase Activities in Extrahepatic Organs of the Rat by Phenobarbital, 3-Methylcholanthrene and Trans Stilbene Oxide. *Xenobiotica* **14(4)**, 295-302

71. deSmidt, P.C., McCarrick, M.A., Darnow, J.N., Mervic, M. & Armstrong, R.N. (1987) Stereoselectivity and Enantioselectivity of Glutathione S-Transferase Toward Stilbene Oxide Substrates. *Biochem.Int.* **14(3)**, 401-408

72. Di Ilio, C., Aceto, A., Del Boccio, G., Casalone, E., Pennelli, A. & Federici, G. (1988) Purification and Characterization of Five Forms of Glutathione Transferase from Human Uterus. *Eur.J.Biochem.* **171**, 491-496

73. Di Ilio, C., Del Boccio, G., Massoud, R. & Federici, G. (1986) Glutathione Transferase of Human Breast is Closely Related to Transferase of Human Placenta and Erythrocytes. *Biochem.Int.* **13(2)**, 263-269

74. Di Ilio, C., Sacchetta, P., Del Boccio, G., Casalone, E. & Polidoro, G. (1986) Glutathione S-Transferase Activity from Rat Placenta. *Placenta* **7**, 155-162

75. Ding, G.J.-F., Ding, V.D.-H., Rodkey, J.A., Bennett, C.D., Lu, A.Y.H. & Pickett, C.B. (1986) Rat Liver Glutathione S-Transferases. DNA Sequence Analysis of a Y_b^2 cDNA Clone and Regulation of the Y_b^1 and Y_b^2 mRNAs by Phenobarbital. *J.Biol.Chem.* **261(17)**, 7952-7957

76. Ding, G.J.-F., Lu, A.Y.H. & Pickett, C.B. (1985) Rat Liver Glutathione S-Transferases. Nucleotide Sequence Analysis of a Y_b^1 cDNA Clone and Prediction of the Complete Amino Acid Sequence of the Y_b^1 Subunit. *J.Biol.Chem.* **260(24)**, 13268-13271

77. Ding, V.D.-H. & Pickett, C.B. (1985) Transcriptional Regulation of Rat Liver Glutathione S-Transferase Genes by Phenobarbital and 3-Methylcholanthrene. *Arch.Biochem.Biophys.* **240(2)**, 553-559

78. DiSimplicio, P., Jensson, H. & Mannervik, B. (1983) Identification of the Isozymes of Glutathione Transferase Induced by *trans*-Stilbene oxide. *Acta Chem.Scand.* **B37(3)**, 255-257

79. Dostal, L.A., Aitio, A., Harris, C., Bhatia, A.V., Hernandez, O. & Bend, J.R. (1986) Cytosolic Glutathione S-Transferases in Various Rat Tissues Differ in Stereoselectivity with Model Polycyclic Arene and Alkene Oxide Substrates. *Drug Metab.Dispos.* **14**, 303-309

80. Dostal, L.A., Guthenberg, C., Mannervik, B. & Bend, J.R. (1986) The Stereoselectivity of Purified Human Glutathione S-Transferases π, μ, and α-ϵ Varies Markedly with Arene and Alkene Oxide Substrates. *Toxicologist* **6**, 148

81. Dostal, L.A., Horton, J.K., Harris, C., Brier, D.F. & Bend, J.R. (1987) Stereoselectivity of Cytosolic Glutathione S-Transferases with Arene Oxide Substrates in Various Tissues and Isolated Hepatic and Pulmonary Cells of the Rabbit. *Carcinogenesis* **8(11)**, 1601-1606

82. Duggleby, R.G. (1981) A Nonlinear Regression Program for Small Computers. *Anal.Biochem.* **110**, 9-18

83. Faulder, C.G., Hirrell, P.A., Hume, R. & Strange, R.C. (1987) Studies of the Development of Basic, Neutral and Acidic Isoenzymes of Glutathione S-Transferase in Human Liver, Adrenal, Kidney & Spleen. *Biochem.J.* **241(1)**, 221-228

84. Federici, G., Di Ilio, C., Sacchetta, P., Polidoro, G. & Bannister, J.V. (1985) The Isolation, Characterisation and Kinetics of Glutathione S-Transferase from Human Platelets. *Int.J.Biochem.* **17(5)**, 653-656

85. Ferdinand, W. (1966) The Interpretation of Non-Hyperbolic Rate Curves for Two-Substrate Enzymes. A Possible Mechanism for Phosphofructokinase. *Biochem.J.* **98**, 278-283

86. Fisher, J.R. (1972) A Guide for Interpreting Substrate Nonlinear Steady State Enzyme Kinetic Data Using Random Models. *Arch.Biochem.Biophys.* **152**, 638-645

87. Foureman, G.L., Hernandez, O., Bhatia, A. & Bend, J.R. (1987) The Stereoselectivity of Four Hepatic Glutathione S-Transferases Purified from a Marine Elasmobranch (*Raja erinacea*) with Several K-Region Polycyclic Arene Oxide Substrates. *Biochim.Biophys.Acta* **914(2)**, 127-135

88. Frey, A.B., Friedberg, T., Oesch, F. & Kreibich, G. (1983) Studies on the Subunit Composition of Rat Liver Glutathione S-Transferases. *J.Biol.Chem.* **258(18)**, 11321-11325

89. Fryer, A.A., Hume, R. & Strange, R.C. (1986) The Development of Glutathione S-Transferase and Glutathione Peroxidase Activities in Human Lung. *Biochim.Biophys.Acta* **883(3)**, 448-453

90. Garfinkel, D. & Fegley, K.A. (1984) Fitting Physiological Models to Data. *Am.J.Physiol.* **246**, R641-R650

91. Garfinkel, L., Kohn, M.C. & Garfinkel, D. (1977) Systems Analysis in Enzyme Kinetics. *CRC Crit.Rev.Bioeng.* **2**, 329-361

92. Grahnén, A. & Sjöholm, I. (1977) The Preparation of Ligandin with Glutathione S-Transferase Activity from Porcine Liver Cytosol by Affinity Chromatography on Bromosulphophthalein-Sepharose. *Eur.J.Biochem.* **80**, 573-580

93. Gulbinsky, J.S. & Cleland, W.W. (1968) Kinetic Studies of *Escherichia Coli* Galactokinase. *Biochemistry* **7(2)**, 566-575

94. Guthenberg, C., Åkerfeldt, K. & Mannervik, B. (1979) Purification of Glutathione S-Transferase from Human Placenta. *Acta Chem.Scand.* **B33**, 595-596

95. Guthenberg, C., Ålin, P., Åstrand, I.-M., Yalçin, S. & Mannervik, B. (1986) Isozymes of Glutathione Transferase in Rat Testis. in *Extrahepatic Drug Metabolism and Chemical Carcinogenesis* (Rydstrom, J., Montelius, J. & Bengtsson, M., eds.), 171-176, Elsevier, Amsterdam

96. Guthenberg, C., Ålin, P. & Mannervik, B. (1985) Glutathione Transferase From Rat Testis. *Methods Enzymol.* **113**, 507-510

97. Guthenberg, C., Åstrand, I.-M., Ålin, P. & Mannervik, B. (1983) Glutathione Transferases in Rat Testis. *Acta Chem.Scand.* **B37**, 261-262

98. Guthenberg, C., Jensson, H., Nyström, L, Österlund, E., Tahir, M.K. & Mannervik, B. (1985) Isoenzymes of Glutathione Transferase in Rat Kidney Cytosol. *Biochem.J.* **230**, 609-615

99. Guthenberg, C. & Mannervik, B. (1979) Purification of Glutathione S-Transferases from Rat Lung by Affinity Chromatography. Evidence for an Enzyme Form Absent in Rat Liver. *Biochem.Biophys.Res.Commun.* **86(4)**, 1304-1310

100. Guthenberg, C. & Mannervik, B. (1981) Glutathione S-Transferase (Transferase π) from Human Placenta is Identical or Closely Related to Glutathione S-Transferase (Transferase ρ) from Erythrocytes. *Biochim.Biophys.Acta* **661**, 255-260

101. Guthenberg, C., Morgenstern, R., DePierre, J.W. & Mannervik, B. (1980) Induction of Glutathione S-Transferases A, B and C in Rat Liver Cytosol by *trans*-Stilbene oxide. *Biochim.Biophys.Acta* **631**, 1-10

102. Guthenberg, C., Warholm, M., Rane, A. & Mannervik, B. (1986) Two Distinct Forms of Glutathione Transferase from Human Foetal Liver. Purification and Comparison with Isoenzymes Isolated from Adult Liver and Placenta. *Biochem.J.* **235**, 741-745

103. Habig, W.H. & Jakoby, W.B. (1981) Glutathione S-Transferases (Rat and Human). *Methods Enzymol.* **77**, 218-224

104. Habig, W.H. & Jakoby, W.B. (1981) Assays for Differentiation of Glutathione S-Transferases. *Methods Enzymol.* **77**, 398-405

105. Habig, W.H., Jakoby, W.B., Guthenberg, C., Mannervik, B. & Vander Jagt, D.L. (1984) 2-Propylthiouracil does not Replace Glutathione for the Glutathione Transferases. *J.Biol.Chem.* **259(12)**, 7409-7410

106. Habig, W.H., Pabst, M.J., Fleischner, G., Gatmaitan, Z., Arias, I.M. & Jakoby, W.B. (1974) The Identity of Glutathione S-Transferase B with Ligandin, a Major Binding Protein of Liver. *Proc.Natl.Acad.Sci. USA* **71(10)**, 3879-3882

107. Habig, W.H., Pabst, M.J. & Jakoby, W.B. (1974) Glutathione S-Transferases: The First Enzymic Step in Mercapturic Acid Formation. *J.Biol.Chem.* **249(22)**, 7130-7139

108. Habig, W.H., Pabst, M.J. & Jakoby, W.B. (1976) Glutathione S-Transferase AA From Rat Liver. *Arch.Biochem.Biophys.* **175**, 710-716

109. Harbury, H.A. & Loach, P.A. (1960) Interaction of Nitrogenous Ligands with the Heme Peptide from Mammalian Cytochrome-c. *J.Biol.Chem.* **235**, 3646-3653

110. Harvey, J.W. & Beutler, E. (1982) Binding of Heme by Glutathione S-Transferase: A Possible Role of the Erythrocyte Enzyme. *Blood* **60(5)**, 1227-1230

111. Hayes, J.D. (1983) Rat Liver Glutathione S-Transferases: A Study of the Structure of the Basic Y_bY_b-Containing Enzymes. *Biochem.J.* **213**, 625-633

112. Hayes, J.D. (1984) Purification and Characterization of Glutathione S-Transferases P, S and N. Isolation from Rat Liver of $Y_b{}^1Y_n$ Protein, the Existence of Which was Predicted by Subunit Hybridization *In Vitro*. *Biochem.J.* **224**, 839-852

113. Hayes, J.D. (1986) Purification and Physical Characterization of Glutathione S-Transferase K. Differential Use of S-Hexylglutathione and Glutathione Affinity Matrices to Isolate a Novel Glutathione S-Transferase from Rat Liver. *Biochem.J.* **233**, 789-798

114. Hayes, J.D. & Mantle, T.J. (1986) Inhibition of Hepatic and Extrahepatic Glutathione S-Transferases by Primary and Secondary Bile Acids. *Biochem.J.* **233**, 407-415

115. Hayes, J.D. & Mantle, T.J. (1986) Use of Immuno-Blot Techniques to Discriminate Between the Glutathione S-Transferase Y_f, Y_k, Y_a, Y_n/Y_b and Y_c Subunits and to Study their Distribution in Extrahepatic Tissues. Evidence for Three Immunochemically Distinct Groups of Transferase in the Rat. *Biochem.J.* **233**, 779-788

116. Hayes, J.D., Strange, R.C. & Percy-Robb, I.W. (1981) A Study of the Structures of the Y_aY_a and Y_aY_c Glutathione S-Transferases from Rat Liver Cytosol. *Biochem.J.* **197**, 491-502

117. Hazelton, G.A. & Lang, C.A. (1983) Gluthathione S-Transferase Activities in the Yellow-Fever Mosquito [*Aedes aegypti* (Louisville)] During Growth and Aging. *Biochem.J.* **210**, 281-287

118. Hirrell, P.A., Collins, M.F., Nimmo, I.A. & Strange, R.C. (1987) The Human Glutathione S-Transferases. Studies on the Kinetic, Stability and Inhibition Characteristics of the Erythrocyte Enzyme. *Biochim.Biophys.Acta* **913(1)**, 92-96

119. Hoesch, R.M. & Boyer, T.D. (1988) Purification and Characterization of Hepatic Glutathione S-Transferases of Rhesus Monkeys. A Family of Enzymes Similar to the Human Hepatic Glutathione S-Transferases. *Biochem.J.* **251(1)**, 81-88

120. Homma, H. & Listowsky, I. (1985) Identification of Y_b-Glutathione-S-Transferase as a Major Rat Liver Protein Labelled with Dexamethasone 21-methanesulfonate. *Proc.Natl.Acad.Sci. USA* **82**, 7165-7169

121. Homma, H., Maruyama, H., Niitsu, Y. & Listowsky, I. (1986) A Subclass of Glutathione S-Transferases as Intracellular High-Capacity and High-Affinity Steroid-Binding Proteins. *Biochem.J.* **235**, 763-768

122. Huang, C.Y., Rhee, S.G. & Chock, P.B. (1982) Subunit Cooperation and Enzymatic Catalysis. *Ann.Rev.Biochem.* **51**, 935-971

123. Hunaiti, A.A., Abu-Orabi, S.T., Sahran, M.A.A. & Owais, W.M. (1988) Interaction of Organic Azides with Purified Camel Glutathione S-Transferase. *Biochem.Med.Metab.Biol.* **39(2)**, 140-147

124. Husby, P., Srai, K.S., Ketterer, B. & Romslo, I. (1981) Effect of Ligandin on the Efflux of co-Deuteroporphyrin from Isolated Rat Liver Mitochondria. *Biochem.Biophys.Res.Commun.* **100(2)**, 651-659

125. Hussey, A.J., Stockman, P.K., Beckett, G.J. & Hayes, J.D. (1986) Variations in the Glutathione S-Transferase Subunits Expressed in Human Livers. *Biochem.Biophys.Acta* **874(1)**, 1-12

126. Inoue, M., Hara, M., Nagashima, F., Matsui, S., Mitsuyasu, N. & Morino, Y. (1981) Affinity Chromatography of Hepatic Glutathione S-Transferases on w-Aminoalkyl Sepharose Derivatives of Glutathione. *Biochim.Biophys.Acta* **659**, 362-369

127. Inskeep, P.B. & Guengerich, F.P. (1984) Glutathione-Mediated Binding of Dibromoalkanes to DNA : Specificity of Rat Glutathione S-Transferases and Dibromoalkane Structure. *Carcinogenesis* **5(6)**, 805-808

128. Ishikawa, T., Esterbauer, H. & Sies, H. (1986) Role of Cardiac Glutathione Transferase and of the Glutathione S-Conjugate Export System in Biotransformation of 4-Hydroxynonenal in the Heart. *J.Biol.Chem.* **261(4)**, 1576-1581

129. Ishikawa, T., Milbert, U., Oesch, F. & Sies, H. (1986) The Major Isozyme of Rat Cardiac Glutathione Transferases. Its Correspondence to Hepatic Transferase X. *Eur.J.Biochem.* **154**, 299-305

130. Ivanetich, K.M. & Thumser, A.E.A. (1987) Reversible Inhibition and Activation of Hepatic GSH S-Transferases by Ethylene Dibromide. *Pharmac.Ther.* **33**, 85-88

131. Ivanetich, K.M., Ziman, M.R., Mennie, R.E.M., Eidne, K.A., Corrigall, A. & Kirsch, R.E. (1984) Inhibition of Rat Glutathione S-Transferases by Ethylene Dibromide. *Res.Commun.Chem.Pathol.Pharmacol.* **45(2)**, 233-242

132. Jakobson, I., Askelöf, P., Warholm, M. & Mannervik, B. (1977) A Steady-State-Kinetic Random Mechanism for Glutathione S-Transferase A from Rat Liver. A Model Involving Kinetically Significant Enzyme-Product Complexes in the Forward Direction. *Eur.J.Biochem.* **77**, 253-262

133. Jakobson, I., Warholm, M. & Mannervik, B. (1979) Multiple Inhibition of Glutathione S-Transferase A from Rat Liver by Glutathione Derivatives: Kinetic Analysis Supporting a Steady-State Random Sequential Mechanism. *Biochem.J.* **177**, 861-868

134. Jakobson, I., Warholm, M. & Mannervik, B. (1979) The Effect of Ethanol on the Steady-State Kinetics of Glutathione S-Transferase A from Rat Liver. *FEBS Lett.* **102(1)**, 165-168

135. Jakobson, I., Warholm, M. & Mannervik, B. (1979) The Binding of Substrates and a Product of the Enzymatic Reaction to Glutathione S-Transferase A. *J.Biol.Chem.* **254(15)**, 7085-7089

136. Jakoby, W.B. (1978) The Glutathione S-Transferases: A Group of Multifunctional Detoxification Enzymes. *Adv.Enzymol.* **46**, 383-414

137. Jakoby, W.B. & Habig, W.H. (1980) Glutathione Transferases. in *Enzymatic Basis of Detoxification* (Jakoby, W.B., ed.), vol. 2, 63-95, Academic Press, New York

138. Jakoby, W.B., Habig, W.H., Keen, J.H., Ketley, J.N. & Pabst, M.J. (1976) Glutathione S-Transferases: Catalytic Aspects. in *Glutathione: Metabolism and Function* (Arias, I.M. & Jakoby, W.B., eds.), 189-211, Raven Press, New York

139. Jakoby, W.B., Ketley, J.N. & Habig, W.H. (1976) Rat Glutathione S-Transferases: Binding and Physical Properties. in *Glutathione: Metabolism and Function* (Arias, I.M. & Jakoby, W.B., eds.), 213-223, Raven Press, New York

140. Jakoby, W.B., Ketterer, B. & Mannervik, B. (1984) Glutathione Transferases: Nomenclature. *Biochem.Pharmacol.* **33**, 2539-2540

141. Jensen, R.A. & Trentini, W.C. (1970) Alternative Allosteric Effects Exerted by End Products upon a Two-Substrate Enzyme in *Rhodomicrobium vannielii*. *J.Biol.Chem.* **245(8)**, 2018-2022

142. Jensson, H., Ålin, P. & Mannervik, B. (1985) Glutathione Transferase Isoenzymes from Rat Liver Cytosol. *Methods Enzymol.* **113**, 504-507

143. Jensson, H., Eriksson, L.C. & Mannervik, B. (1985) Selective Expression of Glutathione Transferase Isoenzymes in Chemically Induced Preneoplastic Rat Hepatocyte Nodules. *FEBS Lett.* **187(1)**, 115-120

144. Jensson, H., Guthenberg, C., Ålin, P. & Mannervik, B. (1986) Rat Glutathione Transferase 8-8. An Enzyme Efficiently Detoxifying 4-Hydroxyalk-2-enals. *FEBS Lett.* **203(2)**, 207-209

145. Kamisaka, K, Habig, W.H., Ketley, J.N., Arias, I.M. & Jakoby, W.B. (1975) Multiple Forms of Human Glutathione S-Transferase and their Affinity for Bilirubin. *Eur.J.Biochem.* **60**, 153-161

146. Kaplowitz, N., Percy-Robb, I.W. & Javitt, N.B. (1973) Role of Hepatic Anion-Binding Protein in Bromsulphthalein Conjugation. *J.Exp.Med.* **138**, 483-487

147. Keen, J.H., Habig, W.H. & Jakoby W.B. (1976) Mechanism for the Several Activities of the Glutathione S-Transferases. *J.Biol.Chem.* **251(20)**, 6183-6188

148. Keen, J.H. & Jakoby, W.B. (1978) Glutathione Transferases: Catalysis of Nucleophilic Reactions of Glutathione. *J.Biol.Chem.* **253(16)**, 5654-5657

149. Keeran, W.S. & Lee, R.F. (1987) The Purification and Characterization of Glutathione S-Transferase from the Hepatopancreas of the Blue Crab *Callinectes sapidus*. *Arch.Biochem.Biophys.* **255(2)**, 233-243

150. Ketley, J.N., Habig, W.H. & Jakoby, W.B. (1975) Binding of Non-Substrate Ligands to the Glutathione S-Transferases. *J.Biol.Chem.* **250(22)**, 8670-8673

151. Ketterer, B. (1986) Detoxication Reactions of Glutathione and Glutathione Transferases. *Xenobiotica* **16(10/11)**, 957-973

152. Ketterer, B., Beale, D. & Meyer, D. (1982) The Structure and Multiple Functions of Glutathione Transferases. *Biochem.Soc.Trans.* **10**, 82-84

153. Ketterer, B., Carne, T. & Tipping, E. (1978) Ligandin and Protein A: Intracellular Binding Proteins. in *Transport by Proteins* (Blauer, G. & Sund, H.,eds.), 79-92, Walter de Gruyter, Berlin

154. Ketterer, B., Ross-Mansell, P. & Whitehead, J.K. (1967) The Isolation of Carcinogen-Binding Protein from Livers of Rats given 4-Dimethylamino-azobenzene. *Biochem.J.* **103**, 316-324

155. Ketterer, B., Tipping, E., Beale, D. & Meuwissen, J.A.T.P. (1976) Ligandin, Glutathione Transferase, and Carcinogen Binding. in *Glutathione: Metabolism and Function* (Arias, I.M. & Jakoby, W.B., eds.), 243-256, Raven Press, New York

156. Kitahara, A., Satoh, K., Nishimura, K., Ishikawa, T., Ruike, K., Sato, K., Tsuda, H. & Ito, N. (1984) Changes in Molecular Forms of Rat Hepatic Glutathione S-Transferase during Chemical Hepatocarcinogenesis. *Cancer Res.* **44(6)**, 2698-2703

157. Klinman, J.P. (1981) Probes of Mechanism and Transition State Structure in the Alcohol Dehydrogenase Reaction. *CRC Crit.Rev.Biochem.* **10**, 39-78

158. Koga, N., Inskeep, P.B., Harris, T.M. & Guengerich, F.P. (1986) S-[2-(N^7-Guanyl)ethyl]glutathione, the Major DNA Adduct Formed from 1,2-Dibromoethane. *Biochemistry* **25**, 2192-2198

159. Koskelo, K. & Valmet, E. (1980) Acid Glutathione S-Transferase from Human Liver: Preliminary Report. *Scand.J.Clin.Lab.Invest.* **40**, 179-184

160. Koskelo, K., Valmet, E. & Tenhunen, R. (1981) Purification and Characterization of an Acid Glutathione S-Transferase from Human Lung. *Scand.J.Clin.Lab.Invest.* **41**, 683-689

161. Kotze, A.C. & Rose, H.A. (1987) Glutathione S-Transferase in the Australian Sheep Blowfly, *Lucilia cuprina* (Weidemann). *Pestic.Biochem.Physiol.* **29(1)**, 77-86

162. Kulkarni, A.P., Nelson, J.L. & Radulovic, L.L. (1987) Partial Purification and Some Biochemical Properties of Neonatal Rat Cutaneous Glutathione S-Transferases. *Comp.Biochem.Physiol.* **B87(4)**, 1005-1009

163. Kulkarni, A.P., Ronan, P., Radulovic, L.L. & Strohm, B. (1984) Glutathione S-Transferase Activity During Pregnancy in the Mouse: Effects of *trans*-Stilbene Oxide Pretreatment. *Biochem.Pharmacol.* **33(20)**, 3301-3303

164. Laemmli, U.K. (1970) Cleavage of Structural Proteins During the Assembly of the Head of Bacteriophage T4. *Nature* **227**, 680-685

165. Lai, H.-C.J. & Tu, C.-P.D. (1986) Rat Glutathione S-Transferases Supergene Family. Characterization of an Anionic Y_b Subunit cDNA Clone. *J.Biol.Chem.* **261(29)**, 13793-13799

166. Lamartiniere, C.A. (1981) The Hypothalamic-Hypophyseal-Gonadal Regulation of Hepatic Glutathione S-Transferases in the Rat. *Biochem.J.* **198**, 211-217

167. Leatherbarrow, R.J. (1987) *Enzfitter*: A Non-Linear Regression Data Analysis Program for the IBM PC, (Software and Manual) p.91, Elsevier-BIOSOFT, Cambridge, UK

168. Leblanc, G.A. & Cochrane, B.J. (1987) Identification of Multiple Glutathione S-Transferases from *Daphnia Magna*. *Comp.Biochem.Physiol.* **88B(1)**, 39-46

169. Lee, C.-Y., Johnson, L., Cox, R.H., McKinney, J.D. & Lee, S.-M. (1981) Mouse Liver Glutathione S-Transferases. Biochemical and Immunological Characterization. *J.Biol.Chem.* **256(15)**, 8110-8116

170. Li, C.-H., Srikumar, K., Burgess, J.R., Hong, Y., Hildenbrandt, G., Rao, M.K., Reddanna, P., Li, N. & Tu, C.-P.D. & Reddy, C.C. (1986) Sheep Lung Glutathione S-Transferases and Eicosanoid Biosynthesis. in *ICSU Short Reports* (Kon, O.L. *et al.*, eds.), vol. 6, 662-663, Cambridge University Press, Cambridge

171. Litwack, G., Ketterer, B. & Arias, I.M. (1971) Ligandin: a Hepatic Protein which Binds Steroids, Bilirubin, Carcinogens and a Number of Exogenous Organic Anions. *Nature (London)* **234**, 466-467

172. Lluis, C. (1984) Lactate Dehydrogenase Associated with the Mitochondrial Fraction and with a Mitochondrial Inhibitor I. Enzyme Binding to the Mitochondrial Fraction. *Int.J.Biochem.* **16(9)**, 997-1004

173. Lowry, O.H., Rosebrough, N.J., Farr, A.L. & Randall, R.J. (1951) Protein Measurement with Folin Phenol Reagent. *J.Biol.Chem.* **192**, 265-275

174. Manchester, D.K. & Jacoby, E.H. (1982) Glutathione S-Transferase Activities in Placentas from Smoking and Non-Smoking Women. *Xenobiotica* **12(9)**, 543-547

175. Mangold, J.B. & Abdel-Monem, M.M. (1980) Stereoselectivity of the Glutathione S-Transferase Catalyzed Conjugation of Aralkyl Halides. *Biochem.Biophys.Res.Commun.* **96(1)**, 333-340

176. Mangold, J.B. & Abdel-Monem, M.M. (1983) Stereochemical Aspects of Conjugation Reactions Catalyzed by Rat Liver Glutathione S-Transferase Isozymes. *J.Med.Chem.* **26**, 66-71

177. Mannervik, B. (1981) Design and Analysis of Kinetic Experiments for Discrimination Between Rival Models. in *Kinetic Data Analysis: Design and Analysis of Enzyme and Pharmacokinetic Experiments* (Endrenyi, L., ed.), 235-270, Plenum Press, New York

178. Mannervik, B. (1982) Regression Analysis, Experimental Error, and Statistical Criteria in the Design and Analysis of Experiments for Discrimination Between Rival Kinetic Models. *Methods Enzymol.* **87**, 370-390

179. Mannervik, B. (1985) The Isoenzymes of Glutathione Transferase. *Adv.Enzymol.Relat.Areas Mol.Biol.* **57**, 357-417

180. Mannervik, B. (1986) Glutathione and the Evolution of Enzymes for Detoxication of Products of Oxygen Metabolism. *Chem.Scr.* **26B**, 281-284

181. Mannervik, B. (1987) The Roles of Different Classes of Glutathione Transferase in the Detoxication of Reactive Products of Oxidative Metabolism. *Chem.Scr.* **27A**, 121-123

182. Mannervik, B., Ålin, P., Guthenberg, C., Jensson, H., Tahir, M.K., Warholm, M. & Jörnvall, H. (1985) Identification of Three Classes of Cytosolic Glutathione Transferase Common to Several Mammalian Species: Correlation between Structural Data and Enzymatic Properties. *Proc.Natl.Acad.Sci. USA* **82**, 7202-7206

183. Mannervik, B., Ålin, P., Guthenberg, C., Jensson, H. & Warholm, M. (1985) Glutathione Transferases and the Detoxication of Products of Oxidative Metabolism. in *Proceedings, 6th International Symposium on Microsomes and Drug Oxidations, Brighton, UK.* (Boobis, A.R., Caldwell, J., De Matteis, F. & Elcombe, C.R., eds.), 221-228, Academic Press, New York

184. Mannervik, B. & Askelöf, P. (1975) Absence of a Ping-Pong Pathway in the Kinetic Mechanism of Glutathione S-Transferase A from Rat Liver. Evidence based on Quantitative Comparison of the Asymptotic Properties of Experimental Data and Alternative Rate Equations. *FEBS Lett.* **56(2)**, 218-221

185. Mannervik, B., Castro, V.M., Danielson, U.H., Tahir, M.K., Hansson, J. & Ringborg, U. (1987) Expression of Class Pi Glutathione S-Transferase in Human Malignant Melanoma Cells. *Carcinogenesis* **8(12)**, 1929-1932

186. Mannervik, B. & Guthenberg, C. (1981) Glutathione Transferase (Human Placenta). *Methods Enzymol.* **77**, 231-235

187. Mannervik, B., Guthenberg, C., Jensson, H., Warholm, M. & Ålin, P. (1983) Isozymes of Glutathione S-Transferases in Rat and Human Tissues. in *Functions of Glutathione: Biochemical, Physiological, Toxicological and Clinical Aspects.* (Larsson, A., Orrenius, S., Holmgren, A. & Mannervik, B., eds.), 75-88, Raven Press, New York

188. Mannervik, B. & Jensson, H. (1982) Binary Combinations of Four Protein Subunits with Different Catalytic Specificities Explain the Relationship Between Six Basic Glutathione S-Transferases in Rat Liver Cytosol. *J.Biol.Chem.* **257(17)**, 9909-9912

189. Mannervik, B., Jensson, H., Ålin, P., Oring, L. & Hammarström, S. (1984) Transformation of Leukotriene A_4 Methyl Ester to Leukotriene C_4 Monomethyl Ester by Cytosolic Rat Glutathione Transferases. *FEBS Lett.* **174(2)**, 289-293

190. Marcus, C.J., Habig, W.H. & Jakoby, W.B. (1978) Glutathione S-Transferase from Human Erythrocytes: Non-Identity with the Enzymes from Liver. *Arch.Biochem.Biophys.* **188(2)**, 287-293

191. Maruyama, H., Arias, I.M. & Listowsky, I. (1984) Distinctions Between the Multiple Cationic Forms of Rat Liver Glutathione S-Transferase. *J.Biol.Chem.* **259**, 12444-12448

192. Meyer, D.J., Christodoulides, L.G., Tan, K.H. & Ketterer, B. (1984) Isolation, Properties and Tissue Distribution of Rat Glutathione Transferase E. *FEBS Lett.* **173(2)**, 327-330

193. Meyer, D.J. & Ketterer, B. (1982) 5α,6α-Epoxy-cholestan-3α-ol (Cholesterol α-oxide): A Specific Substrate for Rat Liver Glutathione Transferase B. *FEBS Lett.* **150(2)**, 499-502

194. Miyaura, S. & Isono, H. (1986) Further Analysis of Multiple Forms of Rabbit Hepatic Glutathione S-Transferase. *Chem.Pharm.Bull. (Tokyo)* **34(7)**, 2919-2925

195. Moore, M.A., Nakagawa, K., Satoh, K., Ishikawa, T. & Sato, K. (1987) Single GST-P Positive Liver Cells - Putative Initiated Hepatocytes. *Carcinogenesis* **8(3)**, 483-486

196. Moore, R.E., Davies, M.S., O'Connell, K.M., Harding, E.I., Wiegand, R.C. & Tiemeier, D.C. (1986) Cloning and Expression of a cDNA Encoding a Maize Glutathione S-Transferase in *E.coli*. *Nucleic Acids Res.* **14(18)**, 7227-7235

197. Morey, K.S. & Litwack, G. (1969) Isolation and Properties of Cortisol Metabolite Binding Proteins of Rat Liver Cytosol. *Biochemistry* **8(12)**, 4813-4821

198. Morgenstern, R. & DePierre, J.W. (1983) Microsomal Glutathione S-Transferase: Purification in Unactivated Form and Further Characterization of the Activation Process, Substrate Specificity and Amino Acid Composition. *Eur.J.Biochem.* **134**, 591-597

199. Morgenstern, R. & DePierre, J.W. (1987) Membrane-Bound Glutathione Transferase. *Biochem.Soc.Trans.* **15(4)**, 719-721

200. Morgenstern, R., DePierre, J.W. & Jörnvall, H. (1985) Microsomal Glutathione Transferase. Primary Structure. *J.Biol.Chem.* **260(26)**, 13976-13983

201. Morgenstern, R., DePierre, J.W., Lind, C., Guthenberg, C., Mannervik, B. & Ernster, L. (1981) Benzo[α]pyrene Quinones can be Generated by Lipid Peroxidation and are Conjugated with Glutathione. *Biochem.Biophys.Res.Commun.* **99(2)**, 682-690

202. Morgenstern, R., Guthenberg, C. & DePierre, J.W. (1982) Microsomal Glutathione S-Transferase: Purification, Initial Characterization, and Demonstration that it is not Identical to the Cytosolic Glutathione S-Transferases A, B, or C. *Eur.J.Biochem.* **128**, 243-248

203. Morgenstern, R., Lundquist, G., Andersson, G., Balk, L. & DePierre, J.W. (1984) The Distribution of Microsomal Glutathione Transferase Among Different Organelles, Different Organs and Different Organisms. *Biochem.Pharmacol.* **33(22)**, 3609-3614

204. Morgenstern, R., Meijer, J., DePierre, J.W. & Ernster, L. (1980) Characterization of Rat-Liver Microsomal Glutathione S-Transferase Activity. *Eur.J.Biochem.* **104**, 167-174

205. Motoyama, N. & Dauterman, W.C. (1977) Purification and Properties of Housefly Glutathione S-Transferase. *Insect Biochem.* **7**, 361-369

206. Mozer, T.J., Tiemeier, D.C. & Jaworski, E.J. (1983) Purification and Characterisation of Corn Glutathione S-Transferase. *Biochemistry* **22**, 1068-1072

207. Mukhtar, H. & Bend, J.R. (1977) Serum Glutathione S-Transferases: Perinatal Development, Sex Difference, and Effect of Carbon Tetrachloride Administration on Enzyme Activity in the Rat. *Life Sci.* **21**, 1277-1286

208. Okuda, A. & Okuda, K. (1983) Physiological Function and Kinetic Mechanism of Human Liver Alcohol Dehydrogenase as 5β-Cholestane-3α,7α,12α,26-tetrol Dehydrogenase. *J.Biol.Chem.* **258(5)**, 2899-2905

209. Okuda, A., Sakai, M. & Muramatsu, M. (1987) The Structure of the Rat Glutathione S-Transferase P Gene and Related Pseudogenes. *J.Biol.Chem.* **262(8)**, 3858-3863

210. O'Leary, K.A. & Tracy, J.W. (1988) Purification of Three Cytosolic Glutathione S-Transferases from Adult *Schistosoma mansoni*. *Arch Biochem.Biophys.* **264(1)**, 1-12

211. Ostlund Farrants, A.-K., Meyer, D.J., Coles, B., Southan, C., Aitken, A., Johnson, P.J. & Ketterer, B. (1987) The Separation of Glutathione Transferase Subunits by Using Reverse-Phase High-Pressure Liquid Chromatography. *Biochem.J.* **245**, 423-428

212. Ottaway, J.H. (1973) Normalization in the Fitting of Data by Iterative Methods. Application to Tracer Kinetics and Enzyme Kinetics. *Biochem.J.* **134**, 729-736

213. Overbaugh, J.M., Lau, E.P., Marino, V.A. & Fall, R. (1988) Purification and Preliminary Characterization of a Monomeric Glutathione S-Transferase from *Tetrahymena thermophila*. *Arch.Biochem.Biophys.* **261(2)**, 227-234

214. Ozawa, N. & Guengerich, F.P. (1983) Evidence for Formation of an S-[2-(N^7-Guanyl)ethyl]glutathione Adduct in Glutathione-Mediated Binding of the Carcinogen 1,2-Dibromoethane to DNA. *Proc.Natl.Acad.Sci.USA* **80**, 5266-5270

215. Pabst, M.J., Habig, W.H., & Jakoby, W.B. (1974) Glutathione S-Transferase A: A Novel Kinetic Mechanism in which the Major Reaction Pathway depends on Substrate Concentration. *J.Biol.Chem.* **249(22)**, 7140-7150

216. Pacifici, G.M. & Rane, A. (1981) Glutathione S-Epoxidetransferase in the Human Placenta at Different Stages of Pregnancy. *Drug Metab.Dispos.* **9**, 472-475

217. Pacifici, G.M., Warholm, M., Guthenberg, C., Mannervik, B. & Rane, A. (1986) Organ Distribution of Glutathione Transferase Isoenzymes in the Human Fetus: Differences Between Liver and Extrahepatic Tissues. *Biochem.Pharmacol.* **35**, 1616-1619

218. Pattinson, N. (1981) Purification by Affinity Chromatography of Glutathione S-Transferases A and C from Rat Liver Cytosol. *Anal.Biochem.* **115**, 424-427

219. Pemble, S.E., Taylor, J.B. & Ketterer, B. (1986) Tissue Distribution of Rat Glutathione Transferase Subunit 7, a Hepatoma Marker. *Biochem.J.* **240(3)**, 885-889

220. Peterson, J., Silver, J., Wilson, M.T. & Morrison, I.E.G. (1980) The Purification and Mössbaur Parameters of the Heme Undecapeptide of Cytochrome-c. *J.Inorg.Biochem.* **13**, 75-82

221. Pettersson, G. (1969) Kinetic Characteristics of the Sequential Random Order Two-Substrate Enzyme Mechanism. *Acta Chem.Scand.* **23**, 2717-2726

222. Pickett, C.B. (1987) Structure and Regulation of Glutathione S-Transferase Genes. *Essays Biochem.* **23**, 116-143

223. Pickett, C.B., Telakowski-Hopkins, C.A., Ding, G.J.-F., Argenbright, L. & Lu, A.Y.H. (1984) Rat Liver Glutathione S-Transferases. Complete Nucleotide Sequence of a Glutathione S-Transferase mRNA and the Regulation of the Y_a, Y_b, and Y_c mRNAs by 3-Methylcholanthrene and Phenobarbital. *J.Biol.Chem.* **259(8)**, 5182-5188

224. Pickett, C.B., Telakowski-Hopkins, C.A., Ding, G.J.-F. & Ding, V.D.-H. (1987) Sequence Analysis and Regulation of Rat Liver Glutathione S-Transferase mRNAs. *Xenobiotica* **17(3)**, 317-323

225. Pickett, C.B., Telakowski-Hopkins, C.A., Ding, G.J.-F., Ding, V.D.-H. & King, R.G. (1987) Structure and Expression of Rat Liver Glutathione S-Transferase Genes. *Fed.Proc.* **46(6)**, 2113

226. Pinkus, L.M., Ketley, J.N. & Jakoby, W.B. (1977) The Glutathione S-Transferases as a Possible Detoxification System of Rat Intestinal Epithelium. *Biochem.Pharmacol.* **26**, 2359-2363

227. Polidoro, G., Del Boccio, G., Di Ilio, C., Piccolomini, R., Ravagnan, G. & Federici, G. (1984) *In Vitro* Interaction of Penicillins and Cephalosporins with Human Placenta GSH S-Transferase. *Res.Commun.Chem.Path.Pharmacol.* **46(3)**, 411-423

228. Polidoro, G., Di Ilio, C., Arduini, A. & Federici, G. (1981) Molecular and Catalytic Properties of Purified Glutathione S-Transferase from Human Placenta. *Biochem.Med.* **25**, 247-259

229. Principato, G.B., Danielson, U.H. & Mannervik, B (1988) Relaxed Thiol Substrate Specificity of Glutathione Transferase Effected by a Non-Substrate Glutathione Derivative. *FEBS Lett.* **231(1)**, 155-158

230. Prohaska, J.R. & Ganther, H.F. (1977) Glutathione Peroxidase Activity of Glutathione S-Transferases Purified from Rat Liver. *Biochem.Biophys.Res. Commun.* **76(2)**, 437-445

231. Radulovic, L.L. & Kulkarni, A.P. (1985) A Rapid, Novel High Performance Liquid Chromatography Method for the Purification of Glutathione S-Transferase: An Application to the Human Placental Enzyme. *Biochem.Biophys.Res.Commun.* **128(1)**, 75-81

232. Radulovic, L.L. & Kulkarni, A.P. (1986) H.P.L.C. Separation and Study of the Charge Isomers of Human Placental Glutathione Transferase. *Biochem.J.* **239**, 53-57

233. Rannug, U. (1980) Genotoxic Effects of 1,2-Dibromoethane and 1,2-Dichloro-ethane. *Mutat.Res.* **76**, 269-295

234. Reddy, C.C., Burgess, J.R. Gong, Z.-Z., Massaro, E.J. & Tu, C.-P.D. (1983) Purification and Characterization of the Individual Glutathione S-Transferases from Sheep Liver. *Arch.Biochem.Biophys.* **224(1)**, 87-101

235. Reddy, C.C., Tu, C.-P.D., Burgess, J.R., Ho, C.-Y., Scholz, R.W. & Massaro, E.J. (1981) Evidence for the Occurence of Selenium-Independent Glutathione Peroxidase Activity in Rat Liver Microsomes. *Biochem.Biophys.Res.Commun.* **101(3)**, 970-978

236. Rhoads, D.M., Zarlengo, R.P. & Tu, C.-P.D. (1987) The Basic Glutathione Transferases from Human Livers are Products of Separate Genes. *Biochem.Biophys.Res.Commun.* **145(1)**, 474-481

237. Ridgewell, R.E. & Abdel-Monem, M.M. (1987) Stereochemical Aspects of the Glutathione S-Transferase Catalyzed Conjugations of Alkyl Halides. *Drug Metab.Dispos.* **15(1)**, 82-90

238. Robertson, I.G.C., Guthenberg, C., Mannervik, B. & Jernström, B. (1986) Differences in Stereoselectivity and Catalytic Efficiency of Three Human Glutathione Transferases in the Conjugation of Glutathione with 7β,8α-Dihydroxy-9α,10α-oxy-7,8,9,10-tetra-hydrobenzo[α]pyrene. *Cancer Res.* **46**, 2220-2224

239. Robertson, I.G.C., Jensson, H., Guthenberg, C., Tahir, M.K., Jernström, B. & Mannervik, B. (1985) Differences in the Occurence of Glutathione Transferase Isoenzymes in Rat Lung and Liver. *Biochem.Biophys.Res.Commun.* **127(1)**, 80-86

240. Robson, C.N., Lewis, A.D., Wolf, C.R., Hayes, J.D., Hall, A., Proctor, S.J., Harris, A.L. & Hickson, I.D. (1987) Reduced Levels of Drug-Induced DNA Cross-Linking in Nitrogen Mustard-Resistant Chinese Hamster Ovary Cells Expressing Elevated Glutathione S-Transferase Activity. *Cancer Res.* **47(22)**, 6022-6027

241. Rothkopf, G.S., Telakowski-Hopkins, C.A., Stotish, R.L. & Pickett, C.B. (1986) Multiplicity of Glutathione S-Transferase Genes in the Rat and Association with a Type 2 Alu Repetitive Element. *Biochemistry* **25(5)**, 993-1002

242. Rudolph, F.B. & Fromm, H.J. (1971) Computer Simulation Studies with Yeast Hexokinase and Additional Evidence for the Random Bi Bi Mechanism. *J.Biol.Chem.* **246(21)**, 6611-6619

243. Rushmore, T.H., Harris, L., Nagai, M., Sharma, R.N., Hayes, M.A., Cameron, R.G., Murray, R.K. & Farber, E. (1988) Purification and Characterization of P-52 (Glutathione S-Transferase P or 7-7) from Normal Liver and Putative Preneoplastic Liver Nodules. *Cancer Res.* **48(10)**, 2805-2812

244. Ryzewski, C.N. & Pietruszko, R. (1980) Kinetic Mechanism of Horse Liver Alcohol Dehydrogenase SS. *Biochemistry* **19**, 4843-4848

245. Sato, K. (1988) Glutathione S-Transferases and Hepatocarcinogenesis. *Jpn.J.Cancer Res.* **79(5)**, 556-572

246. Sato, K., Satoh, K., Hatayama, I., Tsuchida, S., Soma, Y., Shiratori, Y., Tateoka, N., Inaba, Y. & Kitahara, A. (1987) Placental Glutathione S-Transferase as a Marker for (Pre)Neoplastic Tissues. in *Glutathione S-Transferases and Carcinogenesis* (Mantle, T.J., Hayes, J.D. & Pickett, C.B., eds.), 127-137, Taylor & Francis, London

247. Satoh, K., Kitahara, A. & Sato, K. (1985) Identification of Heterogeneous and Microheterogeneous Subunits of Glutathione S-Transferase in Rat Liver Cytosol. *Arch.Biochem.Biophys.* **242(1)**, 104-111

248. Satoh, K., Kitahara, A., Soma, Y., Inaba, Y., Hatayama, I. & Sato, K. (1985) Purification, Induction, and Distribution of Placental Glutathione Transferase: A New Marker Enzyme for Preneoplastic Cells in the Rat Chemical Hepatocarcinogenesis. *Proc.Natl.Acad.Sci. USA* **82**, 3964-3968

249. Schramm, V.L., McCluskey, R., Emig, F.A. & Litwack, G. (1984) Kinetic Studies and Active Site-Binding Properties of Glutathione S-Transferases Using Spin-Labeled Glutathione, a Product Analogue. *J.Biol.Chem.* **259(2)**, 714-722

250. Scriven, A.J., Hume, R., Nimmo, I.A. & Strange, R.C. (1986) Studies on the Relationship between Glutathione S-Transferase Phenotype and Bile Acid Binding by Human Liver Cytosol. *Biochim.Biophys.Acta* **881(1)**, 93-99

251. Scully, N.C. & Mantle, T.J. (1981) Tissue Distribution and Subunit Structures of the Multiple Forms of Glutathione S-Transferase in the Rat. *Biochem.J.* **193**, 367-370

252. Segel, I.H. (1975) Enzyme Kinetics : Behavior and Analysis of Rapid Equilibrium and Steady-State Enzyme Systems, p.957, J.Wiley and Sons, New York

253. Senjo, M., Ishibashi, T. & Imai, Y. (1985) Purification and Characterization of Cytosolic Liver Protein Facilitating Heme Transport into Apocytochrome b_5 from Mitochondria. Evidence for Identifying the Heme Transfer Protein as Belonging to a Group of Glutathione S-Transferases. *J.Biol.Chem.* **260(16)**, 9191-9196

254. Sesay, M.A., Ammon, H.L. & Armstrong, R.N. (1987) Crystallization and a Preliminary X-Ray Diffraction Study of Isozyme 3-3 of Glutathione S-Transferase from Rat Liver. *J.Mol.Biol.* **197(2)**, 377-378

255. Shiratori, Y., Soma, Y., Maruyama, H., Sato, S., Takano, A. & Sato, K. (1987) Immunohistochemical Detection of the Placental Form of Glutathione S-Transferase in Dysplastic and Neoplastic Human Uterine Cervix Lesions. *Cancer Res.* **47(24)**, 6806-6809

256. Silverstein, E. & Boyer, P.D. (1964) Equilibrium Reaction Rates and the Mechanisms of Liver and Yeast Alcohol Dehydrogenase. *J.Biol.Chem.* **239(11)**, 3908-3914

257. Simons, P.C. & Vander Jagt, D.L. (1977) Purification of Glutathione S-Transferases from Human Liver by Glutathione-Affinity Chromatography. *Anal.Biochem.* **82**, 334-341

258. Simons, P.C. & Vander Jagt, D.L. (1980) Bilirubin Binding to Human Liver Ligandin (Glutathione S-Transferase). *J.Biol.Chem.* **255(10)**, 4740-4744

259. Simons, P.C. & Vander Jagt, D.L. (1981) Purification of Glutathione S-Transferases by Glutathione-Affinity Chromatography. *Methods Enzymol.* **77**, 235-237

260. Singh, S.V., Ansari, G.A.S. & Awasthi, Y.C. (1986) Anion-Exchange High-Performance Liquid Chromatography of Glutathione S-Transferases. Separation of the Minor Isozymes of Human Erythrocyte, Heart and Lung. *J.Chromatogr.* **361**, 337-345

261. Singh, S.V. & Awasthi, Y.C. (1986) Cationic Glutathione S-Transferase of Human Erythrocytes has Unique Kinetic Characteristics among Human Glutathione S-Transferases. *Biochem.Biophys.Res.Commun.* **137(3)**, 1174-1180

262. Singh, S.V. & Awasthi, Y.C. (1986) Subunit Composition of Glutathione S-Transferases of Rat Lung. *Enzyme* **35(3)**, 127-136

263. Singh, S.V., Creadon, G., Das, M., Mukhtar, H. & Awasthi, Y.C. (1987) Glutathione S-Transferases of Mouse Lung. Selective Binding of Benzo[α]pyrene Metabolites by the Subunits which are Preferentially Induced by *t*-Butylated Hydroxyanisole. *Biochem.J.* **243(2)**, 351-358

264. Singh, S.V., Dao, D.D., Partridge, C.A., Theodore, C., Srivastava, S.K. & Awasthi, Y.C. (1985) Different Forms of Human Liver Glutathione S-Transferases arise from Dimeric Combinations of at least Four Immunologically and Functionally Distinct Subunits. *Biochem.J.* **232**, 781-790

265. Singh, S.V., Dao, D.D., Srivastava, S.K. & Awasthi, Y.C. (1984) Purification and Characterization of Glutathione S-Transferases in Human Retina. *Curr. Eye Res.* **3**, 1273-1280

266. Singh, S.V., Kurosky, A. & Awasthi, Y.C. (1987) Human Liver Glutathione S-Transferase ψ. Chemical Characterization and Secondary-Structure Comparison with other Mammalian Glutathione S-Transferases. *Biochem.J.* **243(1)**, 61-67

267. Singh, S.V., Leal, T., Ansari, G.A.S. & Awasthi, Y.C. (1987) Purification and Characterization of Glutathione S-Transferases of Human Kidney. *Biochem.J.* **246(1)**, 179-186

268. Singh, S.V., Leal, T., Ansari, G.A.S. & Awasthi, Y.C. (1988) Characterization of Glutathione S-Transferases of Human Kidney. *Fed.Am.Soc.Exp.Biol.* **2(5)**, 6160

269. Singh, S.V., Partridge, C.A. & Awasthi, Y.C. (1984) Rat Lung Glutathione S-Transferases: Evidence for Two Distinct Types of 22 000-M_r Subunits. *Biochem.J.* **221**, 609-615

270. Singh, S.V., Saunders, M.O., Moller, P.C., Haber, B. & Awasthi, Y.C. (1987) Comparative Studies on the Isoenzymes of Glutathione S-Transferase of Rat Brain and Other Tissues. *Comp.Biochem.Physiol.* **86B(1)**, 73-81

271. Smith, D.B., Davern, K.M., Board, P.G., Tiu, W.U., Garcia, E.G. & Mitchell, G.F. (1986) M_r 26 000 Antigen of *Shistosoma japonicum* Recognized by Resistant WEHI 129/J Mice is a Parasite Glutathione S-Transferase. *Proc.Natl.Acad.Sci. USA* **83**, 8703-8707

272. Smith, G.J. & Litwack, G. (1980) Roles of Ligandin and the Glutathione S-Transferases in Binding Steroid Metabolites, Carcinogens and Other Compounds. in *Reviews in Biochemical Toxicology* (Hodgson, E., Bend, J.R. & Philpot, R.M., eds.), vol. 2, 1-47, Elsevier/North Holland, Amsterdam

273. Söderström, M., Hammarström, S. & Mannervik, B. (1988) Leukotriene C Synthase in Mouse Mastocytoma Cells. An Enzyme Distinct from Cytosolic and Microsomal Glutathione S-Transferases. *Biochem.J.* **250(3)**, 713-718

274. Söderström, M., Mannervik, B., Örning, L. & Hammarström S. (1985) Leukotriene C_4 Formation Catalyzed by Three Distinct Forms of Human Cytosolic Glutathione Transferase. *Biochem.Biophys.Res.Commun.* **128(1)**, 265-270

275. Soma, Y., Satoh, K. & Sato, K. (1986) Purification and Subunit-Structural and Immunological Characterization of Five Glutathione S-Transferases in Human Liver and the Acidic Form as a Hepatic Tumor Marker. *Biochim.Biophys.Acta* **869(3)**, 247-258

276. Sugimoto, M., Kuhlenkamp, J., Ookhtens, M., Aw, T.Y., Reeve, J., Jr. & Kaplowitz, N. (1985) γ-Glutamylcysteine: A Substrate for Glutathione S-Transferases. *Biochem.Pharmacol.* **34(20)**, 3643-3647

277. Sugiyama, Y., Sugimoto, M., Stolz, A.W. & Kaplowitz, N. (1984) Comparison of the Binding Affinities of Five Forms of Rat Glutathione S-Transferases for Bilirubin, Sulfobromophthalein and Hematin. *Biochem.Pharmacol.* **33(21)**, 3511-3513

278. Sugiyama, Y., Yamada, T. & Kaplowitz, N. (1981) Glutathione S-Transferases in Elasmobranch Liver. Molecular Heterogeneity, Catalytic and Binding Properties, and Purification. *Biochem.J.* **199**, 749-756

279. Swed, F.S. & Eisenhart, C. (1943) Tables for Testing Randomness of Grouping in a Sequence of Alternatives. *Ann.Math.Stat.* **14**, 66-87

280. Tahir, M.K., Guthenberg, C. & Mannervik, B. (1985) Inhibitors for Distinction of Three Types of Human Glutathione Transferase. *FEBS Lett.* **181(2)**, 249-252

281. Tahir, M.K. & Mannervik, B. (1986) Simple Inhibition Studies for Distinction Between Homodimeric and Heterodimeric Isoenzymes of Glutathione Transferase. *J.Biol.Chem.* **261(3)**, 1048-1051

282. Takikawa, H. & Kaplowitz, N. (1988) Comparison of the Binding Sites of GSH S-Transferases of the Y_a and Y_b Subunit Classes. Effect of Glutathione on the Binding of Bile Acids. *J.Lipid Res.* **29(3)**, 279-286

283. Takikawa, H., Sugiyama, Y. & Kaplowitz, N. (1986) Binding of Bile Acids by Glutathione S-Transferases from Rat Liver. *J.Lipid Res.* **27(9)**, 955-966

284. Takikawa, H., Sugiyama, Y., Stolz, A., Sugimoto, M. & Kaplowitz, N. (1986) Organic Anion-Binding by Human Hepatic GSH S-Transferases. *Biochem.Pharmacol.* **35(2)**, 354-356

285. Tan, K.H., Meyer, D.J., Belin, J. & Ketterer, B. (1984) Inhibition of Microsomal Lipid Peroxidation by Glutathione and Glutathione Transferases B and AA. *Biochem.J.* **220**, 243-252

286. Taylor, J.B., Pemble, S.E., Cowell, I.G., Dixon, K.H. & Ketterer, B. (1987) Molecular Biology of Glutathione Transferases. *Biochem.Soc.Trans.* **15(4)**, 578-581

287. Taylor, J.B., Vidal, A., Torpier, G., Meyer, D.J., Roitsch, C., Balloul, J.-M., Southan, C., Sondermeyer, P., Pemble, S., Lecocq, J.-P., Capron, A. & Ketterer, B. (1988) The Glutathione Transferase Activity and Tissue Distribution of a Cloned Mr28K Protective Antigen of *Schistosoma mansoni*. *The EMBO Journal* **7(2)**, 465-472

288. Telakowski-Hopkins, C.A., King, R.G. & Pickett, C.B. (1988) Glutathione S-Transferase Y_a Subunit Gene: Identification of Regulatory Elements Required for Basal Level and Inducible Expression. *Proc.Natl.Acad.Sci. USA* **85**, 1000-1004

289. Telakowski-Hopkins, C.A., Rodkey, J.A., Bennett, C.D., Lu, A.Y.H. & Pickett, C.B. (1985) Rat Liver Glutathione S-Transferases. Construction of a cDNA Clone Complementary to a Y_c mRNA and Prediction of the Complete Amino Acid Sequence of a Y_c Subunit. *J.Biol.Chem.* **260(9)**, 5820-5825

290. Tew, K.D., Clapper, M.L., Greenberg, R.E., Weese, J.L., Hoffman, S.J. & Smith, T.M. (1987) Glutathione S-Transferases in Human Prostate. *Biochim.Biophys.Acta* **926(1)**, 8-15

291. Tipping, E. & Ketterer, B. (1978) The Role of Intracellular Proteins in the Transport and Metabolism of Lipophilic Compounds. in *Transport by Proteins* (Blauer, G. & Sund, H., eds.), 369-382, Walter de Gruyter, Berlin

292. Tipping, E., Ketterer, B., Christodoulides, L. & Enderby, G. (1976) The Non-Covalent Binding of Small Molecules by Ligandin. Interactions with Steroids and Their Conjugates, Fatty Acids, Bromosulphophthalein, Carcinogens, Glutathione and Related Compounds. *Eur.J.Biochem.* **67**, 583-590

293. Tipping, E., Ketterer, B., Christodoulides, L. & Enderby, G. (1976) Spectroscopic Studies of the Binding of Bilirubin by Ligandin and Aminoazo-Dye-Binding Protein A. *Biochem.J.* **157**, 211-216

294. Tipping, E., Ketterer, B. & Koskelo, P. (1978) The Binding of Porphyrins by Ligandin. *Biochem.J.* **169(2)**, 509-516

295. Trakshel, G.M. & Maines, M.D. (1988) Characterization of Glutathione S-Transferases in Rat Kidney. Alteration of Composition by *cis*-Platinum. *Biochem.J.* **252(1)**, 127-136

296. Tsuchida, S., Izumi, T., Shimizu, T., Ishikawa, T., Hatayama, I., Satoh, K. & Sato, K. (1987) Purification of a New Acidic Glutathione S-Transferase, GST-$Y_{n1}Y_{n1}$, with a High Leukotriene-C_4 Synthetase Activity From Rat Brain. *Eur.J.Biochem.* **170(1-2)**, 159-164

297. Tsutsumi, M., Sugisaki, T., Makino, T., Miyagi, N., Nakatani, K., Shiratori, T., Takahashi, S. & Konishi, Y. (1987) Oncofetal Expression of Glutathione S-Transferase Placental Form in Human Stomach Carcinomas. *Jpn.J.Cancer Res.* **78(7)**, 631-633

298. Tu, C.-P.D., Lai, H.-C.J., Li, N.-Q., Weiss, M.J. & Reddy, C.C. (1984) The Y_c and Y_a Subunits of Rat Liver Glutathione S-Transferases are the Products of Separate Genes. *J.Biol.Chem.* **259(15)**, 9434-9439

299. Tu, C.-P.D., Matsushima, A., Li, N.-Q., Rhoads, D.M., Srikumar, K., Reddy, A.P. & Reddy, C.C. (1986) Immunological and Sequence Interrelationships Between Multiple Human Liver and Rat Glutathione S-Transferases. *J.Biol.Chem.* **261(20)**, 9540-9545

300. Tu, C.-P.D. & Reddy, C.C. (1985) On the Multiplicity of Rat Liver Glutathione S-Transferases. *J.Biol.Chem.* **260(18)**, 9961-9964

301. Tu, C.-P.D., Weiss, M.J., Li, N. & Reddy, C.C. (1983) Tissue-Specific Expression of the Rat Glutathione S-Transferases. *J.Biol.Chem.* **258(8)**, 4659-4662

302. Tuppy, H. & Paléus, S. (1955) Study of a Peptic Degradation Product of Cytochrome-c. 1. : Purification and Chemical Composition. *Acta Chem.Scand.* **9**, 353-364

303. van Bladeren, P.J., Breimer, D.D., Rotteveel-Smijs , G.M.T., De Jong, R.A.W., Buijs, W., Van der Gen, A. & Mohn, G.R. (1980) The Role of Glutathione Conjugation in the Mutagenicity of 1,2-Dibromoethane. *Biochem.Pharmacol.* **29**, 2975-2982

304. Vander Jagt, D.L., Dean, V.L., Wilson, S.P. & Royer, R.E. (1983) Regulation of the Glutathione S-Transferase Activity of Bilirubin Transport Protein (Ligandin) from Human Liver: Enzyme Memory Involving Protein-Protein Interactions. *J.Biol.Chem.* **258(9)**, 5689-5694

305. Vander Jagt, D.L. & Garcia, K.B. (1987) Immunochemical Comparisons of Proteins that Bind Heme and Bilirubin. Human Serum Albumin, α-Fetoprotein and Glutathione S-Transferases from Liver, Placenta and Erythrocyte. *Comp.Biochem.Physiol.* **B87(3)**, 527-531

306. Vander Jagt, D.L., Hunsaker, L.A., Garcia, K.B. & Royer, R.E. (1985) Isolation and Characterization of the Multiple Glutathione S-Transferases from Human Liver. Evidence for Unique Heme-Binding Sites. *J.Biol.Chem.* **260(21)**, 11603-11610

307. Vander Jagt, D.L., Wilson, S.P., Dean, V.L. & Simons, P.C. (1982) Bilirubin Binding to Rat Liver Ligandins (Glutathione S-Transferases A and B). *J.Biol.Chem.* **257(4)**, 1997-2001

308. Vander Jagt, D.L., Wilson, S.P. & Heidrich, J.E. (1981) Purification and Bilirubin Binding Properties of Glutathione S-Transferase from Human Placenta. *FEBS Lett.* **136(2)**, 319-321

309. van Ommen, B., den Besten, C., Rutten, A.L.M., Ploemen, J.H.T.M., Vos, R.M.E., Muller, F. & van Bladeren, P.J. (1988) Active Site-Directed Irreversible Inhibition of Glutathione S-Transferases by the Glutathione Conjugate of Tetrachloro-1,4-benzoquinone. *J.Biol.Chem.* **263(26)**, 12939-12942

310. Vessey, D.A. & Boyer, T.D. (1984) Differential Activation and Inhibition of Different Forms of Rat Liver Glutathione S-Transferase by the Herbicides 2,4-Dichlorophenoxyacetate (2,4-D) and 2,4,5-Trichlorophenoxyacetate (2,4,5-T). *Toxicol.Appl.Pharmacol.* **73**, 492-499

311. Vessey, D.A. & Boyer, T.D. (1988) Characterization of the Activation of Rat Liver Glutathione S-Transferases by Nonsubstrate Ligands. *Toxicol.Appl.Pharmacol.* **93(2)**, 275-280

312. Vessey D.A. & Zakim, D. (1981) Inhibition of Glutathione S-Transferase by Bile Acids. *Biochem.J.* **197**, 321-325

313. Vos, R.M.E., Snoek, M.C., Van Berkel, W.J.H., Mueller, F. & Van Bladeren, P.J. (1988) Differential Induction of Rat Hepatic Glutathione S-Transferase Isoenzymes by Hexachlorobenzene and Benzyl Isothiocyanate. Comparison with Induction by Phenobarbital and 3-Methylcholanthrene. *Biochem.Pharmacol.* **37(6)**, 1077-1082

314. Wang, I.Y., Tung, E., Wang, A.-C., Argenbright, L., Wang, R., Pickett, C.B. & Lu, A.Y.H. (1986) Multiple Y_a Subunits of Glutathione S-Transferase Detected by Monoclonal Antibodies. *Arch.Biochem.Biophys.* **245(2)**, 543-547

315. Warholm, M., Guthenberg, C. & Mannervik, B. (1983) Molecular and Catalytic Properties of Glutathione Transferase μ from Human Liver: An Enzyme Efficiently Conjugating Epoxides. *Biochemistry* **22(15)**, 3610-3617

316. Warholm, M., Guthenberg, C., Mannervik, B. & von Bahr, C. (1981) Purification of a New Glutathione S-Transferase (Transferase μ) from Human Liver Having High Activity with Benzo[α]pyrene-4,5-oxide. *Biochem.Biophys.Res.Commun.* **98(2)**, 512-519

317. Warholm, M., Guthenberg, C., Mannervik, B., von Bahr, C. & Glaumann, H. (1980) Identification of a New Glutathione S-Transferase in Human Liver. *Acta Chem.Scand.* **B34**, 607-621

318. Warholm, M., Guthenberg, C., Von Bahr, C. & Mannervik, B. (1985) Glutathione Transferases From Human Liver. *Methods Enzymol.* **113**, 499-504

319. Warholm, M., Jensson, H., Tahir, M.K. & Mannervik, B. (1986) Purification and Characterization of Three Distinct Glutathione Transferases from Mouse Liver. *Biochemistry* **25(14)**, 4119-4125

320. Wiener, H. (1986) Heterogeneity of Dog-Liver Glutathione S-Transferases. Evidence for a Unique Temperature Dependence of the Catalytic Process. *Eur.J.Biochem.* **157**, 351-363

321. Wilchek, M. (1972) Purification of the Heme Peptide of Cytochrome-c by Affinity Chromatography. *Anal.Biochem.* **49**, 572-575

322. Wolkoff, A.W., Bhargava, M.M., Chung, C. & Gatmaitan, Z. (1979) Purification of Ligandin by Affinity Chromatography on Sulfobromophthalein-Agarose Gel. *Proc.Soc.Exp.Biol.Med.* **160**, 150-153

323. Wolkoff, A.W., Goresky, C.A., Sellin, J., Gatmaitan, Z. & Arias, I.M. (1979) Role of Ligandin in Transfer of Bilirubin from Plasma into Liver. *Am.J.Physiol. 236(6), E638-E648*

324. Wong, L.C.K., Winston, J.M., Hong, C.B. & Plotnick, H. (1982) Carcinogenicity and Toxicity of 1,2-Dibromoethane in the Rat. Toxicol.Appl.Pharmacol. 63, 155-165

325. Yalçin, S., Jensson, H. & Mannervik, B. (1983) A Set of Inhibitors for Discrimination between the Basic Isozymes of Glutathione Transferase in Rat Liver. *Biochem.Biophys.Res.Commun.* **114(2)**, 829-834

326. Yamada, T. & Kaplowitz, N. (1980) Propylthiouracil. A Substrate for the Glutathione S-Transferases that Competes with Glutathione. *J.Biol.Chem.* **255(8)**, 3508-3513

327. Yeung, T.-C. & Gidari, A.S. Purification and Properties of a Chicken Liver Glutathione S-Transferase (1980) *Arch.Biochem.Biophys.* **205**, 404-411